CANADIAN MINING INDUSTRY RESEARCH ORGANIZATION (CAMIRO) EXPLORATION DIVISION

CAMIRO Project 10E01

Quality Control Assessment of Portable XRF Analysers: Development of Standard Operating Procedures, Performance on Variable Media and Recommended Uses

Phase II

Gwendy E.M. Hall

Lilianne Page

Graeme F. Bonham-Carter

August 23, 2012

Revised December 29, 2013

TABLE OF CONTENTS

1. EXECUTIVE SUMMARY

A major component of Phase I of this project was the study of the performance of five portable XRF ('pXRF') instruments from three manufacturers in the analysis of 41 powdered highly varied control reference materials (CRM) - rocks, ores, soils and sediments – in terms of accuracy and precision using the factory calibrations. The objective was not to evaluate the advantages and weaknesses of *individual* instruments but rather to use several instruments in order to gain a comprehensive view of the current capability of the *technique itself*. Although generalities were difficult to make in light of the diversity of sample types, key conclusions comprise:
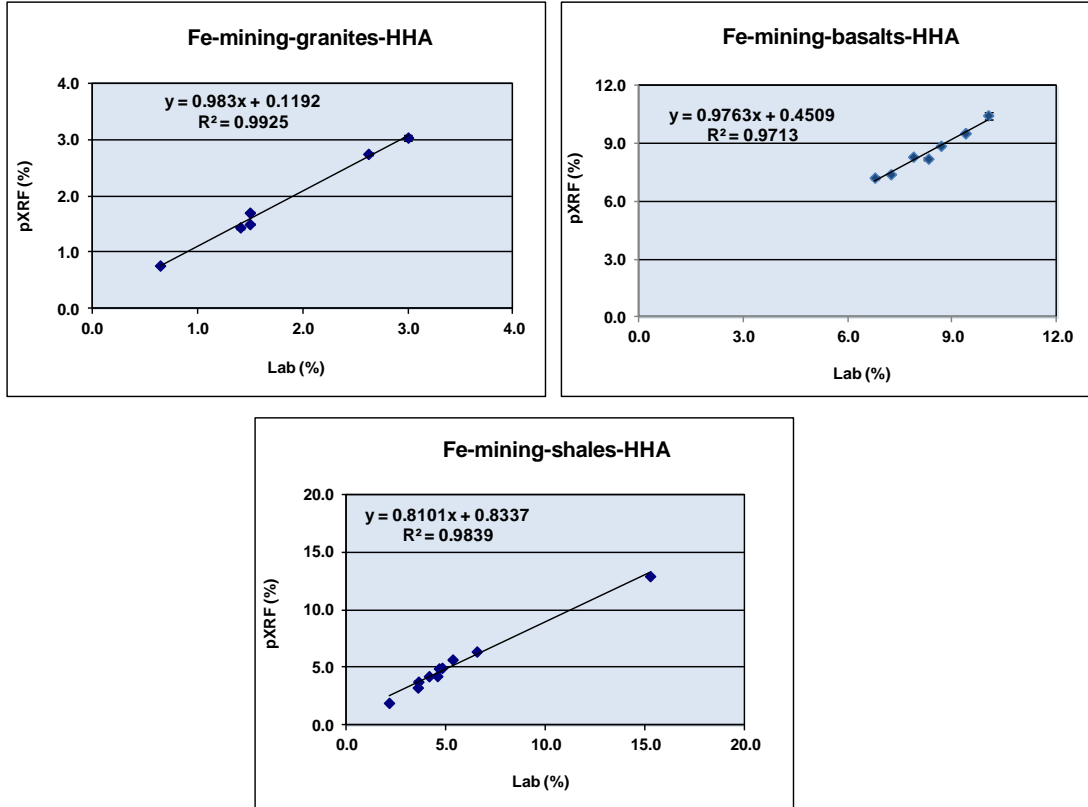
- Inconsistent performance in terms of accuracy in particular was observed across the instruments, even within one manufacturer.
- To use pXRF as a quantitative tool, the user must carry out their own calibrations reflecting the sample matrix under study.
- A beam time of 60 s is a good compromise between efficiency and precision.
- The 4-µm Prolene® thin-film for use with cups provides a good compromise between strength and absorption of low-energy photons of light elements.
- Portable bench-top units were not superior in accuracy or precision to their handheld counterparts.
- Guided by the goodness of fit (r^2) for plots of pXRF value against certified concentration, the overall sequence (across all instruments) of elements in the mining mode from 'good' to 'poor' is Ca, Zn, K, Rb, Sr, Fe, Mn, Cu, S, Ni, Pb, P, Ti, Cr, Al, Si, Mg. In the soil mode, the sequence is Sr, Rb, Cu, Ca, K, Zn, Fe, Ti, Zr, As, Mn, Th, Pb, Nb, Ba, Cd, Cr, U and Sb; elements where ratings were less good include Mo, V, Ni, Co, S and Sn. Elements where highly erroneous results were obtained are those that usually are present at low concentration levels and include Au, Bi, Cs, Hf, Hg, Sc, Pd, Pt, Se, Ta, Te and W. It must be borne in mind that these ratings are based on an extremely varied and often difficult set of sample types, from background granites to ores, and therefore some elements – those which suffer from acute spectral interferences - would fare far better if the sample suite was of a consistent matrix. Severe interferences were observed from the principal elements of ores and from high concentrations of rare-earth elements.
- Repeatability of measurement by pXRF is usually excellent for powders, often better than ± 10 %. From this work, *typical* RSDs (relative standard deviation) for the CRMs fall into the following groups: <2.5 % for Fe, Ca, K, Si; 2.5-4.9 % for Mn, Rb, Sr, Ti, Y, Zn, Zr; 5-10 % for Ag, Cr, Cu, Pb, V, Al, S; 11-20 % for As, Ba, Cd, Co, Ni, S, Th, U, Mg; and > 20 % for Sb, Se, Sn and P.
- 'Real' detection limits in geological materials, particularly for ores or samples enriched in rare-earth elements (REE), can be significantly higher than the ~ 5-50 ppm often quoted. There is a high degree of variability in the manufacturers' software in handling

interferences such that some report erroneous results while others alert the user to the problem by reporting '0', 'VALUE!' or '<LOD'.

In Phase II the focus has been on the performance of pXRF in the *direct* sample analysis of rocks, ores, and soils, most of which have been submitted by the CAMIRO sponsors. The instruments employed are only the two handhelds: the Thermo Niton XL3t GOLDD and the Olympus Innov-X Delta 6000 that were used in Phase I. ALS Laboratories of Vancouver provided the 'lab' results where needed, using 'total' methods such as fusion ICP-MS/-ES. The topics under study for Phase II comprise:

- Calibration strategies and matrix effects;
- Effects due to heterogeneity and particle size in the direct analysis of solid surfaces of rocks and ores;
- Effects of different matrices in soil analysis and the amount of preparation needed for acceptable accuracy and precision; and
- Effect of moisture content in the analysis of soils.

Three suites of control reference materials (CRM) of different rock types – granites, basalts and shales – were analysed by pXRF, using both instruments ('HH-A' and 'HH-C'). Their calibration lines (both mining and soil modes), formed by plots of pXRF results (n=3) versus certified or known values, produced values of goodness of fit ('r^2'), slope and intercept that were compared by element across the three sets to see whether separate calibrations would be required for each. Some elements could reasonably be determined across the different matrices using only one calibration; these include Ca, Rb and Ti by HH-A and Fe, Rb and Zr by HH-C, i.e. not an identical group for each instrument. However, other elements show very significant differences (slope, intercept) in their calibrations across the three matrices using one or both instruments; these include Al, Ba, Cr, Mg, Ni, P, Si and V. Other elements fall in between these two extremes. Below are the calibrations for Fe by HH-A: the slope for the shales is significantly different than that for the granites and basalts (the standard deviations for each point are so small that they cannot be seen). Slopes and intercepts by HH-C differ in that they are essentially the same across all three matrices, illustrating one of the numerous instances of the individual behaviour of pXRF instruments from one manufacturer to another. *Therefore, individual calibration curves are necessary for analysing different sample types.*

Fe-mining-granites-HHA

y = 0.983x + 0.1192
R² = 0.9925

pXRF (%) / Lab (%)

Fe-mining-basalts-HHA

y = 0.9763x + 0.4509
R² = 0.9713

pXRF (%) / Lab (%)

Fe-mining-shales-HHA

y = 0.8101x + 0.8337
R² = 0.9839

pXRF (%) / Lab (%)

Users must compare soil and mining modes for their own samples prior to deciding upon which one to employ. Simply making a decision based on concentration (e.g. soil mode for trace and minor elements and mining for majors) is unwise. The calibration work shows that results even at low levels by the mining mode can be superior (e.g. Pb in shales by HH-A, Ni in basalts and shales by HH-A, and Ba in all three sample types by HH-C). However, high backgrounds are evident in the mining mode for Ag, Bi, Cd, Sb and Sn using HH-A, and for Ce and La using HH-C. The different behaviour of the two instruments supports the conclusion that making a recommendation of soil mode for, say, one element and mining mode for another, or mining mode above a certain concentration, is misguided. This is a decision that is based on the instrument's software, the element, and the sample composition and, because software is changing, it is a moving target. There is clearly a trend amongst manufacturers now to move towards the mining mode for more and more elements but their software needs to be updated to do so.

Calibrations were also studied for ores – namely, for Ni laterite, Ni ultramafic, Cu SEDEX, Zn-Pb-AG SEDEX, and U oxide ores - using the Ore Research and Exploration (OREAS) standards. The objective here was to identify which elements could be determined well within each series and which could not. Factory calibrations for the mining and soil modes can show quite different results, especially for elements subject to interferences (e.g. high background) from the major ore

element(s). Generally the goodness of fit for principal elements is very good. *Again, the ability to handle or mitigate interferences differed between instruments and between modes*. The following elements could be measured well: in the Ni laterite series, Al, Ca, Cr, Fe, Mn, Ni, and Zn; in the Ni ultramafics, As, Co, Cr, Fe, K, Ni, Pb, S, Si, Sr, Ti, Y, Zn and Zr; in the Cu SEDEX series, Ca, Co, Cu, Fe, Pb, S, and Si; in the Zn-Pb-Ag series, Ag, Al, Ba, Ca, Cd, Cu, Fe, Pb, S, Si and Zn; and in the U series, Al, Co, Cr, Fe, K, Mn, Nb, Rb, Si, Sr, Ti, U, Zn and Zr. On the other hand, this set of samples provided numerous demonstrations of spectral interferences such as Pb on As, and U on Mo. The study of three bauxite standards provided by MMG showed once again that one should not assume the preference of the soil mode for traces/minors as Ni, P and Pb proved to be better determined in the mining mode using HH-A. Analysis of bauxites by pXRF was particularly successful for Al, As, Cu, Fe, Mn, Nb, Ni, Pb, Si, Sr, Th, Ti, U, Y and Zn while results for Ca, P and V were just adequate.

How well does a direct analysis by pXRF of a rock or ore sample match that of the prepared powder form analysed by pXRF or by established lab methods such as fusion (lithium metaborate) and ICP-MS/-ES? To answer this question, two groups of samples were analysed: the first is a suite of granodiorites provided by the GSC, in both rock and powder forms, and the second is a diverse suite of 86 rocks and ores provided by the sponsors of this project. As many as 10-15 analyses (both in mining and soil modes) per sample were carried out, in a systematic approach using an unbiased grid system, using both instruments. Comparison was made where possible between analysis of the smooth (usually cut) surface with that of a round or rough surface, again analysing the latter surfaces multiple times. Results show that one can expect a *large deterioration in precision (RSD) in the direct analysis compared to the powder*, obviously depending on the homogeneity and mineralogy of the sample for that element; the magnitude of this deterioration varies enormously, from about fourfold to fortyfold. This is hardly surprising given the very small volume of sample analysed by pXRF (µm to mm depth and area of ~ 50 mm^2) and the inherent heterogeneity of geological materials. Both data-sets, for all elements except Al and Si, indicate that there is no consistent trend in the RSD of multiple analyses of a rock or ore with the texture of the surface, i.e. *analysis of a rough or round surface does not appear to generate an RSD that is inferior to that of a smooth surface*. Of course, individual samples may show a difference in precision across these surfaces but there is no trend. Box-and-whisker plots of RSD by surface and powder analyses below for Ca and Zn in granodiorites illustrate these points.

Granodiorites, HH-C, Mining Mode

Granodiorites, HH-C, Soil Mode
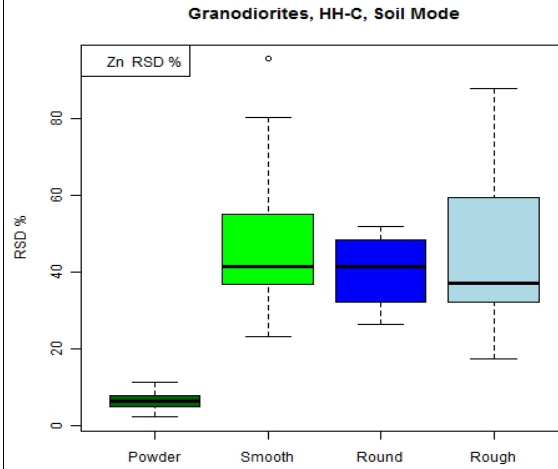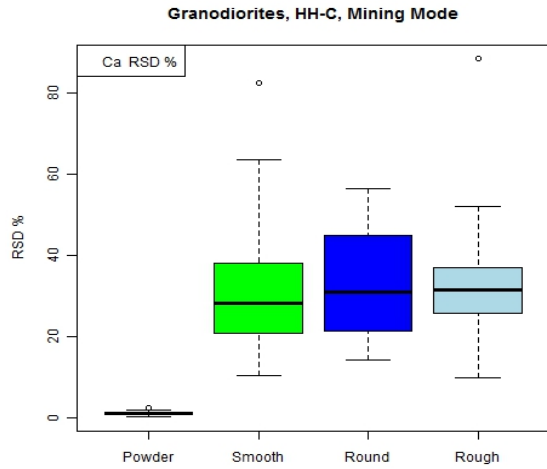
The 86-member rock suite was not ideal for studying the effect of grain size on precision as the coarse/very coarse samples tend to have high RSDs anyway because they comprise ores and high REE samples. However, for numerous elements there is a progression in the RSD of direct smooth surface analysis with grain size, as shown below for Cu in the rock suite. The trend is not always consistent as shown below for Sr in the granodiorite series.

HH-A, Soil Mode

Granodiorites, HH-A, Soil Mode
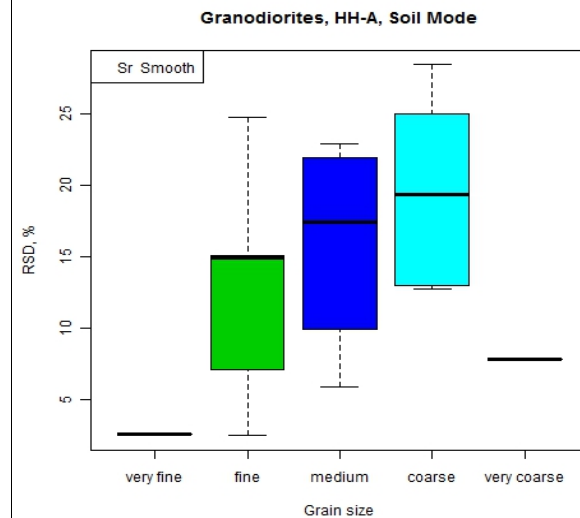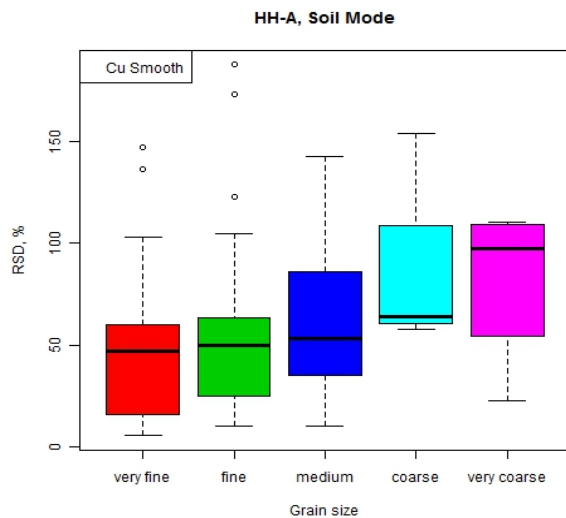
There is quite a strong tendency for results by direct surface analysis to be significantly lower in concentration than those using the powder or those provided by ALS laboratories; this was evident in both data-sets. This phenomenon may be caused by absorption of X-ray photons by large grains/minerals. For example, Cu in a norite sample reports at only 169 ppm (42% RSD) by smooth surface analysis compared to 497 ppm (0.8% RSD) in powder form or 541 ppm by

fusion ICP-MS; in these data-sets, Cu displays this behaviour more severely than other elements. Numerous spectral interferences were observed for the high REE samples, itabirites and various ores. Elements such as Bi, Cs, Te and W could not be determined in this diverse suite, and, as discussed in Phase 1, Au and Hg should not be reported by pXRF unless they are present at exceedingly high levels. However, results for both rock suites showed that excellent performance could be achieved for the trace elements Rb, Nb, Th and Y are very low levels and surface analysis data for Se was extremely encouraging, even at concentrations below 20 ppm.

Repeated measurements, up to 15 per sample, were carried out on the granodiorite smooth and rough surfaces to decide how many measurements (shots) were 'enough'. Because each shot takes on average about 3 minutes to complete, say 20 shots/hour, a cost/benefit approach is critical in deciding how many shots are needed. Monte Carlo simulation experiments on a selection of samples were carried out to evaluate the number of shots needed to be 95% confident that the average of number of measured values is within a selected margin of error of the mean. These results were compared to a formula: $n=4(RSD/D)^2$, where RSD is the relative standard deviation in percent and D is the margin of error as a percentage of the mean. The Monte Carlo results gave very similar results to the formula. The ratio RSD/D is therefore critical: the number of shots needed increases as the square of this ratio. Thus n=4 shots are needed for an element with RSD=20%, using a selected margin of error of D= 20%, but if the RSD increases to 40%, n=16 shots are needed to maintain the same margin of error at 20%. We recommend that a careful analysis of RSD data from an orientation survey be carried out, as well as a decision about an acceptable margin of error for key elements, before deciding on the number of shots. For rocks that are coarse-grained and inhomogenous, with large RSDs for many elements measured on surfaces, grinding to a powder before taking pXRF measurements may be required.

Two sets of soils were used in order to assess whether (a) sample preparation such as ball-milling is required to obtain accurate and precise results and (b) different calibrations are required for organic-rich and mineral (organic-poor) soils. The first set comprises 46 soils collected by the Geological Survey of Canada (GSC) from different eco-regions of Canada, and hence different soil types; these had been coarse-sieved at 2 mm and consisted of ball-milled (BM) and non ball-milled (NBM) suites. *Ball-milling leads generally to a significant improvement in precision for the humus samples* and to a much more subtle one for the mineral soils, such that *this preparation step could be avoided for the mineral soils*. Agreement between the BM and NBM suites for the mineral soils is astoundingly good. Elements differ in the degrees of improvement in precision in the ball-milled humus, presumably due to their distribution and homogeneity in the 'as is' material but for many elements (e.g. As, Rb, Sr) the inferior precision would still be acceptable (i.e. ball-milling not required) but this should be tested for a particular survey. Some elements (e.g. Ca, K, Mn) show a distinct difference in calibration (trend-lines) between humus and mineral soils and therefore *separate calibrations would be required for organic-rich versus*

inorganic-rich media. However, goodness of fit for the plots of pXRF <2-mm ball-milled and <2-mm 'as is' versus the lab result for the *mineral soils* is excellent for elements that are well determined by pXRF (e.g. Ca, Fe, K, As, Cr, Cu, Mn, Nb, Rb, Sr, Zn) so accurate calibration would be obtained across such a suite of fairly diverse soils, i.e. *separate calibrations would not be required for podzol vs brunisol vs chernozem type mineral soils*.

The second set of soils are laterites of high Fe and Al content provided by Vale; they were analysed 'as is' and the results compared with established methods ('total' analysis). Clearly a calibration specific to this matrix is required. The high concentration of Fe has a huge impact on numerous elements, especially on Co and As but also on Ni, Sn, Th, U, and W in samples containing > 25% Fe. These results demonstrate the difference between manufacturers in that one reports an affected element as <LOD while the other reports highly erroneous values, sometimes into the hundreds of ppm. One instrument may correct for a particular interference whereas the other does not; it is not consistent. Elements where at least one instrument shows good results comprise Ca (at > 0.02%), Cu, Fe, K (at > 0.1%), Mn, Nb, Th, Ti, U, V, Y and Zr. With the exception of the elements impacted by high Fe concentration, the overall performance is good in light of the fact that these samples did not undergo any preparation.

Further support to the contention that sample preparation is often not needed in the pXRF analysis of mineral soils is given by comparison of results for a bulk coarse till sample provided by Teck Resources. This sample was analysed after simply separating off large stones and briefly using a pestle and mortar to create a finer grained sample; results were compared with pXRF analyses on the fully prepared 'powder' (ball-milled) and with established lab data. Overall in terms of accuracy the agreement in results is excellent. Examples of degradation in precision in analysing the coarse rather than ball-milled sample, include: Fe, 5.3% RSD (for coarse) from 0.5% (RSD for ball-milled); Ca, 7.0% from 0.9%; Cu, 6.2% from 4.3%; Sr, 10.3% from 0.3%; V, 7.0% from 0.3%; Zn, 6.0% from 3.7%; and Zr, 8.3% from 0.2%. Although these RSDs are inferior to those of the prepared sample, they clearly are reasonable and suggest that a couple of minutes spent sorting and quickly crushing such a sample in the field would be adequate. As very little material is needed to fill a cup or other equivalent vessel for pXRF analysis, using a pestle and mortar to carry out a 1-2 min grind in a field camp would be efficient. A probable cause of the good agreement between 'powder' and 'coarse' results and the fact that precision for the latter analysis remains acceptable is that each cup is repeatedly tapped, prior to analysis, so that the finer fraction of the coarse material settles evenly to the bottom, leaving the larger grains and 'chunks' on top and for the most part invisible to the X-rays.

Three till samples were used to study the effect of moisture content on pXRF results; water was added incrementally and the measurements made at specific intervals after thorough mixing. *Correction for dilution works well up to ~ 30-35% moisture content for most elements*; the light elements Al and Si, however, show a significant degree of under-correction, presumably owing

to absorption of low-energy photons. Correction after the saturation point fails to various degrees depending on the element and sample. Thus, a wet sample can either be analysed 'as is' and a correction made using a simple and inexpensive moisture meter or the sample can be dried in a field camp and subsequently analysed. The former may be more desirable as it would probably be faster and would avoid the need to break up a dry, potentially 'caked' sample. Analysis of a wet clay core provided by Great Western Minerals showed that direct analysis of the core with correction for its 25% moisture content yielded excellent results (except for Al and Si) which compared very well with both established lab analysis of the prepared powder and pXRF analysis of the dried/crushed counterpart.

Portable XRF is capable of producing extremely valuable data in the field, particularly in soil or sediment surveys. If calibrated properly, it can certainly provide data that are 'fit for purpose'. However, geologists should not employ it in the direct analysis of coarse-grained heterogenous rocks and expect the result to be equivalent to a typical 'lab' result on a prepared sample which represents orders of magnitude more volume. Where pXRF should be used is in spatial analysis, such as focussing on a vein, where its small sampling size is an asset, not a detriment.

There is a large amount of information in this report, not all could be extracted in the text. The reader is encouraged to 'mine' the appendices which are clearly laid out and provide the results in numerous graphical formats for easy visualisation and interpretation.

Recommendations to users

• Carry out a calibration to suit your sample type/matrix, in both mining and soil modes. Establish a suite of at least five CRMs, over the expected concentration range, by preparing them to be as homogeneous as possible and having them analysed by several accredited laboratories for total concentrations of the elements of interest. It may well be necessary to create more than five CRMs in order to cover the expected range in concentrations for all elements of interest. Establish which mode is best for which element.
• Become very familiar with the performance of your instrument before taking it to the field. Ascertain the optimum beam time in each mode appropriate for your analytical goals and use both the CRMs supplied with the instrument (usually one or more of the NIST soils) and your own CRMs to establish figures of merit (i.e. *realistic* detection levels, accuracy, precision). Your CRMs may well exhibit data of lesser quality than the NIST standards but that is to be expected.
• Learn to anticipate serious spectral interferences by using the Periodic Table Guide of element lines provided by the manufacturers and in the Phase I report. In most cases, the spectral interferences are not complex. Poor counting statistics precision, provided by the instrument with the actual concentration reading, can alert the user to a likely interference on that element but this is certainly not always the case. Check the spectrum for that element. If the result reported is unexpected (usually high), then analyse again and later check it by a different analytical technique.

• If a *spatial trend* in a survey is being sought and accuracy is not of concern, then prior calibration is not mandatory. However, ensure that a false trend in the data is not generated by any obvious interferences incurred. This could happen when the matrix being analysed changes significantly (e.g. from dry to wet conditions in a soil survey; changing horizons in a soil survey; moving down-core), leading to physical effects, absorption/enhancement effects or direct spectral overlap from hitherto trace-level elements. Data can often be corrected 'after-the-fact' by establishing a calibration to suit the changes in matrix later in the lab/office.

• When carrying out a direct bulk analysis of a rock or core, first measure the variability (RSD) to be expected with that particular rock type (i.e. analyse it in grid format), look up the number of analyses required to be within a specified percentage of the 'true' bulk concentration and ascertain whether it is more efficient and advantageous to grind or mill the sample with portable equipment.

• If a sample is being analysed through a bag of some sort, then that bag's level of contamination must be established and its absorption characteristics for the light elements (Mg, Al, Si) known. Use pure SiO_2 and a low-level CRM as samples to ascertain these figures and correct for them.

• Ensure the depth of sample being analysed is adequate, especially if its density is low. Remember critical penetration depth for light elements such as Si is in the µm range compared to heavy elements in the mm range. Also ensure that the pXRF window fully covers the area of sample being analysed.

• Follow the manufacturer's instructions, e.g. run the supplied coupon/disc as an energy check twice daily. Run the SiO_2 blank at least daily or whenever it is suspected that the window has become dirty (the blank concentration levels should be familiar). The rate at which one or more CRMs is analysed is up to the user/organization but a rate of 1 in 20 to 1 in 40 is recommended. This will facilitate drift correction later if necessary or alert the user to another problem. Running a sample of similar matrix to those under study at a similar rate is also useful, as is replicating an unknown sample to measure precision. Calibrations can be modified using a computer post-analysis; this can be preferable as it is easier to run a regular check on a control sample just using factory calibration (if multiple calibrations are in use).

• Download data from the analyser at least daily and check for any 'oddities' such as change in element order or column shifts. Check the livetime readings: if they are highly variable or decreasing, this may be indicative of a problem with the tube, detector or multichannel analyzer.

• Be consistent!

• Don't combine data from different instruments unless they have been thoroughly cross-calibrated.

• At the present state of the technology, be extremely cautious in using data for the elements Au, Bi, Cs, Hf, Hg, Sc, Pd, Pt, Ta, Te and W. Ensure that results for these elements are verified by established lab methods.

From the manufacturers

In response to questions regarding indications of problems such as a tube dying, these are some comments from the manufacturer of HH-C:

"Key indicators of tube dying are:
- Periodically the analyzer will display "Minimum Count Rate Detected", as if the trigger was being pulled with no sample target;

- Electrical arcing noise; this noise is an indicator that the tube insulator is cracked and the current is arcing;
Key indicators of a failing detector are:
- High V-cool number,
- High resolution,
- High E-scale number.
Key indicators of a failed detector are:
- No spectra,
- Zeroes for results,
- The analyser will display "Minimum Count Rate Detected".

And from the manufacturer of HH-A in response to such questions:
"Our instruments have "smart diagnostic" monitoring which looks at tube and detector data (i.e. voltage, temperature, count rate) that will inform the user and disable the use of the instrument if something looks strange. It will ask for a Cal-Check and then make an assessment. We then advocate the use of good QA/QC to monitor and "catch" any performance changes or drift. This includes:

- *The use or creation of a set of 20-30 lab pulps (per project/area/ore body style) to assess and check the calibration over the desired concentration ranges for all analytes of interest. These are to be used as an initial calibration "orientation" and should then be checked once a week or periodically include in the routine QA/QC protocols.*
- *The constant/daily use of at least 5 good CRMs or matrix-matched SRMs;*
- *Use of one of these CRMs every 20-30 samples, in combination with the blank to check for contamination;*
- *Plus the use of a random duplicate every 20-30 samples, for precision testing;*
- *Near to real time (daily or at least weekly) checking of these data;*
- *We are being the lab, so we should work in the same way and ensure good QA and checking of the instrumentation".*

2. INTRODUCTION

In Phase I of this project we studied the performance of portable XRF (pXRF) in the analysis of 41 powdered control reference materials (CRM) - rocks, ores, soils and sediments – in terms of accuracy and precision using the factory calibrations. We also evaluated the optimum conditions of use (focussing on optimisation of beam time), ease of use, drift, and any problems associated with the operation of three handheld and two bench-top pXRF units, in addition to providing a guide to the theory of XRF, a literature review of pXRF and a study of the best film to employ when using a sample cup.

In Phase II the focus has been on the performance of pXRF in the *direct* sample analysis of rocks, ores, and soils, most of which have been submitted by the CAMIRO sponsors. The instruments employed are only the two handhelds: the Thermo Niton XL3t GOLDD (Ag X-ray tube) and the Olympus Innov-X Delta 6000 (Rh tube) that were used in Phase I. The brand new Bruker S1 Titan handheld pXRF unit was delivered to us but unfortunately still had a few software updates to be worked out and, as time was critical in this short-term project, we had to forego its inclusion in this phase. Our sincere gratitude for all their help go out to John Patterson and Michelle Cameron of Bruker Elemental. We also acknowledge the tremendous help of Aaron Baensch, Todd Houlahan and others of Olympus Innov-X and Keith Grattan, Dave Clifford, Stan Piorek and others at Thermo Niton.

The topics under study for Phase II comprise:
- Calibration strategies and matrix effects
- Effects due to heterogeneity and particle size in the direct analysis of solid surfaces of rocks and ores
- Effects of different matrices in soil analysis and the amount of preparation needed for acceptable accuracy and precision
- Effect of moisture content in the analysis of soils

In Phase I it was evident that the factory calibration (based on fundamental parameters) in the mining mode should be modified to suit the particular samples under study; that is, a group of well characterized samples should be analysed, their results plotted against their known concentrations for the elements of interest and the slope and intercept of the line so formed used to modify future results. Data obtained in the soil mode suggested that this should be done in this mode also. Although good fitting lines were obtained for many elements in the analysis of a diverse suite of 41 CRMs, it was not clear at what point a new calibration was needed to better analyse a different matrix. Therefore in this phase of work, suites of (a) granite, (b) basalt and (c) shale CRMs were gathered and their best-fit lines obtained to compare the different values of r^2, slope and intercept for each element. In other words, could one use a granite calibration for basalts or for shales? Paul Hamlyn of Ore Research and Exploration (http://www.ore.com.au/) kindly provided us with a series of his company's OREAS CRMs for the following matrices: Ni laterites, Ni ultramafics, Cu SEDEX, Zn-Pb-AG SEDEX, and U oxide. We therefore also investigated their calibration lines. Finally, MMG supplied us with three bauxite samples which were intended for use as standards and therefore they were tested and the results compared with those obtained from ALS Laboratories.

How well does a direct XRF analysis of a rock or ore represent the concentration obtained by more conventional analysis using a total methodology such as fusion ICP-MS or ICP-ES (or XRF) following crushing, grinding and ball-milling? The answer to this question was sought by analysing a diverse suite of 86 rocks and ores supplied by the various sponsors. The grain size of these samples was assessed visually. Up to 15 separate analyses were performed on each surface, mostly smooth (i.e. cut) surfaces, but where possible round and rough surfaces were also analysed to see whether their results were inferior. From the relative standard deviations (i.e. precision) obtained, an estimate of the number of shots or pXRF analyses required to generate a result within a selected percentage of the 'truth' could be made. Given the expected range in geochemistry over a whole survey or the constraints of a particular application, one could gauge whether sample preparation was necessary. A more homogenous, less challenging or less interference-prone, suite of samples, granodiorites, was obtained from the GSC to provide another evaluation of the precision of direct pXRF analysis and its comparison with results obtained by sample preparation and established analytical methods.

A group of laterite soils submitted by Vale was analysed 'as is' and results compared with total methods employing ball-milling. This was also carried out with a group of GSC soils of different types (e.g. podsol, chernozem, brunisol) and also of different character (organic-rich and mineral soil). This GSC suite has been coarse-sieved (2 mm) but this fraction was also available in the ball-milled form so that < 2 mm 'as is' and < 2 mm ball-milled could be compared to ascertain whether ball-milling is indeed necessary. A till provided by Teck Resources was also used to assess the necessity of ball-milling.

A soil survey can often cover both well drained and swampy areas and thus it is important to know whether significant differences in concentration are caused simply by moisture content. Three till samples were used for this study: the international standard TILL-2 and two GSC tills. Water was added progressively to them and pXRF analyses carried out at fixed additions. Data obtained were compared with projected results allowing for dilution to see whether a simple correction could be used and, if so, to what maximum concentration of water.

Finally several miscellaneous tests were performed: (a) one on a wet clay core of a high REE sample submitted by Great Western Minerals to compare wet 'as is' results with those on a dry split crushed manually and on a prepared powder; and (b) another on three porphyry Cu pulps submitted by Anglo American to assess accuracy.

3. CALIBRATION

MATRIX CALIBRATIONS (ROCKS)

Calibrations were carried out in both the mining and soil modes for three rock types: granites, basalts and shales. We chose three rock types because of their variation in chemistry and mineralogy: granites (on average, >70% SiO_2, ~15% Al_2O_3, 5-12% total alkalis, <1% MgO, <2% CaO); basalts (on average 45-55 wt% SiO_2, 5-12% MgO, ≥14 % Al_2O_3, 5-14% FeO, ~10% CaO, 2-6 wt% total alkalis); and shales containing mostly clay minerals (~ 50%), quartz and chert, feldspars, limestone and Fe oxides. These are also sample types for which we had an adequate supply of control reference materials (CRM); for some elements, the spread in concentration is limited and therefore not ideal. Table 3.1 shows the CRMs used in these calibrations.

Table 3.1. Control Reference Materials (CRMs) used in study.

Granites		Basalts		Shales	
CRM	**Agency**	**CRM**	**Agency**	**CRM**	**Agency**
GSP-1	USGS	BCR-1	USGS	SCO-1	USGS
GSR-1	IGGE	BHVO-1	USGS	SDO-1	USGS
JG-1	GSJ	BIR-1	USGS	SGR-1	USGS
JG-2	GSJ	BM	ZGI	JSI-1	GSJ
GS-N	CNRS	GSR-3	IGGE	JSI-2	GSJ
GM	ZGI	JB-2	GSJ	8806	U of Ottawa
		JB-3	GSJ	8811	U of Ottawa
		NBS 688	NBS/NIST	8962	U of Ottawa
				8964	U of Ottawa

CNRS: Centre de Recherches Petrographiques et Geochimiques, France
GSJ: Geological Survey of Japan
IGGE: Institute of Geophysical and Geochemical Exploration, China
NBS: National Bureau of Standards, now NIST (National Institute of Science and Technology), USA
USGS: United States Geological Survey
ZGI: Zentrales Geologisches Institut, Germany

The University of Ottawa samples were provided by Mark Hannington, together with total element data from established 'lab' methods such as fusion ICP-MS or XRF. Clearly the 'lab' values for these four samples do not have the same degree of confidence as the recommended values ('RV') of the other reference materials.

The suite of well-homogenised and fine CRMs were loaded into cups, capped with Prolene 4-µm film and analysed by pXRF three times each using HH-A and HH-C. Each time the sample cup was moved so that the analytical variance reflects not only counting statistics but, to a degree, sampling variability.

The actual data, together with recommended (or sometimes only 'provisional' or 'informational') values, are provided with X-Y plots in the Appendix. The X-axis

displays the recommended values (RV), referred to generally as 'Lab' values; the pXRF values are plotted on the Y-axis. Error bars, based on the three pXRF analyses per CRM, are included with all plots. These CRMs are not particularly high in their trace element concentrations, though the shales contain more Cu and Zn than the other two groups and, of course, more Fe at up to ~ 15%. Where element concentrations are too low for the majority of samples, the data are not plotted.

The results are summarized in subsequent pages of this section: Tables 3.2a (granite), 3.2b (basalt), 3.2c (shale) pertain to HH-A while Tables 3.3a, 3.3b and 3.3c show the summary for HH-C. The results are best viewed across all three tables as the statistics of the calibration lines (r^2, slope, intercept) are compared across the three sets of matrix. To make it easier to digest, the results for most elements are colour-coded as follows:

Excellent performance across matrices. Results likely within ~10-20%
Good performance across matrices. Results likely within ~20-30%
Poor performance across matrices. Results likely within ~40-50%
Very poor performance across matrices.

This is a somewhat subjective summary focusing on closeness in slope, intercept (if significant) and goodness of fit, r^2. For interest, data where valid are provided for some elements which are reported in both soil and mining modes. For the most part, major and minor elements are determined using the mining mode and trace elements the soil mode but comparisons were made where possible. The following discussion focuses both on calibration *across* the three rock types and the merits of the *individual* calibrations.

HH-A
Elements which perform well using Handheld A and show an r^2 value of between 0.95 and 1.00 in all their calibrations (except where specifically noted) include Ca, Cr (for basalts and shales), Cu (for basalt and shales), Fe, K, Nb, Ni (basalts), Pb (shale and granite), Rb, S (for shales), Sr, Th (for granites), Ti (for granites and basalts), Y, Zn and Zr.

Elements which show very similar trend-lines across the three calibrations, and hence could be satisfactorily determined using only one calibration (say within ~ 10-20% error), comprise Ca, Rb and Ti (e.g. Ca in Figs. 3.1-3.3). A larger suite of elements, which behave quite well across the calibrations and would probably agree within ~ 20-30% if read using only one calibration, include Cu, Fe, K, Mn, Nb, Pb (for granites and shales), Sr, Y, Zn and Zr (e.g. see Cu and Zr in Figs. 3.4-3.6 and Figs. 3.7-3.9, respectively).

Aluminium and Si are two major elements which certainly have quite different slopes across calibrations, with Al showing a range in slope of 0.72 (granites)-1.04 (basalts) and that of Si being 0.88-1.26; intercepts, too, are variable across the calibrations.

As was demonstrated in Phase 1 of this project, this instrument reports high backgrounds of ~ 200-400 ppm in the mining mode for the trace elements Ag, Cd, Sb and Sn when the soil mode reports correctly values <LOD or close to the LOD. Bismuth is also incorrectly reported in the mining mode in the tens of ppm when in fact this element is

present below 1 ppm. This background in Bi in the mining mode is particularly prevalent in the granites and increases to ~ 160 ppm for the sample highest in Th (105 ppm). If the Bi Lβ line at 13.02 keV is being used for the analysis (the K lines are in too high an energy region, at ~ 77-87 keV), then interference from the Th Lα line at 12.97 keV will be severe.

Most trace element concentrations in the three groups of CRMs are too low for comparison of the calibrations to be made, and/or the goodness of fit, r^2, is very poor. Vanadium (in the soil mode), for example, shows slope values of 2.8 (granites) through 0.37 (basalts) to 0.26 (shales) with corresponding r^2 values of 0.89 through 0.42 to 0.07.

Arsenic in the shale CRMs, with concentrations up to ~ 70 ppm, provides a good calibration with an r^2 value of 0.95 (Fig. 3.10). Cobalt is not well determined at the levels of ~ 10-30 ppm especially if the Fe concentration is high. This effect is evident in the shale calibration, with an r^2 of only 0.44 for the soil mode but the mining mode falsely reports hundreds of ppm Co, to a high of ~ 700 ppm (cf actual value of 56 ppm Co) in the sample containing 15% Fe. The Fe Kα line at 6.40 keV has a huge impact on its Periodic Table neighbour Co whose Kα line is at 6.93 keV. Even the Co Kβ line at 7.65 keV will be affected by the shoulder of the Fe Kβ line at 7.06 keV at high Fe concentrations.

While the soil mode reports mostly <LOD for Ni in the basalt and shale calibrations, with RV concentrations ranging from ~ 13 ppm up to ~ 170 ppm, the mining mode appears to be much preferred, with all values reported above the LOD and an r^2 of 0.97, for example, in the basalt calibration (Fig. 3.11). The superior performance of the mining mode over the soil is also evident for Pb in the shales where an excellent calibration is effected in the former mode but certainly not using the latter (Figs. 3.12 and 3.13). Tungsten, too, appears to be better determined in the granites using the mining mode (only 3 data points >LOD in the soil mode).

Although P is <LOD in most samples, its 3-point basalt calibration, up to ~ 4200 ppm, in the mining mode is encouraging (Fig. 3.14). Sulphur is above detection only in some of the shales, at concentrations from ~ 0.06% up to ~ 5.4%; trend-lines on both modes have associated r^2 values of 1.00, though only four points are available.

An excellent calibration is evident for Th in granites, in the range 14-105 ppm, and standard deviations are extremely small (±1-2 ppm) even at these low concentrations (Fig. 3.15). Uranium was measurable only in four of the granites (at 6-19 ppm); the associated calibration, with an r^2 of 0.93, is nevertheless encouraging.

Table 3.2a. Summary of granite calibration results, HH-A.

	Mining mode			Soil mode			
Element	**Slope**	**Intercept**	**r2**	**Slope**	**Intercept**	**r2**	**<conc**
Al	0.72	1.25	0.85				8%
As		<LOD			Too low values		4 ppm
Ca	1.21	-0.4	0.99	1.05	-0.23	0.99	2%
Co		High bgd, some <LOD			Too low values		70 ppm
Cr		High bgd		0.47	40	0.18	65 ppm
Cu	0.65	23.6	0.88	0.87	2.4	0.94	35 ppm
Fe	0.98	0.12	0.99	0.84	-0.07	0.99	3%
K	1.14	0.21	0.96	0.99	-0.5	0.77	4.5%
Mn	1.23	14.3	0.93	0.88	16.4	0.93	500 ppm
Nb				0.94	-0.34	0.98	40 ppm
Ni		High bgd			<LOD		34 ppm
P		<LOD			<LOD		1200 ppm
Pb	1.16	4.73	0.97	0.85	0.13	0.97	55 ppm
Rb				1.05	-4.1	0.99	500 ppm
S		<LOD			<LOD		400 ppm
Si	0.88	3.91	0.89				36%
Sr				1.04	-4.31	0.99	600 ppm
Th				0.98	4.02	0.99	110 ppm
Ti	1.26	0.05	0.97	0.91	0.001	0.98	0.4%
U				0.75	0.99	0.93	20 ppm
V		Very high variable bgd		2.98	2.28	0.89	70 ppm
W	*0.99*	*18.9*	*0.99*				500 ppm
Y				1.02	-3.13	0.98	90 ppm
Zn		Most <LOD		0.93	0.36	0.98	100 ppm
Zr	1.15	13	0.98	1.15	-8.6	0.99	550 ppm

Italics indicates few points

Table 3.2b. Summary of basalt calibration results, HH-A.

	Basalt calibration						
	Mining mode			Soil mode			
Element	Slope	Intercept	r2	Slope	Intercept	r2	<conc
Al	1.04	-0.11	0.54				9.20%
As	<LOD			Bgd of ~ 20 ppm			13 ppm
Ca	1.14	-0.55	1.00				9.50%
Co	Bgd of ~ 300-500 ppm			Little spread in values			52 ppm
Cr	High SDs cf to soil mode			0.70	22.4	0.97	380 ppm
Cu				0.94	2.88	1.00	230 ppm
Fe	0.98	0.45	0.97				10%
K	1.33	-0.42	1.00				2%
Mn	1.04	-10.1	0.65	1.13	-19.5	0.86	1550 ppm
Nb				1.03	-1.93	1.00	70 ppm
Ni	1.3	48.4	0.97	Most <LOD			170 ppm
P	*1.27*	*-860*	*1.00*	*0.17*	*799*	*0.81*	4100 ppm
Pb	Too low						14 ppm
Rb				1.08	-2.75	0.98	50 ppm
S	<LOD			<LOD			410 ppm
Si	1.26	-5.25	0.87				25%
Sr				1.06	-5.81	1.00	1100 ppm
Th				Too low			6 ppm
Ti	1.16	0.01	0.98				1.70%
U				Too low			2 ppm
V	0.94	320	0.55	0.37	94.4	0.42	600 ppm
W				Too low			<1 ppm
Y				0.96	1.52	0.98	40 ppm
Zn				0.82	9.15	0.96	150 ppm
Zr				1.25	-8.35	1.00	280 ppm

Italics indicates few points

Table 3.2c. Summary of shale calibration results, HH-A.

	Shale calibration						
	Mining mode			**Soil mode**			
Element	**Slope**	**Intercept**	**r2**	**Slope**	**Intercept**	**r2**	**<conc**
Al	0.93	0.63	0.89				10%
As	Many <LOD			0.77	8.84	0.95	70 ppm
Ca	1.24	-0.36	1.00				7.50%
Co	Bgd of ~ 100-200 ppm			0.7	4.29	0.44	56 ppm
Cr	High SDs cf to soil mode			1.36	-6.99	0.98	100 ppm
Cu				0.79	3.09	1.00	580 ppm
Fe	0.81	0.83	0.98				15%
K	1.26	-0.19	0.95				3.50%
Mn	1.24	-6.57	0.95	1.09	34.7	0.94	850 ppm
Nb				0.87	0.00	1.00	70 ppm
Ni	0.54	66.3	0.68	Most <LOD			180 ppm
P	Most <LOD			<LOD			1430 ppm
Pb	1.08	4.12	0.98	*0.08*	*17.3*	*0.03*	40 ppm
Rb				1.05	-5.68	0.99	200 ppm
S	0.83	-0.06	1.00	0.46	-0.04	1.00	5.40%
Si	1.01	0.74	0.96				30%
Sr				0.88	13.6	0.99	420 ppm
Th				1.13	0.85	0.31	13 ppm
Ti	1.26	-0.05	0.91	1.09	-0.04	0.78	0.45%
U				Most <LOD			49 ppm
V	Very high variable bgd			0.26	84.3	0.07	160 ppm
W							
Y				1.16	-5.31	1.00	160 ppm
Zn				0.93	-2.85	1.00	2200 ppm
Zr				1.08	5.21	0.98	290 ppm

Italics indicates few points
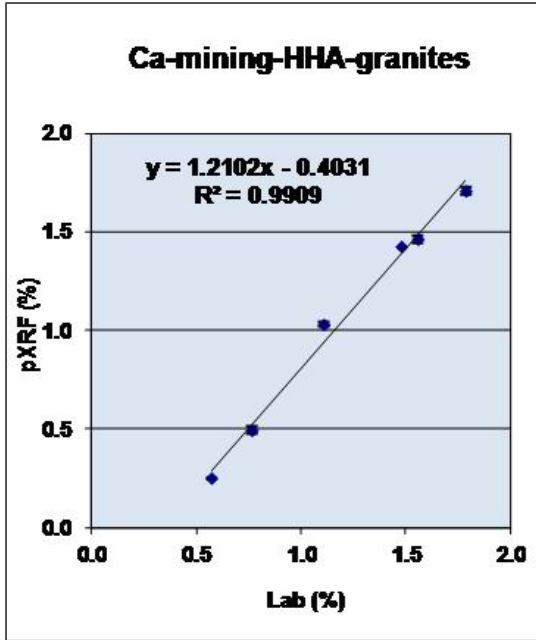
Fig. 3.1. Ca in granite by mining mode, HH-A.
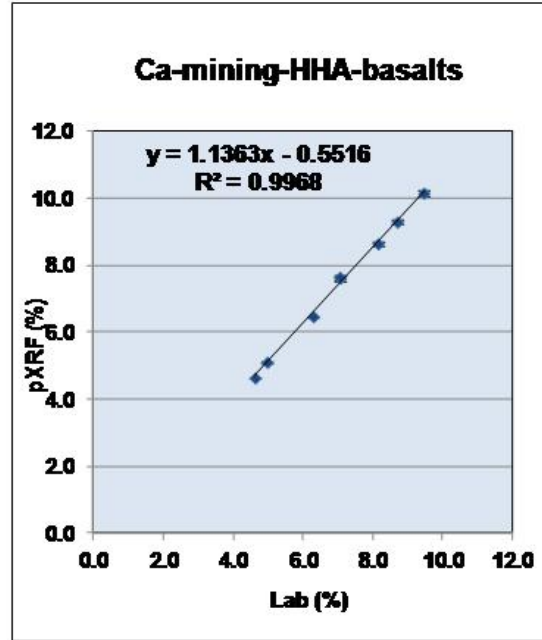
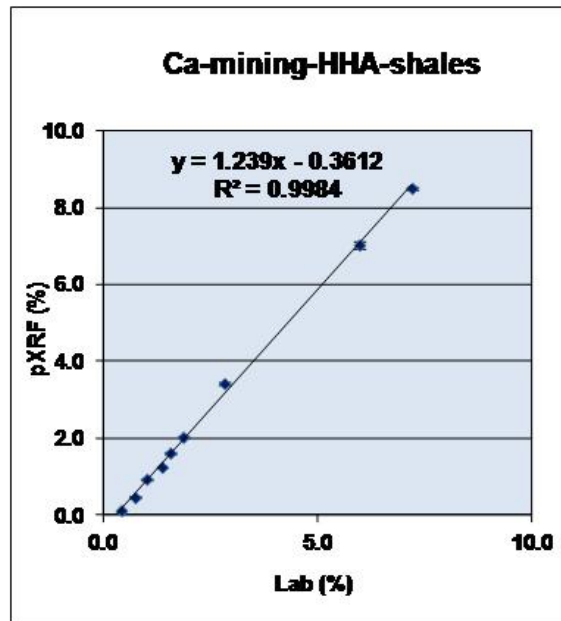**Fig. 3.2. Ca in basalt by mining mode, HH-A.**

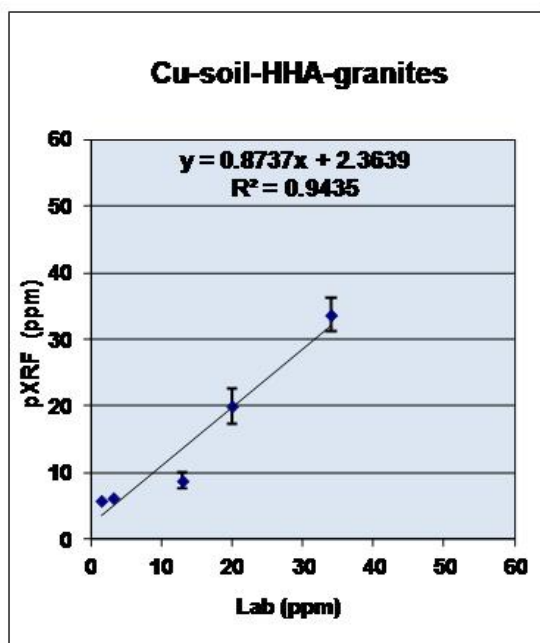Fig. 3.3. Ca in shale by mining mode, HH-A.

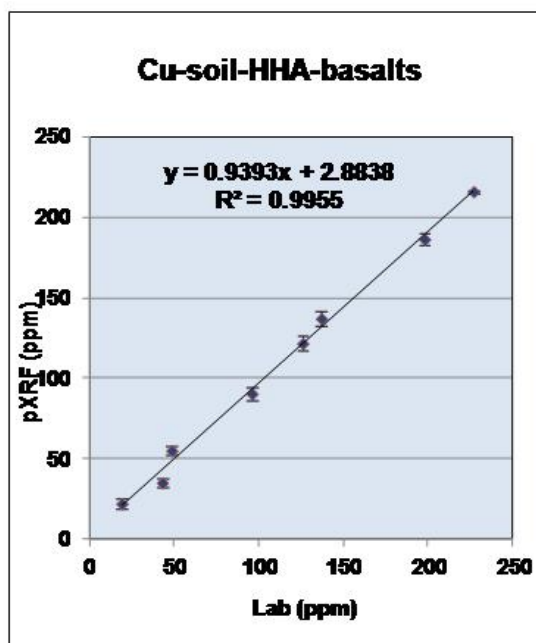Fig. 3.4. Cu in granite by soil mode, HH-A.

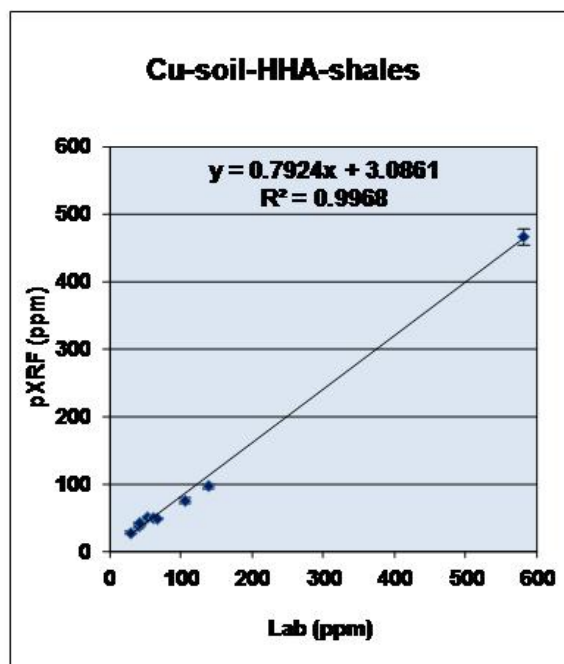Fig. 3.5. Cu in basalt by soil mode, HH-A.

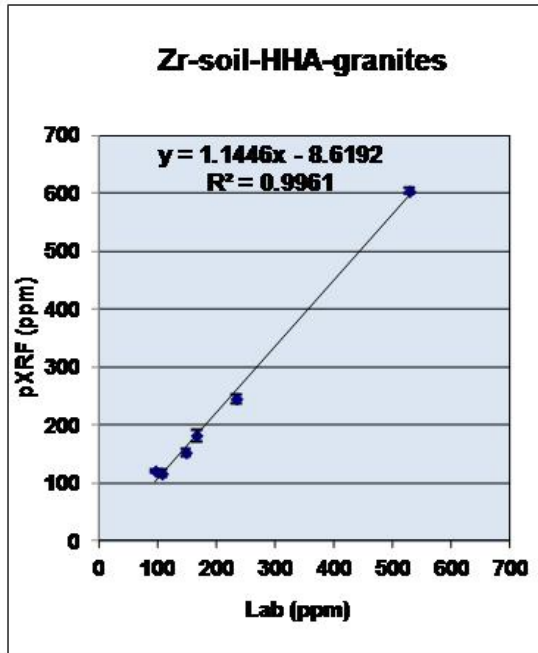Fig. 3.6. Cu in shale by soil mode, HH-A.
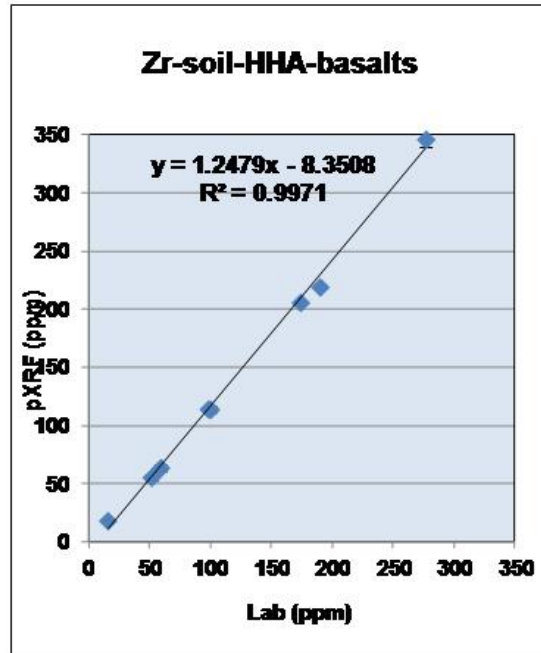
Fig. 3.7. Zr in granite by soil mode, HH-A.

Fig. 3.8. Zr in basalt by soil mode, HH-A.

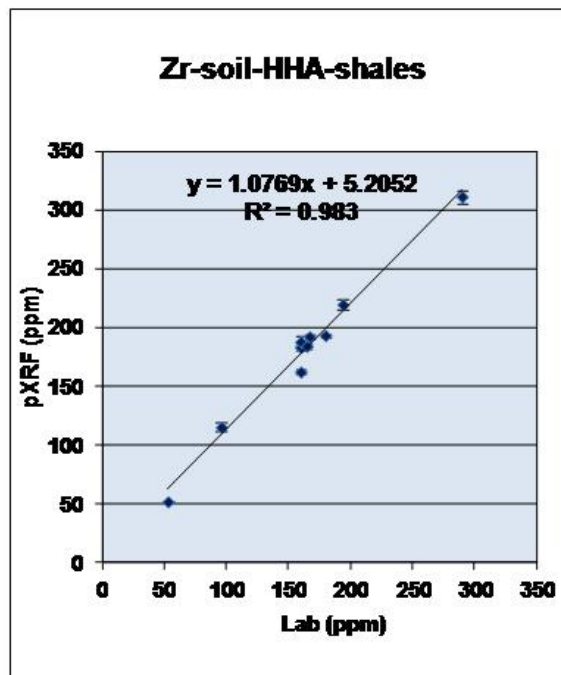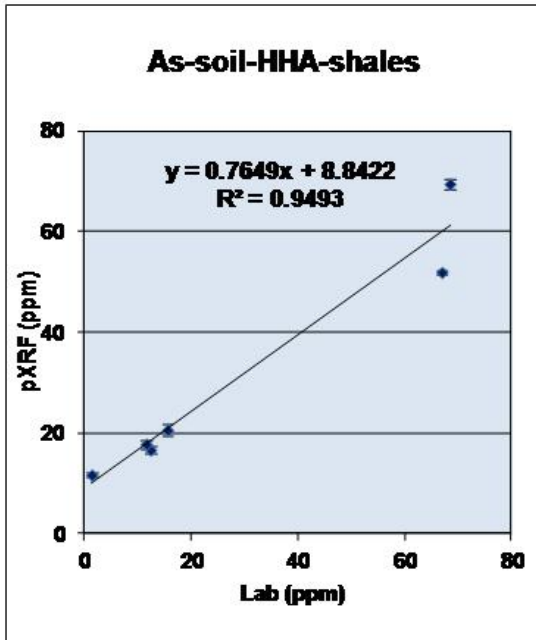Fig. 3.9. Zr in shale by soil mode, HH-A.

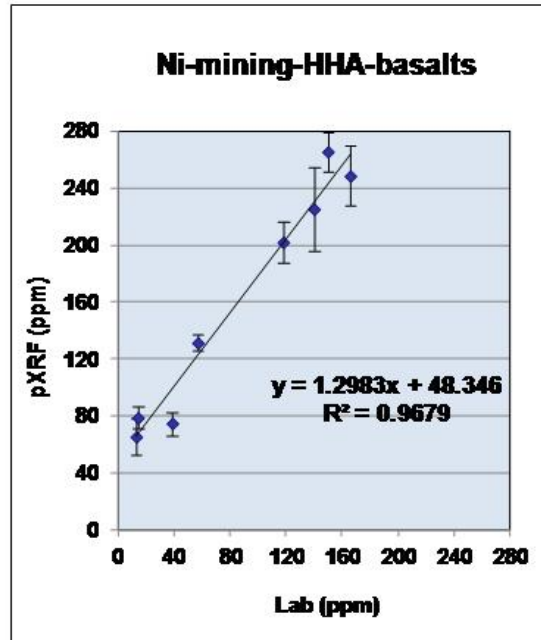**Fig. 3.10. As in shale by soil mode, HH-A.**

Fig. 3.11. Ni in basalt by mining mode, HH-A.

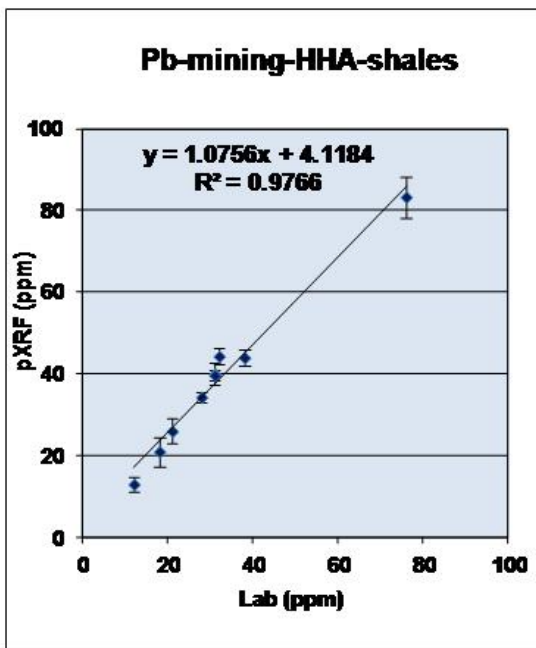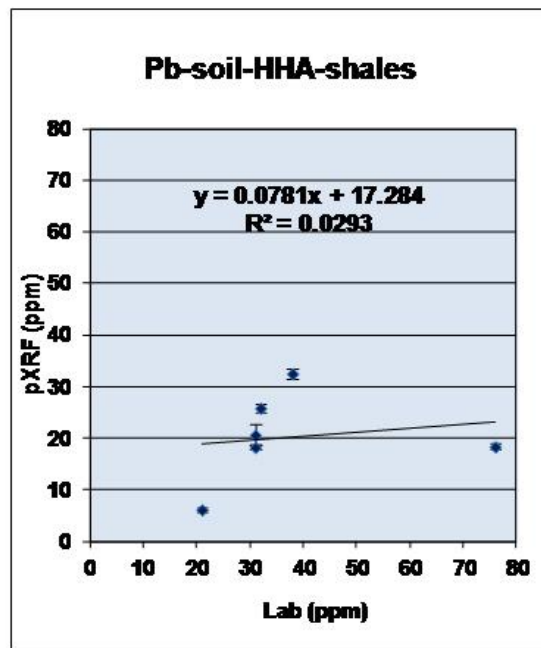**Fig. 3.12 Pb in shale by mining mode, HH-A.**

Fig. 3.13. Pb in shale, by soil mode, HH-A.

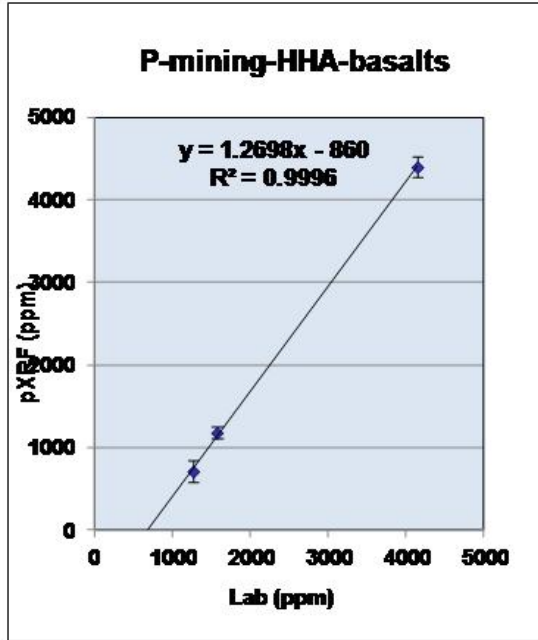**P-mining-HHA-basalts**

$y = 1.2698x - 860$
$R^2 = 0.9996$

pXRF (ppm) vs Lab (ppm)

Fig. 3.14. P in basalt by mining mode, HH-A.

Th-soil-HHA-granites

$y = 0.9833x + 4.0207$
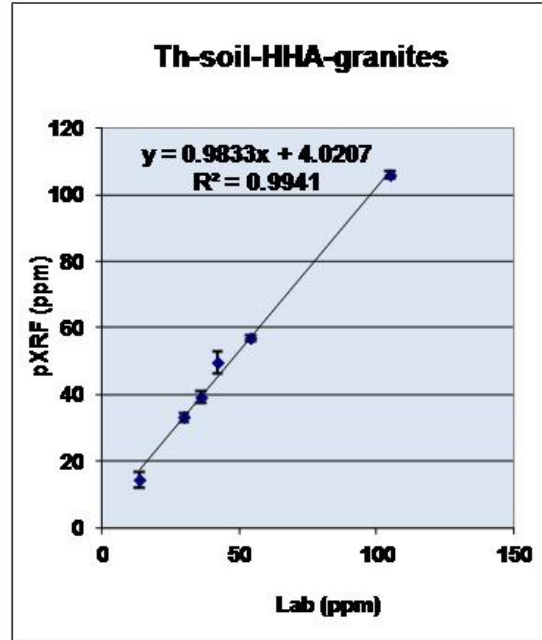$R^2 = 0.9941$

pXRF (ppm) vs Lab (ppm)

Fig. 3.15. Th in granite by soil mode, HH-A.

HH-C

The greater number of 'blue' elements in Tables 3.3a-3.3c compared to Tables 3.2a-3.2c might suggest that the performance of this instrument is inferior to that of HH-A but this is not the case. Rather, HH-C reports to lower values for elements such as Mg, Ni and P.

Elements which perform well using HH-C and show an r^2 value of between 0.95 and 1.00 in all their calibrations (except where specifically noted) include As (for the shales), Ca, Cr (basalts and shales), Cu (basalt and shales), Fe, K (granites and basalts), Ni (basalts), Pb (granites and shales), Rb, S (shales), Sr, Th (granites), Ti (granites and basalts), U (shales), V (granites), Y (granites and shales), Zn, and Zr.

Elements which show very similar trend-lines across the three calibrations, and hence could be satisfactorily determined using only one calibration (say within ~ 10-20% error), comprise Fe, Rb and Zr (e.g. Fe in Figs. 3.16-3.18). A larger suite of elements, which behave quite well across the calibrations and would probably agree to within ~ 20-30% if read using only one calibration, include Ca, Cu, K, Mn (though very poor r^2 values), Pb (granites and shales), Sr, Ti, and Zn (e.g. see Ti in Figs. 3.19-3.21). The calibrations for Al, Ba, Mg, Ni, P, Si and V all differ significantly in slope and intercepts across the three rock types.

As is the case with HH-A, Al and Si show quite different slopes across the rock types; the range for Al is 1.02 (basalts) to 1.32 (granites) and that for Si is 1.05 (granites) to 1.86 (basalts). The actual spread in concentrations within the granite and basalt groups is actually only a few percent, far from ideal for a calibration line.

Arsenic is well determined by HH-C in the basalts and shales, even at these fairly low concentrations of up to ~13 and 70 ppm, respectively (e.g. As in shales, Fig. 3.22). The mining mode appears to provide better analysis in terms of r^2 than the soil mode, for all three calibrations, for Ba (e.g. 0.96 vs 0.80 for granites).

Lanthanum and Ce suffer from a high background of ~200-400 ppm in the basalts and to a slightly lesser extent in the shales, La being more affected; the individual SDs of the pXRF analysis do not necessarily indicate a problem (e.g. 400±50 ppm). As illustrated in Figure 3.23 for Ce in shales and Figure 3.24 for La in granites, these elements are not well determined below several hundred ppm.

A slope of 6.0 and r^2 of 0.62 for Co in the soil mode for the shales indicate the interference of Fe on this element but even for the granite calibration it is obvious that Co at the tens of ppm level is not well determined in geological materials by pXRF (Fig. 3.25, Co in granites).

Table 3.3a. Summary of granite calibration results, HH-C.

	Granite calibration						
	Mining mode			Soil mode			
Element	Slope	Intercept	r2	Slope	Intercept	r2	<conc
Al	1.32	-2.09	0.68				8%
As	<LOD			Too low values			4 ppm
Ba	0.58	88.7	0.96	0.50	115.8	0.80	1500 ppm
Ca	0.93	-0.11	0.99	0.93	-0.14	0.99	2%
Ce	0.57	81.4	0.63				400 ppm
Co	<LOD			1.55	16.34	0.93	70 ppm
Cr	Too low values			Too low values			65 ppm
Cu				0.97	2.46	0.92	35 ppm
Fe	0.97	0.06	0.99	0.73	-0.06	0.99	3%
K	1.22	-0.11	0.98	0.87	0.69	0.95	4.5%
La	0.52	99	0.20				183 ppm%
Mg	0.58	-0.09	0.92				1.50%
Mo							
Mn	1.16	-237	0.68	0.89	-26	0.88	500 ppm
Ni	<LOD			0.40	17.6	0.12	34 ppm
P	1.87	25.4	0.95				1200 ppm
Pb	1.17	-4.4	0.94	1.03	-10.96	0.98	55 ppm
Rb	0.86	-1.91	1.00	0.93	-3.45	1.00	500 ppm
S	SDs too high			SDs too high			400 ppm
Si	1.05	19.01	0.72				36%
Sr				1.03	-3.95	1.00	600 ppm
Th	Too low values			0.97	2.01	1.00	110 ppm
Ti	0.89	0.01	0.98	0.78	0.02	0.96	0.40%
U	<LOD			2.01	8.12	0.72	20 ppm
V				1.46	7.84	0.96	70 ppm
W				0.85	21.23	1.00	500 ppm
Y	0.8	-0.88	0.99				90 ppm
Zn	0.96	-6.56	0.99	0.92	-2.3	0.99	100 ppm
Zr	0.77	-7.32	1.00	1.17	-10.26	1.00	550 ppm

Table 3.3b. Summary of basalt calibration results, HH-C.

	Basalt calibration						
	Mining mode			Soil mode			
Element	Slope	Intercept	r2	Slope	Intercept	r2	<conc
Al	1.02	2.85	0.25				9.20%
As		<LOD		1.00	0.83	0.93	13 ppm
Ba	0.8	193	0.96	0.71	286	0.86	680 ppm
Ca	0.99	-0.4	1.00				9.50%
Ce		High Bgd					
Co		<LOD			Very high SDs		52 ppm
Cr		High Bgd		0.82	-14.4	0.97	380 ppm
Cu				0.90	13.9	0.99	230 ppm
Fe	0.97	0.39	0.97				10%
K	1.33	-0.03	1.00				2%
La		Bgd of ~300 ppm					56 ppm
Mg	0.39	0.1	0.68				6%
Mo							
Mn	1.17	-136	0.94	1.47	-454	0.84	1550 ppm
Ni		<LOD		0.85	53.8	0.98	170 ppm
P	1.81	-240	0.95				4100 ppm
Pb		<LOD			<LOD		14 ppm
Rb		<LOD		0.94	-0.89	0.99	50 ppm
S		<LOD			<LOD		410 ppm
Si	1.86	-2.29	0.90				25%
Sr				1.06	-9.43	1.00	1100 ppm
Th		Too low values			<LOD		6 ppm
Ti	1.03	-0.11	0.99	0.89	-0.06	0.99	1.70%
U		<LOD			Too low values		2 ppm
V				0.64	86.7	0.86	600 ppm
W							
Y		Too low values					40 ppm
Zn				0.85	12.3	0.95	150 ppm
Zr				1.25	-9.88	1.00	270 ppm

Table 3.3c. Summary of shale calibration results, HH-C.

Element	Mining mode			Soil mode			<conc
	Slope	Intercept	r2	Slope	Intercept	r2	
Al	1.19	0.67	0.72				10%
As	1.00	3.26	0.98	0.84	0.09	0.99	70 ppm
Ba	0.34	220	0.32	0.13	269	0.04	600 ppm
Ca	1.08	-0.1	1.00	1.29	-0.33	0.96	7.50%
Ce	0.75	114	0.70				600 ppm
Co		<LOD		5.95	-37.6	0.62	55 ppm
Cr	1.12	104	0.11	0.64	40	0.07	100 ppm
Cu	0.90	-15.3	1.00	0.77	8.48	1.00	580 ppm
Fe	0.91	0.44	0.99	1.14	-1.42	1.00	16%
K	1.15	0.32	0.91	0.92	0.55	0.92	3.50%
La	0.89	135	0.45				287 ppm%
Mg	0.36	0.22	0.53				2.70%
Mo				1.23	-0.53	1.00	135 ppm
Mn	1.23	-140	0.76	0.91	66.2	0.70	850 ppm
Ni		<LOD		0.55	27.6	0.56	180 ppm
P	1.06	246	0.63				1430 ppm
Pb	0.92	-0.05	0.96	1.06	-12.2	0.99	80 ppm
Rb	0.85	-2.29	0.99	0.93	-2.85	0.99	200 ppm
S	1.15	-0.01	1.00	0.53	0.01	1.00	5.40%
Si	1.40	8.66	0.97				30%
Sr				0.87	13.8	0.99	420 ppm
Th		Too low values		0.88	0.46	0.92	13 ppm
Ti	1.06	-0.06	0.85	1.07	-0.06	0.72	0.45%
U		<LOD		1.1	9.44	1.00	49 ppm
V	1.03	76.3	0.63	1.04	27.2	0.83	160 ppm
W							
Y	0.98	-4.55	0.99				160 ppm
Zn	1.01	-11.4	1.00	0.97	-5.26	1.00	2200 ppm
Zr	0.72	2.38	0.97	1.1	5.71	0.99	290 ppm

Data for Cr in the granites and shales suggest that this element cannot be determined at levels below ~ 80-100 ppm but at higher concentrations in the basalts, up to ~ 400 ppm, the calibration is good (r^2 of 0.97).

Considering that Mg is the lightest and therefore worst element in general determined by pXRF, the basalt calibration at ~ 2-6% Mg is not too bad, though the slope is very low (0.39). Although the value of r^2 in the calibration for Mg in granites is better, at 0.92, the individual SDs are very high.

At only several ppm Mo cannot be determined in the suites of granite and basalt CRMs but it performs well in the shale calibration, from ~ 0.4 to 140 ppm (Fig. 3.26).

The calibrations for Ni in the basalts and shales differ markedly: that for the former rock type is excellent, with an r^2 of 0.98 and reasonable SDs but the goodness of fit for Ni in shales deteriorates to 0.56 over the same concentration range. The granites are too low in Ni (< 30 ppm) to be analysed for this element.

The calibrations for P in the granites and basalts are similar, with slopes of 1.8 and r^2 of 0.95, but that for the shales, at the same concentration range as P in granites (up to ~ 1200-1400 ppm), changes dramatically to have a slope of unity and a poor r^2 of only 0.63.

Analysis for Pb in granites and shales is excellent, even at these low ranges of 30-54 and 9-76 ppm, respectively. As for HH-A, Th is extremely well determined in the granites (r^2 of 1.00, at levels up to 110 ppm) and even adequate in the shales at concentrations as low as 5-13 ppm. In light of the low concentrations for U in these samples, this instrument performed well, especially for U in shales at concentrations up to 49 ppm (r^2 of 0.99, Fig. 3.27). The shales, containing up to 5.4% S, can be well calibrated using this instrument, with an r^2 of 1.00 and a slope of 1.15.

Although the calibrations for V vary across the rock types, the individual calibrations are well constrained, even for the granites that contain only up to ~70 ppm. The plots for V in shales using both modes demonstrate the greater noise in the mining mode data (Figs. 3.28 and 3.29); other examples of this include As in shales, Mn in granites and Pb in granites.

There is a significant background of ~ 10-60 ppm for W in the basalts and shales which negates analysis for this element in these samples; the granite calibration is rather misleading in that it is dominated by one high point (490 ppm).

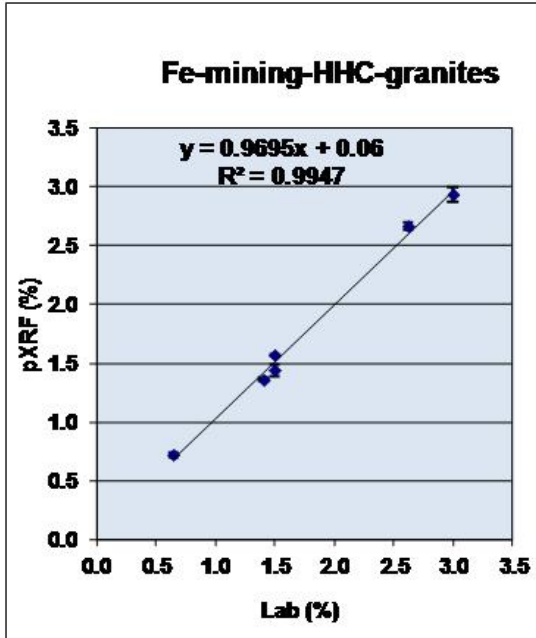Analysis for Y (mining mode) in the granites and shales is superb.

Fe-mining-HHC-granites

$y = 0.9695x + 0.06$
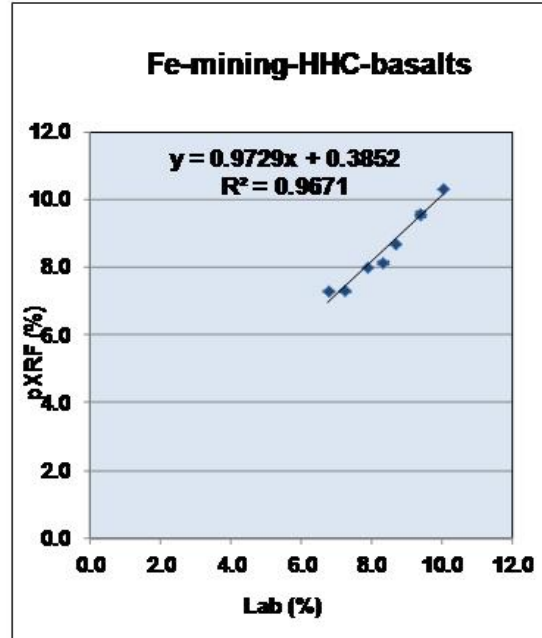$R^2 = 0.9947$

pXRF (%) vs Lab (%)

Fig. 3.16. Fe in granite by mining mode, HH-C.

Fe-mining-HHC-basalts

$y = 0.9729x + 0.3852$
$R^2 = 0.9671$

pXRF (%) vs Lab (%)

Fig. 3.17. Fe in basalt by mining mode, HH-C.

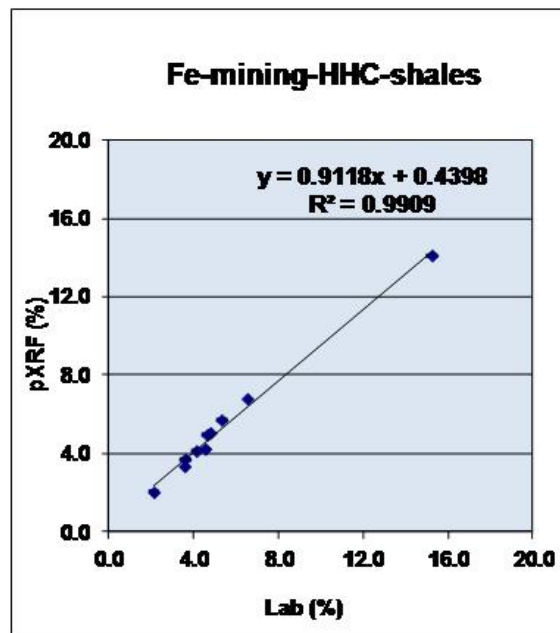### Fe-mining-HHC-shales

$y = 0.9118x + 0.4398$
$R^2 = 0.9909$

pXRF (%) vs Lab (%)

Fig. 3.18. Fe in shale by mining mode, HH-C.
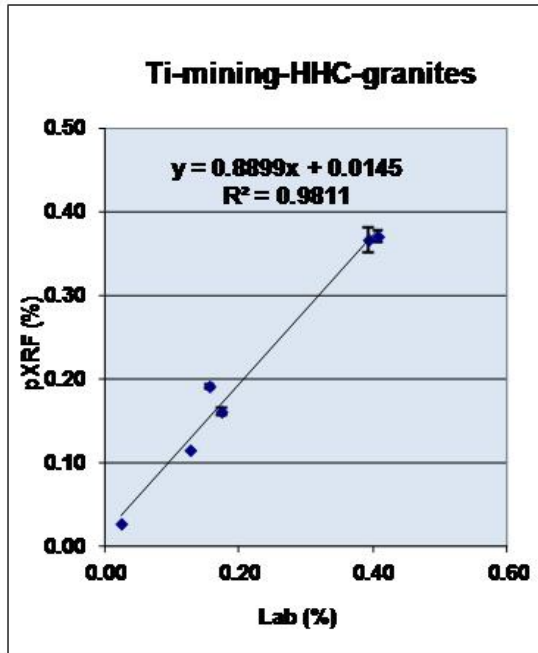
Fig. 3.19. Ti in granite by mining mode, HH-C.
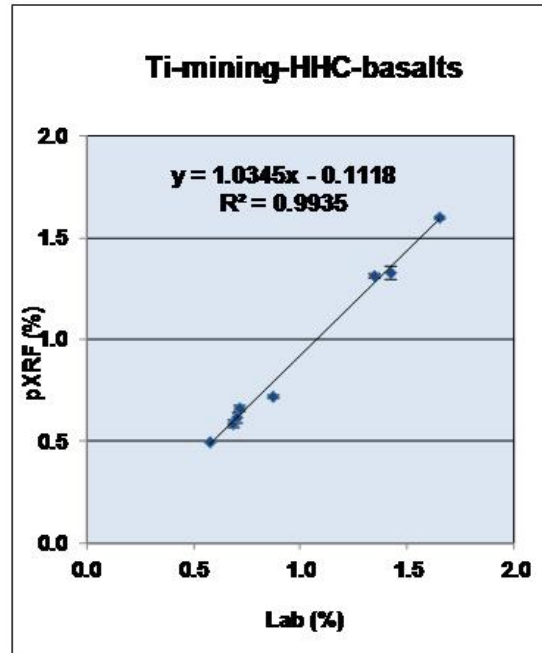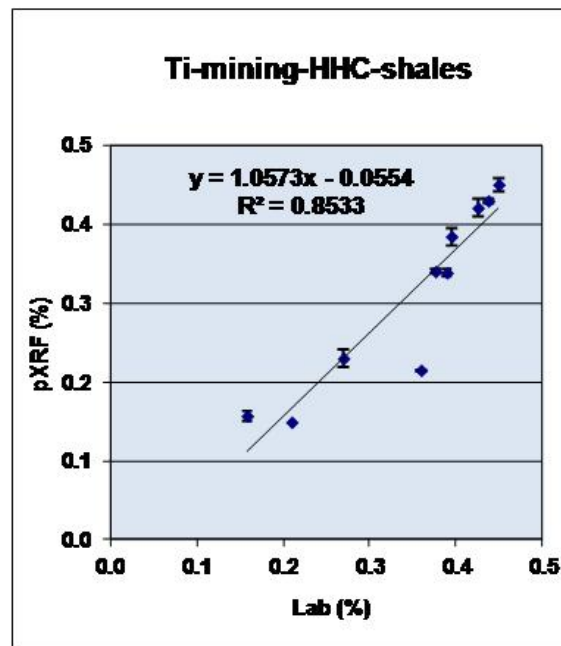

Fig. 3.20. Ti in basalt by mining mode, HH-C.

Fig. 3.21. Ti in shale by mining mode, HH-C.
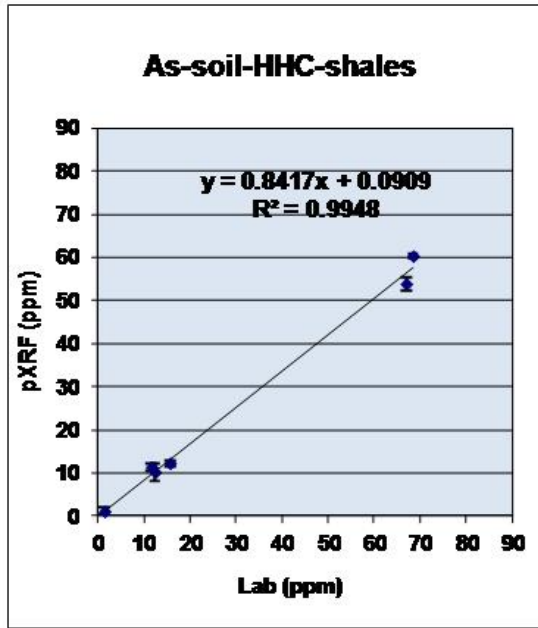
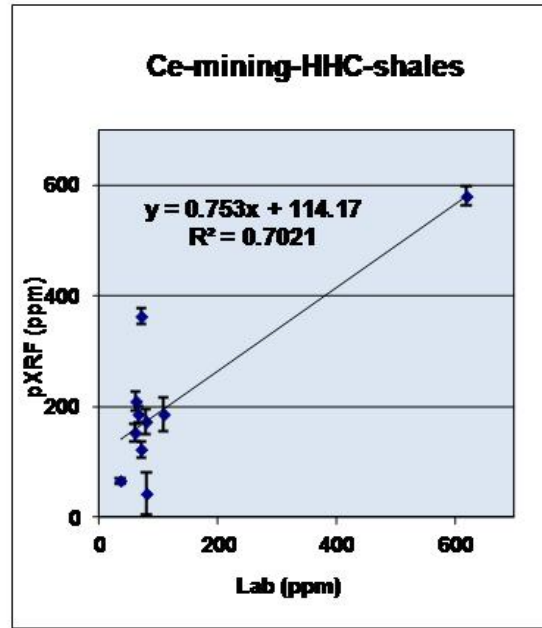**Fig. 3.22. As in shale by soil mode, HH-C.**

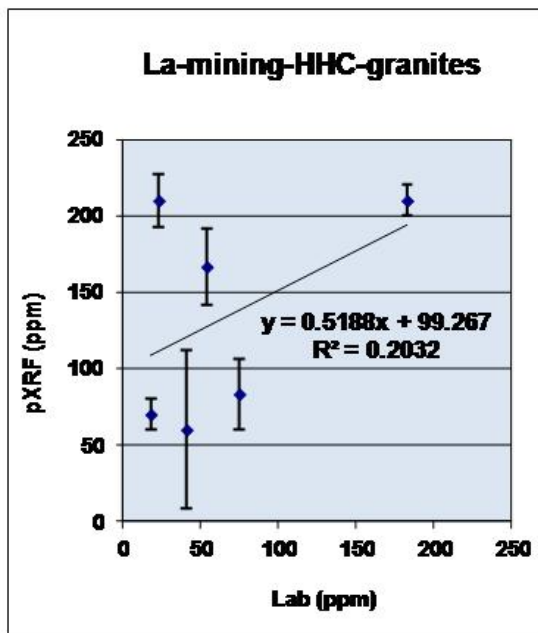**Fig. 3.23. Ce in shale by mining mode, HH-C.**

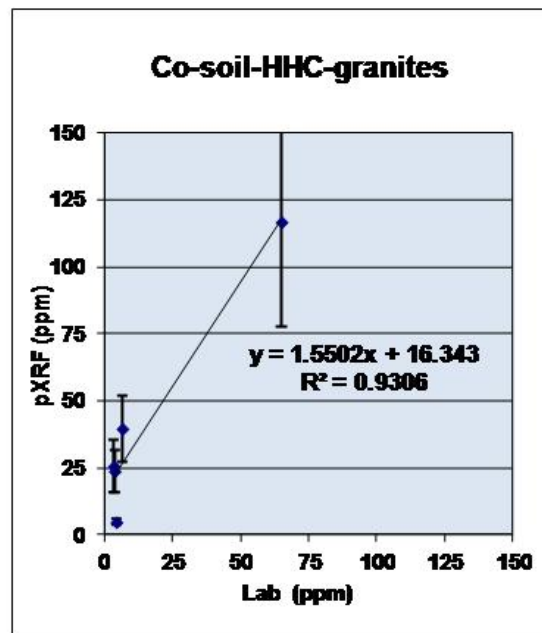**Fig. 3.24. La in granite by mining mode, HH-C.**

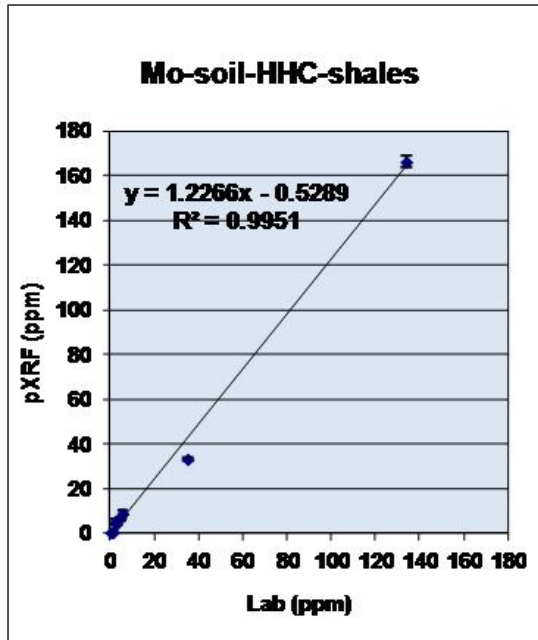**Fig. 3.25. Co in granite by soil mode, HH-C.**
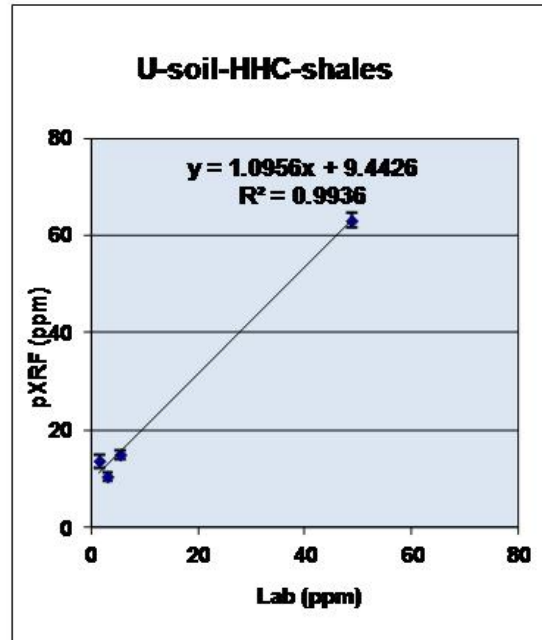
Fig. 3.26. Mo in shale by soil mode, HH-C.

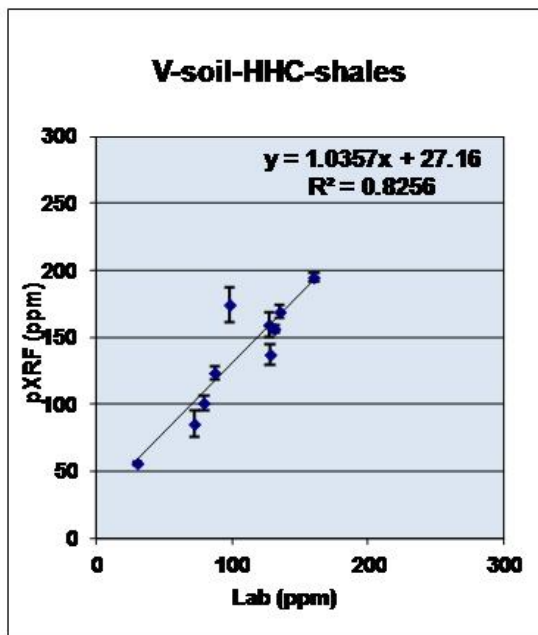**Fig. 3.27. U in shale by soil mode, HH-C.**

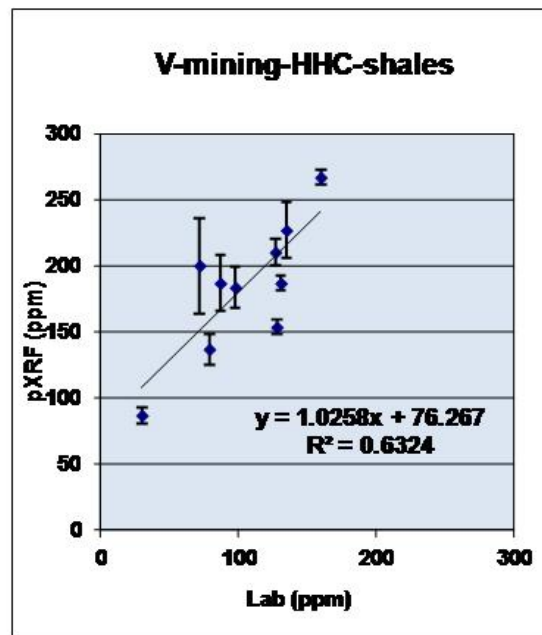
Fig. 3.28. V in shale by soil mode, HH-C.

Fig. 3.29. V in shale by mining mode, HH-C.

Summary of rock calibrations

- Elements which perform very well (r^2 value of 0.95-1.00) in their calibrations (in all three rock types unless specifically noted) include: *by HH-A and HH-C*, Ca, Cr (in basalts and shales), Cu (in basalt and shales), Fe, K (except in shales by HH-C), Ni (in basalts), Pb (in shales and granites), Rb, S (in shales), Sr, Th (in granites), Ti (in granites and basalts), Y (except in basalts by HH-C), Zn and Zr; *by HH-A*, Nb; by *HH-C*, As (in shales), Ni (basalts), U (shales), and V (granites). Some elements are particularly impressive in their calibration at low levels, such as, in the soil mode: Y and Nb at < 40 ppm in basalts and granites, by HH-A (r^2 of 0.98); As at < 70 ppm in shales by HH-A (r^2 of 0.95); Mo at < 135 ppm in shales by HH-C (r^2 of 1.00); and Th at < 13 ppm by HH-C in shales (r^2 of 0.92).
- Users must compare the two modes for their own samples prior to deciding upon which one to employ. Simply making a decision based on concentration (e.g. soil mode for trace and minor elements and mining for majors) is unwise. Results even at low levels by the mining mode can be superior (e.g. Pb in shales (HH-A), Ni in basalts and shales (HH-A), and Ba in all three sample types (HH-C). However, high backgrounds are evident in the mining mode for Ag, Bi, Cd, Sb and Sn using HH-A, and for Ce and La using HH-C. Where there are likely to be spectral interferences, as in the effect of Fe on Co (in shales, HH-A), the mining mode can report highly erroneous results whereas those using soil mode can be acceptable.
- *Using HH-A*, elements which show very similar trend-lines across the three calibrations, and hence could be satisfactorily determined using only one calibration (say within ~ 10-20% error), comprise Ca, Rb and Ti; elements with ~ 20-30% error if read using only one calibration, include Cu, Fe, K, Mn, Nb, Pb (in granites and shales), Sr, Y, Zn and Zr. *Using HH-C*, elements with a probable error of 10-20% determined across calibrations include Fe, Rb and Zr and those within 20-30% error comprise Ca, Cu, K, Mn (though very poor r^2 values), Pb (in granites and shales), Sr, Ti, and Zn. However, the elements showing highly significant differences (slope, intercept) in calibration across the rock types by one or both instruments comprise Al, Ba, Cr, Mg, Ni, P, Si and V. Thus, calibration for each of these sample types is absolutely necessary, suggesting this is mandatory for other rock matrices.

MATRIX CALIBRATIONS (ORES)

Paul Hamlyn of ORE Research and Exploration Pty Ltd in Australia kindly provided us with five series of their ore standards (as fine powders) to test. These CRMs are listed in Table 3.4.

Table 3.4. Ore standards from ORE Research and Exploration ('OREAS')

Ni laterites	Ni ultramafics	Cu SEDEX	Zn-Pb-Ag SEDEX	U series
183	70b	160	131a	120
187	72b	161	132a	121
189	74b	162	133a	122
192	75b	163	134a	123
194	76b	164		124
	77b	165		
		166		

Ni laterites: from Anglo American's Codemin Nickel Mine located in the state of Goiás, Brazil;
Ni ultramafics: from Xstrata Nickel's Prospero and Tapinos nickel mines, Western Australia; typical komatiite-associated, massive sulphide deposit representing an in-situ accumulation of massive and semi-massive primary magmatic Ni-Fe sulphides with minor by-products including Cu, Co and PGEs.
Cu SEDEX: from Xstrata's Mt Isa, northwest Queensland, Australia; ore is hosted by brecciated siliceous and dolomitic rock masses within the Urquhart Shale comprising complex and dissociated veins with chalcopyrite, pyrite and pyrrhotite with grades of 3-4% Cu.
Zn-Pb-Ag SEDEX: from Xstrata's Black Star and George Fisher orebodies, Mt Isa; sediment- hosted 'SEDEX' Zn-Pb-Ag deposits located within the Urquart Shale Formation, composed predominantly of carbonate siltstones, mudstones and shales.
U series: from Mantra Resources' Nyota Prospect, Tanzania; supergene mineralization, hosted in sandstone.

As with the rock CRMs, these ore powders were analysed three times each on the HH-A and HH-C units. The data files, together with all relevant plots (those for which there are recommended values) of results versus recommended values (RV), are provided in the Appendix. Tables 3.5a-e summarise the calibration data using HH-A for the Ni laterites, Ni ultramafics, Cu SEDEX, Zn-Pb-Ag SEDEX and U series, respectively; similarly Tables 3.6a-e provide such information for HH-C. The discussion of results here focuses not on the differences in calibrations across ore types (as one clearly would not attempt to use these calibrations interchangeably!) but rather on the individual calibrations themselves.

Table 3.5a. Summary of Ni laterite calibration results, HH-A.

	Laterite calibration						
	Mining mode			Soil mode			
Element	Slope	Intercept	r2	Slope	Intercept	r2	<conc
Ag							
Al	0.73	-0.2	0.97				1.50%
As							
Ca		Most <LOD		1.46	636	0.93	5100 ppm
Cd							
Co	1.03	432	0.95	0.12	31.5	0.94	640 ppm
Cr	0.92	0.03	0.99	2.14	-0.46	0.99	6800 ppm
Cu							
Fe	1.03	0.14	1.00				13.60%
K							
Mg	1.33	-0.95	0.95				16.50%
Mn	1.04	137	1.00	2.26	-785	0.99	2800 ppm
Nb							
Ni	1.12	0.05	1.00	1.6	-0.19	1.00	2.10%
Pb							
Rb							
S							
Sb							
Si	0.91	4.02	0.84				21.80%
Sr							
Th							
Ti		Mostly <LOD		4.14	344	0.91	215 ppm
U							
V							
W							
Y							
Zn				0.75	20.8	0.96	200 ppm
Zr							

Table 3.5b. Summary of ultramafic calibration results, HH-A.

	Mining mode			Soil mode			
Element	**Slope**	**Intercept**	**r2**	**Slope**	**Intercept**	**r2**	**<conc**
Ag							
Al	0.95	0.14	0.99				4.80%
As				1.01	-53.2	1.00	2100 ppm
Ca		No spread					
Cd							
Co	1.1	404	0.98	0.21	0.57	0.99	1600 ppm
Cr	1.41	-219	0.96	1.18	197	0.35	1250 ppm
Cu				1.12	-60.5	0.99	2300 ppm
Fe	0.87	1.48	1.00				29%
K	1.36	-0.47	0.99	0.98	0.32	0.51	1.10%
Mg	1.89	-5.13	1.00				13.50%
Mn	1.43	-393	0.94	1.23	352	0.11	1150 ppm
Nb							
Ni	0.97	0.18	1.00	1.94	-0.74	0.99	11.20%
Pb	1.03	2.49	0.95		<LOD		58 ppm
Rb				0.56	10.3	0.38	23 ppm
S	0.83	0.68	0.99				22.20%
Sb							
Si	1.15	-0.42	1.00				24%
Sr				1.21	-12	0.99	61 ppm
Th							
Ti	1.48	-0.05	0.99				0.21%
U							
V		Mostly <LOD		0.45	78.1	0.02	77 ppm
W							
Y				0.96	0.02	0.96	15 ppm
Zn				1.31	-39.3	0.99	200 ppm
Zr				1.19	-3.52	0.99	48 ppm

Table 3.5c. Summary of Cu SEDEX calibration results, HH-A.

	Cu SEDEX calibration						
	Mining mode			**Soil mode**			
Element	**Slope**	**Intercept**	**r2**	**Slope**	**Intercept**	**r2**	**<conc**
Ag				1.02	8.9	0.83	12 ppm
Al	1.03	-0.06	0.98				2.60%
As							
Ca		Mostly <LOD		1.82	-0.18	1.00	9.40%
Cd							
Co	0.92	331	1.00	Very suppressed signal			2500 ppm
Cr							
Cu	1.01	0.07	1.00	1.27	-0.35	0.99	8.80%
Fe	0.92	0.36	1.00				11.50%
K							
Mg							
Mn							
Nb							
Ni							
Pb				0.93	-10.8	0.98	460 ppm
Rb							
S	0.97	-0.08	0.99				11.30%
Sb							
Si	0.98	3.2	0.97				41.50%
Sr							
Th							
Ti							
U							
V							
W							
Y							
Zn	*1.09*	*0.01*	*0.97*		<LOD		102 ppm
Zr							

Italics: Misleading as not all points plotted

Table 3.5d. Summary of Zn-Pb-Ag SEDEX calibration results, HH-A.

	Zn-Pb-Ag calibration						
	Mining mode			Soil mode			
Element	Slope	Intercept	r2	Slope	Intercept	r2	<conc
Ag				1.81	-46.6	0.99	200 ppm
Al	1.01	0.5	0.98				4.70%
As							
Ca	1.12	-0.19	0.99				5.60%
Cd				2.06	-139	0.98	550
Co		<LOD		0.61	27.8	0.74	100 ppm
Cr							
Cu	0.82	2.11	0.99	2.11	-261	1.00	1300 ppm
Fe	0.79	1.2	1.00				12.30%
K							
Mg							
Mn							
Nb							
Ni							
Pb	0.91	0.45	1.00	1.21	-0.04	1.00	13.00%
Rb							
S	1	0.02	1.00				19.40%
Sb				1.83	10.5	0.65	175
Si	1.04	1.87	1.00				21%
Sr							
Th							
Ti							
U							
V							
W							
Y							
Zn	0.88	0.66	1.00	1.04	1.87	1.00	17.50%
Zr							

Table 3.5e. Summary of uranium series calibration results, HH-A.

	Uranium calibration						
	Mining mode			Soil mode			
Element	Slope	Intercept	r2	Slope	Intercept	r2	<conc
Ag							
Al							
As							
Ca				1.11	-579	0.92	990 ppm
Cd							
Co							
Cr							
Cu							
Fe							
K							
Mg							
Mn							
Nb							
Ni							
Pb							
Rb							
S							
Sb							
Si							
Sr				1.01	-0.77	1.00	190 ppm
Th							
Ti							
U				1.04	1.23	1.00	1850 ppm
V							
W							
Y							
Zn							
Zr							

Table 3.6a. Summary of Ni laterite calibration results, HH-C.

	Laterite calibration						
	Mining mode			**Soil mode**			
Element	**Slope**	**Intercept**	**r2**	**Slope**	**Intercept**	**r2**	**<conc**
Ag							
Al	1.15	-0.15	1.00				1.50%
As							
Ba							
Ca	0.97	-291	0.99	1.18	-1230	0.99	5100 ppm
Cd							
Ce							
Co				0.85	140	0.74	640 ppm
Cr	0.79	377	0.95	0.92	813	0.97	6800 ppm
Cu							
Fe	1.16	-0.28	1.00				13.60%
K							
Mg	0.26	3.8	0.84				16.50%
Mn	1.26	-197	0.99	2.01	-852	0.97	2800 ppm
Nb							
Ni	0.95	0.01	1.00	0.87	-0.08	1.00	2.10%
Pb							
Rb							
S							
Sb							
Si	1.41	7.39	0.95				21.80%
Sr							
Th							
Ti				1.4	-88.6	0.93	215 ppm
U							
V							
W							
Y							
Zn				0.78	27.2	0.95	200 ppm
Zr							

Table 3.6b. Summary of ultramafic calibration results, HH-C.

	Ultramafic calibration						
	Mining mode			Soil mode			
Element	Slope	Intercept	r2	Slope	Intercept	r2	<conc
Ag							
Al	0.28	3.95	0.25				4.80%
As	1	-5.98	1.00	0.97	-49.5	1.00	2100 ppm
Ba	-0.13	417	0.02	-1.37	820	0.38	340 ppm
Ca							
Cd							
Ce		High background					43 ppm
Co	0.69	-154	0.99	2.25	-100	0.99	1600 ppm
Cr	0.51	735	0.83	1.29	-206	0.98	1250 ppm
Cu							2300 ppm
Fe	1.02	0.55	1.00				29%
K	1.28	-0.08	1.00				1.10%
Mg	0.32	3.6	0.80				13.50%
Mn	0.13	946	0.08				1150 ppm
Nb							
Ni	0.91	0.02	1.00	1.05	-0.39	0.99	11.20%
Pb				1.8	-21.3	1.00	58 ppm
Rb				0.53	10.7	0.47	23 ppm
S	1.18	0.79	0.99				22.20%
Sb							
Si	1.68	2.01	1.00				24%
Sr				0.7	20.8	0.96	61 ppm
Th							
Ti				1.09	-0.04	0.99	0.21%
U							
V				0.92	22.2	0.99	77 ppm
W							
Y	1.15	-4.32	0.96				15 ppm
Zn				1.56	-53	0.99	200 ppm
Zr				1.63	-38.9	0.96	48 ppm

Table 3.6c. Summary of Cu SEDEX calibration results, HH-C.

	Cu SEDEX calibration						
	Mining mode			**Soil mode**			
Element	**Slope**	**Intercept**	**r2**	**Slope**	**Intercept**	**r2**	**<conc**
Ag				3.77	-3.91	0.64	12 ppm
Al	1.12	0.77	0.83				2.60%
As							
Ba							
Ca	1.08	-0.05	1.00				9.40%
Cd							
Ce							
Co				2.27	-224	0.97	2500 ppm
Cr							
Cu	0.94	-0.02	1.00	1.22	-0.34	0.99	8.80%
Fe	1.06	-0.06	1.00				11.50%
K							
Mg	0.6	0.5	0.86				
Mn							
Nb							
Ni							
Pb	1.09	13.8	1.00	0.95	7.33	1.00	460 ppm
Rb							
S	1.24	0.04	1.00				11.30%
Sb							
Si	1.38	11.9	0.98				41.50%
Sr							
Th							
Ti							
U							
V							
W							
Y							
Zn	*0.9*	*0.4*	*0.90*	*0.72*	*-2.15*	*1.00*	102 ppm
Zr							

Italics: Misleading as not all points plotted

Table 3.6d. Summary of Zn-Pb-Ag SEDEX calibration results, HH-C.

	Zn-Pb-Ag calibration						
	Mining mode			**Soil mode**			
Element	**Slope**	**Intercept**	**r2**	**Slope**	**Intercept**	**r2**	**<conc**
Ag	1	-0.03	1.00	2.45	-31	0.99	200 ppm
Al	1.34	2.03	0.84				4.70%
As							
Ba	1.23	-47.3	0.95	4.97	-2615	0.91	1370 ppm
Ca	1.08	-1.27	0.94				5.60%
Cd	0.88	56.1	0.93	2.17	-86	0.99	550
Ce							
Co		<LOD			<LOD		100 ppm
Cr							
Cu	1.09	31	0.99	3.05	-430	0.97	1300 ppm
Fe	0.93	1.17	0.99				12.30%
K							
Mg							
Mn							
Nb							
Ni							
Pb	0.89	0.53	1.00	1.39	-0.77	1.00	13.00%
Rb							
S	1.23	0.99	1.00				19.40%
Sb							175
Si	1.85	2.28	1.00				21%
Sr							
Th							
Ti							
U							
V							
W							
Y							
Zn	0.91	0.39	1.00	2.62	-5.07	0.99	17.50%
Zr							

Table 3.6e. Summary of uranium series calibration results, HH-C.

| Element | Uranium calibration | | | | | | |
| | Mining mode | | | Soil mode | | | |
	Slope	Intercept	r2	Slope	Intercept	r2	<conc
Ag							
Al							
As							
Ba							
Ca	0.92	-295	0.93				990 ppm
Cd							
Ce							
Co							
Cr							
Cu							
Fe							
K							
Mg							
Mn							
Nb							
Ni							
Pb							
Rb							
S							
Sb							
Si							
Sr				0.41	73.2	0.99	190 ppm
Th							
Ti							
U	1.3	48.1	1.00	1.5	38.8	1.00	1850 ppm
V							
W							
Y							
Zn							
Zr							

HH-A
The goodness of fit for the elements Al, Co (mining mode), Cr, Fe, Mg, Mn, Ni and Zn in the laterite series is excellent, with r^2 values better than 0.95; intercepts can, however, be very large (e.g. 432 ppm for Co). The elements Co, Cr, Mn and Ni would be best calibrated using the mining mode; the slopes for Cr, Mn and Ni in the soil mode are high (2.1, 2.3 and 1.6, respectively) (Figs. 3.30 and 3.31, Ni by soil and mining modes, respectively). The response for Co, an element sandwiched between Fe and Ni in the Periodic Table and hence subject to a high degree of interference in this matrix, is severely suppressed in the soil mode, with a slope of only 0.12. There is about a factor of ten times difference between Co results by mining and soil modes. Although the individual SDs for Mg are high, the calibration is robust (Fig. 3.32, Mg). Given the drastically different chemistry of the ores from silicate rocks and soils etc used to generate factory calibrations, it is not surprising that large values in intercepts (e.g. for Ca, Si, Ti and Co) and deviations from unity in slope values (e.g. 4.1 for Ti in the soil mode) are encountered here.

The calibration lines for almost all elements determined in the ultramafic series are excellent, i.e. for Al, As, Co (mining), Cr (mining), Cu, Mg, Fe, K (mining), Mn (mining), Ni, S, Si, Sr, Ti (mining), Y, Zn and Zr. Cobalt in the soil mode suffers from severe suppression (slope of 0.20), as in the laterite calibration. Unlike the responses in the mining mode, those for Cr, K and Mn in the soil mode are extremely poor, with r^2 values between 0.1 and 0.5. Phosphorus reports in the thousands of ppm range (<LOD ~ 5100 ppm) whereas the RVs are in the 90-270 ppm range. The calibration for Rb, normally an excellent element by pXRF, is non-existent, with an r^2 value of only 0.38 (Fig. 3.33, Rb in soil mode). These are examples where Compton normalization, used to mitigate matrix effects, fails. Vanadium too cannot be determined at these levels (~ < 100 ppm) in this sample type. Although Pb is reported at levels <LOD in the soil mode, its determination in the mining mode, even at concentrations below ~ 60 ppm is very good (Fig. 3.34, Pb). Yttrium appears to be measured accurately at concentrations below 20 ppm in the soil mode.

Analysis of the Cu SEDEX suite for the elements Al, Ca, Co, Cu, Fe, Pb, S, and Si is excellent; values for goodness of fit are in the range 0.97-1.00 and SDs are very low. Silver can be determined at concentrations below 12 ppm (Fig. 3.35, Ag)! Although Cu *could* be determined using the soil mode, at these concentrations (up to ~ 9%) the mining mode is certainly superior. Zinc is affected by the high concentrations of Cu and can be determined using the soil mode only up to ~ 2% Cu; the signal is completely suppressed over 3% Cu (CRMs 165, 166). Zinc, present in the range 7-102 ppm, was reported as <LOD in the mining mode. Cobalt by the soil mode is again highly suppressed.

The elements Ag, Al, Ca, Cd, Cu, Fe, Pb, S, Si and Zn are very well determined in the suite of Zn-Pb-Ag sulphides, with r^2 values of 0.98-1.00 and good individual SDs. Cobalt is less suppressed in the soil mode than seen previously but the calibration (25-100 ppm) is very noisy, the r^2 being only 0.74. Goodness of fit (0.65) is also poor for Sb, present in the range 50-175 ppm. The interference of Pb on As (from Pb Lα 10.55 keV line) is well demonstrated here where pXRF (soil mode) reports As in the range 244-4142 ppm when

in fact the range is 91-218 ppm. Arsenic is reported as <LOD in the mining mode. Figure 3.36, a plot of As by pXRF versus Pb in these samples, shows this spectral interference clearly.

Unfortunately most of the elements in the U series of samples are present at very restricted ranges and therefore creating X-Y plots is negated. However, results using factory calibration for Co, Cr, Al, Fe, K, Mn, Nb, Rb, Si, Sr, Ti, U, Zn and Zr are reasonably close to the recommended values. Arsenic appears to be suppressed as results are low, at only 4-7 ppm whereas the actual concentrations range from 3 to 46 ppm; As can usually be measured quite well, in the absence of high Pb, at these levels. Results for Mo, present at 6.9-7.5 ppm in these samples, increases with increasing U concentration, from 7 through 11, 19, 27 and finally to 44 ppm. The U Lβ line at 17.22 keV is close to the Mo Kα line at 17.48 keV and therefore at concentrations of U up to 1845 ppm a spectral overlap ensues. Phosphorus appears to have a background of several hundred ppm in the soil mode (<LOD in the mining mode, RVs in the range 120-330 ppm). It is interesting that Rb, whose Kα line at 13.4 keV is very close to the U Lα line at 13.61 keV, is apparently unaffected but its concentration in these samples is much higher than that of Mo, at ~ 87 ppm.

HH-C
The goodness of fit for the elements Al, Ca, Cr, Fe, Mn, Ni, Si and Zn in the laterite series is excellent, with r^2 values better than 0.95. Although the slope for Co in the soil mode is not nearly as suppressed as it is for HH-A (0.85 vs 0.12), the individual SDs are so high that the goodness of fit falls to 0.74 (e.g. for CRM 189, Co is 361±102 ppm vs 68.3±1.8 pm by HH-A, RV is 326 ppm) (Fig. 3.37, Co). In contrast, the signal for Mg is very suppressed, generating a slope of only 0.26 but the SDs are certainly acceptable. Titanium (soil mode), present at levels of only 215 ppm or less, is well determined, with an r^2 value of 0.93 and a slope of 1.4 (cf slope of 4.1 by HH-A). Copper, next to Ni in the Periodic Table is present at ~ 20-40 ppm in the CRMs but, not surprisingly, cannot be determined in this matrix (reports as '1' in the mining mode and as negative numbers in the soil mode).

In the ultramafic series, elements that show excellent performance, with r^2 values better than 0.95 and reasonable slopes, include As, Co (mining mode slightly better than soil), Cr (soil mode), Fe, K, Ni, Pb, S, Si, Sr, Ti, Y, Zn and Zr. It is difficult to understand why Al behaves so badly, with a slope of 0.28 and very poor fit of 0.25. Barium, at concentrations of ~ 120-335 ppm, cannot be determined in this matrix and displays a negative slope in both the soil and mining modes. There is a large background of 200-500 ppm (reported in mining mode) for Ce in these samples where the actual concentrations are 27-43 ppm. Lanthanum has a similar background which also increases with ore concentration. A similar background, though not quite as high, is evident for these REEs in the other suites of ores but there are no recommended values for those samples. Calibration for Mg shows a poor fit of 0.80 with a low slope of only 0.32; that for Mn is even worse with a fit of 0.08 and slope of 0.13. It is interesting how the two instruments can perform so differently, these two elements being good examples. As is the case for HH-A, Rb cannot be determined in this suite of ultramafics (r^2 of 0.47, slope of 0.53)

where its concentration ranges from ~ 7 to 50 ppm. Vanadium, however, at levels of 34-77 ppm can be determined quite well even though the individual SDs are high (Fig. 3.38, V); the same is true for Y at concentrations below 16 ppm.

Elements that are well determined in the Cu SEDEX series comprise Ca, Co (steep slope of 2.27), Cu (mining mode preferred), Fe, Pb (both modes excellent), S, and Si. Although r^2 for Zn by the soil mode is 1.00, only the first four CRMs in this series are plotted; pXRF values for the other CRMs (2-9% Cu; 37-47 ppm Zn) are negative and noisy. This suppression is less severe in the mining mode and therefore this is the preferred mode in this sample type, but is effective only to ~ 3% Cu at these fairly low Zn levels. Although for Ag the range in concentration is extremely low (~ 1-12 ppm) and the SDs are significant, it does seem possible to distinguish, say, 12 ppm from 4 ppm. Not surprisingly, the fit for Mg is only 0.86 and the slope is 0.68.

In the suite of Zn-Pb-Ag sulphides, the elements Ag (mining mode preferred), Cd (soil mode), Cu (mining preferred), Fe, Pb (mining preferred), S, Si and Zn (mining preferred) behave extremely well, with values of r^2 of 0.98-1.00. Aluminium and Ca calibrations are noisier, with r^2 values of 0.84 and 0.94, respectively. Results for Co, present in the range 24-100 ppm, by the soil mode are highly negative and '1' by the mining mode (i.e. all <LOD; designation differs according to the user setting for results <LOD). The Pb interference on As was again evident in this suite: for example, CRM 134a (12.95% Pb) is reported as ~ 6400 ppm in the soil mode and 1455 ppm in the mining mode (cf actual value of 218 ppm As). The mining mode, however, reports the other three CRMs as <LOD, as should be the case with such interferences that cannot be handled by the software. Barium, at 850-1370 ppm, is well determined using the mining mode (r^2 of 0.95 and slope of 1.23) but not by the soil mode where the slope increases to 5.0.

In the U series, as mentioned previously, many of the elements are constant in their concentration, other than U of course. With increasing U concentration from 41 (CRM 120) to 1845 ppm (CRM 124), Al by pXRF shows a progressive decrease, from 6.1 through to 5.3% (RVs are 4.6% for all five samples) and Ba decreases from 660 through to 228 ppm whereas the RVs range from 973 to 1017 ppm. Some elements, whose concentrations in the five CRMs are more or less constant, show a significant drop (i.e. suppression) in concentration for the last or penultimate sample in the series (i.e. highest [U]) and these include Ce, Cr, Fe, K, La, Mn, Rb and Zr. Molybdenum, on the other hand, shows a progressive increase in concentration with U, from 8 to 68 ppm (actual range is 7.0-7.4 ppm), as discussed for HH-A. Again, As is severely suppressed, with reported values of 2.5-5.7 ppm (cf 2.6-46 ppm RVs). Phosphorous and Si are reading extremely high: P by pXRF is in the range 1450-2325 ppm compared to RVs of 120-330 ppm and Si is reported at 60-63% compared to RVs of 38%. Results for Ca, Ti, Sr, Ni, U, V, Y, Zn and Zr (except CRM 124) appear to be valid, except that recalibration is obviously needed for Ca, Ni, and V. Calibrations in both modes are excellent for U, with r^2 values of 1.0 and slopes of 1.0 in the soil mode and 1.3 in the mining mode.
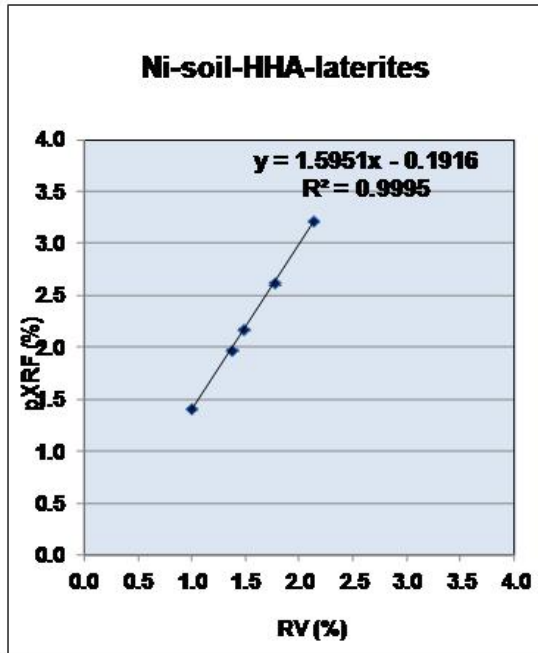
Fig. 3.30. Ni in laterite by soil mode, HH-A
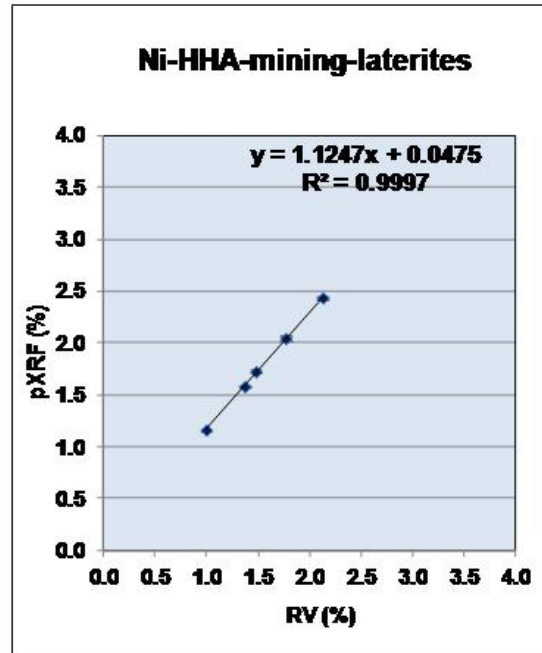
Fig. 3.31. Ni in laterite by mining mode, HH-A.
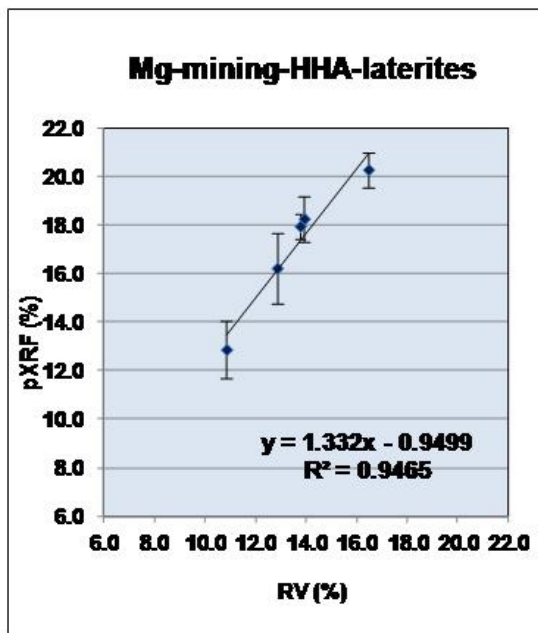
Fig. 3.32. Mg in laterite by mining mode, HH-A.
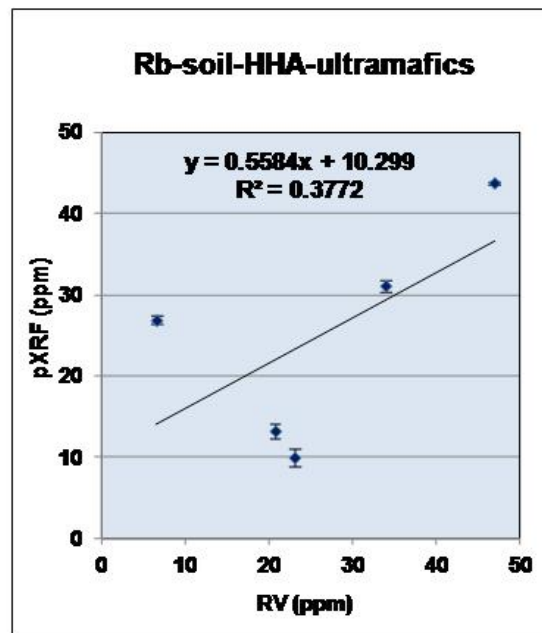
Fig. 3.33. Rb in ultramafics by soil mode, HH-A.

Pb-mining-HHA-ultramafics

$y = 1.0236x + 2.4951$
$R^2 = 0.9518$
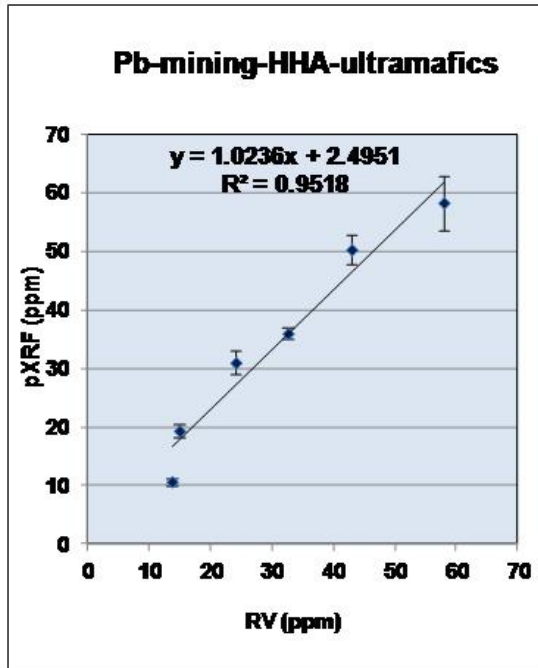
Fig. 3.34. Pb in ultramafics by mining mode, HH-A.

Ag-soil-HHA-Cu SEDEX

$y = 1.0238x + 8.9048$
$R^2 = 0.8254$
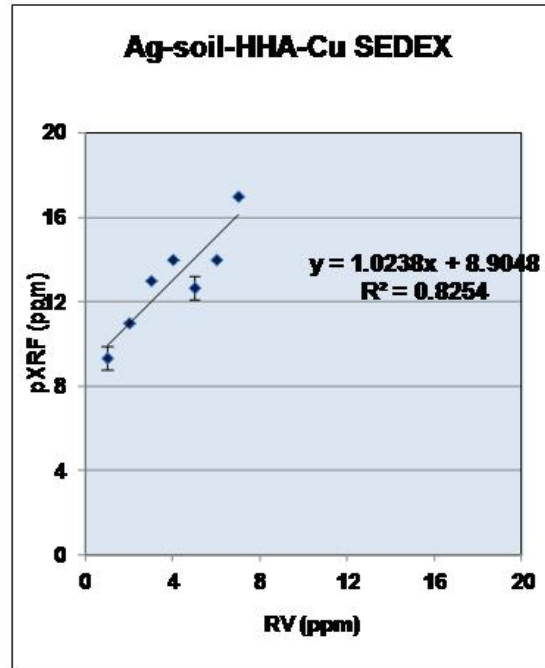
Fig. 3. 35. Ag in Cu-sedex suite by soil mode, HH-A.

As vs Pb in the Zn-Pb-Ag suite, HHA

$y = 353.27x - 480.76$
$R^2 = 0.9938$
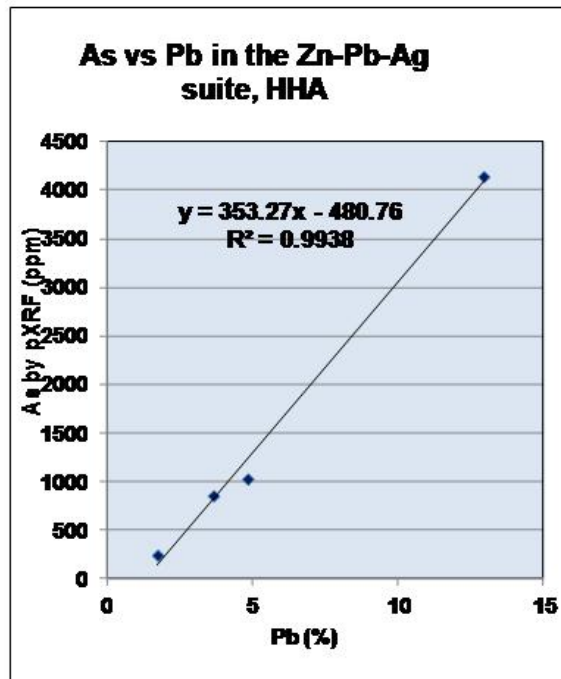
Fig. 3.36. As versus Pb in the Zn-Pb-Ag suite, HH-A.

Co-soil-HHC-laterites

$y = 0.8487x + 139.88$
$R^2 = 0.7357$

V-soil-HHC-ultramafics

$y = 0.9217x + 22.227$
$R^2 = 0.9939$
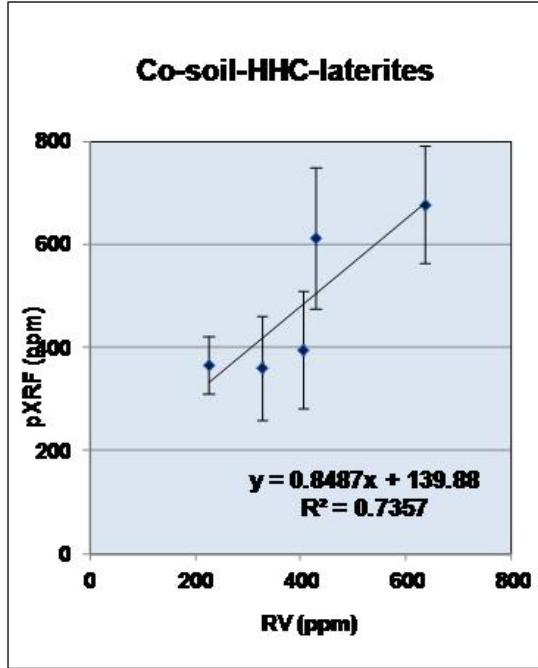
Fig. 3.37. Co in laterites by soil mode, HH-C.   **Fig. 3.38. V in ultramafics by soil mode, HH-C.**
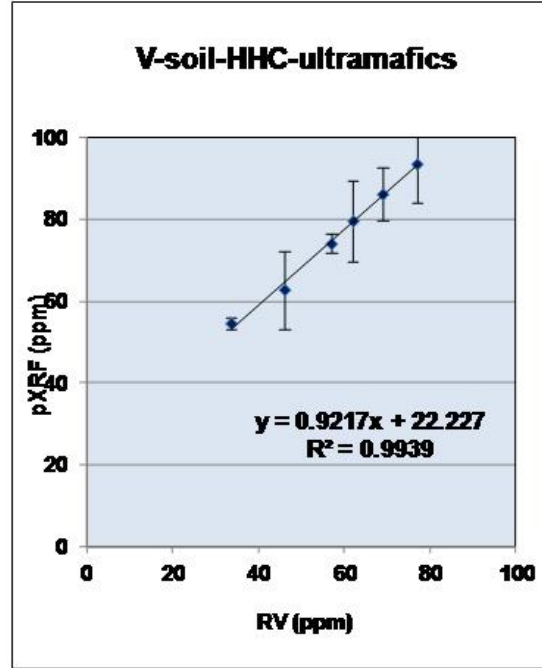
Summary of ore calibrations

- Factory calibrations for the mining and soil modes can show quite different results, especially for elements subject to interferences (e.g. high background) from the major ore element(s). Slopes and intercepts, not surprisingly, for these ores, can vary widely from 1 and 0, respectively, but goodness of fit in the plot of pXRF vs recommended value is usually very good.

- The Ni laterite series can be analysed well (r^2>0.9, often >0.95) for Al, Ca, Cr, Fe, Mn, Ni, and Zn. The HHs differ markedly in their performance for Co, Mg, Si and Ti. Cobalt and Cu suffer severely from Ni interference, though the mining mode can generate good results for Co using HH-A.

- Depending on the mode used, As, Co, Cr, Fe, K, Ni, Pb, S, Si, Sr, Ti, Y, Zn and Zr can be determined well in the Ni ultramafic series. Differences in performance between the two instruments are evident for Al (very poor by HH-C) and V (very poor by HH-A). Cobalt can be determined by the mining mode but in the soil mode is greatly suppressed using HH-A and enhanced using HH-C. Barium and Rb could not be determined in this matrix.

- In the Cu SEDEX series, Ca, Co, Cu, Fe, Pb, S, and Si are well determined by one or two modes. Aluminium performs well by HH-A but is noisy using HH-C. Zinc, Cu's neighbour in the Periodic Table, could be determined by HH-A using the soil mode, only up to ~ 2% Cu and by HH-C using the mining mode to ~ 3% Cu.

- In the suite of Zn-Pb-Ag sulphides, at least one mode reports well for the elements Ag, Al, Ba, Ca, Cd, Cu, Fe, Pb, S, Si and Zn. Calibration for Co in these samples (25-100 ppm) is possible using the soil mode on HH-A but the goodness of fit is only 0.74. The interference of Pb on As is demonstrated in the soil mode where CRM 134a, containing 218 ppm As and 13% Pb, is reported at 4140 ppm As by HH-A and 6400 ppm by HH-C.

- In the U series, HH-A performs well for Al, Co, Cr, Fe, K, Mn, Nb, Rb, Si, Sr, Ti, U, Zn and Zr. Aluminium and Ba show progressively lower results with increasing U concentrations by HH-C; other elements such as Ce, Cr, Fe, K, La, Mn, Rb and Zr seem to be affected/suppressed at U concentrations above ~ 1000-1500 ppm. Arsenic is reported by both instruments at 3-7 ppm whereas the range in RV values is 3-46 ppm. High concentrations of U create a positive interference on Mo; for example, CRM 124, at 1845 ppm U, is reported to contain 44 or 68 ppm Mo whereas its RV is 7.4 ppm.

- High backgrounds in the order of 200-500 ppm are present for Ce and La in many samples, the most severe being for the ultramafic series.

BAUXITE CALIBRATIONS

Three new bauxite standards in fine powder form were supplied to us by MMG for testing. We analysed them three times by pXRF, again moving the cup each time, and compared the results with those obtained by ALS Laboratories. As there are only three samples and little spread in many of the element concentrations, the results are compared mostly in tabular rather than graphic format (see Table 3.7 below).

Elements whose results agree well with those by ALS, either 'as is' or with adjustment through re-calibration comprise Al, As, Cu, Fe, Mn, Nb, Ni, Pb, Si (HH-C needs a major re-calibration, slope is 1.7), Sr, Th, Ti, Y and Zn. Standard deviations are by and large similar to those reported by ALS. Results for Nb at 30-46 ppm and Th at 32-41 ppm are particularly impressive.

Barium, with values of 44-73 ppm (JB1-JB3), cannot be determined in this matrix by HH-C: the plot of the soil mode results (96-56 ppm) would be highly negative and the slope in the mining mode is ~ 5 (35-203 ppm Ba).

Results for Ca (500-715 ppm) by HH-A (soil mode) and HH-C (mining mode) are quite noisy and while the agreement with ALS values is good for HH-C, re-calibration for HH-A is significant (Fig. 3.39, Ca).

Cadmium at 12-22 ppm is below detection by HH-A but at ~ 20 ppm it does seem to be measurable by HH-C but with high individuals pXRF SDs (~ 5 ppm).

The backgrounds in Ce and La evident for other calibrations is seen here, though not as significant as for others: the range in $LiBO_2$ fusion ICP-MS results is 231-248 ppm in Ce and 210-319 ppm in La but by HH-C these respective ranges are 399-418 and 413-450 ppm.

Cobalt, in the presence of 12-14% Fe, cannot be determined by HH-C in either soil or mining mode but results for JB2 and JB3 by HH-A agree well with those by fusion ICP-MS, at 55-57 and 47-48 ppm, respectively. However, JB1, at the greatest concentration of Fe at 14.8%, reports high at 72 ppm Co compared to the ALS value of 29 ppm. In the mining mode, however, the high background due to Fe is very apparent (~350-550 ppm).

Phosphorus, which does show a good spread in values (1077-3840 ppm), is well determined by both instruments (r^2 of 1.0) but they have large negative intercepts (e.g. Fig. 3.40, P).

Uranium, at 7.6-15.4 ppm, is below detection by HH-A but is well determined by HH-C at these low levels.

Vanadium, at 303-568 ppm, has a high positive bias by both instruments but the calibration is excellent (e.g. Fig. 3.41, V).

Table 3.7. Comparison of results for three bauxite standards analysed by pXRF using HH-A and HH-C and by ALS. Results for Al, Fe, Si, Ti in %, rest in ppm.

	ALS		HH-A		HH-C			ALS		HH-A		HH-C	
Element	Mean	SD	Mean	SD	Mean	SD	Element	Mean	SD	Mean	SD	Mean	SD
Al-JB1	25.42	0.11	22.76	0.45	25.23	0.51	Ni-JB1	191	1.5	175	11.0	185	9.4
Al-JB2	25.37	0.34	22.81	0.18	25.83	0.48	Ni-JB2	569	8.1	598	25.0	470	4.4
Al-JB3	26.38	0.21	22.93	0.10	26.15	0.24	Ni-JB3	821	19.7	813	24.7	633	17.2
As-JB1	68.7	4.0	105	2.6	59.8	3.8	P-JB1	1076	25.2	229	51.4	700	73.5
As-JB2	50.0	3.0	80.9	2.0	39.6	1.2	P-JB2	1964	43.6	1172	76.6	1921	63.9
As-JB3	26.7	3.5	59.2	1.8	22.2	1.3	P-JB3	3840	43.6	2781	27.8	3935	65.6
Ba-JB1	43.6	0.2			95.7	2.7	Pb-JB1	60.3	0.6	69.0	3.6	52.7	2.7
Ba-JB2	55.0	1.1			69.0	8.8	Pb-JB2	70.3	2.1	79.7	3.2	67.1	1.2
Ba-JB3	73.0	1.9			56.3	4.0	Pb-JB3	82.3	0.6	89.3	7.8	77.6	1.0
Ca-JB1	596	41.3	645	27.7	639	98.5	Si-JB1	0.67	0.02	0.63	0.02	1.22	0.02
Ca-JB2	500	0.0	288	76.0	497	55.9	Si-JB2	0.36	0.00	0.31	0.01	0.69	0.02
Ca-JB3	715	0.0	824	84.7	719	21.7	Si-JB3	0.09	0.00	0.07	0.01	0.24	0.02
Cd-JB1	11.7	0.5	<LOD		Too low		Sr-JB1	126	1.0	117	1.5	117	0.4
Cd-JB2	21.9	0.3	<LOD		16.3	2.0	Sr-JB2	171	1.4	162	2.3	170	2.1
Cd-JB3	19.5	0.9	<LOD		12.1	2.4	Sr-JB3	272	2.6	255	2.6	264	3.5
Ce-JB1	231	1.0			399	13.4	Th-JB1	31.5	0.2	29.7	4.2	31.8	0.9
Ce-JB2	283	6.5			417	42.0	Th-JB2	35.2	1.0	33.3	1.2	36.7	1.5
Ce-JB3	348	7.0			418	37.4	Th-JB3	41.0	0.3	39.3	2.1	41.5	2.0
Co-JB1	28.9	1.0	71.7	5.0	High -ve #s		Ti-JB1	1.49	0.01	1.55	0.01	1.61	0.03
Co-JB2	55.3	2.3	57.0	1.7			Ti-JB2	1.38	0.02	1.48	0.02	1.54	0.01
Co-JB3	47.4	0.6	48.3	4.5			Ti-JB3	1.40	0.01	1.47	0.02	1.55	0.01
Cr-JB1	680	10.0	1114	7.1	844	13.6	U-JB1	7.6	0.1	<LOD		9.1	2.7
Cr-JB2	667	15.3	1135	15.5	881	27.6	U-JB2	10.1	0.2	<LOD		14.7	1.4
Cr-JB3	587	5.8	1009	20.0	808	32.5	U-JB3	15.4	0.1	<LOD		19.5	2.1
Cu-JB1	45.7	0.6	49.3	2.1	52.6	8.3	V-JB1	568	3.5	737	42.9	720	38.7
Cu-JB2	88.3	2.1	88.7	4.9	93.6	6.1	V-JB2	435	11.2	652	11.5	620	10.8
Cu-JB3	134	1.5	125	1.5	133	3.2	V-JB3	303	1.5	568	1.7	507	6.9
Fe-JB1	14.78	0.04	14.89	0.10	16.98	0.13	Y-JB1	80.3	1.0	78.1	1.9	71.8	0.5
Fe-JB2	13.49	0.11	13.79	0.12	15.78	0.03	Y-JB2	403	3.5	416	1.5	361	2.7
Fe-JB3	12.43	0.15	12.42	0.05	14.41	0.08	Y-JB3	551	8.1	552	2.6	480	1.7
La-JB1	210	1.0			413	9.9	Zn-JB1	205	0.0	159	1.0	172	5.6
La-JB2	258	6.0			432	22.3	Zn-JB2	272	4.2	231	2.3	245	1.7
La-JB3	319	6.7			450	12.7	Zn-JB3	361	8.7	296	4.7	314	9.7
Mn-JB1	1626	0	1536	33	1730	35	Zr-JB1	479	5.0	565	20.6	571	10.4
Mn-JB2	3873	77	3801	92	4227	63	Zr-JB2	411	13.1	547	3.8	577	11.5
Mn-JB3	4802	155	4496	198	5009	154	Zr-JB3	252	2.1	567	4.4	582	4.6
Nb-JB1	46.0	0.3	42.9	0.7	41.8	2.1							
Nb-JB2	39.0	1.7	43.1	0.6	39.2	2.3							
Nb-JB3	30.0	0.7	46.5	2.2	42.3	1.4							

For HH-A, results for Al, Fe, Mn, Ni, P, Pb and Si were by the mining mode (soil mode for Ni, P, Pb was not as sensitive as the mining mode)

For HH-C, results for Al, Ca, Ce, Fe, La, Mn, P, Si, Ti and Y were by the mining mode

It is interesting that both instruments in both modes report Zr in the range 547-582 ppm for all three standards. However, the fusion ICP-MS result for JB3 differs in that it is much lower, at 252 ppm. This is puzzling.

Summary of bauxite calibrations

- With recalibration, the elements Al, As, Cu, Fe, Mn, Nb (superb), Ni, Pb, Si, Sr, Th, Ti, U (HH-C only), Y and Zn are well determined in three bauxite standards.
- The elements Ca, P and V can be determined reasonably well following recalibration but they can be noisy (Ca) or have large intercepts (P, negative; V, positive).
- One instrument (HH-A) can determine Co at the tens of ppm level in the presence of < 14% Fe.
- Barium, at < 75 ppm, cannot be determined in this matrix.
- Again, one should not assume the preferences of the soil mode for traces/minors and the mining mode for majors as for example, Ni, P and Pb proved to be better determined in the mining mode (HH-A).

57
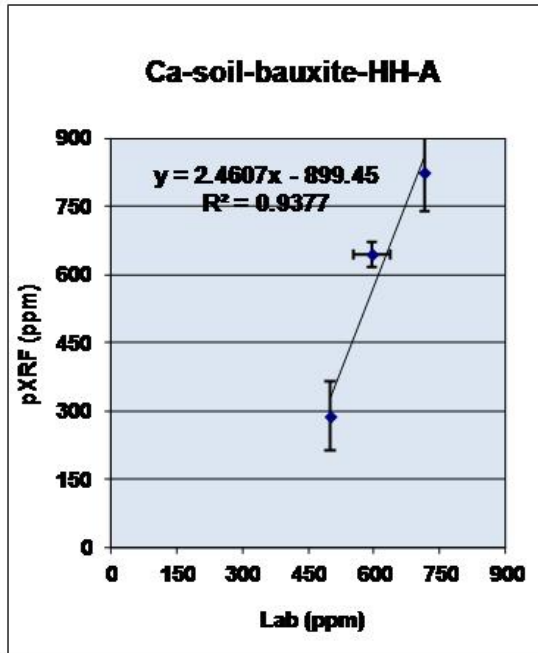
Fig. 3.39. Ca in bauxite by soil mode, HH-A.
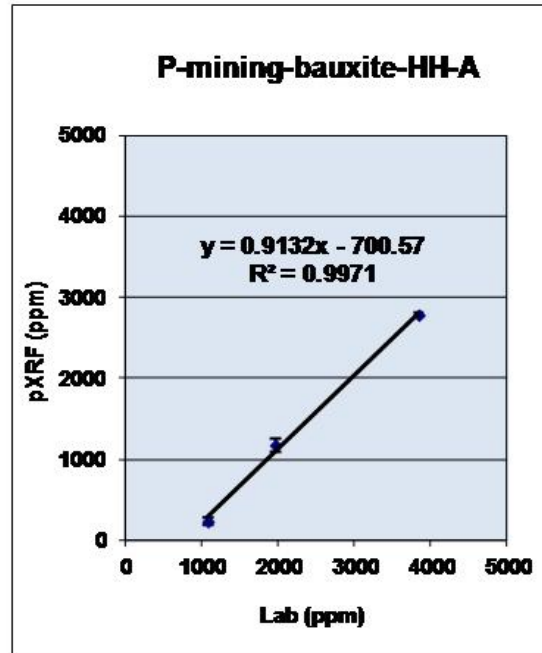
Fig. 3.40. P in bauxite by mining mode, HH-A.
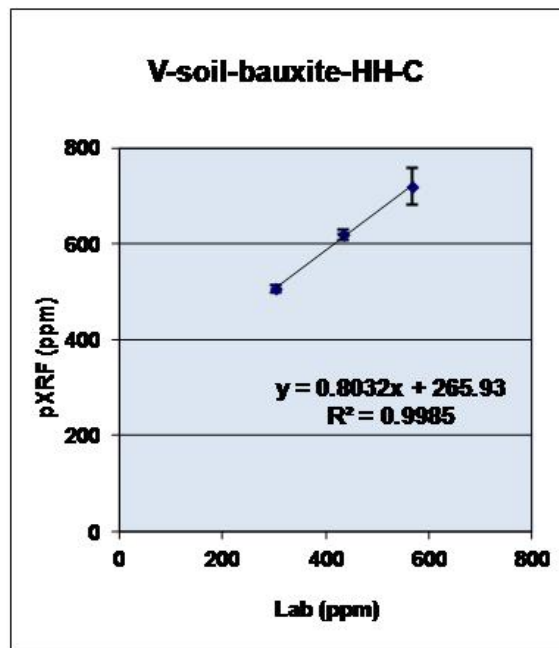
Fig. 3.41. V in bauxite by soil mode, HH-C.

4. HOW MANY MEASUREMENTS (SHOTS) PER SAMPLE?

Introduction

One of the experiments carried out on a suite of granodiorite rocks (see Section 5) was designed to help determine how many 'shots' (analyses) are required with the pXRF technique for samples of various types. Because each shot takes 2-3 minutes to complete on average (i.e. 20-30 shots/hour), the fewer shots the better from a cost point of view. There is obviously a big cost difference between situations where 1 or 2 shots are sufficient, versus a situation requiring 5-10 shots. For samples with noisy analytical data by pXRF, it may in some situations be more cost effective to do some sample preparation (e.g. grinding to a powder) before taking pXRF measurements, to control the variability.

How many shots (measurements) are needed to obtain a sufficiently precise estimate of the element content for the elements of interest? Clearly this depends also on how the data are to be used. In some situations, for example in a regional survey for exploration, the contrast between background levels and anomalous levels may be large enough that relatively imprecise data will do the job, where in other situations, anomalies may be much more subtle, and precise analytical data are essential.

The most frequently used measure of analytical precision in geochemistry is the RSD (relative standard deviation), simply defined as the standard deviation divided by the mean, and multiplied by 100 to give a percentage. Depending on the element, an RSD of 5-10% is usually good, even 20% acceptable, but greater than 30% often problematic. For a particular value of RSD, what is the relationship between the margin of error (deviation from the mean) and the number of measurements?

Data used as example

The granodiorite experiments were carried out here on several surface types: a smooth (cut) surface, a rough (broken) surface, a round (as on a core) surface, and a powdered sample. For most samples, the number of shots (n) was n=15 for smooth, n=10 for rough, n=10 for round, and n=3 for powdered—but these changed sometimes depending on circumstances. For each element (in both mining and soil modes of the pXRF), estimates of mean, standard deviation and RSD were calculated for each surface type, as illustrated in Table 4.1 for Fe in the mining mode by instrument HH-A. The independent lab value for each sample is also shown for comparison.

It is clear from Table 4.1 that the RSD values for Fe of powdered samples are excellent (always less than 2%), whereas the RSD values of smooth, rough and rounded surfaces are much greater, occasionally less than 20%, but mostly greater than 30%, and sometimes as high as 70%. How does RSD vary with number of shots? If we select a desired margin of error (defined as half the confidence interval about the mean) we need to determine the smallest number of shots, 'n', that

will ensure that the estimated mean is within the specified *margin of error*, at some level of confidence. For example, given a particular value of RSD, what is the minimum number of shots that will guarantee that the average measured value is within 10% of the actual mean? Or within 20% of the mean, and so on?

Table 4.1. RSD values in % for 20 granodiorite samples (Fe, mining mode, HH-A).

No	Powder	Smooth	Rough	Round
1	0.66	44.80	50.44	
2	0.26	28.95	21.30	
3	1.82	22.74	18.76	
4	1.46	56.06		
5	1.20	69.42	37.90	81.54
6	1.35	37.20	40.46	
7	1.76	45.60	32.63	
8	1.18	31.85	43.00	
9	0.58	69.68	75.48	
10	0.30	24.76	21.89	
11	1.02	34.03	34.45	
12	0.23	38.21		
13	0.59	18.74	55.48	22.53
14	0.68		44.07	41.41
15	0.57	20.55		17.48
16		36.44	41.68	
17		48.90	29.62	
18		12.66	20.10	
19		36.94	42.07	
20		35.24	25.82	

Methods of determining 'n'

Here we used two approaches, and compared them on actual samples. One is a simulation approach, using a Monte Carlo method, the other using a statistical formula. The Monte Carlo method makes no assumptions about the statistical distribution of the measurements, but requires a computer code to be run on a particular sample. The formula approach is much easier to compute a value of n, but makes some statistical assumptions. The comparison of results was to find out whether the easily applied formula could be safely used for data of this type.

Monte Carlo Approach

Table 4.2 shows the measured values of Ca in four samples of the granodiorite suite, with widely differing RSDs, ranging from less that 10% to over 40%. These are used to illustrate and compare results from the Monte Carlo and formula approach.

Table 4.2. Values for Ca for four samples (3 rough, 1 smooth surface) measured with 15 shots by HH-A in mining mode. The # sign indicates the sample number. The number of shots (n) is shown at the bottom for a desired margin of error of 15% of the mean, 19 times out of 20 from Equation (2).

Shot	Ca, %			
	#2, Rough	#3, Rough	#17, Rough	#7, Smooth
1	2.68	3.47	0.82	0.44
2	2.87	3.29	0.56	0.64
3	2.92	2.93	0.7	0.32
4	3.31	3.1	0.63	0.35
5	3.58	3.08	0.98	0.42
6	3.2	2.71	0.7	0.45
7	2.63	2.74	0.87	0.39
8	2.93	4.04	0.72	0.27
9	2.89	3.47	0.49	0.4
10	3.32	3.44	0.56	0.89
11	2.6	1.36	0.77	0.47
12	3.21	2.54	0.81	0.04
13	3.22	3.34	0.73	0.37
14	2.73	4.07	0.48	0.6
15	3.33	2.63	0.2	0.25
Mean	3.03	3.08	0.67	0.42
St. Dev	0.3	0.66	0.19	0.19
RSD,%	9.97	21.53	28.61	45.76
n (D=15%)	2	9	15	38

For example, consider the 15 values of Ca measured for sample #2 (rough). Can we get close enough to the mean (estimated from 15 shots) by taking a smaller number? We could use these measurements and select subgroups of differing size from them to estimate on average how much the 'test' estimate of mean differs from the mean of all 15, starting with taking groups of 2 out of the 15 measurements at random, computing the 'test' mean, and calculating the % difference from the 'true' mean. We can repeat this, say 1000 times, and select the 950th largest % difference obtained. This is like selecting coloured balls from a bag of 15, with replacement. We now have a good idea that 95% of the time we will be within this % difference if we take 2

measurement shots. Then we repeat the process for taking groups of 3 measurements at a time, obtain the 950th largest % difference from the 'true' mean; then groups of 4 measurements at a time, etc., up to taking all 15. Then we can plot the results on a graph, such as Figure 4.1 for sample #2.

We see that for this sample (#2 on a rough surface), we can get within a margin of error of about 10% (i.e +/- 10%) 95% of the time with n=4 shots. But if we want to be more stringent and get a margin of error of 5%, then we need n=15 shots. If we are happy with a 20% margin of error, then n=1 shot is enough.

For a situation where the RSD is a little over 20%, as for the second column of Table 4.2, a similar experiment results in the graph shown in Figure 4.2. Here n=3 shots give a margin of error of about 25%, and we need n=15 to get close to +/- 10%. Figures 4.3 and 4.4 show similar patterns, but for samples with progressively larger RSDs of about 28% and 45%. As one would expect, the larger the RSD, the greater the number of shots needed to obtain a selected margin of error. For the example with 45% RSD, about n=7 shots are needed to obtain a margin of error of about +/- 30%.

Formula Method

From these examples, it can be seen that the formula approach (blue line) is a close approximation to the Monte Carlo solution, possibly a little on the conservative side, because the red dots (Monte Carlo) are usually a little below the blue line (formula), indicating that the margin of error for a particular value of n is slightly better by the Monte Carlo experiment, than by the formula. But the results are close, and give confidence that, despite the assumptions, the formula approach can be relied upon to give an adequate answer.

When estimating the true mean with 95% confidence the following equation can be used to obtain an approximate value of n:

$n = 4 s^2 / d^2$ (1)

where n is the number of measurements (shots), s is the standard deviation and d is the margin of error. (For a good introduction on this, online, see http://www.sjsu.edu/faculty/gerstman/StatPrimer/). Substituting RSD for s, and expressing the margin of error as a percentage of the mean, D=d/xbar * 100, we get equation (2):

$n = 4 RSD^2 / D^2$ (2)

or

$n = 4 (RSD / D)^2$ (3).

Thus, given the RSD and selecting the desired value of the margin or error, this formula can be used to calculate the minimum number of shots (after rounding up to the nearest integer). Notice that the number of shots, n, increases as the square of the ratio of RSD to the selected margin or error. Thus if RSD/D=1, we only need 4 shots, but if RSD/D=2, we need 16 shots—obviously a huge difference in practical terms.

Applying this to the Ca values in the first column of Table 4.2, we get for a margin of error that is within 5% of the mean (95% of the time) n=4(9.9)^2/5^2=15.68, which rounds up to 16 shots. On the other hand, if we are satisfied with a margin or error of 10% of the mean, then n=4(9.9)^2/10^2=3.9, and rounds up to 4.

Selecting a margin of error of D= 15% of the mean for each of the 4 sets of measurements in Table 4.2, we get n=2, 9, 15 and 37 for RSDs=9.97%, 21.53%, 28.61% and 45.76%, respectively. Figure 4.5 summarizes these relationships graphically. The lines on the graph were generated using equation (3).

In applying this approach to the rock data collected in this project, the value of the RSD is only known approximately, because the true RSD could only be estimated from a relatively small number of measurements. For example, the number of measurements made on rock surfaces was usually 10, so the estimate of the RSD is itself not very precise. Here we have assumed, however, that these estimates of RSD on a rock specimen (for a particular element) are sufficiently precise to be used in equation (3). In many situations, the RSD is so large (sometimes more than 50%) that for a margin of error on the mean of, say, +/- 10%, leads to a huge number of required observations per sample—obviously simply not practical for routine use. Table 4.3 contains Al values (%) measured 10 times (i.e. 10 shots) per specimen on a smooth rock surface by the HH-C instrument in mining mode, using the rock data discussed in Section 5.2 of the report.

In general, the 'very coarse' grained rocks have large RSD values (not surprisingly) and the number of shots required to achieve a 10 or even 20% margin of error on the mean is so high that analysis by pXRF is probably impractical. One solution for any samples with high RSD is to use a portable grinder and and carry out the analysis on the resulting powder, which greatly reduces the spatial inhomogeneity, as reflected in much reduced RSDs and subsequent number of required shots to achieve a reasonable margin of error. Aluminum was selected for this example because in general the precision of Al by pXRF measurements is good, in comparison with some other elements.

Table 4.3. Estimated number of shots, n, needed to achieve +/- 10% and 20% margins of error of the mean, 19 times out of 20. Data are for Al using smooth cut surfaces and mining mode.

Rock type	Grain size	% Mean	St Dev	RSD	n (D=10%)	n (D=20%)
Granite breccia	medium	8.61	0.608	7.1	2	1
Diabase	very fine	13.84	0.533	3.9	1	1
Norite	fine	8.59	1.742	20.3	17	5
Norite	medium	12.60	0.721	5.7	2	1
Norite	medium	12.11	0.648	5.3	2	1
Argillite	very fine	13.48	0.889	6.6	2	1
Dolostone	very fine	0.32	0.117	36.8	55	14
Rhyolite	fine	7.50	2.097	28.0	32	8
Gabbro	fine	3.52	0.807	22.9	22	6
Sericite-alt	fine	6.64	0.747	11.3	6	2
Basalt	very fine	11.00	0.747	6.8	2	1
Gneiss	medium	12.18	1.025	8.4	3	1
Clay-alt regolith	medium	15.53	1.921	12.4	7	2
Chlorite-alt	very fine	14.95	0.265	1.8	1	1
Rhyolite	medium	4.54	1.666	36.7	54	14
Chalcocite-alt	fine	15.57	1.228	7.9	3	1
Dolostone	very fine	0.83	0.251	30.2	37	10
Argillite	very fine	0.89	0.077	8.6	3	1
Porphyry Cu	very coarse	4.38	4.574	104.4	436	109
Sed. Cu oxide	very coarse	11.23	3.863	34.4	48	12
Basalt	fine	14.56	0.352	2.4	1	1
Zn-Pb ore	fine	0.66	0.149	22.7	21	6
High REE	very coarse	11.28	2.131	18.9	15	4
High REE	very coarse	6.22	2.380	38.3	59	15

Summary and recommendation

We recommend that an orientation survey be carried out on a typical suite of samples, using n=15 to 20 shots per sample. Determine the RSDs for the elements of interest, and decide on a desired margin of error that can be tolerated (this clearly depends on how the data are to be used). Calculate the minimum number of shots, using equation (3) for each sample.

If the number of shots makes the project too costly (given that on average you need about 3 minutes per shot, given setup time as well as beam time), consider either grinding the sample to produce a more homogenous material (pXRF measurements on powdered values always have lower RSDs than those taken on surfaces), or using conventional lab analyses for problematic materials.

Comment

Geochemists are accustomed to getting precise and accurate analyses of their samples, and usually analytical error is small compared to other sources of variation. Data from pXRF on rock samples, particularly coarse-grained ones, are much noisier than conventional lab analyses, and care needs to be exercised to avoid compounding errors to the point where the results can no longer be safely interpreted. Not surprisingly, data from soils, or from powdered materials, usually gives much lower RSDs than rock surfaces, because they are more homogeneous and the pXRF window is large enough to "see" a representative sample in the ~ 50-mm^2 field of view.
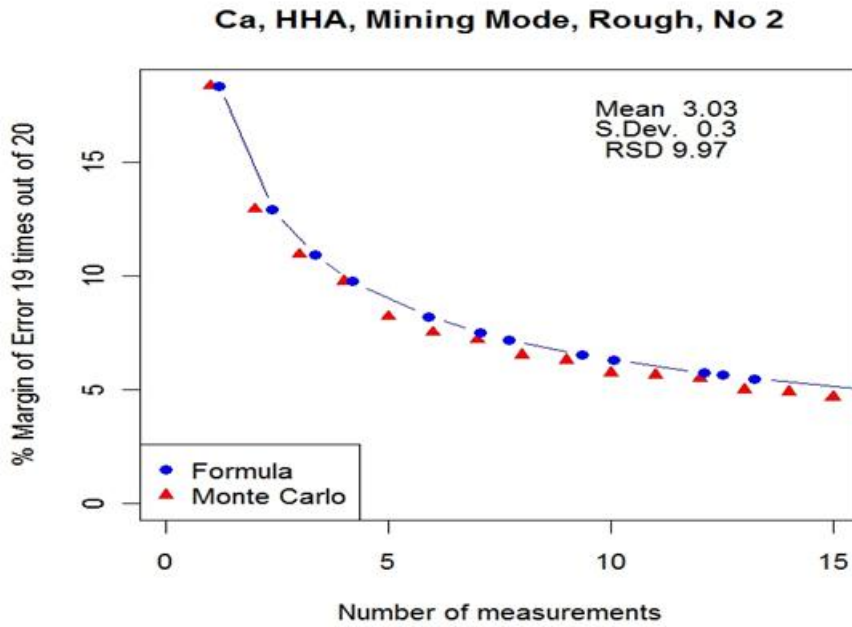
Fig. 4.1. Sample # 2. Number of measurements (shots) needed to obtain selected margins of error (deviations from the mean) 19 times out of 20 (i.e. 95% of the time).
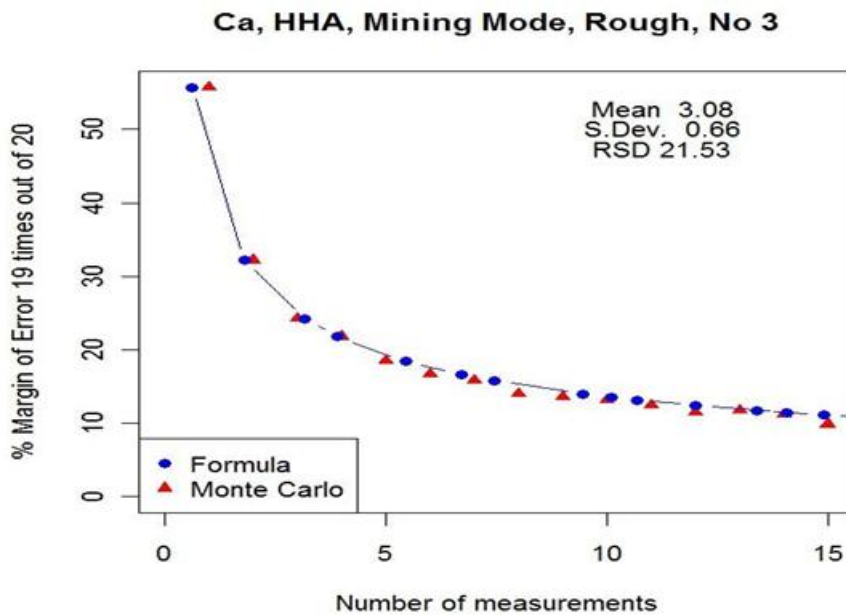
Fig. 4.2. Sample # 3. Number of measurements (shots) needed to obtain selected margins of error (deviations from the mean) 19 times out of 20 (i.e. 95% of the time).
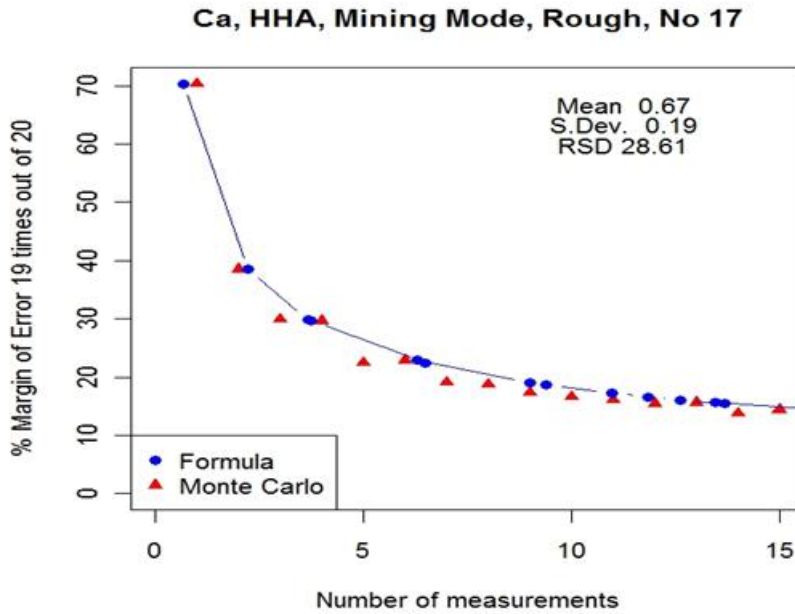
Fig. 4.3. Sample # 17. Number of measurements (shots) needed to obtain selected margins of error (deviations from the mean) 19 times out of 20 (i.e. 95% of the time).
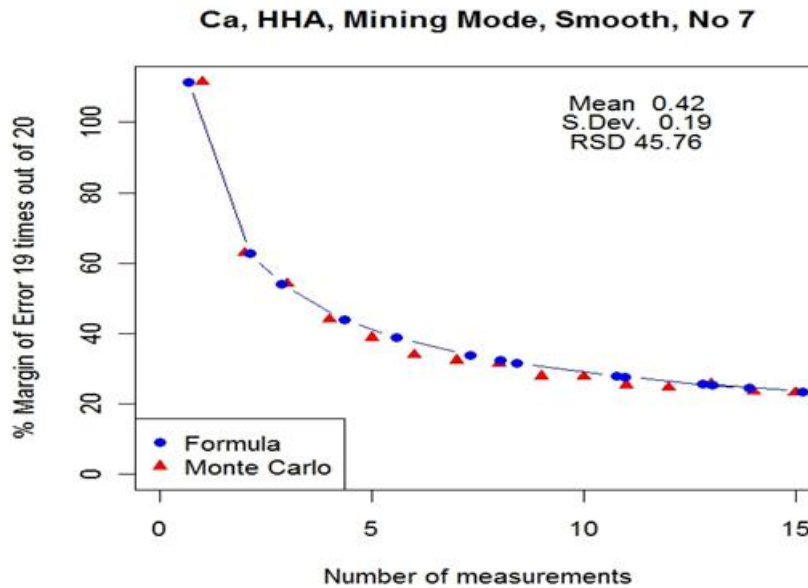
Fig. 4.4. Sample # 7. Number of measurements (shots) needed to obtain selected margins of error (deviations from the mean) 19 times out of 20 (i.e. 95% of the time).
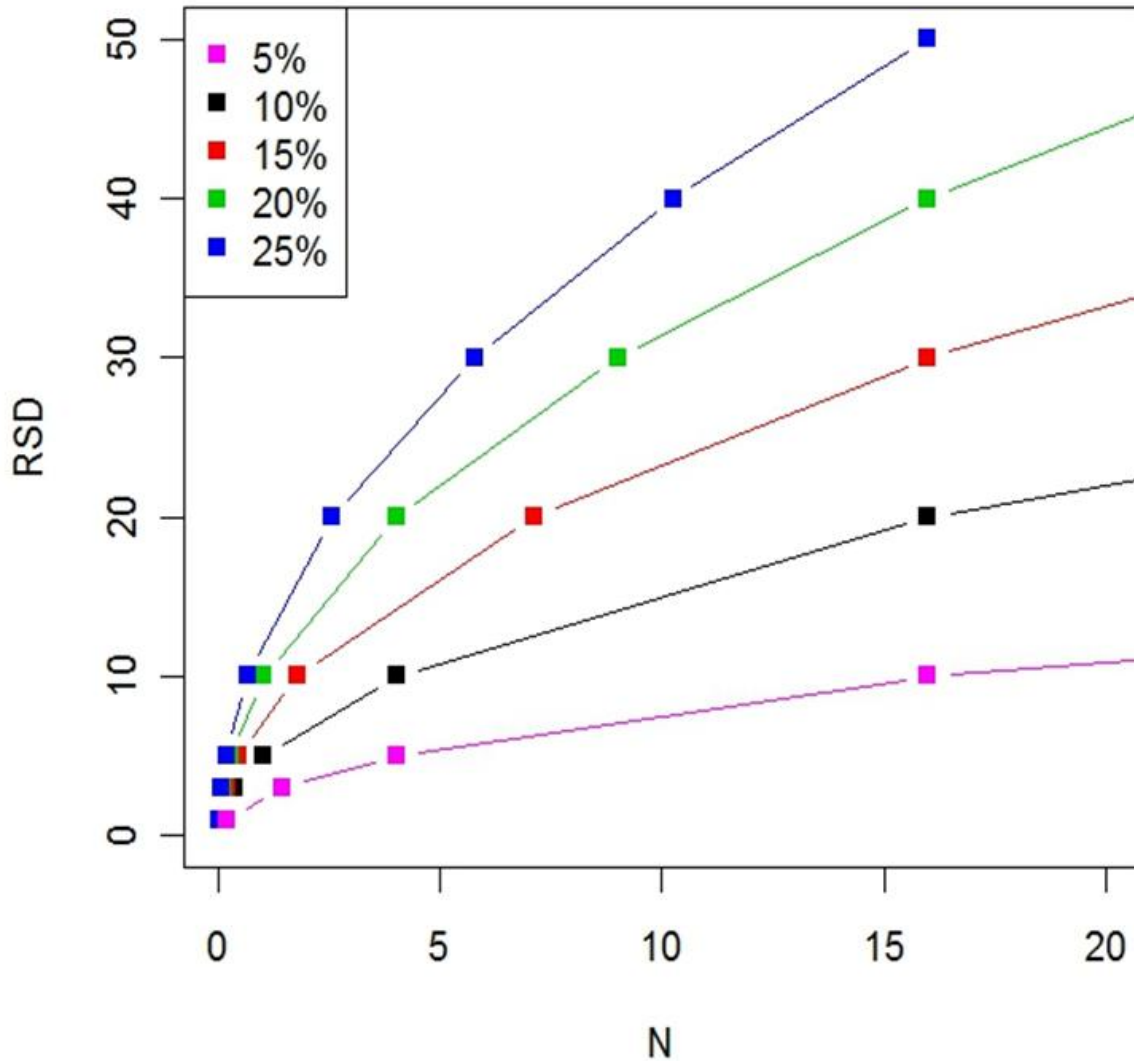
Fig. 4.5. Use this graph to select a value of N for a selected margin of error, given a sample RSD. For example, assuming an RSD of 30% and a 25% margin or error (blue curve), about N=6 measurement shots should be taken and averaged to be certain of being within +/-25% of the true mean 19 times out of 20.

5. ROCK SURFACE STUDY

5.1. Group of granodiorites

Samples and methodology

Twenty granodiorites were lent to the project by John Chapman of the GSC. Fifteen of these also had the prepared counterparts (labelled 'powders') together with fusion (lithium metaborate) ICP-MS and ICP-ES data. Most of the rock chips had 'smooth' (cut) and 'rough' surfaces and four had a 'round' surface. Up to 15 analyses per surface per sample were carried out using each instrument (HH-A and HH-C). Thus, in total in terms of mean analyses, there should be 15 powder, 19 smooth (sample 14 does not have a smooth surface), 17 rough and 4 round analyses per element but these are often lower in number if the concentration of the element is too low. Attention is focussed on the comparison of the two surface analysis sets: smooth and rough. It is unadvisable to compare summary data (e.g. median RSD) with the round set as there are so few samples so that the two populations of samples would be quite different.

The rocks were classified visually into: very fine (1), fine (5), medium (4), coarse (9), and very coarse (1). Besides evaluating the RSD by surface type, the goal was also to examine whether there is a relationship between RSD and grain size distribution.

Powder samples were cupped and capped with the usual 4-µm Prolene film. Three analyses were made for the powder samples, moving the cup to a different position over the pXRF window each time. Test stands were used for the rocks. A systematic approach was taken to analyse the rough, smooth and round surfaces of the various core and rocks in this study. Each sample was analysed using the same grid of points for both machines. For each point, data were first collected in the soil mode, and then mining mode, without moving the sample between these two readings. This grid of points was unbiased and attempted to capture an accurate reading of the sample as a whole. Weathered surfaces were avoided as much as possible. In some cases the rocks had to be propped up using glass microscope slides to minimize the distance between the analyser and sample. Care was taken to ensure the slides did not cover any part of the window. Beam times were 60 s each.

If some of the 15 or so shots per sample returned results below detection or that were eliminated by the software because of interference then the remaining results were still used and the average taken over those positive shots. These situations are obvious as 'n', provided in each element's table, is lower than expected.

Results

The data are presented in the Appendix for the actual pXRF results (both original lab data, and merged and cleaned-up), and as plots in numerous formats, by element:
- A colour-coded sequence plot of concentration in powder, smooth, round, rough surfaces
- An x-y plot of concentration in surface type vs powder with statistics
- An x-y plot of concentration in powder vs lab with statistics
- Box-and-whisker ('B&W') plots of concentration by lab, powder, various surface types
- Box-and-whisker plots of RSD by powder, smooth, round, rough surfaces
- Box-and-whisker plots of RSD by grain size in smooth surface
- Box-and-whisker plots of RSD by grain size in powder
- An x-y plot of rough versus smooth with statistics

These plots are followed for each element by an Excel file containing three summary tables:
- a table of mean, SD and RSD for the lab (the lab usually has only 1 value), powder and different surface types in the 20 samples;
- a table in ascending order of sample by RSD indicating how many pXRF analyses would be necessary to achieve a result within a particular RSD of the mean (e.g. 10, 20, 30% etc) when analysing the smooth surface;
- a table (at the bottom of the page) providing the statistics for the concentration plots of powder vs smooth, vs rough and vs round results and smooth vs rough.

There is also a summary table for all elements showing median RSD for each sample type (powder, smooth, rough, round) ranked by increasing median RSD of smooth.

Results are discussed by element, the mining mode being used mostly for the majors and soil mode for the traces and minors. The concentration range using the lab data is provided in brackets at the beginning of each element's section.

Mining mode

Al, aluminium (7.0-9.4%)
A glance at the sequence plot for either instrument shows that (a) the smooth and round surface results are higher than those for the powder and (b) the rough surface results are consistently lower than all others (Fig 5.1.1). The reasons are two-fold: firstly, the powder is analysed in a cup capped with a Prolene film which absorbs the low-energy X-ray photons of light elements such as Al (and Si) and hence powder results will be lower than smooth or round; and (b) the presence of air between the sample and pXRF window in the rough surface analysis leads to more absorption and hence lower results compared to those for smooth or round surfaces.

The calibration graphs of pXRF vs lab value for the powder are very poor (r^2 values of 0.2 and 0.1 for HH-A, HH-C). The plot for HH-A data would be much better except for two fliers: sample # 13 (9.0 pXRF vs 8.2% lab) and # 15 (10.7 vs 8.1% lab) (Fig 5.1.2); the plot of HH-C is extremely noisy. The box-and-whisker plot of the median values of Al by HH-A shows the lower concentration for the rough surface analysis at ~ 7.3%, compared to ~ 8.2% Al for the smooth. [The higher mean value for the round surface analysis cannot be truly compared as these are not the same suite of samples, n being only 4 for the round]. A gradation in median RSD is shown in Figure 5.1.3 for HH-A: it increases from ~ 2% in the powder, through ~ 11% for the smooth surface analysis, and 16% for the round to 20% for the rough surface (Fig 5.1.3). Given the added complication of air absorbing photons, it is hardly surprising that the median RSD for rough surface analysis is twice that for smooth.

Both HH-A and HH-C show a dependency of median RSD for the smooth surface set on grain size: for example, the RSD for the fine grained samples is ~ 7.5% and ~ 17-21% for the medium to coarse grained (Fig. 5.1.4).

With an RSD of 11%, the median for smooth surface analysis by HH-A, only one analysis would be required to obtain a mean value of Al within 30% of the 'true' concentration (and two for 20%; see Granodiorite_HHA_mining_Al-summary.xls in the Appendix).

Ca, calcium (0.2-3.9%)
The calibration plots for Ca of powder vs lab are excellent, with r^2 values of 1.0 and slopes of 1.2 and 1.0, respectively, for HH-A and HH-C. The B&W plots of Ca values across lab, powder and different surface analyses do not show any significant differences in median values. The median RSDs across these different analyses are also very similar, at ~ 27-35% for HH-A and ~ 28-31% for HH-C. However, the trend in RSDs differs from one sample to another: for example, by HH-A, sample # 2 (medium grain) has an RSD of 29% by rough surface analysis and only 10% by smooth but the same figures for sample # 6, also of medium grain size, are 178 and 29%, respectively. Thus it is very hard to generalise across samples.

The RSD of 27% for HH-A analysis of smooth surfaces breaks down to: ~ 15% for the very fine grained sample, through 25-29% for fine to coarse and 38% for the one very coarse sample. The HH-C smooth surface data is more gradual, from ~ 10% RSD (very fine) through 20% (fine), 28% (medium), 38% (coarse) to 52% for the very coarse grained sample (Fig. 5.1.5).

With an RSD of 28%, the median for smooth surface analysis by HH-C, four analyses would be required to obtain a mean value of Ca within 30% of the true concentration.

Fe, iron (0.3-5.1%)

Both calibrations are excellent for Fe: slopes are unity for both instruments and r^2 values are 0.99 and 1.0. The B&W plots for HH-A and HH-C show distinctly lower median values for powder and lab, at 3-3.2% Fe, compared to ~ 1.9% for all three surface analyses (Fig. 5.1.6). Part of this is probably due to the fact that the five samples for which they are no powder or lab analyses tend to be low in Fe compared to the rest but the sequence plot by both HH-A and HH-C show that this trend is real, particularly for the smooth data-set (Fig. 5.1.7).

Median RSDs are high: at 36% for both smooth and rough surface analysis by HH-A; and 49 and 46%, respectively, for smooth and rough, by HH-C. There is not an obvious dependency of the RSD on grain size. The HH-A results for smooth surface analysis show similar median RSDs for very fine, fine, medium and coarse, only the one very coarse sample shows a high RSD of 56%. HH-C results show a median RSD of ~ 38% for fine grained samples and ~ 46-60% for the rest but not in any order.

The table below (Table 5.1.1) for the samples with all three surface types shows similar tendencies in RSD for both HH-A and HH-C with sample. For example, both instruments display low RSDs (17-27%) for surface analysis of sample # 15 and high RSDs (69-88%) for the smooth and round analyses of sample # 5. Clearly the variation in RSD between smooth and rough (or round) surface analysis is very sample dependent. The lower RSDs (38, 46%) for the rough surface analysis of sample # 5 are hard to explain. These data support the observation that RSDs are independent of grain size for Fe.

Table 5.1.1. Results for Fe in granodiorites with different surface analyses, values in %

Sample #		Lab	Powder		Smooth		Rough		Round	
			Mean	RSD	Mean	RSD	Mean	RSD	Mean	RSD
5	fine	0.85	0.92	1.20	0.48	69	0.84	38	0.91	82
5	*fine*	*0.85*	*0.83*	*0.92*	*0.53*	*88*	*0.62*	*46*	*0.72*	*83*
13	coarse	3.34	3.32	0.59	2.51	19	4.33	55	2.63	23
13	*coarse*	*3.34*	*3.22*	*1.79*	*2.80*	*35*	*6.30*	*68*	*2.95*	*47*
14	coarse	2.99	2.85	0.68			1.71	44	1.17	41
14	*coarse*	*2.99*	*2.85*	*0.66*			*1.28*	*36*	*1.13*	*58*
15	coarse	5.01	4.90	0.57	3.43	21			3.93	17
15	*coarse*	*5.01*	*4.91*	*0.44*	*3.26*	*27*			*3.79*	*22*

HH-A results in Roman, *HH-C results in italics*

With an RSD of 36%, the median for smooth surface analysis by HH-A, six analyses would be required to obtain a mean value of Ca within 30% of the true concentration.

Mg, magnesium (0.04-1.53%), HH-C only
HH-C reports on the 11 of the 15 samples, for which there are lab values, that contain Mg > 0.1%. The fit of the calibration is quite good, at 0.81, but the slope is far from 1, at 0.54 (Fig. 5.1.8).

The agreement between smooth and rough surface analysis with powder is very poor, with r^2 values of 0.35 and 0.57, respectively (Fig. 5.1.9). The median RSDs are 28 and 31% for smooth and rough surface analyses. There is no relationship between RSD and grain size.

K, potassium (1.4-6%)
The calibration graphs for both HH-A and HH-C have excellent r^2 values of 0.98 and 0.99, respectively; both have positive slopes (1.3, 1.2) and hence results are higher than those of the lab (Fig. 5.1.10). Median RSDs for HH-A are all very close: 44% for smooth, 40% for rough and 42% for round; corresponding figures for HH-C are 42%, 40% and 41%. RSDs for the four round surface analyses are similar.

HH-C shows a rather mixed progression in median RSD of smooth surface analysis with grain size distribution: 5%, very fine – 34% fine – 55% medium – 42% coarse – 70% very coarse. HH-A is similar in that the very fine sample has a median RSD of 5% but the other samples are in the range ~ 40-65% with the fine being at the top end of this scale.

With an RSD of 44%, the median for smooth surface analysis by HH-A, nine analyses would be required to obtain a mean value of K within 30% of the true concentration.

Si, silicon (29-36%)
As for Al, another light element, values for Si by smooth and round surface analysis are higher than those for the powder due to the absence of Prolene film and values for rough surface analysis are lower owing to the larger effect of absorption of photons by air (Fig. 5.1.11). The incorrect factory calibration for Si is evident in the B&W plot of Si results for lab, powder and surface analyses where the lab results are so much lower than all the others by pXRF (Fig. 5.1.12). Hence the calibration plot for HH-C has a large intercept of 13.5% but its fit, at 0.88, is not bad; the r^2 value for HH-A is 0.76, quite noisy.

Both instruments show a progression in median RSD with surface: for example, by HH-A, the median RSD changes from 6% for smooth, through 8% for round to 13% for rough (Fig. 5.1.13). Corresponding figures for HH-C are 6, 8 and 10%. Both smooth surface data-sets show a dependency of RSD on grain size. For example, by HH-A, the median RSD increases from ~ 2% for the very fine sample, through 3.2% (fine) and 6% (medium) to 7-8% for coarse and very coarse.

Ti, titanium (0.066-0.396%)
The calibration (powder vs lab results) by HH-C is very good, with an r^2 of 0.98 and slope of 0.89. That for HH-A, however, shows a translational effect, with a significant intercept of 0.14%, r^2 of 0.85 and slope of 1.0 (Fig. 5.1.14).

The median RSDs of smooth, rough and round are essentially the same for HH-A data, at 28-29%; those by HH-C are higher, at 53, 47 and 40%, respectively. Only the very fine-grained sample shows a significantly lower RSD in smooth surface analysis than the other samples, at 10% for HH-A (cf 23-35% for the rest) and 32% for HH-C (cf 52-58% for the others).

With an RSD of 28%, the median for smooth surface analysis by HH-A, four analyses would be required to obtain a mean value of Ti within 30% of the true concentration.

P, phosphorus (87-1264 ppm)
HH-A reports on only 4 samples (# 1, 9, 10, 13) and these are not the highest in P concentration. By HH-C, smooth surface analysis results tend to be lower than those of the powder and rough surface analysis higher (Fig. 5.1.15). Although there is a large intercept of 520 ppm, the calibration by HH-C is quite good, with an r^2 value of 0.90 and a slope of 1.6 (Fig. 5.1.16).

Median RSDs are similar for the three surface analyses, at 46% for smooth, 57% for rough and 52% for round. There does not appear to be any control by grain size.

S, sulphur (<100-33900 ppm)
Both instruments report on only 4 samples (1, 13-15), those that are high in S concentration. There are sporadic results >LOD in the smooth and rough surface analysis, but not in the powder analysis, a phenomenon that is evident for other elements at concentrations close to the LOD. The calibrations afforded by the four samples have a good fit of 0.99 for both HH-A and HH-C, but fairly high intercepts of 797 and 165 ppm, respectively (Fig. 5.1.17).

Results for the three S-enriched granodiorites are given below. Note: (a) in general, RSDs are sample dependent (e.g. for samples 13 and 14, both instruments show RSDs in surface analyses of 63-113% but only 29-66% for sample 15); (b) there is no consistent difference between smooth, rough and round RSDs (e.g. smooth or round is not consistently better than rough); and (c) mean values can differ considerably across surface analyses (e.g. 1.6-6.7% S in sample 13 by HH-C). The individual 15 pXRF analyses display large ranges in concentration for the same sample: e.g. in sample 13, by smooth surface analysis, HH-A reports 0.27-2.8% S and HH-C reports 0.4-5.1% S, a range of a decade.

Table 5.1.2.Results for S (in ppm, RSD in %) in three granodiorites, different surface analyses

Sample	Lab	Powder		Smooth		Rough		Round	
		Mean	RSD	Mean	RSD	Mean	RSD	Mean	RSD
13	17800	10796	1.8	10687	69	25041	113	11576	63
13	*17800*	*12897*	*8.2*	*16142*	*84*	*66632*	*97*	*22310*	*112*
14	23000	16284	1.7			10023	96	5144	85
14	*23000*	*20860*	*2.0*			*6891*	*82*	*8007*	*103*
15	33900	20906	2.6	12550	48			11171	29
15	*33900*	*25763*	*0.9*	*13978*	*66*			*14224*	*45*

HH-A results in Roman. *HH-C results in italics*

Soil mode

Ag, silver (0.25-4.8 ppm)
These concentrations for Ag are too low to evaluate accuracy or precision. All Ag values by HH-A in the soil mode are <LOD and in the mining mode there is a large background of several hundred ppm. HH-C does report Ag in most samples but, not surprisingly at these concentrations, the calibration has an r^2 of only 0.4. Median RSDs for smooth and rough analyses are 52 and 39%, respectively. The plots of surface analysis by HH-C versus powder results show that (a) there is no relationship between these sets of data and (b) the rough surface analysis data are all higher than those for the smooth (Fig. 5.1.18).

As, arsenic (0.2-38.9 ppm)
Only two samples contain As greater than 2.5 ppm, at 17.9 and 38.9 ppm. Although the analytical RSDs by HH-C are much higher than those by HH-A (48% vs 9%, powder), the agreement of powder and surface results with lab values is far better. The median RSDs for smooth and rough surface analysis are 24 and 23% for HH-A and 65 and 60% for HH-C, i.e. there is no difference in variability between smooth and rough surface analysis on a general basis. Concentrations are too low to form any conclusion with respect to RSD variation with grain size.

Ba, barium (1190-5210 ppm)
Only HH-C reports Ba. The calibration is good, with an r^2 value of 0.97 and slope of 0.82. The median RSDs for smooth and rough surface analysis are essentially equal, at 52 and 55%, respectively (round surface analysis is similar). The plot of smooth surface analysis versus powder is quite good, regardless of high standard deviations: it has an r^2 value of 0.92, far better than that for the rough surface analysis which is only 0.43 (Fig. 5.1.19). There is no obvious dependency of RSD on grain size, only that the very fine sample has a very low RSD of 5% (4% for rough) compared to all the rest. Samples 2 and 3 which have the highest RSDs of 170 and

131% in the smooth surface analysis are also highest in the rough surface analysis, at 132 and 156%, respectively.

With an RSD of 52%, the median for smooth surface analysis by HH-C, 13 analyses would be required to obtain a mean value of Ba within 30% of the true concentration.

Cd, cadmium (< 0.5 ppm)
The lab values are based on four-acid digestion, not fusion, and are all below the detection limit of 0.5 ppm. All samples are <LOD in the soil mode by HH-A; there is a large background of ~ 200-300 ppm in the mining mode. HH-C reports Cd in the range 1-7 ppm but, not surprisingly, the RSDs for the powder are very high, at 27-106%.

Ce, cerium, HH-C only
There are no lab values for this element. Given the evidence from the other rock data (Section 5.2) that there is a large and variable background (few hundreds of ppm) for Ce using HH-C, the data for these granodiorites – in the range ~ 200 to 300 ppm – is discounted. The same is true for La.

Co, cobalt (1-53 ppm)
There are 14 samples containing less than 10 ppm Co. Most of the data by HH-C are so noisy, interspersed with negative numbers, that they are not reported here. The calibration graph (powder vs lab) by HH-A is odd in that below ~ 10 ppm there is a good fitting line but the three higher samples form a much lower slope (Fig. 5.1.20). The results for these three by direct surface analysis remain low, suggesting the lab values may be in error. Regardless of the noisy data, the plot of rough versus smooth surface results is good, with an r^2 of 0.87 (Fig. 5.1.21). Median RSDs are similar, at 27, 28 and 33% for smooth, round and rough analysis. With the exception of the RSD for smooth surface analysis of the very fine sample (31%), there does seem to be a relationship with grain size: from 18% (fine), through 23% (medium), 30%, (coarse) to 63% (very coarse).

With an RSD of 27%, the median for smooth surface analysis by HH-C, four analyses would be required to obtain a mean value of Co within 30% of the true concentration.

Cr, chromium (10-50 ppm)
As for many of the trace elements, Cr is very low in concentration, most are reported at 10 ppm by the lab (fusion ICP-MS). Almost all the data by HH-C are negative numbers and results by HH-A are high compared to the lab values (Fig. 5.1.22). It is interesting that both smooth and rough surface analyses are consistently lower than those using the powder (Fig. 5.1.23). Given the uncertainty in accuracy for Cr, evaluating precision is not justified. The sample containing 50

ppm Cr is reported by HH-A at: 75 ppm (powder, 4% RSD); 62 ppm (smooth surface, 13% RSD); 74 ppm (rough surface, 23% RSD); and 61 ppm (round surface, 22% RSD).

Cs, caesium (0.1-10.2 ppm), by HH-C only
Caesium obviously suffers from interferences and cannot be measured at this concentration range. The results by HH-C for the powder are in the range 14-72 ppm, with those for the surface analyses even higher, and they bear no correlation whatsoever to the lab results (Fig. 5.1.24). It is interesting that this phenomenon of higher results by smooth or rough (or round) surface analyses compared to powder is evident for other elements (e.g. Cd, Ni, Sb, Sn) which are poorly determined by HH-C.

Cu, copper (1-4820 ppm)
There are two populations of Cu: < 30 ppm and > 1000 ppm (1390, 1655, 2140, 4820 ppm). The calibration graphs, dominated by the high Cu samples, are excellent, with r^2 values of 1.0. Only 7 samples are reported for Cu by HH-A (others <LOD) and, for some of these, not all individual analyses were >LOD (i.e. 'n' is much lower than the 15 smooth surface analyses, etc). The high median RSD of 22% in the HH-C powder data is caused by many samples containing only a few ppm of Cu.

The median RSD by HH-C for smooth and rough surface analyses are 49 and 62%, respectively. There does appear to be a dependency of median RSD with grain size in the smooth analysis, with that for very fine and fine grained samples being ~ 40% and that for medium and coarse being ~ 50%.

The table below presents data for three coarse granodiorites. Note: (a) the similarity in RSD for the same sample analysed by different instruments; and (b) the large range in mean values across the different surface and powder analyses. For example, in sample 13 the range is 497 to 3768 ppm by HH-C (459 to 3674 ppm by HH-A) and in sample 15 it is 274 to 1716 ppm by HH-C (328 to 1792 ppm by HH-A). The difference encountered between, say, smooth and rough (sample 13) results is similar for both instruments. These differences are extreme; there is a tendency towards lower mean values by the surface analysis compared to powder.

Table 5.1.3 Results for Cu (in ppm, RSD in %) in coarse granodiorites with different surface analyses

Sample	Lab	Powder		Smooth		Rough		Round	
		Mean	RSD	Mean	RSD	Mean	RSD	Mean	RSD
13	1390	1146	2.0	497	58	3768	115	561	113
13	*1390*	*1186*	*0.2*	*459*	*55*	*3674*	*120*	*713*	*85*
14	4820	4248	1.7			1082	85	942	123
14	*4820*	*4338*	*0.6*			*1017*	*89*	*767*	*104*

| 15 | 2140 | 1716 | 1.7 | 723 | 97 | | 274 | 57 |
| *15* | *2140* | *1792* | *0.6* | *604* | *67* | | *328* | *48* |

HH-A results in italics. HH-C in Roman.

With an RSD of 49%, the median for smooth surface analysis by HH-C, 11 analyses would be required to obtain a mean value of Cu within 30% of the true concentration.

Mn, manganese (~ 100-1394 ppm)
Calibration graphs are excellent for both instruments, with r^2 values of 0.99 and 0.97 (Fig. 5.1.25). There is no real difference in median RSDs: for the smooth and rough surface analysis, they are 35 and 43%, respectively, for HH-A and 40 and 33% for HH-C. Similarly there is no relationship between grain size and RSD in the smooth surface analysis (Fig. 5.1.26).

Table 5.1.4. Results for Mn (in ppm, RSD in %) in granodiorites with different surface analyses

Sample		Lab	Powder		Smooth		Rough	
			Mean	RSD	Mean	RSD	Mean	RSD
7	coarse	387	370	2.4	267	107	999	142
7	*coarse*	*387*	*325*	*0.7*	*338*	*89*	*1103*	*143*
9	coarse	1006	973	1.1	500	66	593	70
9	*coarse*	*1006*	*967*	*0.9*	*533*	*84*	*609*	*69*
11	fine	387	369	1.8	263	16	804	43
11	*fine*	*387*	*374*	*7.5*	*377*	*39*	*654*	*32*

HH-A in Roman. *HH-C in italics*

Table 5.1.4 shows the same trends as were evident for Cu, that is: there can be a large range in mean values across different surface morphologies and powder (e.g. 325 to 1103 ppm in sample 7); and similar RSDS are obtained for the same sample by the different instruments.

With an RSD of 33%, the median for smooth surface analysis by HH-C, five analyses would be required to obtain a mean value of Mn within 30% of the true concentration.

Mo, molybdenum (<1 -333 ppm)
Only three samples contain Mo above 1 ppm; these results are provided in the table below. The number of results >LOD by pXRF for smooth and rough analysis of sample # 11 is only 2-7, well below the usual 10-15, and are shown for interest only. Note the huge RSDs for the rough and round surface analyses of samples 13 and 14, up to 229%! Thus it is not surprising that the mean values differ so much, from 5 to 70 (powder) ppm in sample 13 and 28 to 382 (powder) ppm in sample 14. As seen for other elements, the mean values in the surface analyses are considerably lower than those of the powder.

Table 5.1.5. Results for Mo (in ppm, RSD in %) in granodiorites with different surface analyses

Sample	Lab	Powder		Smooth		Rough		Round	
		Mean	RSD	Mean	RSD	Mean	RSD	Mean	RSD
13	62	65	2.5	6.8	52	352	229	7	51
13	*62*	*70*	*1.1*	*9.6*	*112*	*334*	*201*	*5*	*120*
14	333	331	1.4			178	176	28	90
14	*333*	*382*	*2.8*			*87*	*198*	*70*	*151*
15	11	11	5.7	5.5	25			3	22
15	*11*	*14*	*3.7*	*4.0*	*130*			*2*	*59*

Results by HH-A in Roman. *Results by HH-C in italics*

The calibrations (3-point for HH-A, 4-point for HH-C) are good, both r^2 values are 1 and slopes are close to unity.

Nb, niobium (1.4-11.1 ppm), by HH-A
Niobium is reported in the mining mode only by HH-C and the values are too low to report. The calibration line (r^2 0.94, slope 0.97) by HH-A is superb, especially at these concentrations! (Fig. 5.1.27). The median RSDs of smooth and rough surface analysis are essentially the same, at 37 and 38%. There appears to be a slight dependency of RSD on grain size in the smooth analysis, from 29% for the very fine, through 36% (fine and medium), to 41-43% for the coarse and very coarse (Fig. 5.1.28). Though the individual SDs are high, the plot of rough versus smooth surface analysis is good, with a slope of unity and r^2 of 0.79.

With an RSD of 37%, the median for smooth surface analysis by HH-A, seven analyses would be required to obtain a mean value of Nb within 30% of the true concentration.

Ni, nickel (1-18 ppm)
Nickel by HH-A in the soil mode is mostly <LOD and in the mining mode there is a background of ~ 60-90 ppm making measurement at these levels of Ni impossible. Unfortunately this is also the case for Ni by HH-C: there is a background of ~ 30-90 ppm for all the samples when in fact most contain 1-3 ppm (Fig. 5.1.29). The individual pXRF SDs on each analysis are high: for example, Ni reported at ~ 60 ppm has an SD of ~ 14-15 ppm.

Pb, lead (6-27 ppm)
Only 8 out of the 15 powder samples are reported for Pb by HH-A (the rest are <LOD); 13 are reported by HH-C. The calibration by HH-C is actually quite good (r^2 0.94, slope 0.95 but large negative intercept of -6.8 ppm) in light of the low concentration range (Fig. 5.1.30). The median RSDs for smooth and rough analyses are 27% by HH-A and 60 and 80%, respectively, by HH-C.

HH-A does appear to show a dependency of median RSD with grain size (8%, very fine - 20%, fine+ medium - 50%, coarse - 41%, very coarse) but HH-C does not, possibly because of its higher individual SDs.

Several examples of different surface analyses are given below. Note the low mean values for the smooth analysis of sample 11 by HH-A and HH-C (3-7 ppm, cf rough at 18-30 ppm). The actual individual data provide more information on heterogeneity. The 15 smooth values are all fairly low and scattered but the rough values, for both instruments, are very low (<LOD for HH-A and a few ppm for HH-C) for ~ 7-8 shots and then increase to ~ 25-38 ppm for the rest. Clearly a region higher in Pb, and homogeneous in Pb, was analysed in the second half of the shots.

Table 5.1.6. Results for Pb (in ppm, RSD in %) in granodiorites with different surface analyses

Sample		Lab	Powder		Smooth		Rough		Round	
			Mean	RSD	Mean	RSD	Mean	RSD	Mean	RSD
11	fine	27	26.7	3	6.8	37	29.6	47		
11	*fine*	*27*	*21.9*	*9*	*3.4*	*60*	*18.0*	*79*		
13	coarse	18	8.1	14	7.3	57	10.3	69	23.3	59
13	*coarse*	*18*	*8.9*	*7*	*6.8*	*95*	*28.5*	*103*	*22.2*	*68*
14	coarse	17	8.5	21			7.7	28	11.8	41
14	*coarse*	*17*	*8.6*	*5*			*6.3*	*58*	*7.4*	*64*

HH-A results in Roman. *HH-C in italics*

With an RSD of 27%, the median for smooth surface analysis by HH-A, four analyses would be required to obtain a mean value of Pb within 30% of the true concentration.

Rb, rubidium (21-199 ppm)
Rubidium is a superb element by pXRF and this is well demonstrated by these results. The r^2 and slope values by HH-A are unity (1.0 and 0.92 by HH-C) and the plots of smooth, rough and round surface analysis versus powder are excellent, with slopes of unity and r^2 values of 0.93, 0.97 and 0.97, respectively (Figs. 5.1.31 and 5.1.32).

The median RSDs for smooth and rough analysis by HH-A are 30 and 27%, respectively, and 39 and 46% by HH-C, i.e. there is no difference for the performance of Rb between smooth and rough analysis (round is similar). The only dependency of median RSD on grain size is seen for the extreme sample, the very fine-grained # 16 which has RSDs of 7 and 9% for smooth and rough analyses by HH-A (6, 11% by HH-C), much lower than the others.

Some examples are given below.

Table 5.1.7. Results for Rb (in ppm, RSD in %) in granodiorites with different surface analyses

Sample		Lab	Powder		Smooth		Rough		Round	
			Mean	RSD	Mean	RSD	Mean	RSD	Mean	RSD
1	fine	149	150	0.9	111	49	145	36		
1	*fine*	*149*	*133*	*1.9*	*93*	*35*	*159*	*55*		
3	medium	35	39	1.0	22	29	35	76		
3	*medium*	*35*	*33*	*1.3*	*22*	*81*	*30*	*94*		
5	fine	21	26	1.2	18	40	15	20	17	43
5	*fine*	*21*	*22*	*4.4*	*17*	*30*	*10*	*32*	*12*	*55*
13	coarse	165	167	0.3	166	15	182	19	174	20
13	*coarse*	*165*	*151*	*1.0*	*148*	*24*	*165*	*28*	*161*	*22*

HH-C in italics

With an RSD of 30%, the median for smooth surface analysis by HH-A, four analyses would be required to obtain a mean value of Rb within 30% of the true concentration.

Sb, antimony (< 1 ppm)
The lab values for Sb are all below 1 ppm. HH-A reports Sb only in the mining mode and there is a very high background of ~ 300-400 ppm, making measurement below these levels impossible. HH-C reports this suite of samples in the soil mode up to 13 ppm Sb but the RSDs are very high for the powder, at ~ 25-80%, alerting the user that these values are highly suspect. The plots of surface analyses versus powder or each other show that there is no relationship amongst them.

Se, selenium (0.1-4.2 ppm)
Only three samples contain > 0.4 ppm Se. Impressively, HH-C reports well on these three (Fig. 5.1.33) and HH-A reports above LOD only on the powder form for them (though a few of the surface analyses report a couple of ppm, most of the 15 are <LOD). The results for these three samples are presented in the table below. Given that the RSD for the powder by HH-A is better than that for HH-C, this instrument probably could report lower but it is wise to cut off at ~ 1-2 ppm.

Table 5.1.8. Results for Se (in ppm, RSD in %) in the three samples above 0.4 ppm Se

		Powder		Smooth		Rough		Round	
Sample	Lab	Mean	RSD	Mean	RSD	Mean	RSD	Mean	RSD
13	3.3	3.6	15.1	3.1	55	6.7	80	3.5	83
13		*2.9*	*1.1*						
14	3.8	4.5	9.3			2.2	48	2.3	40
14		*3.4*	*0.6*						
15	4.2	5.1	20.0	1.6	31			2.4	45
15		*4.1*	*0.2*						

HH-A results in italics, HH-C results in Roman.

Sn, tin (<1-5 ppm)
HH-A reports <LOD for all the samples in the soil mode and in the mining mode there is a large background of several hundred ppm. While HH-C reports 6 ppm for Sn in sample 13 (lab, 5 ppm), 4 ppm in # 14 (lab, 3 ppm) and 10 ppm in # 15 (lab, 5 ppm), it also reports these magnitudes in other samples which contain ≤ 1 ppm and therefore the data cannot be trusted (Fig. 5.1.34).

Sr, strontium (26-1240 ppm)
Like Rb, Sr is another excellent element by pXRF and these results confirm this. Calibration plots are superb, with an r^2 of 1.0 and slope of 1.1 by HH-A and r^2 and slope of unity by HH-C (Fig. 5.1.35). Plots of smooth, rough and round surface analyses against powder by HH-A are excellent, with r^2 values of 0.98, 0.98 and 1, respectively (Fig. 5.1.36); HH-C behaves similarly. Median RSDs by HH-A are also similar for smooth (15%), rough (17%) and round (16% HH-A) analyses; corresponding figures for HH-C are 15, 24 and 22%. The plot of rough versus smooth surface analyses is excellent for both instruments (Fig. 5.1.37).

Both instruments tend to show an increase in median RSD with grain size, with the exception of the very coarse sample (# 4) which has an unusually low RSD of 8% for the smooth analysis. Median RSDs by HH-C for smooth surface analysis increase from 3%, very fine, through 15%, fine, and 22%, medium to 25% for coarse grain (Fig. 5.1.38).

With an RSD of 15%, the median for smooth surface analysis by HH-A, only two analyses would be required to obtain a mean value of Sr within 30% of the true concentration.

Th, thorium (0.25-15.1 ppm)
The calibration plot for HH-A is very poor (r^2 of 0.3, large intercept) but that by HH-C is impressive (r^2 of 0.96, slope of 1.1), given this low concentration range (Fig. 5.1.39). Nevertheless, the plot of rough versus smooth surface analyses for HH-A is good (r^2 of 0.88, slope of 1.2) (Fig. 5.1.40). The median RSDs for smooth and rough surface analysis are 19 and

20% for HH-A and 37 and 42% for HH-C. At this concentration range it is unwise to evaluate RSD with grain size. Some examples of data for the samples containing higher concentrations of Th are given in Table 5.1.9.

Table 5.1.9. Results for Th (in ppm, RSD in %) in granodiorites with different surface analyses

Sample		Lab	Powder Mean	Powder RSD	Smooth Mean	Smooth RSD	Rough Mean	Rough RSD	Round Mean	Round RSD
11	Fine	10.4	26.0	7.7	24.4	14	28.7	13		
11	*Fine*	*10.4*	*15.6*	*1.6*	*13.2*	*23*	*13.1*	*13*		
12	Coarse	15.1	22.2	11.1	14.3	57				
12	*Coarse*	*15.1*	*16.6*	*3.9*	*4.2*	*107*				
13	Coarse	8.7	14.1	6.9	14.1	14	14.8	15	15.0	16
13	*Coarse*	*8.7*	*10.4*	*11.0*	*9.0*	*23*	*9.7*	*28*	*9.1*	*18*
14	Coarse	13.4	16.7	3.5			14.3	73	10.4	34
14	*Coarse*	*13.4*	*17.1*	*2.2*			*7.8*	*34*	*7.9*	*53*

HH-C in italics

With an RSD of 19%, the median for smooth surface analysis by HH-A, only two analyses would be required to obtain a mean value of Th within 30% of the true concentration.

U, uranium (0.1-13.7 ppm)
HH-A reports only on four samples and HH-C reports on all samples, at 8-26 ppm. The calibration is poor; these levels of U are too low to estimate differences in RSDs with surface and grain size (Fig. 5.1.41).

V, vanadium (7-134 ppm)
The calibration using HH-A is so poor (r^2 of 0.09 and a large positive intercept of 153 ppm) that its data will not be used. The calibration by HH-C is certainly acceptable (r^2 of 0.91, slope of 1.2, intercept of 13 ppm) (Fig. 5.1.42). Regardless of high individual SDs, the graphs of smooth, rough and round versus powder and rough versus smooth surface analyses show good fit but the slopes are rather low (~ 0.8) (Figs. 5.1.43 and 5.1.44). Both instruments report lower in general for the smooth surface analyses compared to the powder, a difference noted for several other elements (e.g. Fe) (Fig. 5.1.45). Median RSDs are 56 and 58% for smooth and rough surface analysis but as the table below indicates, the differences between smooth and rough RSDs are very sample dependent (cf sample 1 and 2).

Table 5.1.10. Results for V (in ppm, RSD in %) by HH-C in selected granodiorites

Sample		Lab	Powder		Smooth		Rough		Round	
			Mean	RSD	Mean	RSD	Mean	RSD	Mean	RSD
1	fine	78	102	1.8	85	30	136	70		
2	medium	62	82	17.7	64	72	71	37		
13	coarse	81	131	4.6	119	10	108	17	103	10
14	coarse	74	89	4.1			87	58	81	48
15	coarse	100	162	0.5	130	38			155	18

There does not appear to be a dependency of RSD with grain size.

With an RSD of 56%, the median for smooth surface analysis by HH-C, 15 analyses would be required to obtain a mean value of V within 30% of the true concentration.

W, tungsten (1-43 ppm)

Only three samples contain more than 2 ppm W. HH-A reports on only these three but HH-C reports on all, and obviously has a high background of 13-29 ppm for the samples containing <2 ppm W (Fig. 5.1.46). Results for the three samples are shown below. HH-A reports low for the means (probably corrected through recalibration) and, as mentioned, HH-C is high. These samples are too few to examine variation in RSD with surface but the data do suggest that the rough surface analysis is inferior to smooth for sample 13 but, given the opposite trends between instruments for samples 14 and 15, general conclusions are precarious.

Table 5.1.11. Results for W (in ppm, RSD in %) in (coarse) granodiorites containing W > 2 ppm

Sample	Lab	Powder		Smooth		Rough		Round	
		Mean	RSD	Mean	RSD	Mean	RSD	Mean	RSD
13	43	20.7	14.0	25.1	34	27.8	51	25.0	36
13	*43*	*62.3*	*9.0*	*61.3*	*38*	*75.3*	*57*	*58.4*	*48*
14	30	17.3	14.5			13.0	34	13.1	63
14	*30*	*54.2*	*14.5*			*32.1*	*50*	*44.6*	*32*
15	42	28.3	2.0	16.0	44			18.6	30
15	*42*	*73.3*	*9.0*	*49.1*	*38*			*44.0*	*45*

HH-A results in Roman. *HH-C in italics*

Yttrium, Y (1.4-18.8 ppm)

HH-C reports Y in the mining mode but only three decimal places were used and hence the results are rounded to the nearest decade, not adequate at this low level. The calibration by HH-A is excellent, with an r^2 of 0.96 and slope of unity (Fig. 5.1.47). The median RSDs are 41% for smooth surface analysis and 33% for rough. The plot of rough versus smooth is actually good (r^2

of 0.85, slope of unity), even at these low levels (Fig. 5.1.48). There is no obvious dependency of RSD on grain size: the RSD for smooth surface analysis of the very fine sample is only 13% but the median RSDs for other grain size categories all hover around 40%.

With an RSD of 41%, the median for smooth surface analysis by HH-A, seven analyses would be required to obtain a mean value of Y within 30% of the true concentration.

Zn, zinc (13-131 ppm)
The calibration plots are excellent for Zn by both instruments (HH-A, r^2 of 0.98, slope of 0.83; HH-C, r^2 of 1.0, slope of 0.89) (Fig. 5.1.49). However, the plots of smooth and rough versus powder for both are quite noisy (HH-A, r^2 of 0.75 and 0.58; HH-C, r^2 of 0.69 and 0.64) (Fig. 5.1.50). The graphs of rough versus smooth for both have steep slopes of 1.7 which is caused by samples 1, 3 and 19 especially reporting higher means in the rough analysis, presumably owing to an area more concentrated in Zn being analysed (Fig. 5.1.51).

Median RSDs for the smooth and rough surface analysis are 36 and 33% for HH-A and 41% and 37% for HH-C, all very similar, as are the figures for the few round surface analyses. There is no dependency of RSD with grain size (Fig. 5.1.52).

With an RSD of 36%, the median for smooth surface analysis by HH-A, 6 analyses would be required to obtain a mean value of Zn within 30% of the true concentration.

Zr, zirconium (64-234 ppm)
Calibration graphs are excellent for Zr, with r^2 values of 0.94 and 0.92 for HH-A and HH-C, and slopes of 1.1 (Fig. 5.1.53). The sequence plots, together with those of smooth and rough versus powder, show that the smooth and rough surface analyses often result in lower values than those for the powder (Figs. 5.1.54 and 5.1.55). The agreement in mean values between smooth and rough surface analysis is excellent for both HH-A and HH-C (Fig. 5.1.56). The median RSDs for smooth and rough analysis are 23 and 22% for HH-A and 33 and 27% for HH-C. The only real distinction in median RSD with grain size for both instruments is that the very fine sample has an usually low RSD (3.7 and 8.0% by HH-A and HH-C, smooth surface).

The table below demonstrates the lower mean values for the smooth and rough surface analysis compared to powder, a phenomenon that is evident for other elements.

Table 5.1.12. Results for Zr (in ppm, RSD in %) in selected granodiorites

Sample		Lab	Powder		Smooth		Rough	
			Mean	RSD	Mean	RSD	Mean	RSD
1	fine	119	130	5	62	46	86	38
1	*fine*	*119*	*83*	*7*	*40*	*59*	*65*	*70*
2	medium	123	157	9	107	21	114	21
2	*medium*	*123*	*103*	*15*	*64*	*29*	*73*	*30*
4	very coarse	171	184	2	93	26		
4	*very coarse*	*171*	*127*	*9*	*70*	*43*		
9	coarse	137	127	3	80	56	96	64
9	*coarse*	*137*	*77*	*27*	*33*	*65*	*44*	*67*

HH-A results in Roman. *HH-C in italics*

With an RSD of 23%, the median for smooth surface analysis by HH-A, three analyses would be required to obtain a mean value of Zr within 30% of the true concentration.

Summary of granodiorite surface study

Below are tables summarising the median RSD values for the different surface analyses of the granodiorites; elements where performance was very poor (interferences or concentrations too low) have been removed. Some of the median RSDs for HH-C (Table 5.1.14) are significantly higher than those for HH-A (Table 5.1.13) but this is due mostly to the fact that the former instrument reports on many more samples with low concentrations of that particular element (e.g. As, Cu, Mo).

- There is an overwhelming difference between the RSDs of powder and direct surface analysis, as can be seen in these tables. Consequently, in many cases, it may be necessary to grind samples to powder before analysis.
- With a few exceptions (Cu, Al, Si), the median RSD of smooth surface analysis is equivalent to that of rough surface analysis, and to that of round surface analysis (note there were only four samples in the rough suite). This is not necessarily true on an *individual* sample basis but certainly the data by both instruments show that, in general, it is. Rough surface analysis for Al and Si is inferior to that of the smooth because of the (variable) presence of air, which absorbs low-energy photons, between sample and XRF window.
- In the surface analysis, many elements such as Al, Ca, Co, Cu, Nb, Pb, Si and Sr show an increase in RSD with grain size, whereas other elements such as Fe, K, Mg, Mn, P, Rb, S, Ti, Y, Zn and Zr do not. There is no relationship between RSD and grain size in powdered samples, as expected.

- There is a tendency for results by smooth surface analysis, and to a lesser degree by rough surface analysis, to be lower in concentration than those using the powder. These elements include Fe, Mo, Mn, V and Zr.
- Quite often a value above detection limit will be reported in a direct surface analysis but not in the corresponding powder (presumably owing to a dilution effect in the powder).
- The granodiorite matrix allows for the accurate determination by pXRF of some trace elements at very low concentrations; these include Nb, Se, Th and Y.

It should be borne in mind that these conclusions pertain to this sample matrix.

Table 5.1.13. Summary of median RSDs using HH-A

	A. Mining mode			
	Median RSD, %			
	Smooth	**Rough**	**Round**	**Powder**
Si	6	13	8	1.5
Al	13	21	16	2.5
S	23	34	48	1.8
Ca	27	35	24	0.9
Ti	28	29	29	3.6
Fe	36	38	32	0.7
K	44	40	38	1.1
	B. Soil mode			
	Median RSD, %			
	Smooth	**Rough**	**Round**	**Powder**
Sr	15	17	16	0.9
Th	19	20	17	7.7
Zr	23	22	39	3.0
As	24	23	39	8.1
Cu	26	69	85	1.2
Pb	27	27	46	6.1
Co	27	33	33	4.4
Rb	30	27	29	1.1
Mn	35	43	35	1.6
Zn	36	33	41	3.3
Nb	37	37	21	6.2
Mo	38	93	51	2.5
Y	41	32	46	6.4

Table 5.1.14. Summary of median RSDs using HH-C

A. Mining mode			
Median RSD, %			
Smooth	**Rough**	**Round**	**Powder**
Si	6	10	7	1.0
Al	16	22	13	2.7
Mg	28	31	34	14.7
Ca	28	31	31	1.0
K	42	40	36	0.9
P	46	57	50	11.2
Fe	49	46	53	1.1
Ti	53	47	38	3.2
S	54	81	74	5.6

B. Soil mode			
Median RSD, %			
Smooth	**Rough**	**Round**	**Powder**
Sr	15	24	22	0.8
Zr	34	27	45	5.5
Th	37	42	48	11.0
Rb	39	46	31	1.3
Mn	40	33	26	4.0
Zn	41	37	41	6.5
Cu	49	62	97	24.9
Ba	52	55	43	1.9
V	56	58	33	4.8
Pb	60	80	66	9.1
Se	62	67	44	33.7
As	65	60	60	44.2
Mo	112	105	120	15.5
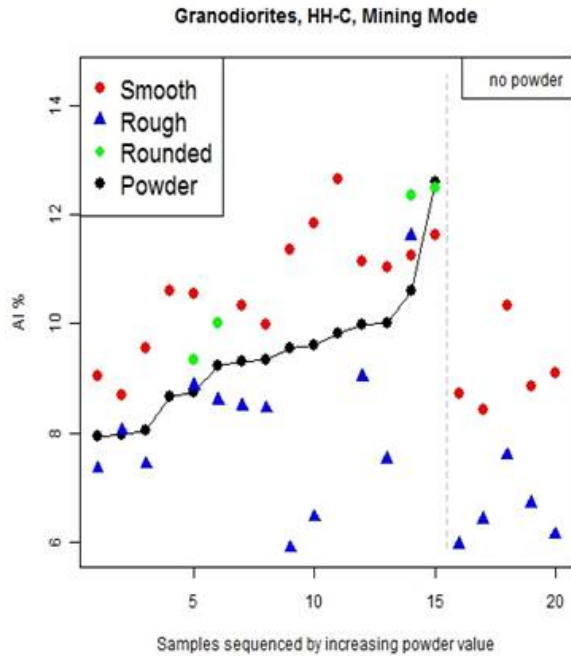
Fig 5.1.1. Granodiorite_HHC_mining_Al.1.jpg.
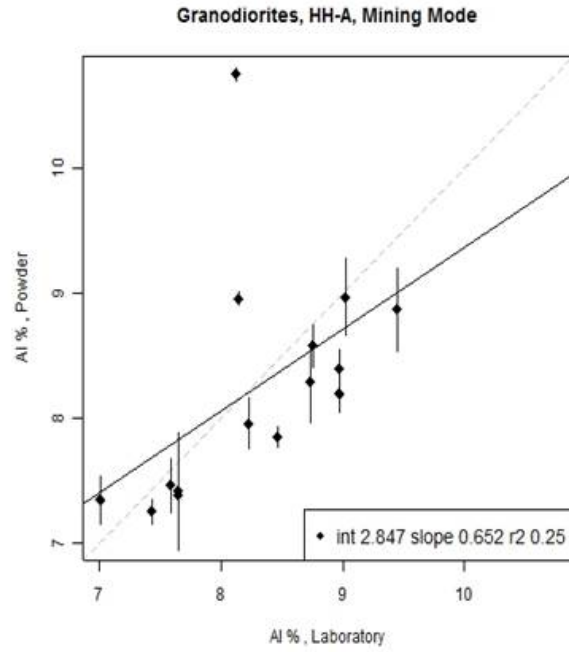
Fig. 5.1.2. Granodiorite_HH-A_mining_Al.3.jpg.
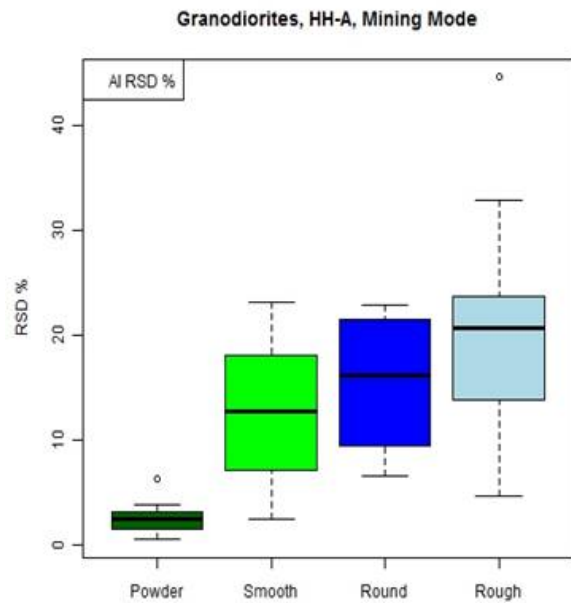
Fig. 5.1.3. Granodiorite_HHA_mining_Al.5.jpg.
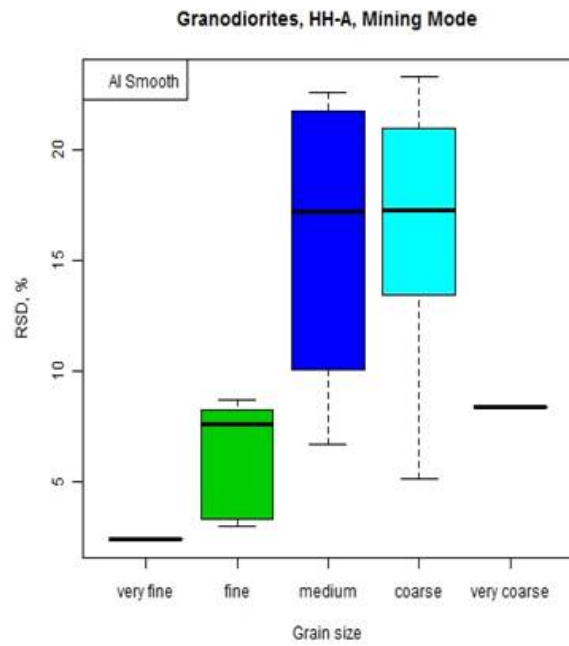
Fig. 5.1.4. Granodiorite_HHA_mining_Al.6.jpg.
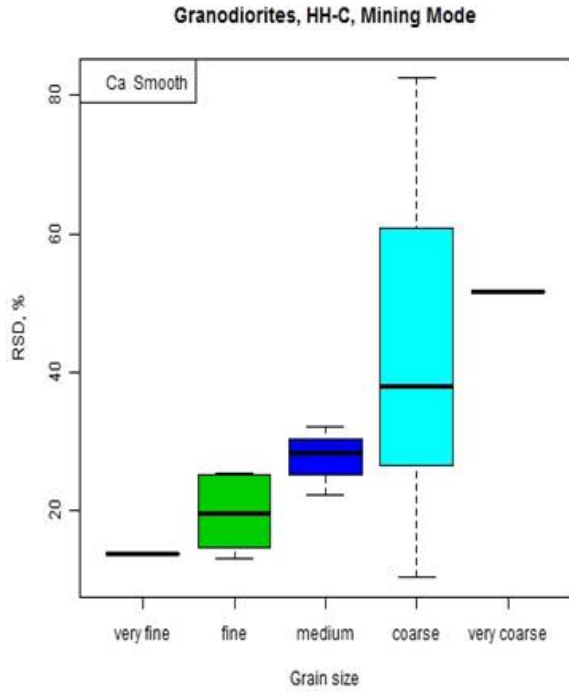
Fig. 5.1.5. Granodiorite_HHC_mining_Ca.6.jpg
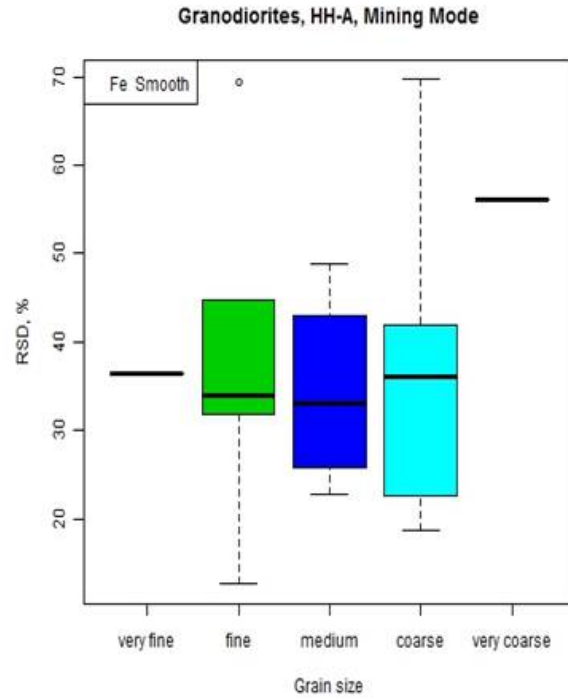
Fig. 5.1.6. Granodiorite_HHA_mining_Fe.6.jpg
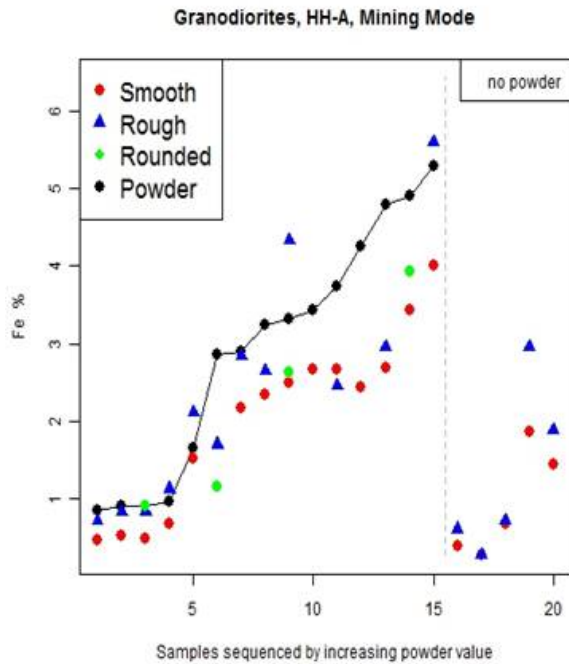
Fig. 5.1.7.
Granodiorite_HHA_mining_Fe.1.jpg.
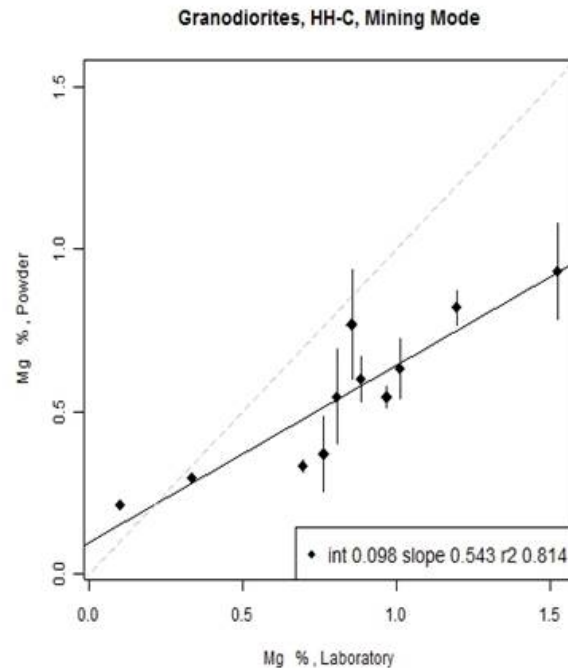
Fig. 5.1.8.
Granodiorite_HHC_mining_Mg.3.jpg.

Granodiorites, HH-C, Mining Mode
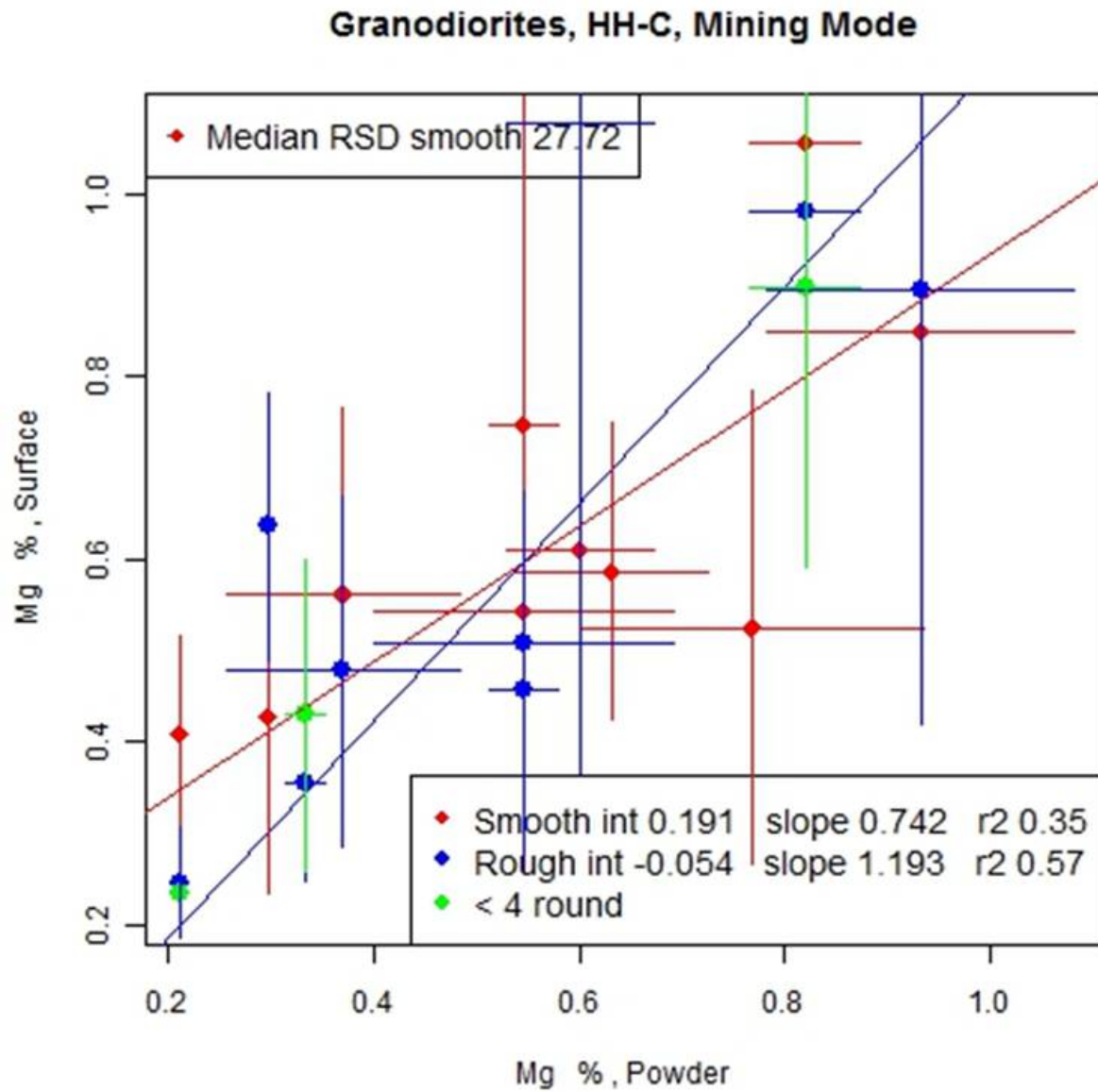
Fig. 5.1.9. Granodiorite_HHC_mining_Mg.2.jpg.

Granodiorites, HH-A, Mining Mode

int -0.177 slope 1.306 r2 0.983
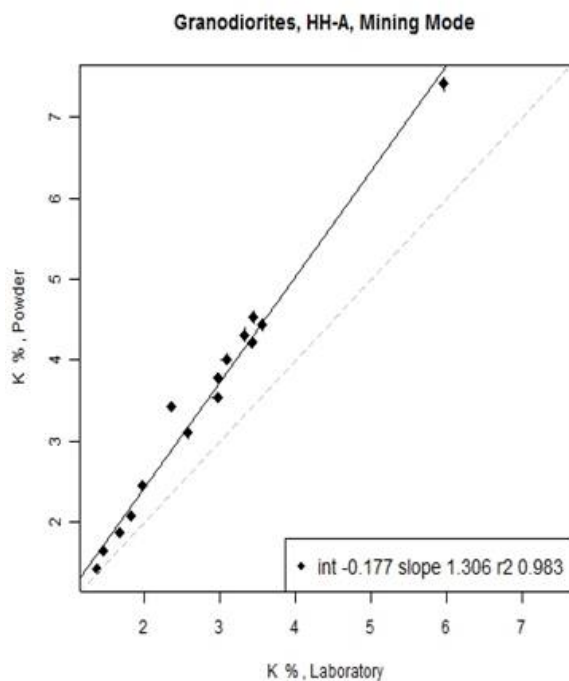
Fig. 5.1.10.
Granodiorite_HHA_mining_K.3.jpg.

Granodiorites, HH-A, Mining Mode

Smooth
Rough
Rounded
Powder

no powder

Si %

Samples sequenced by increasing powder value
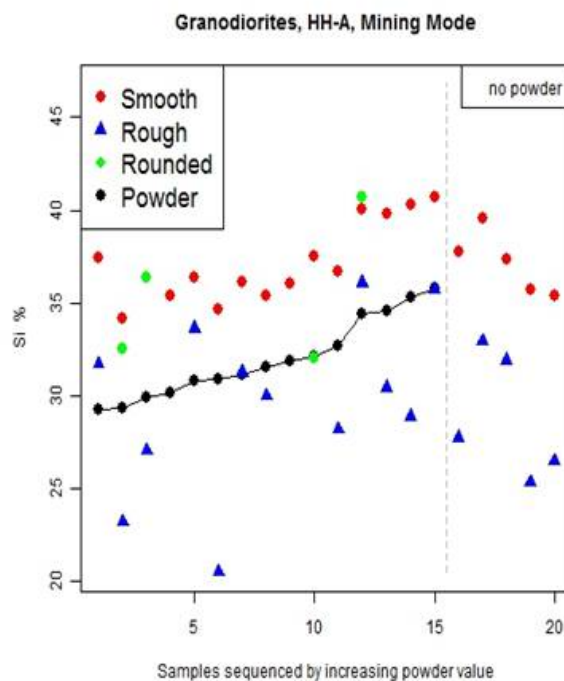
Fig. 5.1.11.
Granodiorite_HHA_mining_Si.1.jpg.

Granodiorites, HH-C, Mining Mode

Mean Si %

Si %

Lab Powder Smooth Round Rough
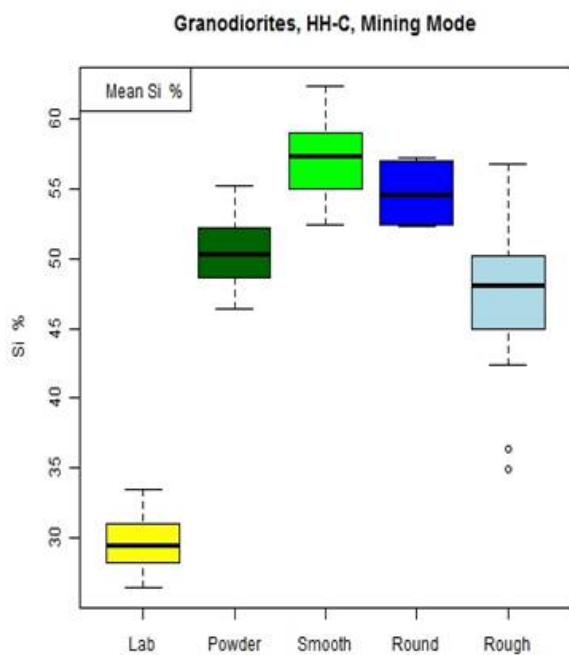
Fig. 5.1.12.
Granodiorite_HHC_mining_Si.4.jpg.

Granodiorites, HH-A, Mining Mode

Si RSD %

RSD %

Powder Smooth Round Rough
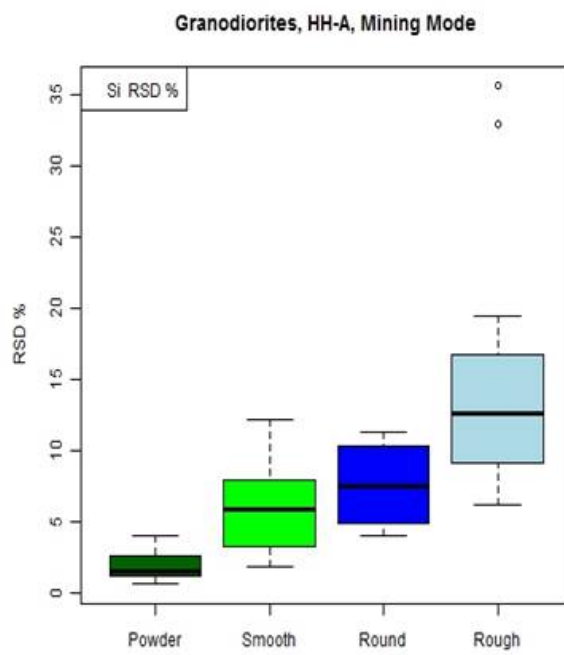
Fig. 5.1.13.
Granodiorite_HHA_mining_Si.5.jpg.
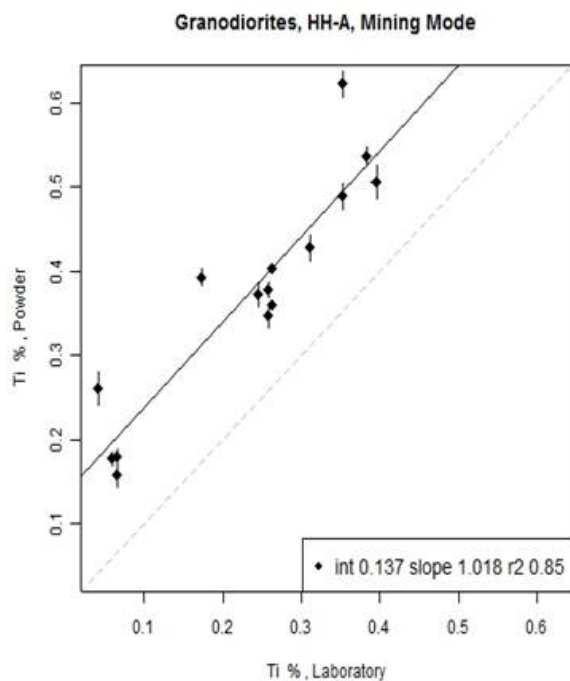
Fig. 5.1.14.
Granodiorite_HHA_mining_Ti.3.jpg.
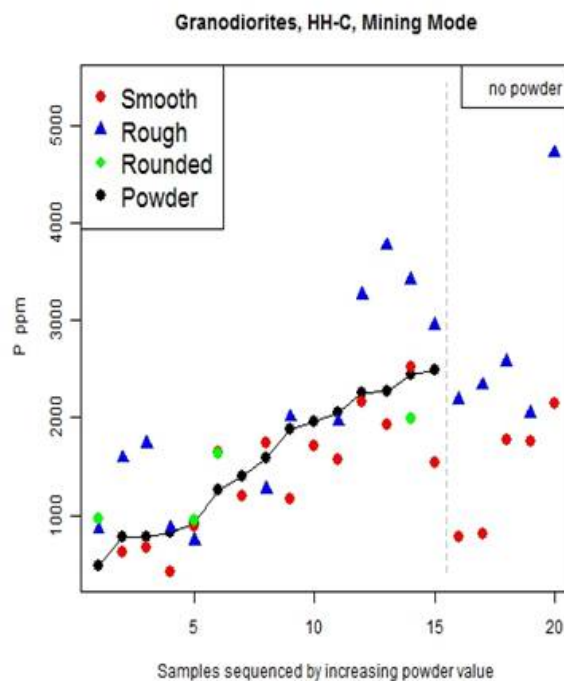
Fig. 5.1.15.
Granodiorite_HHC_mining_P.1.jpg.
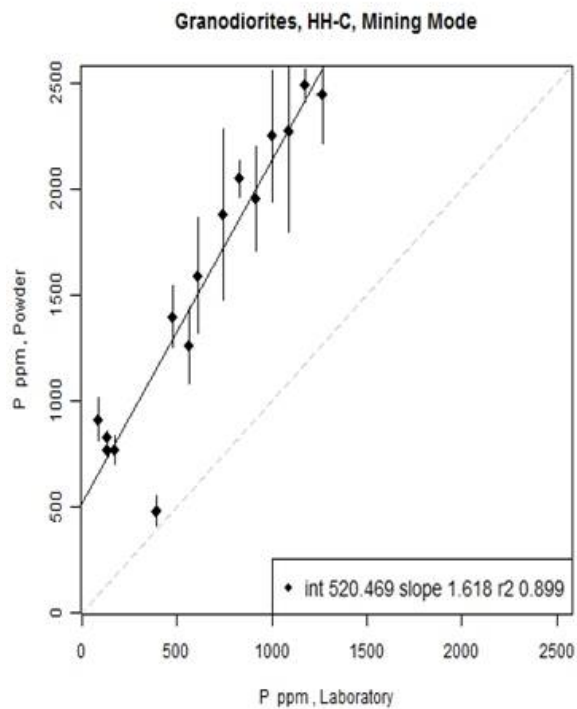
Fig. 5.1.16.
Granodiorite_HHC_mining_P.3.jpg.
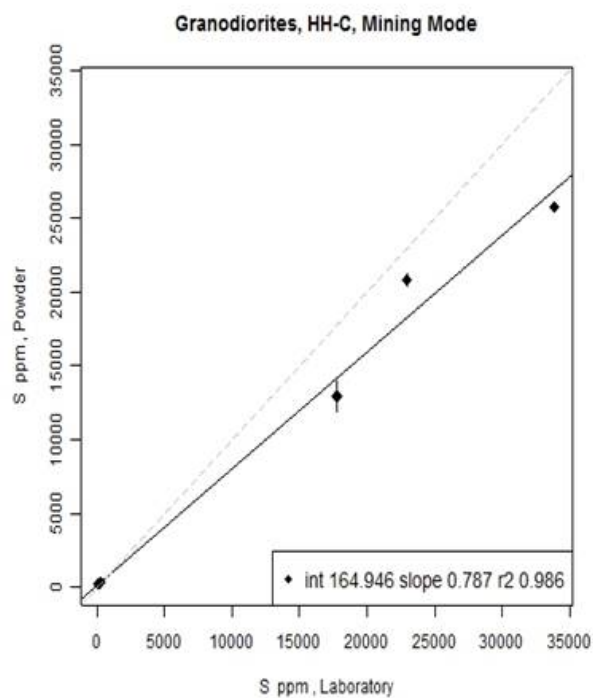
Fig. 5.1.17.
Granodiorite_HHC_mining_S.3.jpg.
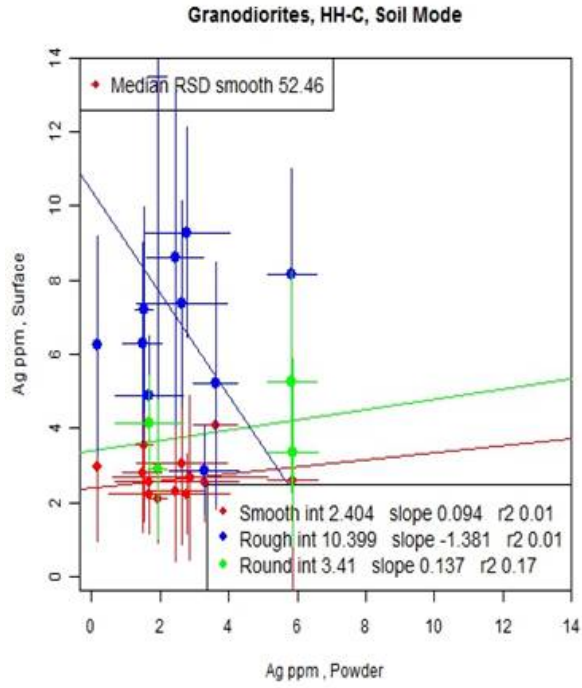
Fig. 5.1.18. Granodiorite_HHC_soil_Ag.2.jpg.
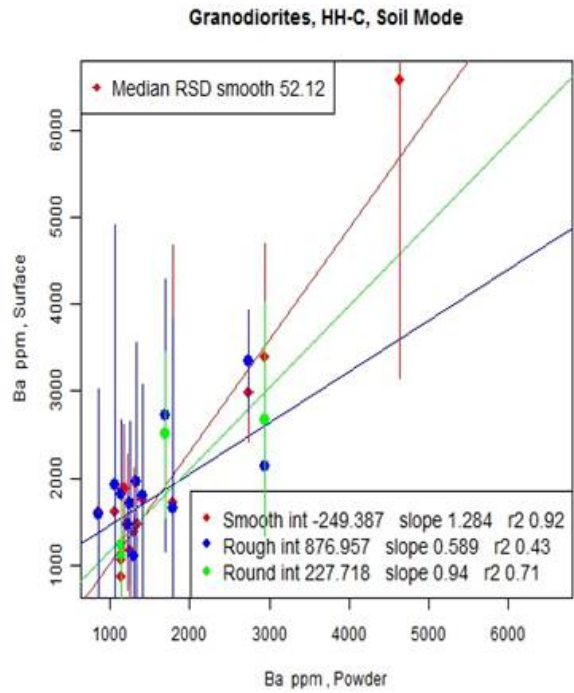
Fig. 5.1.19. Granodiorite_HHC_soil_Ba.2.jpg.

Granodiorites, HH-A, Soil Mode
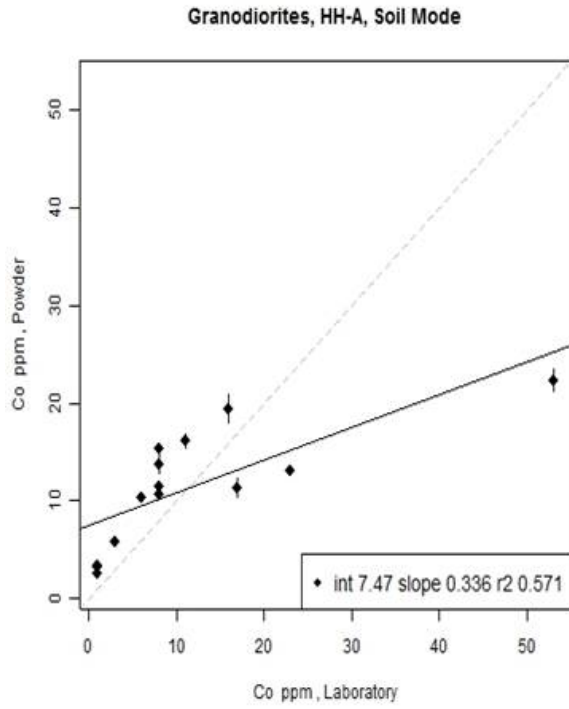
Fig. 5.1.20. Granodiorite_HHA_soil_Co.3.jpg.

Granodiorites, HH-A, Soil Mode
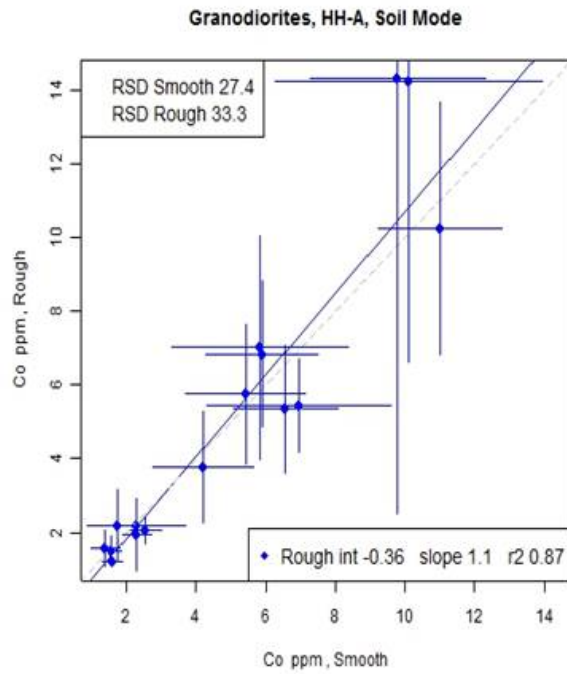
Fig. 5.1.21. Granodiorite_HHA_soil_Co.2.jpg.

Granodiorites, HH-A, Soil Mode
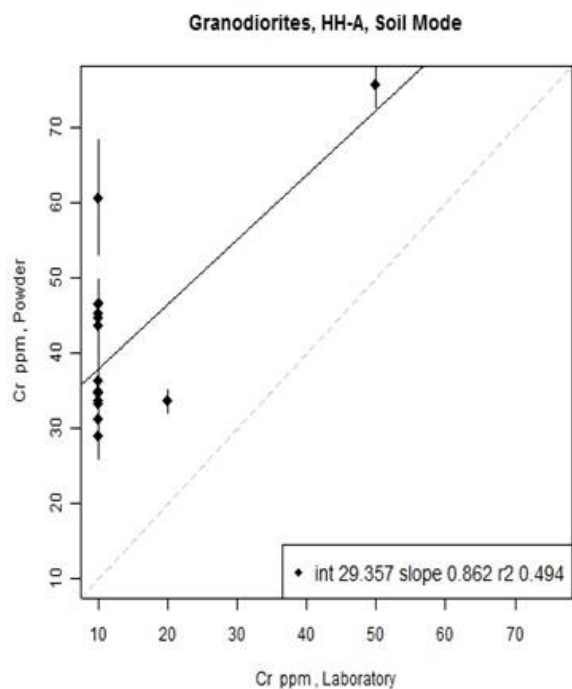
Fig. 5.1.22. Granodiorite_HHA_soil_Cr.3.jpg.

Granodiorites, HH-A, Soil Mode
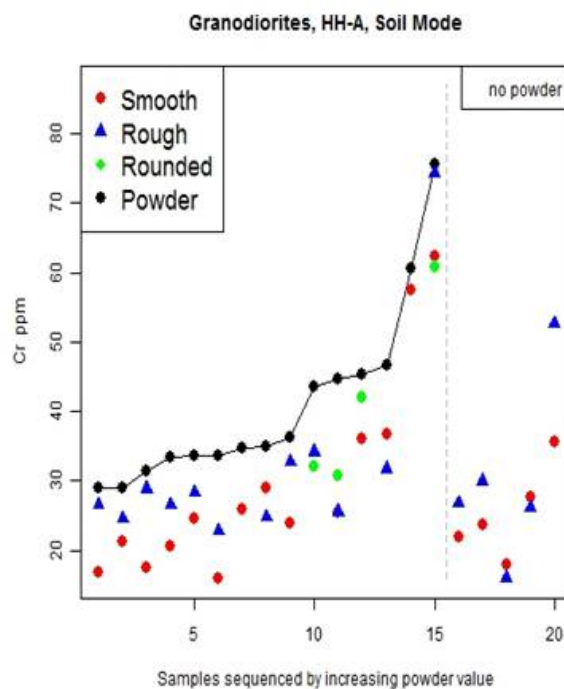
Fig. 5.1.23. Granodiorite_HHA_soil_Cr.1.jpg.

Granodiorites, HH-C, Soil Mode
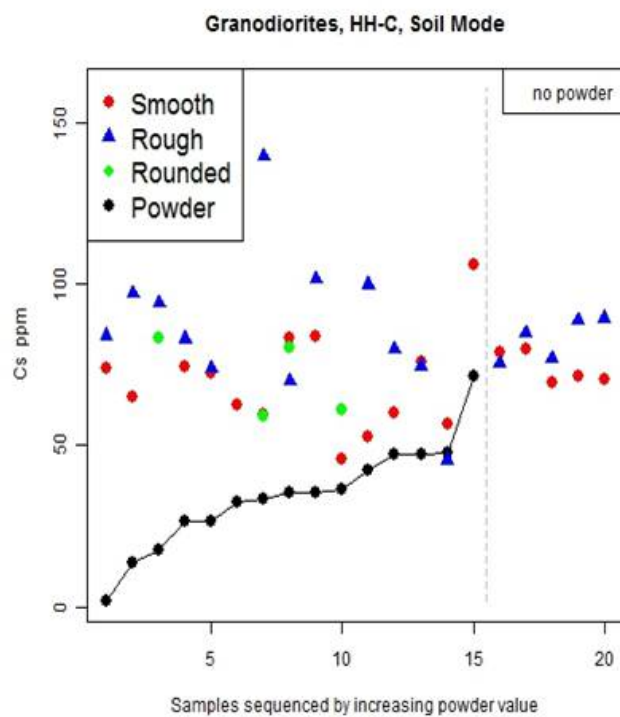
Fig. 5.1.24. Granodiorite_HHC_soil_Cs.1.jpg.

Granodiorites, HH-A, Soil Mode
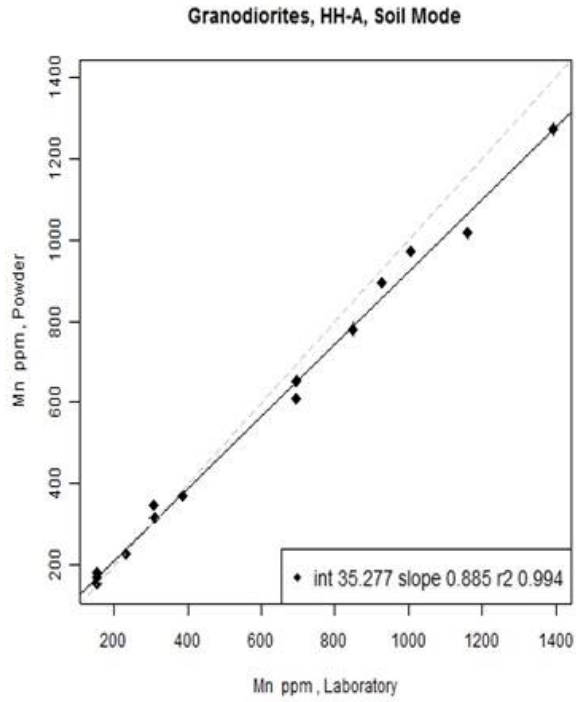
Fig. 5.1.25. Granodiorite_HHA_soil_Mn.3.jpg.

Granodiorites, HH-A, Soil Mode
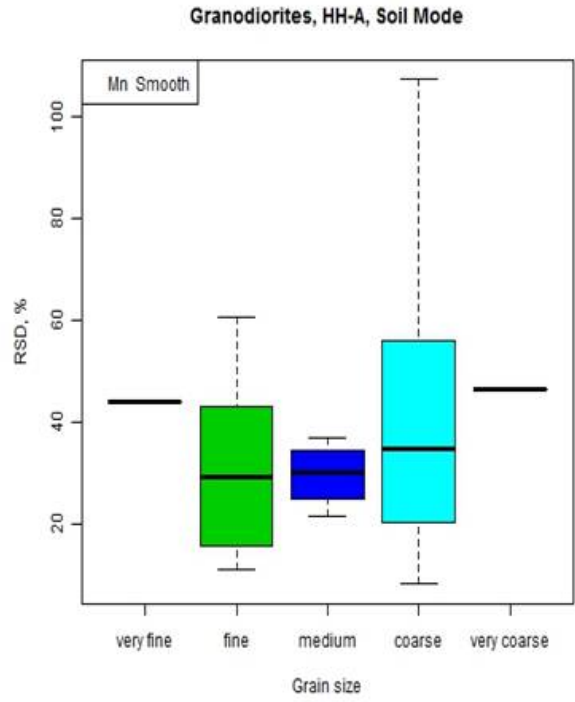
Fig. 5.1.26 Granodiorite_HHA_soil_Mn.6.jpg.

Granodiorites, HH-A, Soil Mode
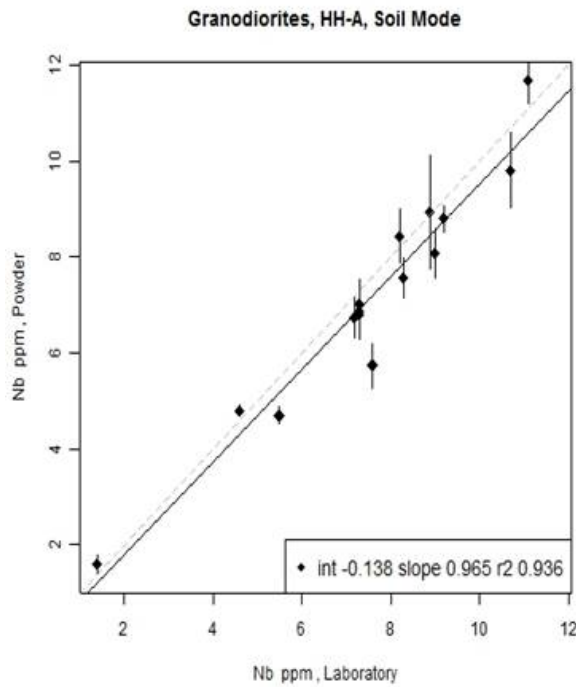
Fig. 5.1.27. Granodiorite_HHA_soil_Nb.3.jpg.

Granodiorites, HH-A, Soil Mode
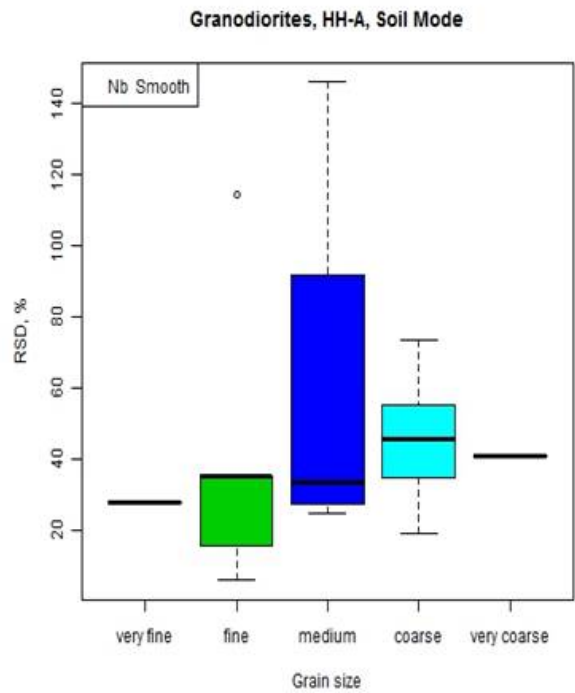
Fig. 5.1.28. Granodiorite_HHA_soil_Nb.6.jpg.

Granodiorites, HH-C, Soil Mode

Ni ppm, Powder

◆ int 45.15 slope 0.39 r2 0.016

Ni ppm, Laboratory
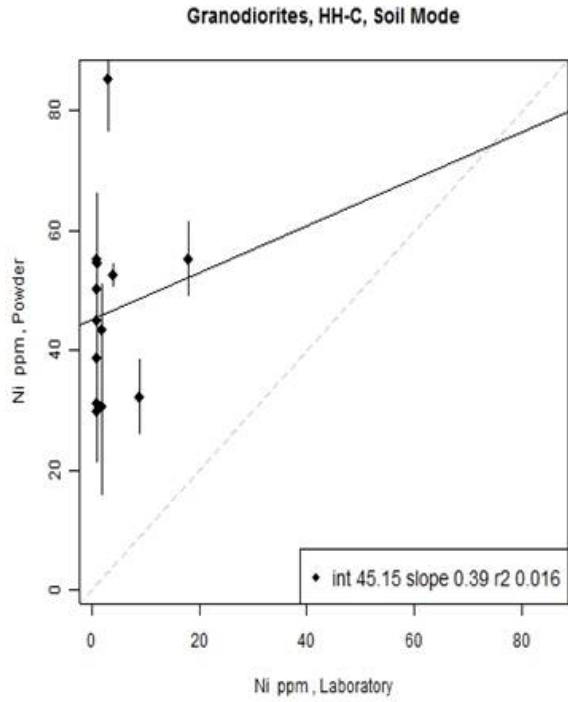
Fig. 5.1.29. Granodiorite_HHC_soil_Ni.3.jpg.

Granodiorites, HH-C, Soil Mode

Pb ppm, Powder

◆ int -6.813 slope 0.945 r2 0.939

Pb ppm, Laboratory
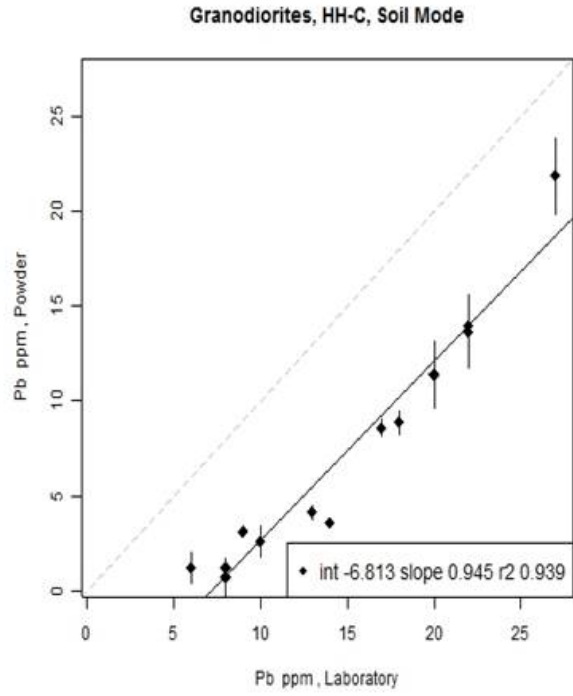
Fig. 5.1.30. Granodiorite_HHC_soil_Pb.3.jpg.

Granodiorites, HH-A, Soil Mode

Rb ppm, Powder

◆ int 6.25 slope 0.996 r2 0.995

Rb ppm, Laboratory
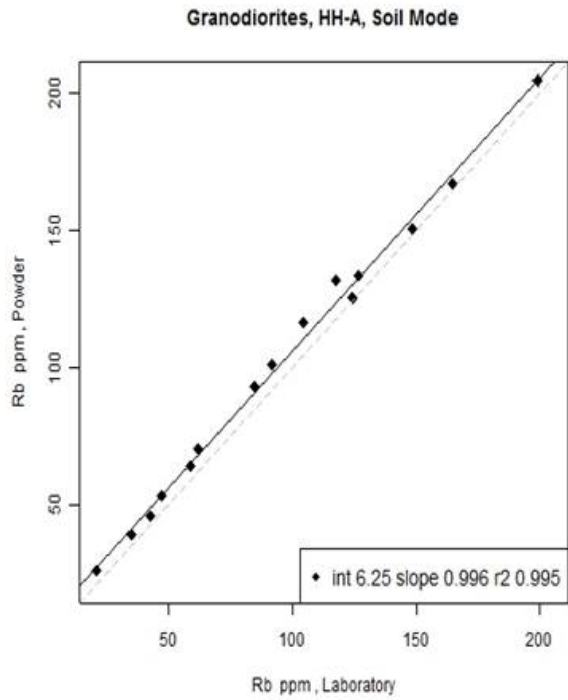
Fig. 5.1.31. Granodiorite_HHA_soil_Rb.3.jpg.

Granodiorites, HH-A, Soil Mode

Rb ppm, Surface

● Median RSD smooth 30.34

Smooth int -10.44   slope 1.011   r2 0.93
Rough int -13.474   slope 1.062   r2 0.97
Round int -7.308   slope 0.973   r2 0.97

Rb ppm, Powder
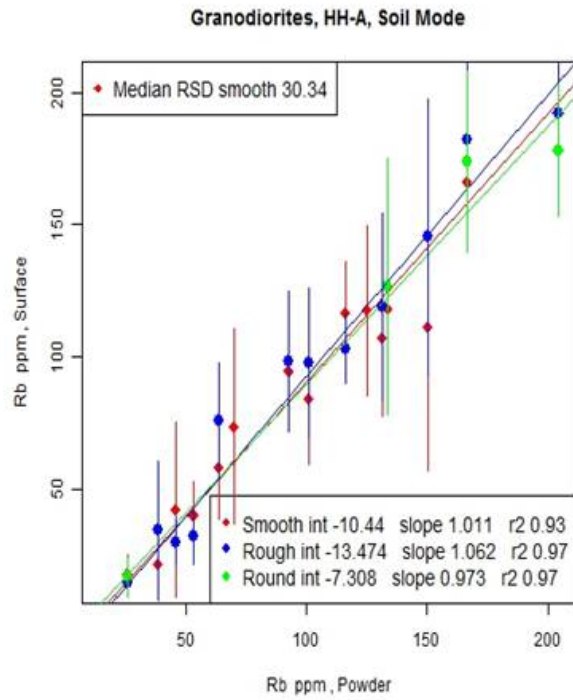
Fig. 5.1.32. Granodiorite_HHA_soil_Rb.2.jpg.

Granodiorites, HH-C, Soil Mode

int 0.818 slope 0.961 r2 0.911
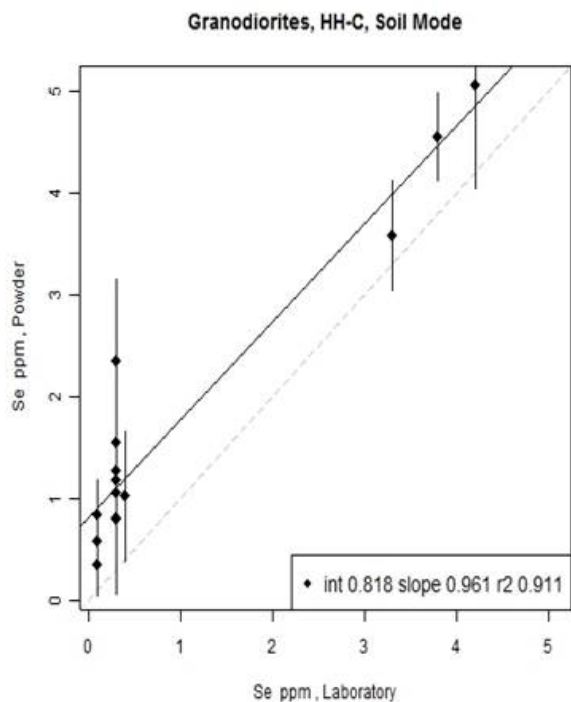
Fig. 5.1.33. Granodiorite_HHC_soil_Se.3.jpg.

Granodiorites, HH-C, Soil Mode

int 4.204 slope 0.653 r2 0.091
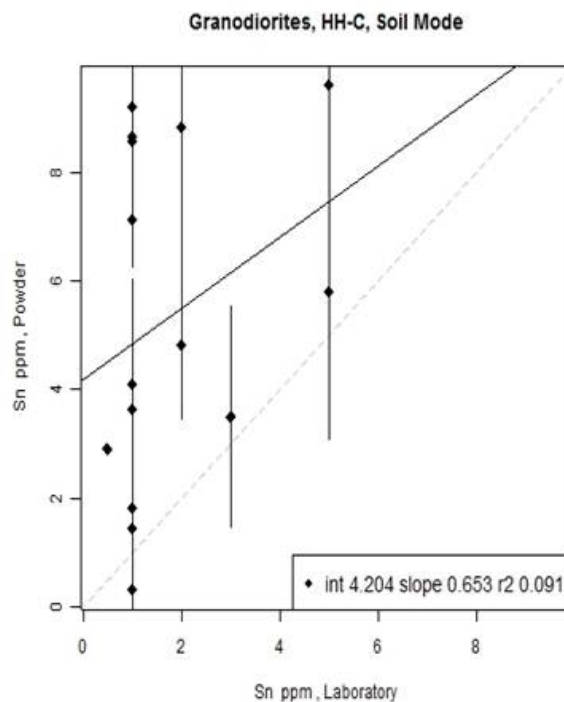
Fig. 5.1.34. Granodiorite_HHC_soil_Sn.3.jpg.

Granodiorites, HH-C, Soil Mode

int -10.163 slope 1.029 r2 0.997
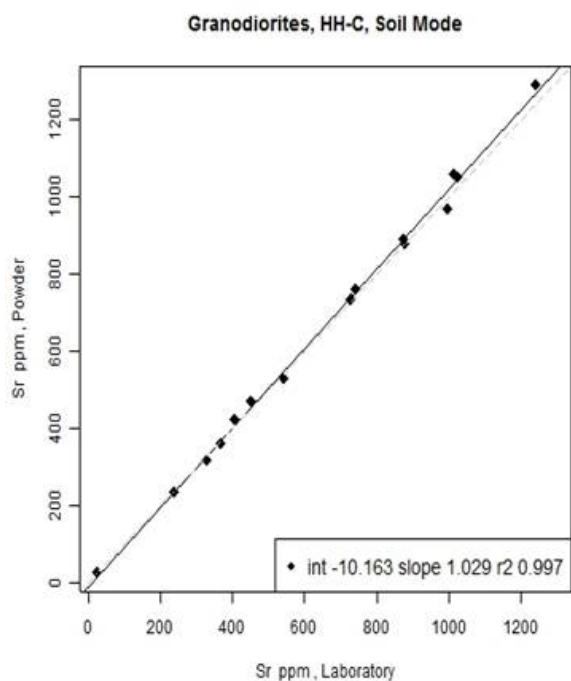
Fig. 5.1.35. Granodiorite_HHC_soil_Sr.3.jpg.

Granodiorites, HH-A, Soil Mode

Median RSD smooth 14.92

Smooth int -11.196 slope 1.058 r2 0.98
Rough int -53.277 slope 1.081 r2 0.98
Round int -1.406 slope 1.014 r2 1
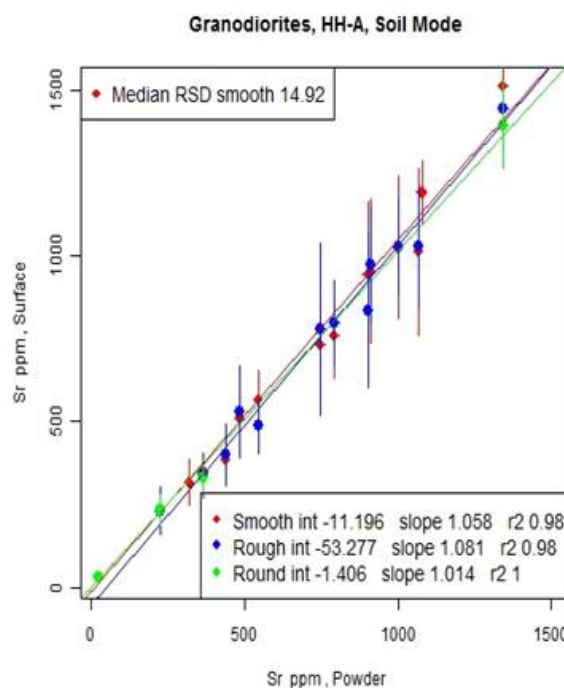
Fig. 5.1.36. Granodiorite_HHA_soil_Sr.2.jpg.
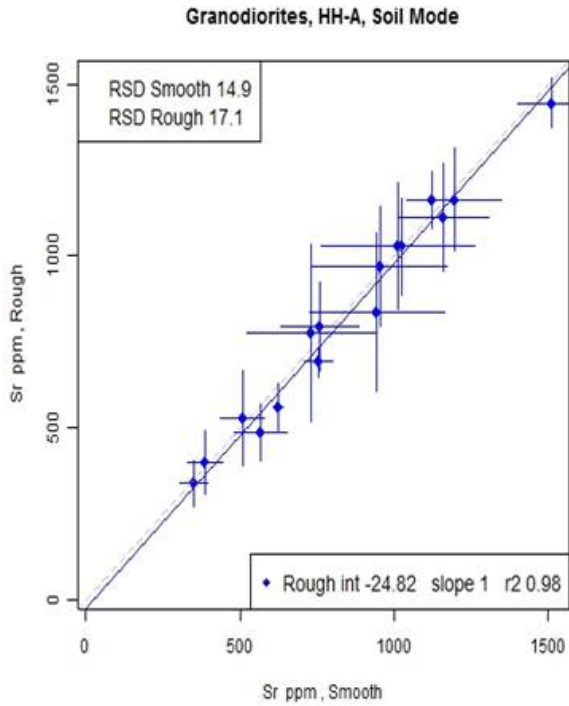
Fig. 5.1.37 Granodiorite_HHA_soil_Sr.8.jpg.
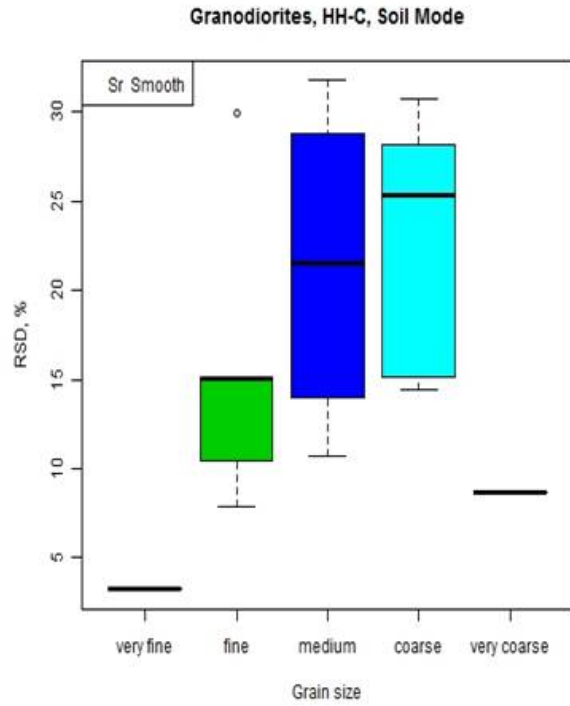
Fig. 5.1.38. Granodiorite_HHC_soil_Sr.6.jpg.
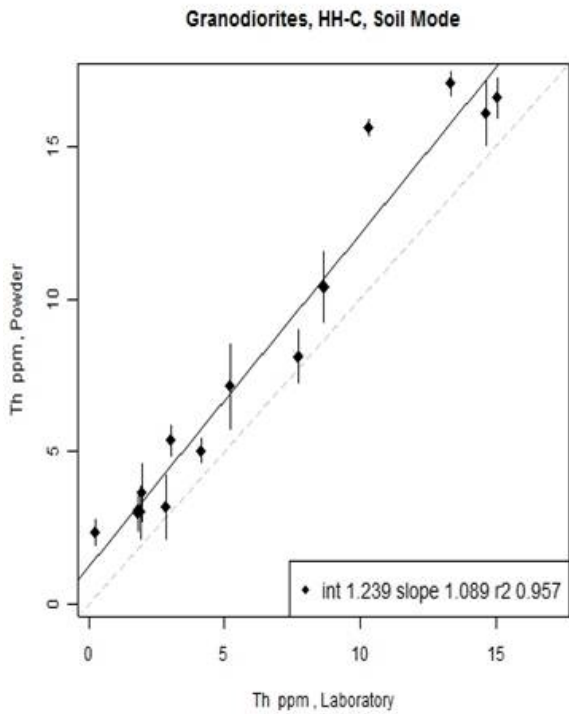
Fig. 5.1.39. Granodiorite_HHC_soil_Th.3.jpg.
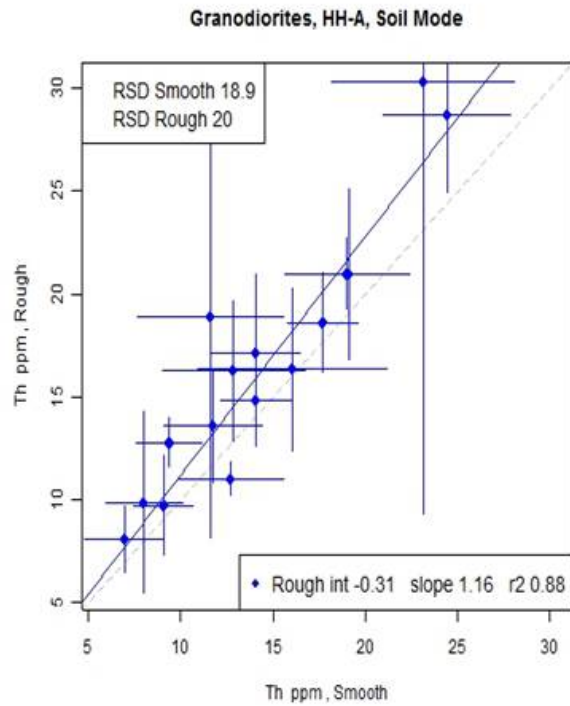
Fig. 5.1.40. Granodiorite_HHA_soil_Th.8.jpg.
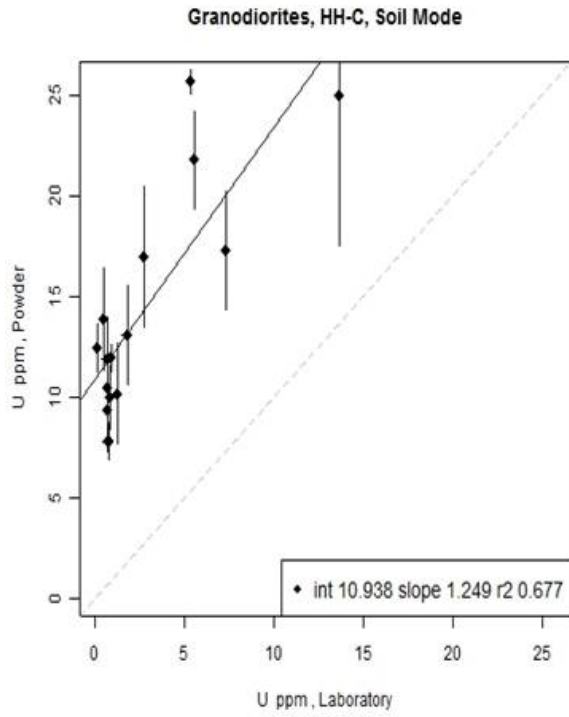
Fig. 5.1.41. Granodiorite_HHC_soil_U.3.jpg.
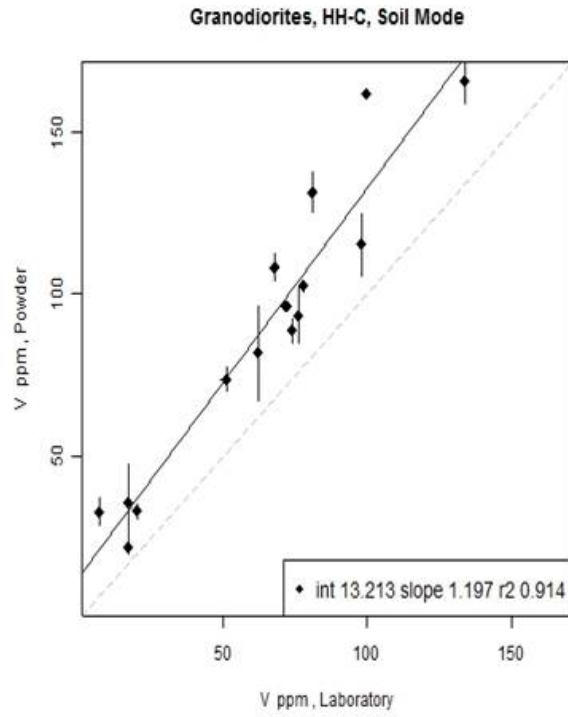
Fig. 5.1.42. Granodiorite_HHC_soil_V.3.jpg.
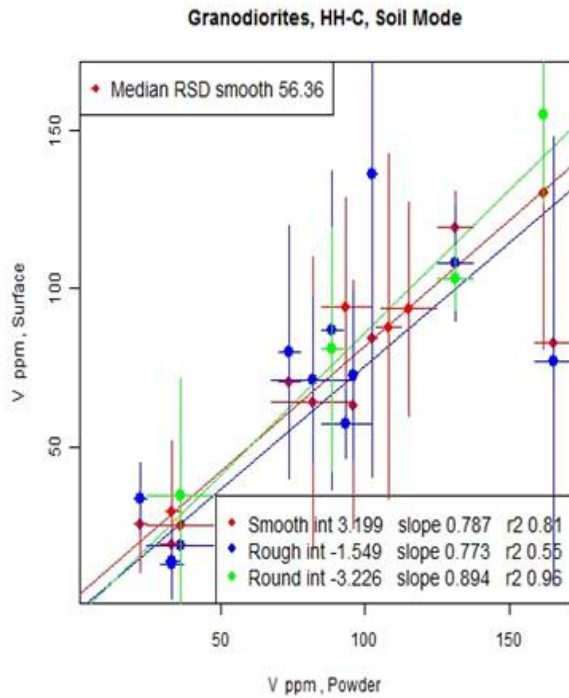
Fig. 5.1.43. Granodiorite_HHC_soil_V.2.jpg.
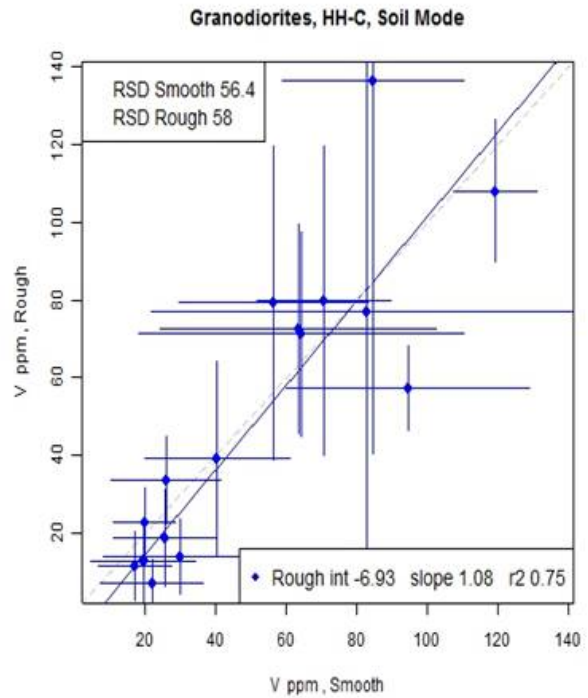
Fig. 5.1.44. Granodiorite_HHC_soil_V.8.jpg.

Granodiorites, HH-C, Soil Mode
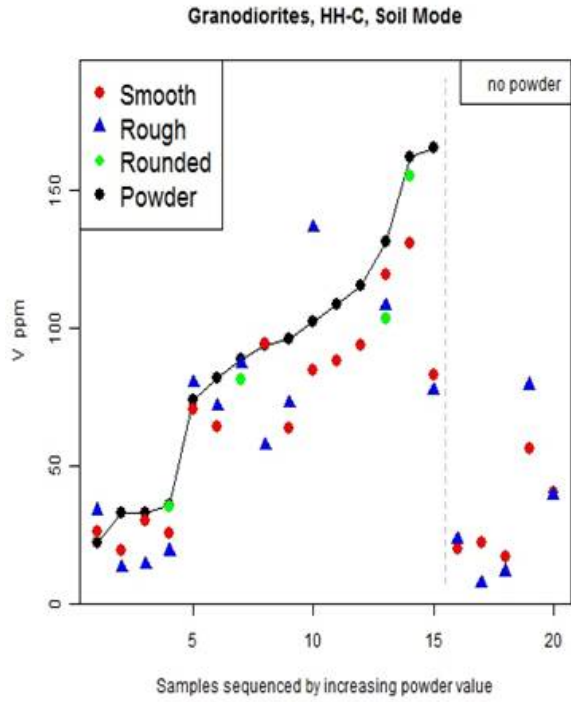
Fig. 5.1.45. Granodiorite_HHC_soil_V.1.jpg.

Granodiorites, HH-C, Soil Mode

int 23.848 slope 1.028 r2 0.808
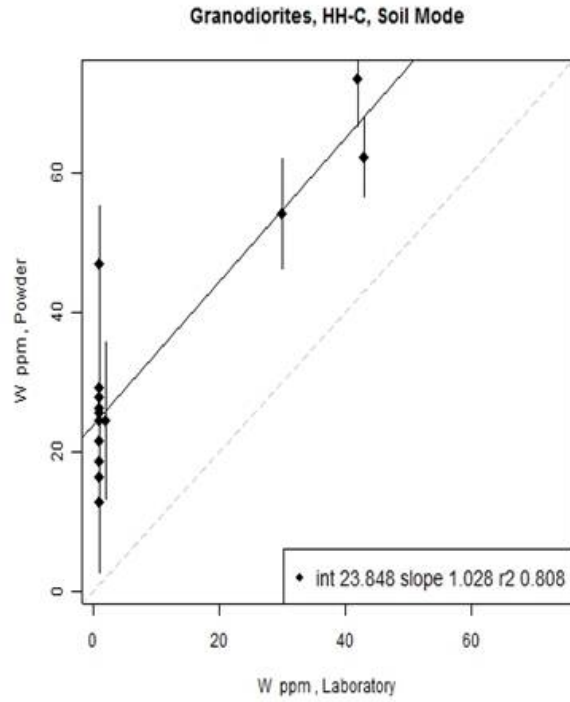
Fig. 5.1.46. Granodiorite_HHC_soil_W.3.jpg.

Granodiorites, HH-A, Soil Mode

int 0.461 slope 1.009 r2 0.961
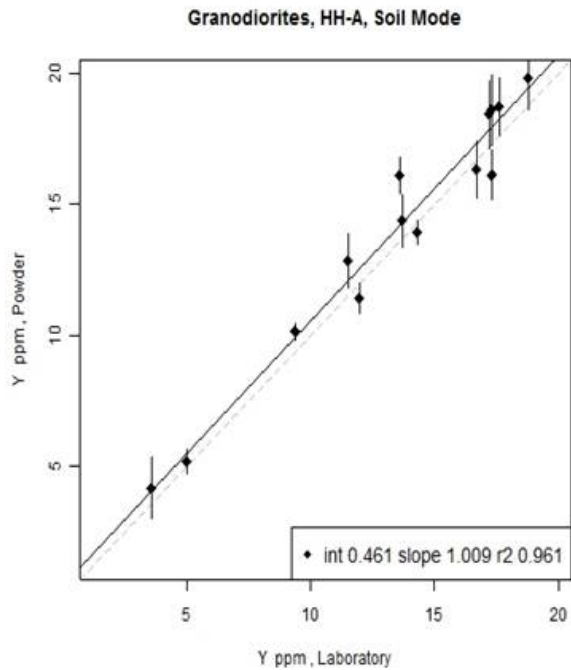
Fig. 5.1.47. Granodiorite_HHA_soil_Y.3.jpg.

Granodiorites, HH-A, Soil Mode

RSD Smooth 41.1
RSD Rough 32.5

Rough int 0.3   slope 1.04   r2 0.85
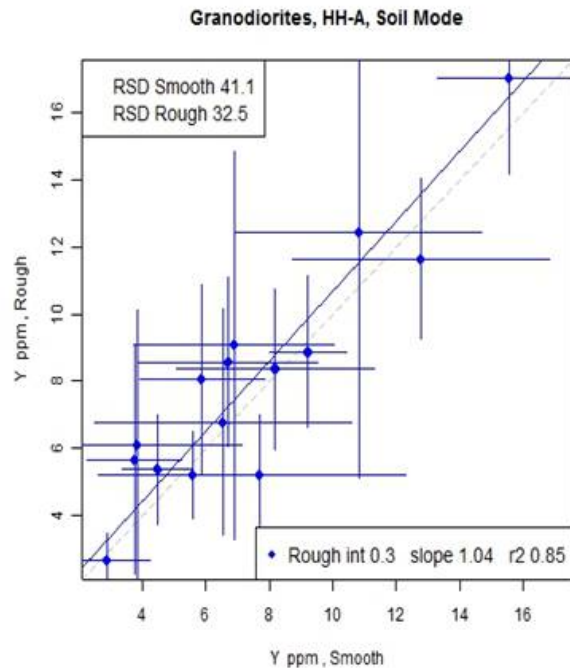
Fig. 5.1.48. Granodiorite_HHA_soil_Y.8.jpg.
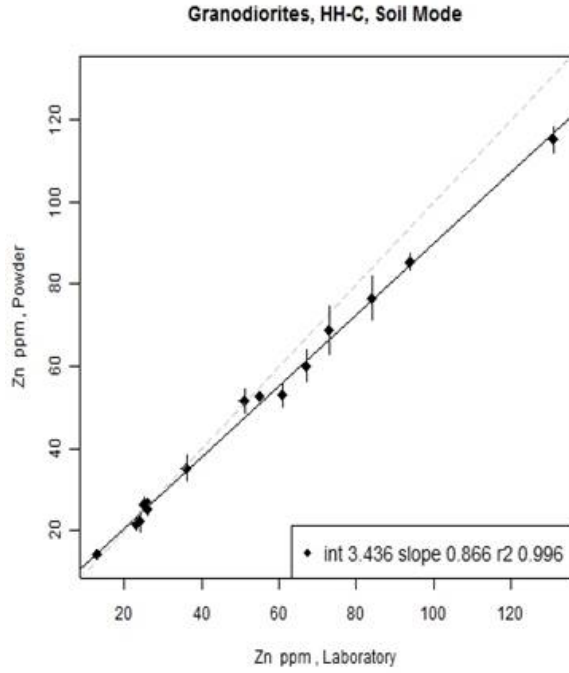
Fig. 5.1.49. Granodiorite_HHC_soil_Zn.3.jpg.
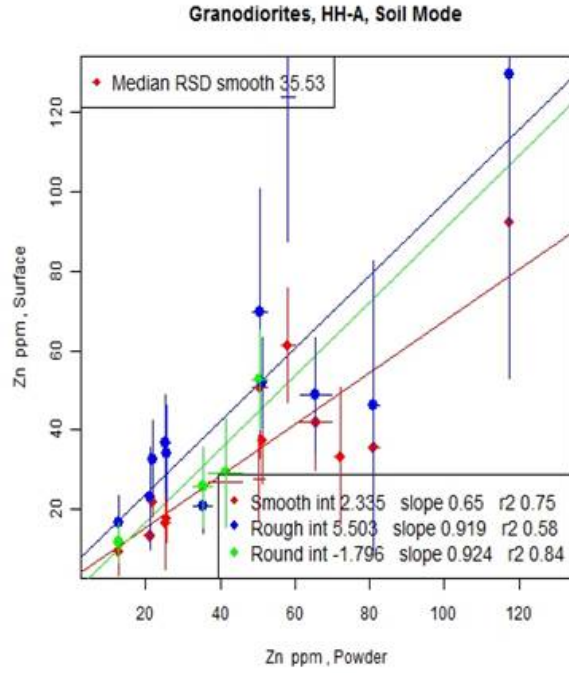
Fig. 5.1.50. Granodiorite_HHA_soil_Zn.2.jpg.
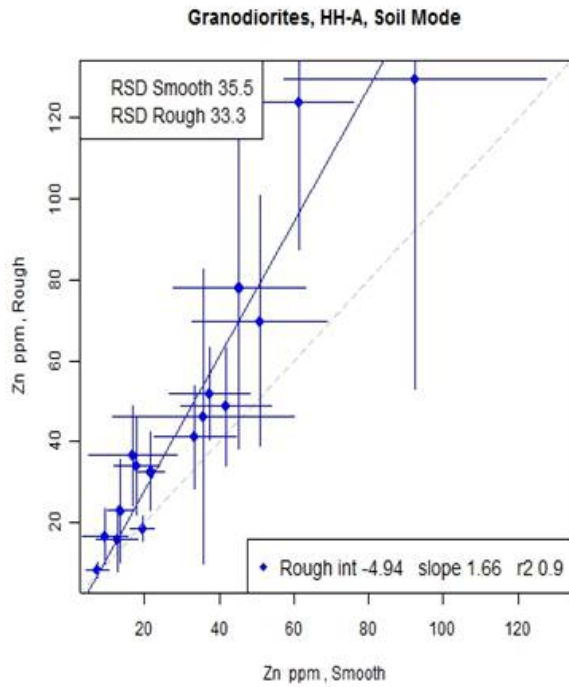
Fig. 5.1.51. Granodiorite_HHA_soil_Zn.8.jpg.
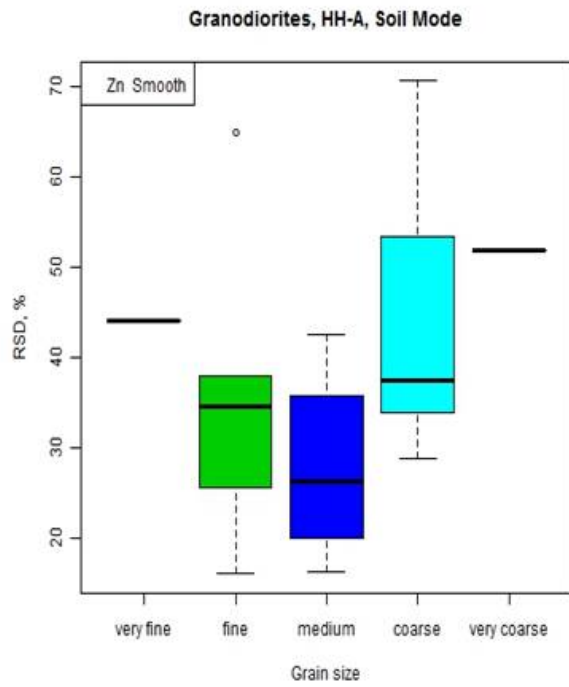
Fig. 5.1.52. Granodiorite_HHA_soil_Zn.6.jpg.

Granodiorites, HH-A, Soil Mode
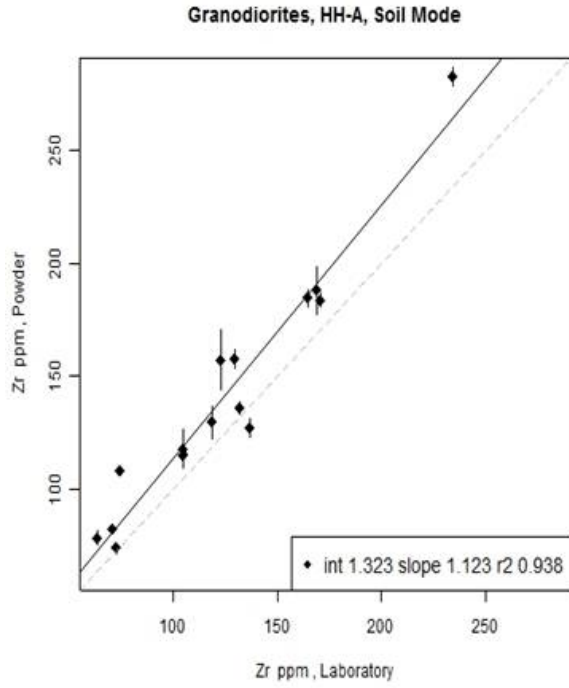
Fig. 5.1.53. Granodiorite_HHA_soil_Zr.3.jpg.

Granodiorites, HH-A, Soil Mode
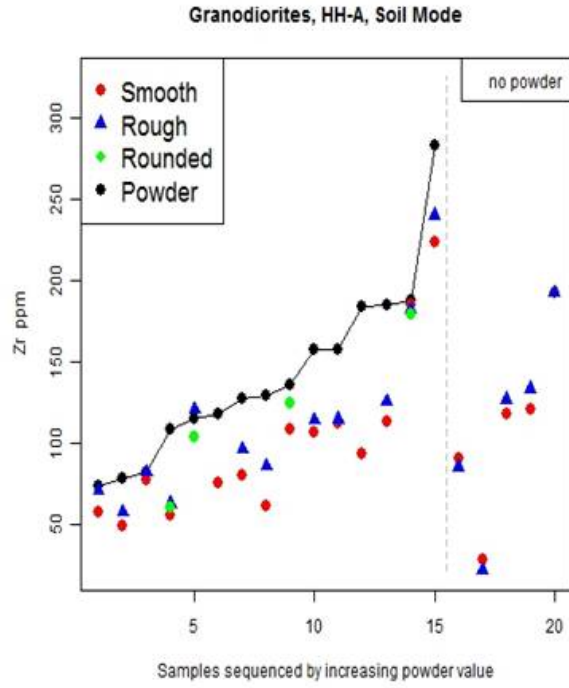
Fig. 5.1.54. Granodiorite_HHA_soil_Zr.1.jpg.

Granodiorites, HH-A, Soil Mode
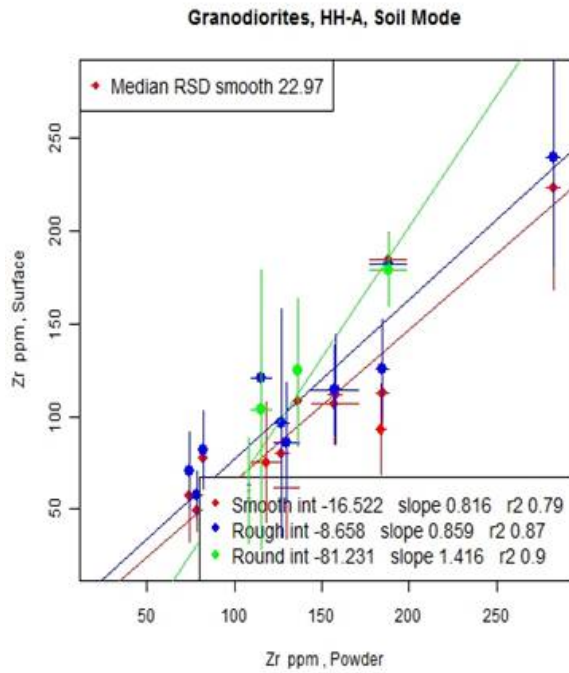
Fig. 5.1.55. Granodiorite_HHA_soil_Zr.2.jpg.

Granodiorites, HH-A, Soil Mode
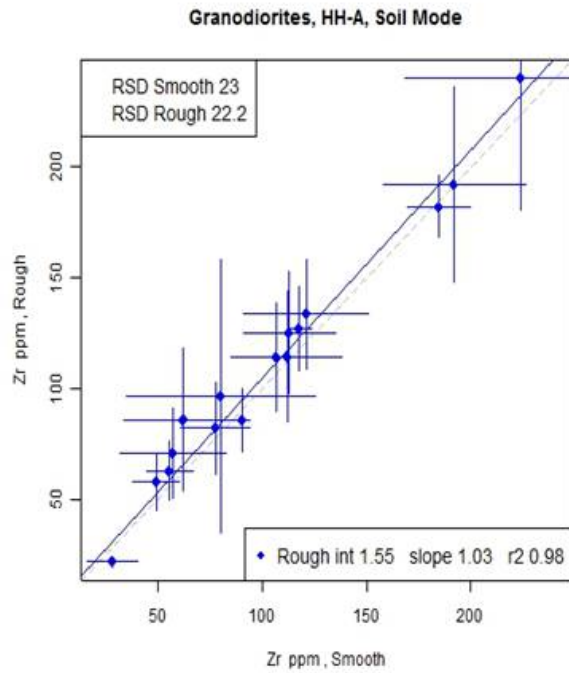
Fig. 5.1.56. Granodiorite_HHA_soil_Zr.8.jpg.

5.2. Group of 86 diverse rocks and ores from companies

Samples and methodology

Various sponsors submitted rock, core, and ore samples of particular interest to them and representative of the types of samples they would want to analyse by pXRF. They are listed in Table 5.2.1, together with the reference number used in this project, the classification we have used to group them, and their grain size as determined through visual inspection only. Note that sample numbers assigned have some gaps (numbers go up to 91, although only 86 samples analysed). Pictures of these samples are attached in the Appendix; they illustrate well the range in grain size and the heterogeneity of some of the ores and high REE samples in particular.

Table 5.2.1 Various rock and ore samples analysed by HH-A and HH-C

Sample #	Sample ID	Company	Rock Type	Reclassified	Grain Size
1	558931	V-metal	Zn-Pb ore, Murray Brook VMS	Ores	fine
2	558932	V-metal	Zn-Pb ore	Ores	medium
3	558933	V-metal	Zn-Pb ore	Ores	fine
4	558934	V-metal	Zn-Pb ore	Ores	fine
5	558935	V-metal	Zn-Pb ore	Ores	medium
6	558936	V-metal	Zn-Pb ore	Ores	fine
7		Anglo	Dacite	Felsic	medium
8	DDH 014 696	Anglo	Porphyry Cu	Ores	coarse
9	DDH 014 662	Anglo	Porphyry Cu	Ores	coarse
10	DDH 017 429	Anglo	Porphyry Cu	Ores	fine
11	DDH 015 351	Anglo	Porphyry Cu	Ores	fine
12		Vale	Granite breccia - core	Felsic	medium
13		Vale	Diabase core	Mafic	very fine
14		Vale	Norite core, sub layer	Mafic	fine
15		Vale	Norite core, felsic	Mafic	medium
16		Vale	Norite, mafic with minor sulphide	Mafic	medium
17		Hudson Bay	Argillite	Other	very fine
18		Hudson Bay	Dolostone	Other	very fine
19		Hudson Bay	Rhyolite	Felsic	fine
20		Hudson Bay	Gabbro	Mafic	fine
21		Hudson Bay	Sericite-altered	Other	fine
22		Hudson Bay	Basalt	Mafic	very fine
23		Hudson Bay	Gneiss	Felsic	medium
24		Hudson Bay	Clay-altered regolith	Other	medium
25		Hudson Bay	Chlorite-altered rock	Other	very fine
26		Hudson Bay	Rhyolite	Felsic	medium
27		Hudson Bay	Granite blank	Felsic	medium

28	SJC 04	Teck	Chalcocite-alt, Cu oxide, Chile	Other	fine
29	SJC 02	Teck	Calp float, cf to dolostone	Other	very fine
30	SJC 03	Teck	Argillite, disseminated sulphide, Red Dog	Other	very fine
31	SJC 11	Teck	Coarse Cu-Mo porphyry, Highland Valley	Ores	very coarse
32	SJC 07	Teck	Sedimentary Cu oxide, Namibia	Ores	very coarse
33	SJC 09	Teck	Basalt, Chilcotin, BC	Mafic	Fine
34	SJC 06	Teck	High-grade SEDEX Zn-Pb ore, Red Dog	Ores	Fine
35	GWM-PR	GWM	High REE	High REE	very coarse
36	GWM-HL	GWM	High REE	High REE	very coarse
37	598901-a	GWM	High REE, clay core	High REE	Fine
38	598901-b	GWM	High REE, clay core	High REE	Fine
39	598901-c	GWM	High REE, clay core	High REE	Fine
40	598902-a	GWM	High REE, clay core	High REE	Fine
41	598902-b	GWM	High REE, clay core	High REE	Fine
42	598902-c	GWM	High REE, clay core	High REE	Fine
46	Itabirite-1	Rio Tinto	Fe formation	Ores	Medium
47	Itabirite-2	Rio Tinto	Fe formation	Ores	Medium
48	Itabirite-3	Rio Tinto	Fe formation, friable	Ores	Fine
50	1689334	Newmont	Quartz diorite, orogenic Au deposit, West Africa	Felsic	very fine
51	1689342	Newmont	Quartz diorite, orogenic Au deposit, West Africa	Felsic	Medium
52	1689345	Newmont	Quartz diorite, orogenic Au deposit, West Africa	Felsic	Medium
53	1689347	Newmont	Quartz diorite, orogenic Au deposit, West Africa	Felsic	Medium
54	1689350	Newmont	Quartz diorite, orogenic Au deposit, West Africa	Felsic	Fine
55	1689352	Newmont	Quartz diorite, orogenic Au deposit, West Africa	Felsic	Fine
56	1689359	Newmont	Quartz diorite, orogenic Au deposit, West Africa	Felsic	Medium
57	1689365	Newmont	Quartz diorite, orogenic Au deposit, West Africa	Felsic	very fine
58	1689367	Newmont	Quartz diorite, orogenic Au deposit, West Africa	Felsic	Medium
59	1689368	Newmont	Quartz diorite, orogenic Au deposit, West Africa	Felsic	very fine
60	1689374	Newmont	Quartz diorite, orogenic Au deposit, West Africa	Felsic	Fine
61	1689375	Newmont	Quartz diorite, orogenic Au deposit, West Africa	Felsic	very fine
62	1689379	Newmont	Quartz diorite, orogenic Au deposit, West Africa	Felsic	Fine
63	1689380	Newmont	Quartz diorite, orogenic Au deposit, West Africa	Felsic	very fine
64	1689383	Newmont	Quartz diorite, orogenic Au deposit, West Africa	Felsic	Fine
65	1689385	Newmont	Quartz diorite, orogenic Au deposit, West Africa	Felsic	Fine
66	1689388	Newmont	Quartz diorite, orogenic Au deposit, West Africa	Felsic	Fine
67	1689391	Newmont	Quartz diorite, orogenic Au deposit, West Africa	Felsic	Fine
68	1689393	Newmont	Quartz diorite, orogenic Au deposit, West Africa	Felsic	Medium
69	1689396	Newmont	Quartz diorite, orogenic Au deposit, West Africa	Felsic	Fine
70	LM01	Barrick	Cu-rich schist, with metamorphic minerals	Other	Fine
71	LM02	Barrick	Cu-rich schist, with metamorphic minerals	Other	Fine
72	LM03	Barrick	Cu-rich schist, with metamorphic minerals	Other	Fine

73	LM04	Barrick	Cu-rich schist, with metamorphic minerals	Other	Fine
74	LM05	Barrick	Cu-rich schist, with metamorphic minerals	Other	Fine
75	LM06	Barrick	Cu-rich schist, with metamorphic minerals	Other	Fine
76	LM07	Barrick	Cu-rich schist, with metamorphic minerals	Other	fine
77	LM08	Barrick	Cu-rich schist, with metamorphic minerals	Other	fine
79	SUH-327-XRF-1	Goldfields	Peridotite	Mafic	coarse
80	SUH-327-XRF-2	Goldfields	Microgabbronorite	Mafic	very fine
81	SUH-327-XRF-3	Goldfields	Pyroxenite	Mafic	very fine
82	SUH-327-XRF-4	Goldfields	Gabbro	Mafic	fine
83	SUH-327-XRF-5	Goldfields	Gabbro	Mafic	fine
84	SUH-327-XRF-6	Goldfields	Quartz Diorite	Felsic	fine
85	SUH-327-XRF-7	Goldfields	Quartz Diorite	Felsic	medium
86	SUH-327-XRF-8	Goldfields	Quartz Diorite	Felsic	medium
87	AU08803	U of Ottawa	Shale	Other	fine
88	AU08808	U of Ottawa	Shale	Other	fine
89	AU08818	U of Ottawa	Shale	Other	fine
90	AU08819	U of Ottawa	Shale	Other	fine
91	AU08825	U of Ottawa	Shale	Other	fine

Thus, there are 29 felsic rocks, 12 mafic, 16 ores, 8 high REE samples, and 21 'other' which includes shales and Cu-rich schists. In terms of grain size distribution, there are 14 very fine, 45 fine, 20 medium, 3 coarse (two porphyry Cu ores and 1 peridotite) and 4 very coarse (2 high REEs, 2 ores). The small number and type of coarse and very coarse samples suggest that evaluation of RSD with grain size should focus more on the larger and more diverse very fine, fine and medium groups.

Samples 1-48 of the rocks and ores were split by the GSC preparation facility and one-half shipped off to ALS Laboratories (Sudbury and Vancouver) for preparation (crushing, ball-milling to a fine powder) and analysis. Some of the prepared 'powder' was sent back to Ottawa for analysis by pXRF. Thus the portion analysed directly by pXRF is not the *exact* portion prepared to powder form. The 'lab' results for these samples are based mostly on fusion (lithium metaborate) ICP-MS and ICP-ES; only a few elements (e.g. As, Cd, Hg, Se, Te) not determined in this package were reported using an $HF-HClO_4-HNO_3-HCl$ ('four-acid') near-total digestion. Major elements in the ores were determined by assay methods (designated 'OG62', specialised four-acid digestion). Carbon and sulphur were determined by combustion and IR spectrometry (Leco). The lab results used for the Newmont samples were supplied by the company and are based on (1) whole rock fusion using XRF for the majors and minors (and Nb), and (2) four-acid digestion for the trace elements. The Barrick and Goldfield suites arrived fairly late in the project, without adequate time to have them analysed or prepared by ALS, and therefore the lab data used are those supplied by the companies. These are based on the partial aqua regia

digestion for the Goldfields suite and mixed (unclear) methods (e.g. Cu by XRF) for the Barrick suite.

The powders were analysed by pXRF in duplicate, moving the cup between analyses. Prepared samples matching the rocks were provided by Newmont for their suite (samples 50-69) so they were used for the pXRF 'powder' analysis. Similarly the University of Ottawa shale samples supplied by Mark Hannington (#s 87-91) had matching powders.

The intent in this work was not so much to examine the accuracy of results, since the sample group is so diverse in matrix and specific calibrations were not created, but rather to investigate the variability in results obtained by analysing the surface directly. 'Smooth' surfaces were sought for this purpose and in the first 48 samples 10 analyses on average were carried out on each sample exposing a different area to the window of each instrument. The exceptions to this are the samples 37-42 (three splits each of the two REE-rich clay cores) and sample 48 (friable itabirite) which did not have any smooth surfaces so the 'rough' were substituted. Owing to time constraints, only five analyses (different areas of the sample) were performed for the Barrick and Goldfields suites and three for the Newmont suite.

It was also desirable to compare the results of the 'smooth' surface analysis with those of the 'round': this was done for the samples # 1-6 (Zn-Pb ores), 8-11 (porphyry Cu ores), 36 (GWM-HL, REE-rich) and 87-91 (shales), 16 samples in total. The 14 'rough' surface analyses comprise those for sample #s: 27 (granite); 35-42 (high REE); 46 and 48 (two itabirites); 87, 89 and 91 (three shales). Since the round and rough surface suites are much smaller in number than the smooth surface suite, and constitute a different cross-section of sample types, it is unwise to compare them in a general sense. When comparisons are made of variability between these surface analyses it is done on an individual sample basis where both smooth and round (or rough) surface analysis has been carried out on the *same* sample. This contrasts with the granodiorite suite where there was an adequate number of samples with both smooth and rough surface analyses.

A systematic approach was taken to analyse the rough, smooth and rounded surfaces of the various core and rocks in this study. Each sample was analysed using the same grid of points for both machines. For each point, data were first collected in the soil mode, and then mining mode, without moving the sample between these two readings. This grid of points was unbiased and attempted to capture an accurate reading of the sample as a whole. Phenocrysts in the shot window were noted, but not avoided. Weathered surfaces were avoided as much as possible. In some cases the rocks had to be propped up using glass microscope slides to minimize the distance between the analyser and sample. Care was taken to ensure the slides did not cover any part of the window.

If some of the 10 or so shots per sample returned results below detection or that were eliminated by the software because of interference then the remaining results were still used and the average taken over those positive shots. These situations are obvious as 'n', provided in each element's table, is lower than expected. Where the lab has reported only greater than a particular concentration, that lab value is set to 1 + the maximum concentration. For example, ALS reports As > 250 ppm in the Zn-Pb ores; therefore, the lab concentration is set to 251 ppm.

Results

The pXRF measurements are provided in the Appendix for HH-A and HH-C. They are also presented in numerous plot and table formats in the Appendix, by element:
- A colour-coded sequence plot of concentration in powder, smooth, round, rough surfaces
- A colour-coded surface x-y plot of concentration in surface type vs powder with statistics
- X-Y plot of concentration in powder vs lab with statistics
- Box-and-whisker plots of concentration by lab, powder, various surface types
- Box-and-whisker plots of RSD by powder, smooth, round, rough surfaces
- Box-and-whisker plots of RSD by grain size in smooth surface
- Box-and-whisker plots of RSD by grain size in powder
- Box-and-whisker plots of RSD by rock type in smooth surface
- Box-and-whisker plots of RSD by rock type in powder

These plots are followed by an Excel file containing three tables:
- a table of mean, SD and RSD for the lab (the lab usually has only 1 value), powder and different surface types in the 86 samples;
- a table in ascending order of sample by RSD indicating how many pXRF analyses would be necessary to achieve a result within a particular RSD of the mean (e.g. 10, 20, 30% etc) when analysing the smooth surface (explained in an earlier section);
- a table (at the bottom) providing the statistics for the concentration plots of powder vs smooth, vs rough and vs round results. The number of smooth pairs (powder vs smooth) is higher than that for either of the others.

There is also a summary table for all elements showing median RSD for each sample type (powder, smooth, rough, round) ranked by increasing median RSD of smooth.

Some of these plots, such as those of the RSD of the powder analysis by grain size or rock type, do not provide much additional information but are there for interest or further interpretation.

To reiterate, accuracy, by comparison with the lab data, is not that pertinent in this study: we have analysed many different rocks or matrices and hence, since we are not calibrating to match these diverse groups of samples, we do not expect really good values of r^2 or slope in an x-y plot

of pXRF versus lab result. Rather it is the *change in relative standard deviation, RSD,* with surface texture or grain size or rock type that is under study here. The number of data points for the round and rough surface analyses is much lower than the number of smooth surfaces analysed. This must be borne in mind when reviewing the results, especially for the box and whisker plot which compares the median concentrations across the different surfaces with the powder value.

The elements are reviewed using both instruments. Where one instrument shows significantly different behaviour from the other this is indicated in the discussion; otherwise the plots of one instrument represent the results to be expected.

Three Zn-Pb ores from V-metals - 558934 (sample # 3), 558935 (sample # 4) and 558936 (sample # 5) – and the Anglo dacite (sample # 7) were re-analysed in powder form by pXRF towards the end of the project because their pXRF powder results did not match at all with the lab values or with the surface analyses. The lab values for Zn in the ores are 4.38%, 18.65% and 6220 ppm for samples 3-5, respectively, but their powder pXRF values are 17.9-18.2%, 0.74-0.80% and 187-199 ppm, respectively. Similarly, the lab values for Pb are 1.1%, 5.2% and 1780 ppm, respectively, but the pXRF values are 5.18-5.24%, 2118-2395 ppm and 118-124 ppm, respectively. The pXRF values of elements such as Cu, Ca and S in the dacite are much higher than those of the lab or surface analyses. The pXRF powder results, after taking another completely separate portion from the powder prepared by ALS, confirmed the earlier data. Thus there is no mix-up in the pXRF analysis but there is definitely something amiss in the powders returned to us. Therefore the powder data by pXRF for these four samples have not been used, but their surface analyses have.

Mining mode

Al, aluminium (0.03-12%)
Figures 5.2.1-5.2.4 (HH-A) show the B&W plots of the medians and RSDs for surface type, grain size and rock type, respectively. It is clear (Fig. 5.2.1) that the median Al value for the rough surface is considerably lower than that for the others (~ 4% vs 6-7% Al). This could be due to the fact that the populations of samples differ, or that more air exists in the path between sample and pXRF window which thereby reduces the X-rays for this light element via absorption. Figure 5.2.2 illustrates the increase in RSD with surface texture, from < 2% for the powder, through ~ 10% for smooth (n=53) and ~ 20% for round (n=12) to ~ 22% for a rough surface (n=8). Figure 5.2.3 shows the increase in RSD with grain size for the smooth surface analysis, from ~ 5% for the very fine, through ~ 7% for medium, 11% for fine to ~ 35% for coarse and very coarse rocks. In the analysis of the smooth surface, all RSDs are < ~ 12% (median is 10%; 8% by HH-C) except for the high REE (only 2 analysed in the 'smooth' mode) and ore samples where the RSD is ~ 28% (Fig. 5.2.4).

Ca, calcium (0.007-33.4%)
The x-y plots of Ca concentrations by surface against powder for HH-A all have different slopes but r^2 values are better than 0.90, and indeed the plot of powder vs lab value is excellent with an r^2 of 0.99 and slope of unity (HH-A, Fig. 5.2.5). HH-C behaves similarly in all respects. The B&W plot of RSDs by HH-A shows values of ~ 18% for smooth surfaces compared to ~ 25% for rough and ~ 40% for round, all of course much higher than the < 1% RSD for the powder (Fig. 5.2.6). An RSD of ~ 75% is evident for the very coarse samples (smooth surface), considerably higher than for finer grained samples at ~ 8%, very fine – 12%, medium – 17%, coarse – 23%, fine (Fig. 5.2.7). Again the 'high REE' samples dominate the RSD B&W plot by rock type, at ~ 72%, vs < 43% for the rest of the rock types (other > ores > felsic > mafic) (Fig. 5.2.8).

The second table in the summary Excel file for Ca (Rock_HHA_mining_Ca-summary.csv, see the Appendix) shows that only a couple (≤ 3) of pXRF analyses are required to achieve a value within 20% of the true mean for 32 samples (mostly igneous rocks) but the Cu-rich schists, for example, would require > 24.

Fe, iron (0.36-55%)
The calibration plots for Fe of pXRF versus lab value are good; the r^2 value for HH-C is 0.99 and slope of 1 (Fig. 5.2.9, HH-C). The table below shows examples where the mean concentrations across the different surfaces agree quite well despite fairly high RSDs (e.g. shale AU08818, 1.30 to 1.55%) together with the opposite situation where the mean concentrations differ significantly (e.g. shale AU08825, 1.68-3.20% by HH-C), indicating considerable heterogeneity. The mean values for the surface analysis for this last sample are considerably lower than those of the powder or lab.

Table 5.2.2. Results for Fe by pXRF in different surface media for selected samples, all in %

	Sample ID	Type	Lab	Powder			Smooth			Round		
				Mean	SD	RSD	Mean	SD	RSD	Mean	SD	RSD
HH-A	014 662	Por Cu	2.40	2.43	0.01	0.34	1.79	0.54	30	1.86	0.51	27
HH-C	014 662	Por Cu	2.40	2.76	0.00	0.09	1.23	0.40	32	1.78	0.53	30
HH-A	017 429	Por Cu	3.96	3.68	0.02	0.45	4.46	1.20	27	3.73	1.33	36
HH-C	017 429	Por Cu	3.96	1.82	0.00	0.14	3.63	1.72	47	4.48	1.64	37
HH-A	AU08825	Shale	6.29	5.88	0.01	0.16	1.94	0.60	31	2.88	1.08	37
HH-C	AU08825	Shale	6.29	5.83	0.04	0.66	1.68	0.84	50	3.20	3.40	106
HH-A	AU08818	Shale	2.03	2.05	0.04	1.92	1.30	0.27	21	1.54	0.98	64
HH-C	AU08818	Shale	2.03	1.92	0.07	3.63	1.30	0.32	25	1.55	1.39	90
HH-A	GWM-HL	High REE	2.53	2.95	0.00	0.07	2.47	0.59	24	3.28	0.45	14
HH-C	GWM-HL	High REE	2.53	2.81	0.02	0.82	2.08	0.65	31	3.30	0.96	29

Using HH-A data, the median RSDs for the different surfaces range from 18% for the smooth through ~ 23% for rough and ~ 26% for round; the RSDs for the powder are overwhelmingly under 1-2%. Median RSDs for smooth surfaces based on grain size range from ~ 5% for the very fine through ~ 15% for the medium, ~ 20% for coarse, ~ 23% for fine to ~ 46% for the very coarse (HH-A, Fig. 5.2.10) and based on rock type range from ~ 8% for mafic rocks to ~ 42% for the high REE samples. The overall median RSD for smooth surface analysis by HH-A is 18% and 20% by HH-C.

Independent of the grain-size rating, there is a large range in RSDs within a group of 'like' samples (e.g. Cu-rich schists or the quartz diorites) and hence in the number of analyses required to obtain a result within a selected deviation from the 'true' value. For example, 1 to 63 analyses would be required to obtain a value within 20% of the 'true mean' for the Cu-rich schists and 1 to 46 for the quartz diorites (HH-A Fe summary table). This dependency on an individual sample makes it difficult to form general conclusions.

K, potassium (<0.01-4.7%)
The overall calibration for K by HH-C is good, with an r^2 of 0.94 and slope of 1.3 (HH-A is similar). A glance at the HH-C x-y plot of K concentration in surface rock vs powder shows that, above ~ 2% K, the RSDs for individual samples increase dramatically, especially for the round surfaces (Fig. 5.2.11). This results in median RSDs of ~ 35% for round, 25% for rough and 20% for smooth surfaces. The RSDs for the smooth suite are in the range 40-48% for coarse-grained samples and ≤ 20% for the others (HH-C, Fig. 5.2.12); again high REE and ore samples result in the noisiest signals (median RSDs of 35-40% vs ~ 18-19% for the others).

Mg, magnesium (<0.01-14.6%)
There are far more data points >LOD by HH-C compared to HH-A so those plots are used here; it is mostly the ores and high REE samples for which Mg is not reported. It is clear that the analytical precision for Mg carries some control here which is not the case for other major elements: note Fig. 5.2.13 where the median RSD for the powder is in the range ~ 7-13% across the grain sizes, far higher than the usual RSDs below 2% for powder. In the analysis of the smooth surface samples, the very coarse-grained materials still generate the highest RSDs (~ 40%) and the very fine the lowest (~ 10%); the median RSD overall is 24%. As was evident for Al, Ca and Fe, the median RSD of the fine group is higher than that of the medium grained rocks (~ 32% vs 25%). Median RSD by rock type decreases in the order high REE > ores ~ 'other' ~ felsic > mafic.

Si, silicon (0.76-42.4%)
Both HH-A and HH–C show Si values for smooth surfaces higher in general than for the powder counterparts, probably owing to the absence of the Prolene film (used for the powders in cups) which absorbs Si photons (HH-C, Figs. 5.2.14 and 5.2.15). The large positive bias we have seen for Si using HH-C is evident in the powder vs lab x-y plot (Fig. 5.2.15); the few 'fliers' are ore samples.

The median RSD for the analysis of the smooth surface on the very coarse samples is 22% by HH-C (6% by HH-A), much higher than the other RSDs at ≤ 4%. As usual, it is the ores and high REE samples which show high RSDs of ~ 15-16% (cf ≤ 6% for the others) for the smooth surface, the median RSD overall being only 3.9%.

Note the results for Si in the shales given in Table 5.2.3 below. There is little difference in the RSDs associated with the three different surface analyses for samples 8803 and 8818, though the RSDs for the rough and round surface analysis of 8825 are considerably higher than that for the smooth (12.6 and 15.6%, cf 5.1%). This contrasts with the impression obtained from the B&W plot of RSD with surface texture: ~ 16% for rough, 9% for round and 4% for smooth. The 'rough' results are dominated by the high REE samples and the 'round' by ores and hence this does not represent a true comparison of surface texture.

Table 5.2.3. Results for Si in % for several shale samples, by HH-A

Sample	Powder		Smooth		Rough		Round	
	Mean	RSD	Mean	RSD	Mean	RSD	Mean	RSD
AU08803	49.3	0.3	54.0	8.8	52.4	7.6	54.1	6.8
AU08818	54.6	2.1	55.6	6.4	58.5	7.7	56.5	9.8
AU08825	46.9	0.3	54.1	5.1	44.4	12.3	55.4	15.6

Ti, titanium (<0.01-1.59%)
Figure 5.2.16 shows that the noise associated with the determination of Ti in the powders can be quite high (up to 27% RSD, HH-A), even for several samples containing well above 0.1% Ti. However, analytical median RSDs are better than ~ 3%. The overall median RSD of 20% for smooth surface analysis breaks out to ~ 18-22% for very fine to medium grained rocks and ~ 32-52% for the coarse and very coarse groups (Fig. 5.2.17). The order in median RSD based on rock type is high REE (~ 55%)>ores>mafic~other>felsic rocks (~ 13%), (HH-A, Fig. 5.2.18).

P, phosphorus (44-25792 ppm)
More samples were reported above LOD by HH-C and therefore it is highlighted here. The calibration is quite good, with an r^2 of 0.92 which could probably be improved upon by grouping into matrix-specific calibrations. The absolute concentrations of the rough surface samples seem to be significantly higher than the other populations for P but this is simply because these samples constitute the high REE samples. The RSDs for the powder samples are quite high, ranging from medians of ~ 4 to 12% (Fig. 5.2.19). The median RSD (overall is 24%) for the smooth surfaces ranges up to ~ 80% for the coarse-grained samples, much higher than the 25-30% for the others (i.e. no dependency of RSD with grain size from very fine to medium categories); similarly, the high REE samples show the greatest RSDs at ~ 85% (cf ≤ 40% for other rock types) (Fig. 5.2.20).

S, sulphur (10 ppm-47.4%)
Almost all samples are reported by HH-C for S (unlike the case for HH-A). Perhaps not surprisingly, the overall median RSD for S in the smooth surface measurements is high, at 49%; this does not appear to be controlled by grain size (very coarse > very fine > medium > fine > coarse) (Fig. 5.2.21). For this element, the ores show the lowest RSDs, with a median of ~ 25% (cf ~ 60-100% for the other rock types) (Fig. 5.2.22).

Table 5.2.4 below shows that the absolute concentration of S can vary greatly across the powder, smooth and round surface analysis of the same sample, even though the RSDs of 10 readings on different parts of the surface can be reasonable (e.g. < 20%). This is the case for Zn-Pb ore 558931 (2.6-6.3% S), porphyry Cu ore 014 662 (3-12% S), and shales AU08808 (1.3-6.5% S) and AU08819 (0.8-7.5% S).

Table 5.2.4. Results for S in % by HH-C in different surface media for four ores and four shales

Sample ID	Type	Lab	Powder			Smooth			Round		
			Mean	SD	RSD	Mean	SD	RSD	Mean	SD	RSD
558931	Zn-Pb	7.27	6.33	0.02	0.3	2.56	1.08	42.1	5.49	2.39	43.6
558932	Zn-Pb	8.5	5.81	0.01	0.2	4.49	2.26	50.4	7.86	4.03	51.2
014 662	Por Cu	2.09	2.59	0.04	1.4	11.80	0.29	24.3	2.81	0.67	23.8
017 429	Por Cu	2.92	2.84	0.01	0.3	1.77	0.52	29.7	4.04	1.29	31.9
AU08808	Shale		6.46	0.13	2.1	1.26	1.20	94.9	1.25	0.68	54.6
AU08818	Shale		0.97	0.04	4.4	0.65	0.24	36.0	0.97	1.45	150
AU08819	Shale		7.48	0.22	3.0	0.83	0.11	13.1	1.19	0.13	11.0
AU08825	Shale		2.91	0.02	0.8	1.28	0.65	51.2	2.13	1.33	62.6

Ba, barium by HH-C (2-9040 ppm)
Only HH-C reports Ba and in the soil mode there are negative values associated with the high REE samples and therefore the mining mode data are also reviewed briefly here (the Ba Kα and Kβ lines at 4.47 and 4.83 keV are so close to the L lines of La and Ce). The goodness of fit in the plot of powder vs lab is 0.95, with three high values off the line for the splits of the high REE core 598902 (e.g. 2598 ppm vs 1960 ppm by lab). Results for the two high REEs – GWM-PR and –HL – are quite good. GWM-PR reports 556 ppm in the powder (cf 475 ppm, lab), 601 ppm (39% RSD, n=10) by smooth surface analysis and 413 ppm (12% RSD) by rough surface analysis; GWM-HL reports 9040 ppm in the powder (cf 7193 ppm, lab), 8371 ppm (59% RSD) by smooth surface analysis and 3179 ppm (50%) by rough surface analysis. Thus it seems that the mining mode can handle the high REE samples quite well.

It is interesting that the many of the mean values by smooth surface analysis are considerably higher than those of the powder (r^2 of 0.97, positive intercept of 189 ppm).

Ce, cerium by HH-C (0.2 ppm->1.0%)
There is a very high and variable background in Ce which destroys confidence in concentrations reported below ~ 400 ppm. It is not only the ores which show erroneously high concentrations: for example, sample 13, a diabase containing 18 ppm Ce reports 245 ppm in the powder; sample 22, a basalt containing 9.9 ppm Ce reports 202 ppm; sample 23, a gneiss containing 4.7 ppm Ce reports 265 ppm; sample 27, a granite, containing 32.4 ppm reports 95 ppm Ce, etc. The Zn-Pb ores contain in the tens of ppm Ce (or less) but report in the ~ 300-460 ppm range.

Well above this threshold of variable background, the results for the high REE samples agree quite well with the lab values (Table 5.2.5). Results for the GWM-PR and –HL are encouraging but it is interesting that the one value for a round surface analysis, that of 3930 ppm with an RSD

of 26% (n=10) for GWM-HL, is considerably lower than that for the smooth (8310 ppm). For this sample, one would need 16 analyses of the smooth surface to be within 30% of the 'true value' and 6 to be within 50%.

Table 5.2.5. Results for Ce by HH-C in high REE samples, mean in ppm, RSD in %

Sample #	Sample ID	Lab	Powder		Smooth		Rough	
			Mean	RSD	Mean	RSD	Mean	RSD
35	GWM-PR	816	852	8.4	703	51	761	31
36	GWM-HL	7870	6045	1.4	7576	60	8310	51
37	598901-a	2320	1974	3.6			1560	25
38	598901-b	3850	3587	3.4			2375	40
39	598901-c	2310	1844	5.6			2024	65
40	598902-a	>10000	22345	0.3			11927	27
41	598902-b	>10000	17083	1.4			10232	20
42	598902-c	>10000	14922	2.0			13814	41

Cu, copper at high concentrations (full range is 0.5-18.8%)
Both instruments show excellent calibrations with the lab values, with r^2 values of unity and slopes of 1.1. As there are essentially two populations of Cu because of the Cu ores, rather than evaluating the plots containing all the data, the results for the high-Cu samples only are discussed here. Table 5.2.6 below for various Cu-rich samples shows: (a) powder values match the lab values quite well; (b) the variation encountered in analysing the smooth surface is not controlled by the grain size; (c) there can be a very large range in mean values across surface and powder analysis (e.g. 8647, powder – 3511, smooth – 1347, round ppm in sample # 8); and (d) overall, the RSDs of the smooth and round surfaces are equivalent.

Table 5.2.6. Results for Cu by HH-A in Cu-rich samples, mean in ppm, RSD in %

Sample #	Sample ID	Type	Texture	Lab	Powder		Smooth		Round	
					Mean	RSD	Mean	RSD	Mean	RSD
8	014 696	Por Cu	coarse	7470	8647	0.4	3511	57	1347	133
9	014 662	Por Cu	coarse	5270	5986	0.1	3809	64	1086	60
10	017 429	Por Cu	fine	2230	2392	0.1	2037	100	2634	72
11	015 351	Por Cu	fine	4150	4602	0.3	1819	78	1850	51
16		Norite	medium	5040	6011	1.0	3074	93		
28	SJC 04	Chalc-alt	fine	9940	13704	0.5	9010	14		
31	SJC 11	Por Cu	v. coarse	8820	9943	0.2	6252	78		
32	SJC 07	Sed. Cu ox	v. coarse	188000	216855	0.7	203269	62		

Table 5.2.7 below, presenting the results for the Cu-rich schist series shows (a) major discrepancies between the lab values provided and the pXRF analyses for several samples

(LM04 and LM06), and (b) similar RSDs in general between instruments. The much lower results in the direct pXRF analysis of the Cu schists suggest that mineralisation is very inhomogeneously distributed and not likely to identified by such a limited spatial area of measurement (50^2 mm).

Table 5.2.7. Results of smooth surface analysis for Cu schist series, mean in ppm, RSD in %

Sample #	Sample ID	Lab	HH-A		HH-C	
			Mean	RSD	Mean	RSD
70	LM01		162	45	161	42
71	LM02		467	171	99	57
72	LM03	29100	17648	80	7097	83
73	LM04	13500	78	48	27	93
74	LM05	7740	616	53	1704	143
75	LM06	4110	171	100	84	120
76	LM07	2870	1671	186	738	101
77	LM08	167	99	59	70	37

Taking the porphyry Cu ores (samples 8-11) as examples, one would need 15-45 pXRF analyses of the smooth surface to obtain a mean value within 30% of the 'true' mean.

La, lanthanum by HH-C (0.2 ppm->1.0%)
Like Ce, La suffers from a high and variable background in these samples. The Zn-Pb ores, itabirites and Cu-rich schists all report La in the hundreds of ppm (~ 200-500 ppm) whereas they contain La in the tens of ppm or less. Other examples include sample 13, a diabase containing 8.3 ppm but reported as 284 ppm, sample 23, a gneiss at 299 ppm (cf lab 1.7 ppm), and sample 91, a shale at 237 ppm (cf lab 37 ppm).

Table 5.2.8 lists the results for the REE-enriched samples which contain La above the problematic background. Except for sample 598902-a, agreement between powder and rough surface analysis is good and RSDs are reasonable. Analysis of the round surface for sample GWM-HL (the only round surface analysis for this group) reports a mean of 2260 ppm and an RSD of 25%. Using sample 598901-a as an example, one would need two analyses of the rough surface to be within 30% of the 'true value' and one to be within 50%.

Table 5.2.8. Results for La by HH-C in high REE samples, mean in ppm, RSD in %

Sample #	Sample ID	Lab	Powder		Smooth		Rough	
			Mean	RSD	Mean	RSD	Mean	RSD
35	GWM-PR	337	507	0.2	489	35	502	20
36	GWM-HL	3830	3293	1.2	4401	67	4414	53
37	598901-a	1115	1139	2.1			1021	20
38	598901-b	1590	1751	3.7			1334	34
39	598901-c	1055	978	1.1			1020	35
40	598902-a	10001	13189	1.2			6522	22
41	598902-b	7210	8848	1.2			5428	19
42	598902-c	5920	7327	0.2			6341	33

Nb, niobium by HH-C (0.1->2500 ppm)
There are two clear populations of Nb: concentrations below ~ 25 ppm and those above 2000 ppm in the REE-enriched clay cores (#s 598901 and 598902 and splits thereof). The lab reported mostly > 2500 ppm for these latter samples; pXRF concentrations in the powders range from 3000 to 7550 ppm with RSDs equal to or better than 1%.

The x-y plot of the rough surface, essentially the high REE samples (and a few shales), shows the high RSDs associated with these samples, from 38 to 102% (Fig. 5.2.23); hence the goodness of fit is only 0.58. The majority of the data for Nb in smooth surfaces are much lower in concentration (< 25 ppm) and therefore do not appear on this plot; by and large, they actually agree well with the powder results (Fig. 5.2.24, Nb < 200 ppm only) (the 'flier' is the Zn-Pb ore SJC 06). The median RSDs for the powder range from ~ 9 (fine) to 19% (medium), clearly controlled by nearness to LOD. The median RSD of 32% for the smooth analysis breaks down to: ~ 88% for very coarse, through 35% for fine to 20-22% for very fine and medium, based on grain size; and ~ 88% for ores, through ~ 72% for high , ~ 35% for 'other', 30% for mafic to ~ 25% for felsic rocks, based on rock type.

Pb, lead at high concentrations (full range is 1 ppm-9.6%)
Only high-level Pb is discussed here; low-level results are found in the soil mode section. Calibration plots against lab values are excellent, with r^2 values of 1.0 and slopes of 0.9. (Figs. 5.2.25 and 5.2.26 for HH-A and HH-C, respectively). The median RSD over all samples for the smooth surface analysis is 22% for HH-A and 36% by HH-C; corresponding RSD values for the ores are ~ 34% and 50%, respectively.

Most of the results for the high Pb samples are summarised in Table 5.2.9. Note: there is essentially no difference in RSD between smooth and round surface analysis; lower mean values in the surface analysis compared to powder or lab for some samples (e.g. Zn-Pb ores 558933,

558935 and the argillite SJC 03); significantly lower RSDs (~ 25 vs 50%) for smooth and round analysis of Zn-Pb ores 558933 and 558934 compared to those for 558932 and 558935, making generalisations inaccurate; and the extremely high RSDs of 115 and 74% for the smooth surface analysis of Zn-Pb ore SJC 06.

Table 5.2.9. Results for Pb in various samples by HH-A and HH-C (italics), mean in ppm, RSD in %

Sample #	Sample ID	Type	Lab	Powder		Smooth		Round	
				Mean	RSD	Mean	RSD	Mean	RSD
2	558932	Zn-Pb ore	974	1150	1.6	609	42	1037	66
2	*558932*	*Zn-Pb ore*	*974*	*1131*	*0.0*	*646*	*43*	*778*	*41*
3	558933	Zn-Pb ore	4210	3948	0.2	2093	23	2233	20
3	*558933*	*Zn-Pb ore*	*4210*	*4921*	*1.5*	*2761*	*22*	*2767*	*24*
4	558934	Zn-Pb ore	11000		2.4	5413	27	6790	20
4	*558934*	*Zn-Pb ore*	*11000*		*2.7*	*9484*	*23*	*7376*	*30*
5	558935	Zn-Pb ore	52000		0.7	22216	44	17138	36
5	*558935*	*Zn-Pb ore*	*52000*		*0.8*	*19425*	*58*	*17030*	*52*
30	SJC 03	Argillite	974	1079	0.3	435	34		
30	*SJC 03*	*Argillite*	*974*	*1081*	*0.3*	*405*	*29*		
32	SJC 07	Cu oxide	490	584	2.3	397	80		
32	*SJC 07*	*Cu oxide*	*490*	*534*	*0.9*	*457*	*98*		
34	SJC 06	Zn-Pb ore	95500	86780	0.6	82513	115		
34	*SJC 06*	*Zn-Pb ore*	*95500*	*86424*	*0.5*	*52539*	*74*		

Y, yttrium by HH-C (<0.5-2330 ppm)

The plot of powder vs lab results for Y is excellent, with r^2 and slope values of unity; similarly the x-y plots of smooth and rough vs powder are very good (r^2 values of 0.99, 0.97) (Figs. 5.2.27 and 5.2.28). Some of the Zn-Pb ores (#s 3-6), however, erroneously report Y up to ~ 25 ppm, mostly by round surface analysis, when in fact they contain < 3 ppm.

The median RSD of 24% for the smooth surface analysis breaks down to: ~ 100% for the two high REEs, 55% for the ores, 40% for 'other' and ~ 20% or better for the mafic and felsic rocks; or alternatively ~ 75% for the very coarse-grained samples, 36% for the coarse, 26% for fine, and 20% for the very fine and medium grain size rocks.

Table 5.2.10 presents the data for the high REE samples. Given the very coarse and heterogeneous appearance of the two solid GWM-PR and –HL samples, the range in mean values across the different forms is acceptable. Analysis of the smooth surface does not provide a superior RSD to the rough, in fact it is worse. The two clay cores, 598901 and 598902, are much more homogenous and fine-grained: this is apparent in the results.

Table 5.2.10. Results for Y in ppm (RSD in %) for high REE samples, by HH-C

Sample	Lab	Powder Mean	Powder SD	Powder RSD	Smooth Mean	Smooth SD	Smooth RSD	Rough Mean	Rough SD	Rough RSD
GWM-PR	1035	1031	1.79	0.17	557	636	114	569	375	66
GWM-HL	162	151	2.58	1.71	91	77	84	272	113	42
598901-a	693	723	13.93	1.93				516	85	16
598901-b	798	833	9.35	1.12				620	82	13
598901-c	854	881	0.56	0.06				601	114	19
598902-a	2330	2311	1.52	0.07				1544	532	34
598902-b	1720	1801	36.04	2.00				1280	165	13
598902-c	1750	1906	13.00	0.68				1599	504	32

Zn, zinc at high concentrations (full range is 1 ppm-30.0%)
Samples containing less than 1100 ppm Zn (lab value) are discussed under the soil mode. The calibration plots for Zn are excellent by both HH-A and HH-C, with r^2 values of 1.0 and slopes of 1.1 (Figs. 5.2.29 and 5.2.30, respectively).

Results for the high Zn samples are shown in Table 5.2.11, below. It has been seen for other elements that quite often the results for the surface analysis can be significantly lower than those for the powder or lab and this is again the case (e.g. Zn-Pb ores 558933 and 598935; shale AU08803). Note, for example, the range in surface analyses for Zn-Pb ore 558933, from 0.46% to 2.4%, compared to a lab value for the powder of 2.14%. The concentrations for the rhyolite (sample # 26) are remarkably low, at 70 and 48 ppm compared to 3281-3802 ppm (confirmed in the soil mode); this is difficult to understand. Good agreement is evident in the RSDs for the same sample by each instrument, a measure of variability over 5-10 analyses of different areas on each sample (i.e. the identical 'spot' of measurement is not necessarily the same for each instrument). For example, both instruments suggest that shale AU08819 is very homogeneous whereas both find that the argillite is quite heterogeneous. Only in shale AU08818 does the round surface analysis appear to be inferior to the smooth (RSDs of 134, 147% compared to 30, 38%).

Table 5.2.11. Results for Zn in various samples by HH-A and HH-C (italics), mean in ppm, RSD in %

Sample #	Sample ID	Type	Lab	Powder		Smooth		Round	
				Mean	RSD	Mean	RSD	Mean	RSD
2	558932	Zn-Pb ore	3220	3736	0.6	1459	51	1900	31
2	*558932*	*Zn-Pb ore*	*3220*	*3206*	*0.5*	*1893*	*52*	*1832*	*50*
3	558933	Zn-Pb ore	21400	19561	0.6	24210	113	5592	65
3	*558933*	*Zn-Pb ore*	*21400*	*20949*	*0.1*	*5658*	*58*	*4604*	*55*
4	558934	Zn-Pb ore	43800		0.8	30943	36	45811	30
4	*558934*	*Zn-Pb ore*	*43800*		*1.1*	*74796*	*39*	*41845*	*44*
5	558935	Zn-Pb ore	186500		1.0	100226	58	69051	36
5	*558935*	*Zn-Pb ore*	*186500*		*0.9*	*92400*	*59*	*56299*	*55*
21		Seric-alt	2410	3007	0.5	2249	63		
21		*Seric-alt*	*2410*	*2529*	*0.7*	*1901*	*70*		
26		Rhyolite	3450	3802	0.2	70	66		
26		*Rhyolite*	*3450*	*3281*	*0.4*	*48*	*18*		
30	SJC 03	Argillite	19700	20650	0.3	6783	102		
30	*SJC 03*	*Argillite*	*19700*	*19217*	*0.5*	*5779*	*166*		
34	SJC 06	Zn-Pb ore	300001	327373	0.2	296371	48		
34	*SJC 06*	*Zn-Pb ore*	*300001*	*323517*	*0.2*	*276576*	*37*		
87	AU08803	Shale	2420	2914	4.2	1092	32	1413	55
87	*AU08803*	*Shale*	*2420*	*2557*	*2.2*	*939*	*39*	*1154*	*68*
88	AU08808	Shale	3140	3627	0.7	2119	43	1721	42
88	*AU08808*	*Shale*	*3140*	*3207*	*2.0*	*1244*	*16*	*1310*	*35*
89	AU08818	Shale	2450	2776	1.5	2851	30	3440	134
89	*AU08818*	*Shale*	*2450*	*2287*	*5.6*	*2441*	*38*	*3229*	*147*
90	AU08819	Shale	2460	2786	1.1	2237	8	1753	8
90	*AU08819*	*Shale*	*2460*	*2450*	*1.2*	*2062*	*16*	*1668*	*12*
91	AU08825	Shale	1430	1622	4.0	2119	33	2371	59
91	*AU08825*	*Shale*	*1430*	*1363*	*1.5*	*2141*	*22*	*2050*	*36*

The median RSD overall for the smooth surface analysis is 26% by HH-A (specifically the median for the ores is ~ 48%) and 25% by HH-C (RSD for ores is ~ 35%). Using the HH-C data, one would need anywhere from 6 to 43 surface analyses of the Zn-Pb ore series to obtain a mean value of Zn within 30% of the true value.

Soil mode

Ag, silver (0.02-221 ppm)
Very few samples are reported for Ag by HH-A (and in the mining mode there is a background of several hundred ppm) and hence results by HH-C are discussed here. There are many pXRF results (for ~ 57 samples), be it for powders or the various surfaces, which are in the range ~ 1-10 ppm Ag whereas the lab values are ≤ 0.5 ppm or ≤ 0.05 ppm. These erroneous values can be detected by the value of n: if it is below 10 (or 5 for several suites) some of the analyses are <LOD (i.e. blank) and only the positive records are used in the computation. The high median RSD for the powders, at ~ 25%, also indicates analytical problems as concentrations are near detection limit. The three itabirites (#s 46-48), highly enriched in Fe, report from 14 to 47 ppm (n=10) Ag in powder or surface media but the lab values are 0.25 ppm; HH-A does not report on these samples.

Table 5.2.12 provides results for samples where Ag is indeed reported to be significant by the lab as well as by pXRF. Note: (a) the highest powder RSDs are for the two samples containing only 5 and 13 ppm Ag, showing the effect of analytical precision; (b) the very high RSDs (60-195%) for the smooth surface samples which contain several hundred ppm Ag; and (c) there is no deterioration in results for the round surfaces compared to the smooth. So, in 10 analyses of the sedimentary Cu oxide ore (SJC 07), for example, Ag is reported anywhere from 9.0 to 4794 ppm!

Table 5.2.12. Results for Ag in ppm (RSD in %) for ore samples containing significant [Ag], by HH-C

Sample	Type	Lab	Powder			Smooth			Round		
			Mean	SD	RSD	Mean	SD	RSD	Mean	SD	RSD
SJC 06	Zn-Pb	145	366	8.4	2.3	237	143	60.3			
SJC 07	Cu ox	221	247	1.9	0.8	749	1459	195			
558932	Zn-Pb	4.8	13.4	1.7	12.8	7.0	2.5	35.8			
558933	Zn-Pb	13.3	75.1	19.4	25.9	70.1	8.9	12.6	24.8	5.5	22.3
558934	Zn-Pb	26.3			0.3	67.5	22.1	32.8	29.0	5.2	18.0
558935	Zn-Pb	158			1.6	336	431	128	236	330	140
558935	*Zn-Pb*	*158*			*7.8*	*156*	*214*	*138*	*1069*	*1569*	*147*

Italics indicates the last sample was reported by HH-A

As, arsenic (.05->250 ppm)
As is well known, Pb interferes with As in XRF and causes false positives, especially difficult in geoanalysis as Pb is usually so much higher in concentration than As. Unfortunately the Zn-Pb ores (sample #s 1-6 and 34), which report in the range 367-3454 ppm by HH-A (380-5745 pm by HH-C) in powder by pXRF, have associated lab values of > 250 ppm so it is impossible to

estimate how much of the As can be attributed to Pb interference. Much of the data for As is below 10 ppm but results for selected samples are tabled below. These indicate that: (a) large absolute differences in concentration can exist between powder and surface, beyond that suggested by the RSDs (e.g. by HH-C, 379 for powder vs 70 or 80 ppm for surface analysis in sample 55931; 212 vs 86 ppm in 598901-a; 191 vs 51 vs 32 ppm in AU08808); (b) RSDs for the smooth surfaces are generally equivalent to those for rough or round surfaces; and (c) the instruments are comparable in performance for these particular samples.

Table 5.2.13. Results for As (in ppm) in selected samples, n=10 or 9 for the surface analyses, RSD in %

Sample	Type	Lab	Powder		Smooth		Rough		Round	
			Mean	RSD	Mean	RSD	Mean	RSD	Mean	RSD
558931	Zn-Pb	>250	379	1.4	70	72			80	73
558931	*Zn-Pb*		*367*	*0.4*	*67*	*46*			*106*	*42*
558935	Zn-Pb	>250		0.8	3276	56			1853	49
558935	*Zn-Pb*			*0.1*	*2600*	*25*			*2301*	*26*
	Sericite-alt	54	33	6	13	23				
	Sericite-alt		*38*	*3*	*14*	*45*				
SJC 03	Argillite	42	39	4	13	37				
SJC 03	*Argillite*		*28*	*5*	*12*	*39*				
SJC 06	Zn-Pb	>250	5745	4	4849	96				
SJC 06	*Zn-Pb*		*3454*	*0.8*	*7518*	*154*				
GWM-HL	High REE	12	13	15	9	68	26	53	15	56
GWM-HL	*High REE*		*29*	*4*	*26*	*32*	*52*	*35*	*27*	*34*
598901-a	High REE	187	212	3			86	35		
598901-a	*High REE*		*131*	*3*			*78*	*32*		
598902-a	High REE	199	307	5			234	60		
598902-a	*High REE*		*206*	*1.4*			*170*	*64*		
AU08808	Shale		191	0.9	51	85			32	68
AU08808	*Shale*		*194*	*2*	*56*	*62*			*35*	*42*
AU08818	Shale		21	13	27	80	39	106	4.6	125
AU08818	*Shale*		*25*	*11*	*24*	*73*			*5.4*	*70*
AU08825	Shale		1.6	82	3.0	34	1.8	49	1.4	56
AU08825	*Shale*		*11*	*11*	*5.9*	*17*			*5.4*	*35*

Italics indicate results by HH-A; Roman font indicates HH-C

Examining all the data, median RSDs for the powder by HH-A are better than 7% whereas they are quite high by HH-C, at ~ 40% for the felsic and mafic rocks probably indicating their low concentrations in As and hence control by analytical precision, but are below ~ 10% for the other rock types (Figs. 5.2.31 and 5.2.32 for HH-A and HH-C, respectively). The median RSD for smooth surface analysis is 61% using HH-C, progressing gradually from 54% for the very fine

samples through to ~ 78% for coarse; the precision using HH-A is 26% and a greater, less gradual spread is evident in RSD with grain size, from ~ 15% for the very fine to 20%, medium and coarse – 40%, fine - ~ 50%, very coarse. (Figs. 5.2.33 and 5.2.34 for HH-A and HH-C, respectively).

As examples, using HH-C data, to obtain a result within 30% of the true mean it would take seven analyses for the argillite SJC 03 and 24 for the Zn-Pb ore 558931.

Au, gold (<0.001-6.93 ppm)
HH-C reports Au for the majority of rocks and ores, samples which contain for the most part < 0.1 ppm Au; these are reported mostly in the range ~ 1-10 ppm (i.e. data are nonsense). HH-A does not do this and reports only very few results. Some examples of results where Au is indeed > 0.1 ppm comprise: SJC-06 (lab=0.24, HH-C=40 ppm); 558933 (lab=0.2, HH-C=18 ppm); 1689374 (lab=6.9, HH-C=9, HH-A=9 ppm); 1689379 (lab=5.4, HH-C=2.6 ppm). The splits of the high REE cores 598901 and 598902 are reported by HH-C to contain 6-27 and 16-32 ppm Au, respectively, when in fact they contain <0.03 ppm.

Ba, barium by HH-C (2-9040 ppm)
The goodness of fit for the calibration of powder versus lab is 0.83, with a slope of 0.69 and large intercept of 202 ppm. The major flier in this set is the Zn-Pb ore SJC 06 which reports in the powder at 3219 ppm but the lab value (based on fusion) is 998 ppm. The Zn-Pb ores #s 3-6 all report high, in the range 424-610 ppm by smooth surface analysis but they actually contain < 42 ppm Ba. The itabirites also suffer interference: they contain 6-85 ppm Ba but are reported in the powder at 482-546 ppm.

There is a significant trend in that most of the smooth surface analyses are higher than those of the powder (or lab), and this occurs for samples with low RSDs. Some examples include: the quartz diorite series, # 59 at 726 ppm with 3% RSD (cf 490 ppm in the powder and 501 ppm lab) or # 60 at 706 ppm with 11% RSD (cf 455 ppm in powder and 412 ppm lab); #30, argillite at 286 ppm with 33% RSD (cf 145 ppm in powder and 175 ppm lab); and # 33, basalt, at 655 ppm with 2% RSD (cf 432 ppm in powder and 266 ppm lab).

The low median RSD of only 11% for the smooth surface analysis breaks down to: by particle size, ~ 8% very fine – 10% medium – 13% fine – 20% coarse – 65% very coarse; and by rock type, ~ 8% mafic – 10% fine – 18% 'other' – 25% ore – 65% high REE.

Bi, bismuth (<0.01->250 ppm)
Bismuth is reported by HH-A for only nine samples – two Zn-Pb ores, high REEs and itabirite – at 25-832 ppm whereas in fact they contain a mere 0.1-44 ppm Bi. Bismuth is not detected in Cu

ore SJC 07 which contains 45 ppm Bi, nor in the surface analysis of Zn-Pb ore 558936 (sample # 6) which contains > 250 ppm.

Cd, cadmium (<0.05->1000 ppm)
Only eight samples have results for Cd by HH-A and six of these match well with the lab values in the range 8-64 ppm; the other two are ores containing > 1000 ppm. Many more values are provided by HH-C but most are erroneously high, up to ~ 20 ppm when the lab reports < 0.5 or < 0.05 ppm.

Co, cobalt (0.5-575 ppm)
A quick glance at the x-y plot of powder vs lab and the summary table tells the viewer that Co by HH-C suffers extreme interferences, mainly of course from Fe. In most of the ores and shales (containing ~ 6% Fe) Co is reported in the hundreds of ppm (cf lab values in the tens of ppm) and yet Co is not detected in a sample such as the felsic gneiss (# 23) which contains 42 ppm. The x-y plot using HH-A data is much better: some points remain high on the y-axis (ores) and two are high along the x-axis (a mafic norite and a Zn-Pb ore) but most of the points cluster on a calibration line (Fig. 5.2.35, HH-A). The Cu-rich schist series appears to be suppressed in the analysis of the smooth surface for Co (e.g. 28 vs 61 ppm by lab; 10 vs 70 ppm; 13 vs 113 ppm).

Given that many of the samples are ores (and therefore interference-prone) and there are significant gaps in the data, comparing the RSD plots by grain size and rock type is not valid. Table 5.2.14 compares the analysis of the powder with the smooth surface analysis for the quartz diorite series. The agreement is excellent, especially at these low levels. The mean RSD for the powder is 9% and that for the smooth surface is 22%.

Table 5.2.14. Results for Co by HH-A in felsic quartz diorite series, mean in ppm, RSD in %

Sample	Texture	Powder Mean	Powder RSD	Smooth Mean	Smooth RSD
1689334	very fine	20.4	5.9	18.7	7.7
1689342	medium	12.3	1.7	12.7	9.5
1689345	medium	14.5	0.5	7.1	30.9
1689347	medium	23.8	5.1	23.5	13.5
1689350	fine	21.3	4.6	19.9	65.7
1689352	fine	22.5	6.3	20.7	35.9
1689359	medium	25.9	1.6	14.8	16.6
1689365	very fine	22.7	5.0	20.5	7.7
1689367	medium	18.6	2.3	11.4	21.6
1689368	very fine	18.3	0.8	14.5	18.4
1689374	fine	20.3	5.6	14.4	26.0
1689375	very fine	17.0	14.1	14.9	34.0
1689379	fine	17.9	0.4	21.6	16.8
1689380	very fine	27.4	2.3	26.8	1.7
1689383	fine	4.6	3.1	12.6	29.6
1689385	fine	12.2	25.5	16.5	8.1
1689388	fine	13.3	18.7	16.0	6.6
1689391	fine	12.3	13.8	15.7	18.7
1689393	medium	19.0	61.8	18.3	64.1
1689396	fine	14.3	0.5	15.2	12.1

Cr, chromium (5-2410 ppm)

Chromium suffers from interference by the REE L lines and hence the results for the REE-enriched series are very high and this is evident on both x-y plots of powder vs lab result (e.g. in 598901-c, HH-A reports 1050 in the powder and 966 ppm for the rough surface, cf 80 ppm by lab; # 598902-a reports 9768 ppm in the powder and 5361 ppm for the rough surface, cf 100 ppm by lab).

In some of the Cu-rich schists and SUH series (sample #s 72-82), there is considerable disagreement between the lab value (supplied by the companies) and the smooth surface pXRF data (both HH-A and HH-C). The fact that the pXRF data agree with each other suggests that the lab value may be in error or low: the lab values for the SUH series are based on an aqua regia digestion which is known to be partial, especially for Cr mineralogy.

The x-y plot of smooth vs powder is excellent for HH-A, with an r^2 and slope of 0.95 (HH-C is slightly worse, at 0.87 and 0.92, respectively). The median RSD of 23% for the smooth surface data breaks down to: a gradual progression from ~ 12% for the very fine to ~ 64% for the very

coarse-grained samples; and 18% ('other') to 30 % (ores) by rock type, ignoring the high REEs (Fig. 5.2.36, HH-A).

Table 5.2.15 for the fine-grained shales shows that the RSDs for the round surface are not significantly different from those for the smooth surface analysis (note the lab results provided are not for the *exact* same subsample).

Table 5.2.15. Results for Cr by HH-A in the shale series, mean in ppm, RSD in %

Sample ID	Lab	Powder		Smooth		Round	
		Mean	RSD	Mean	RSD	Mean	RSD
AU08803	5	57.7	5.6	44.2	14.8	46.1	21.3
AU08808	39	79.0	6.6	59.4	16.7	64.6	9.2
AU08818	21	45.7	3.3	43.2	11.8	48.3	14.9
AU08819	54	86.3	5.7	74.3	7.7	83.0	7.7
AU08825	24	60.3	5.1	51.1	18.3	54.8	18.9

Cs, caesium (0.05-10.5 ppm)
This element is measured by HH-C but the results are entirely unacceptable, not only for ore samples. For example, Cs is reported as 57 ppm in a diabase (cf 0.6 ppm by lab), 110 ppm in a norite (cf 0.23 ppm) and 47 ppm in a gabbro (cf 0.4 ppm by lab).

Cu, copper at low concentrations, < 1100 ppm (full range is 0.5-18.8%)
Having discussed Cu in enriched samples in the mining mode, the data-base in the soil mode was restricted to samples with concentrations below 1100 ppm Cu, a natural break. The calibration by HH-A is good, with an r^2 value of 0.96, and that for HH-C would be excellent except for the one datum for Zn-Pb ore SJC 06 (30% Zn) which contains 395 ppm Cu and is reported in the powder at 2491 ppm (340 ppm by HH-A), probably owing to an overlap of the Cu K lines with the shoulder of the Zn Kα line (8.64 keV) (Figs. 5.2.37 and 5.2.38 for Cu< 1100 ppm, for HH-A and HH-C, respectively.)

Numerous samples display significantly different mean values from powder to smooth surface analysis, as shown in Table 5.2.16, below. As has been noted previously, the mean values for the surface (smooth) analysis are lower than those for the powder (or lab). For example, compare: in the chlorite-altered regolith (# 25) 848 (powder) vs 32 ppm (smooth) by HH-A (769 vs 51 ppm, HH-C); in the rhyolite (# 26), 335 vs 53 ppm by HH-A (312 vs 51 ppm, HH-C); in the basalt (# 33), 241 vs 48 ppm by HH-A (224 vs 57 ppm by HH-C); and in the shale (# 88), 158 vs 45 ppm

by HH-A (162 vs 31 ppm, HH-C). Most of the results (except sample # 2 by HH-A) for the round surface are similar to those for the smooth, indicating a significant difference from the powder result. This presumed heterogeneity is not always suggested by the RSD for the surface analysis which, for example, is low (4-33%) for shale sample # 90. The fact that *lower* results are consistently obtained in the surface analysis compared to the powder is interesting and bears no relationship to the particle size classifications of the samples. This discrepancy between powder and direct surface results is probably the most severe for Cu.

The median RSD for smooth surface analysis is high for Cu compared to other elements, at 53% by HH-A and 54% by HH-C, for these levels of Cu below 1100 ppm. This breaks down by particle size to: HH-A - ~ 40-45% for very fine and fine and 55-65% for medium and very coarse; HH-C - ~ 25% for very fine, 45% for fine and medium and ~ 80% for very coarse.

Taking the rhyolite (# 26) as an example, one would need 27 (HH-A) or 10 (HH-C) pXRF analyses of the smooth surface to obtain a mean value within 30% of the 'true' mean.

Table 5.2.16. Results for Cu in various samples by HH-A and HH-C (in italics), mean in ppm, RSD in %

Sample #	Type	Lab	Powder		Smooth		Round	
			Mean	RSD	Mean	RSD	Mean	RSD
2	Zn-Pb ore	339	325	0.9	91	39	279	93
2	*Zn-Pb ore*	*339*	*336*	*0.5*	*77*	*85*	*59*	*116*
14	Norite	541	524	1.1	160	57		
14	*Norite*	*541*	*497*	*0.8*	*169*	*42*		
22	Basalt	175	134	2.6	42	53		
22	*Basalt*	*175*	*134*	*4.0*	*56*	*100*		
23	Gneiss	103	92	3.9	48	70		
23	*Gneiss*	*103*	*89*	*9.9*	*51*	*62*		
25	Chlorite-alt	1050	848	0.8	32	103		
25	*Chlorite-alt*	*1050*	*769*	*1.5*	*51*	*117*		
26	Rhyolite	387	335	0.0	53	77		
26	*Rhyolite*	*387*	*312*	*1.2*	*51*	*47*		
33	Basalt	303	241	1.5	48	19		
33	*Basalt*	*303*	*224*	*0.7*	*57*	*14*		
56	Qua. dior	128	111	2.6	24	64		
56	*Qua. dior*	*128*	*113*	*3.3*	*54*	*64*		
59	Qua. dior	94.5	80	2.7	25	42		
59	*Qua. dior*	*94.5*	*79*	*5.7*	*43*	*13*		
87	Shale	298	257	4.6	75	60	82	62

87	*Shale*	*298*	*267*	*5.1*	*93*	*55*	*94*	*59*
88	Shale	181	158	2.0	45	81	28	16
88	*Shale*	*181*	*162*	*2.4*	*31*	*88*	*31*	*50*
89	Shale	116	87	1.3	38	25	33	49
89	*Shale*	*116*	*86*	*8.2*	*44*	*45*	*35*	*60*
90	Shale	347	286	4.4	102	11	83	9
90	*Shale*	*347*	*311*	*3.4*	*108*	*33*	*77*	*4*
91	Shale	333	253	1.4	80	53	54	44
91	*Shale*	*333*	*253*	*4.3*	*77*	*38*	*81*	*90*

Hg, mercury (<0.005-25.1 ppm)

The results for Hg are nonsense: HH-C generates many more data than HH-A but most are for samples that contain Hg at concentrations well below 0.1 ppm and they are reported in the range ~ 1-12 ppm. Where a sample does contain Hg, as for the rhyolite (# 26) at 2.93 ppm, it is reported by pXRF at 7.3 ppm, but how would one know if this is real when so many samples, containing < 0.01 ppm, are reported at this high level? The Zn-Pb ore, SJC 06, with a true Hg content of 25 ppm, is reported as 685 ppm!

Mn, manganese (39 ppm-3.3%)

Both HH-A and HH-C behave similarly and show good calibration graphs between lab values and powders with r^2 values of 0.99 and slopes of 1.4 and 2.2, respectively. The mean RSD for HH-A data of 20% for the smooth set comprise: ~ 8%, for the very fine, through 20-25% for fine to coarse, to 54% for the very coarse-grained samples; and ~ 10% for the mafic rocks, through 20% for felsic and 'other', and 35% for ores to 56% for high REEs.

Table 5.2.17 provides examples of the excellent RSDs for the smooth and round surface sets of shales and the ranges in means across the different media of a sample. Once again, mean values for the surface analysis, be it smooth or round, can be considerably lower than those for the powder sample (e.g. 153 and 179 ppm in AU08808, cf powder at 454 ppm).

Table 5.2.17. Results for Mn by HH-A in various samples, mean in ppm, RSD in %

Sample #	Sample ID	Type	Lab	Powder Mean	RSD	Smooth Mean	RSD	Round Mean	RSD
1	558931	Zn-Pb ore	155	153	1.8	55	34	104	109
2	558932	Zn-Pb ore	4105	4708	1.9	1234	66	2178	35
11	015 351	Por Cu	232	267	1.3	139	54	147	13
36	GWM-HL	High REE	620	1065	1.5	773	29	849	14
88	AU08808	Shale	387	454	5.6	153	39	179	27
89	AU08818	Shale	542	530	0.1	328	22	401	24

Mo, molybdenum (0.05-99 ppm)

Most of the samples contain < 10 ppm of Mo and some, such as the quartz diorites, much less. Hence there are numerous non-detects, especially in the HH-A data-set. Nevertheless, the calibration for Mo (powder vs lab, r^2 of 0.98, slope of 1.1) by HH-A is superior to that by HH-C because the latter erroneously reports very high Mo in the high REE samples (Figs. 5.2.39 and 5.2.40 for HH-A and HH-C, respectively). Most of the samples with significant Mo concentration are tabled below. The shales have high RSDs for the different surfaces owing in large part to nearness to detection limit but the porphyry Cu ores demonstrate also heterogeneity (sample # 9). The analyses of the rough surface of the three shales (in the summary table) are of the same variability essentially as the round or smooth surface counterparts.

In the analysis of the Cu-rich schists (smooth surface), Mo in LM04 at 33 ppm (lab) was not detected in any of the five shots, and was reported as 5 ppm (102% RSD) in LM08 (cf 16 ppm lab). Molybdenum in sample LM07 was reported as 40 ppm (94% RSD), the lab value being 17 ppm.

Table 5.2.18. Results for Mo by HH-C in various samples, mean in ppm, RSD in %

Sample #	Sample	Type	Lab	Powder		Smooth		Round	
				Mean	RSD	Mean	RSD	Mean	RSD
9	014 662	Por Cu	99	110.4	1.1	68.2	186	85.9	161
10	017 429	Por Cu	13	16.9	4.9	8.9	139	10.0	120
11	015 351	Por Cu	10	13.6	2.9	8.3	95	8.7	83
34	SJC 06	Zn-Pb ore	24	86.3	11.4	54.9	54		
40	598902-a	High REE	16	62.6	2.8			46.5*	70*
89	AU08818	Shale	9	9.8	16.5	4.7	45	4.5	146
91	AU08825	Shale	4.3	6.7	20.1	8.9	49	7.9	67

These are 10 rough surface analyses

Nb, niobium by HH-A (0.1->2500 ppm)

As mentioned previously, Nb is divided into two populations, that governed by the high REEs and the rest which are mostly under 20 ppm in Nb. Agreement at the low level between powder and lab values is very good, given this concentration level.

The mean RSD of 24% for the smooth data-set breaks out: by grain size, from ~ 15% for the very fine, through ~ 25% for fine to coarse, to 50% for the very coarse; and by rock type, from ~ 20-25% for all but the high REEs which are at ~ 60%.

Table 5.2.19 illustrates the good RSDs achieved in the analysis of the rough surfaces encountered for these high REE samples.

Table 5.2.19. Results for Nb by HH-A in high REE samples, mean in ppm, RSD in %

Sample #	Sample ID	Lab	Powder Mean	Powder RSD	Rough Mean	Rough RSD
35	GWM-PR	193.5	199	1.1	102	55
36	GWM-HL	9.7	11.05	9.6	7.9*	57*
37	598901-a	>2500	1938	0.9	1199	44
38	598901-b	>2500	2254	0.3	1484	28
39	598901-c	>2500	1949	0.9	1698	25
40	598902-a	2310	1061	0.3	1035	26
42	598902-c	>2500	1125	0.7	1073	26

round rather than rough surface in this instance

Ni, nickel (0.05 ppm-2.0%)

There are many non-detects in the HH-A data-set, presumably owing to programming set to eliminate reporting of results subject to interferences. It is surprising that most of the quartz diorite series are not reported as (a) they do not pose the challenge of ores or high REEs and (b) they contain Ni in the range 30-135 ppm. Eliminating interference-prone results is wise as the HH-C data-set provides examples of severe interferences on Ni, in the: Zn-Pb ores (e.g. sample # 3 at 226 ppm, cf 3 ppm, lab), the high REEs (e,g sample # 41 at 1102 ppm, cf 102 ppm lab), and the itabirites (e.g. sample # 48 at 336 ppm, cf lab <1 ppm). The median RSD of 18% for smooth surface analysis breaks down to: based on grain size, ~ 14%, very fine – 17%, medium – 20%, fine and coarse – 46% very coarse; based on rock type, ~ 14%, mafic – 17%, felsic – 20% for ores and 'other' – 45%, high REEs.

Table 5.2.20 presents results for the diorite series by HH-C: RSDs for the smooth surfaces are excellent, particularly in light of the relatively high analytical RSDs for the powder. Also shown are data by both instruments for a few shales; results are comparable, with similar RSDs for particular samples.

Table 5.2.20. Results for Ni in various samples mostly by HH-C, mean in ppm, RSD in %

Sample #	Sample ID	Type	Lab	Powder Mean	Powder RSD	Smooth Mean	Smooth RSD
50	1689334	Quartz diorite	100	92	11.5	126	9.4
51	1689342	Quartz diorite	50	33	17.6	84	19.8
52	1689345	Quartz diorite	75	66	4.6	98	21.1
53	1689347	Quartz diorite	135	109	19.1	177	3.4
54	1689350	Quartz diorite	40	51	8.4	181	44.0
55	1689352	Quartz diorite	100	109	9.2	117	64.9
88	AU08808	Shale	283	198	5.2	103	46.9
88	*AU08808*	*Shale*	*283*	*192*	*2.1*	*87*	*67.1*
89	AU08818	Shale	160	77	27.8	91	13.3
89	*AU08818*	*Shale*	*160*	*101*	*12.4*	*66*	*26.2*
90	AU08819	Shale	349	221	2.2	195	14.3
90	*AU08819*	*Shale*	*349*	*208*	*5.9*	*241*	*13.9*

Italics indicates analysis by HH-A

Again, Table 5.2.21 shows similar RSDs by HH-A and HH-C in the smooth surface analysis of various samples, indicating that the inherent homogeneity (sample # 82, gabbro) or heterogeneity (sample 79, peridotite) of the sample controls the variability. Thus only one analysis of the

Table 5.2.21. Results for Ni in the Goldfields suite by HH-A (italics) and HH-C (Roman), mean in ppm, RSD in %

Sample #	Sample ID	Type	Lab	Smooth Mean	Smooth RSD
79	*327-XRF-1*	*Peridotite*	*1280*	*1186*	*47.7*
79	327-XRF-1	Peridotite	1280	2048	56.3
80	*327-XRF-2*	*Microgabbronorite*	*53.8*	*199*	*3.9*
80	327-XRF-2	Microgabbronorite	53.8	199	9.4
81	*327-XRF-3*	*Pyroxenite*	*275*	*640*	*14.1*
81	327-XRF-3	Pyroxenite	275	841	18.4
82	*327-XRF-4*	*Gabbro*	*47.2*	*199*	*5.9*
82	327-XRF-4	Gabbro	47.2	193	5.2
83	*327-XRF-5*	*Gabbro*	*1580*	*560*	*57.6*
83	327-XRF-5	Gabbro	1580	1093	48.3
84	*327-XRF-6*	*Quartz diorite*	*2190*	*586*	*42.0*
84	327-XRF-6	Quartz diorite	2190	914	25.7
85	*327-XRF-7*	*Quartz diorite*	*741*	*561*	*10.6*
85	327-XRF-7	Quartz diorite	741	670	17.9

smooth surface would be required to obtain a result within 30% of the true mean in the gabbro but 15 analyses would be required for the peridotite. The means tends to be lower at high concentration by HH-A which is probably a calibration difference.

In the mining mode, the norite sample (sample # 16) containing 2.01% Ni reports by HH-A as 2.19% (0.4% RSD) for the powder and 1.48% (36% RSD) for the smooth surface, and by HH-C as 1.01% (0.3% RSD) for the powder and 1.42% (28% RSD) for the smooth surface.

Pb, lead at low concentrations, < 300 ppm (full range is 1 ppm-9.6%)
In order to examine the low level data, results for samples containing greater than 300 ppm by the lab value were eliminated; these results and plots are grouped at the end of the file. Samples which are high enough in Pb to have been reported but where the majority of results are <LOD by HH-A include: norites, sample # 15 and 16 (14, 16 ppm Pb by lab); high REE, GWM-HL (46 ppm lab); microgabbronorite, sample # 80 (25.8 ppm lab); and several quartz diorites (8, 12 ppm). All but the microgabbronorite were reported by HH-C. Unlike HH-A, HH-C reports very high (for powder and rough surface analysis) for the three splits of REE-enriched sample 598902, in the range 508-786 ppm (powder) compared to lab values of 229-282 ppm Pb. Disregarding these three points, the calibration of powder versus lab value would be very good (Fig. 5.2.41, HH-C for Pb <300 ppm).

Most of the results for samples containing significant levels of Pb are summarised in Table 5.2.22. Note: the lower mean values for the surface analysis compared to powder for several samples (Zn-Pb ore 558931; high REE 598901-a); the extremely high RSD (150, 170%) for the rough surface analysis of high REE sample GWM-PR; the apparent interference on Pb using HH-A in the sample Itabirite-3 (700 and 431 ppm, cf 16 ppm, lab); and the sample-dependent comparison of smooth versus round versus rough RSDs.

Table 5.2.22. Results for Pb in various samples by HH-A (Roman) and HH-C (italics), mean in ppm, RSD in %

#	Sample ID	Type	Lab	Powder		Smooth		Rough		Round	
				Mean	RSD	Mean	RSD	Mean	RSD	Mean	RSD
1	558931	Zn-Pb ore	139	122	2.3	51	61			58	35
1	*558931*	*Zn-Pb ore*	*139*	*131*	*0.2*	*50*	*97*			*68*	*78*
21		Sericite-alt	24	20	2.8	14	18				
21		*Sericite-alt*	*24*	*16*	*7.9*	*6*	*51*				
35	GWM-PR	High REE	136	108	4.6			54	170		
35	*GWM-PR*	*High REE*	*136*	*113*	*5.4*	*3*	*81*	*161*	*150*		
37	598901-a	High REE	176	99	2.9			52	42		
37	*598901-a*	*High REE*	*176*	*188*	*0.8*			*88*	*26*		

40	598902-a	High REE	282	387	0.5			328	56		
40	*598902-a*	*High REE*	*282*	*786*	*0.2*			*664*	*49*		
48	Itabirite-3	Fe friable	16	700	1.9			431	41		
48	*Itabirite-3*	*Fe friable*	*16*	*36*	*80.4*			*53*	*35*		
83	327-XRF-5	Gabbro	240			189	20				
83	*327-XRF-5*	*Gabbro*	*240*			*167*	*21*				
87	AU08803	Shale	88	65	4.6	46	55			59	52
87	*AU08803*	*Shale*	*88*	*74*	*2.8*	*64*	*61*	*29*	*95*	*66*	*41*
89	AU08818	Shale	50	45	1.0	36	16			44	37
89	*AU08818*	*Shale*	*50*	*38*	*11.5*	*29*	*28*	*28*	*81*	*38*	*72*

Rb, rubidium (0.2-303 ppm)

The calibration against lab values for HH-A is good, with an r^2 value of 0.92 and slope of 1.1; the few fliers include Itabirite-3 (81.5 ppm by powder pXRF, lab 0.7 ppm), a quartz diorite, sample # 55 (40 vs 0.2 ppm) and the REE-enriched sample, GWM-PR (303 vs 396 ppm). With the exceptions of these fliers, the calibration by HH-C is also very good (r^2 of 0.94, slope of 0.97).

The median RSD of 19% in the smooth surface analysis by HH-A comprises: ~ 12-21% for the fine and medium grain size samples (medium being lowest at 12%) and ~ 32% for the coarse; by rock type, ~ 15% for felsics, 22% for mafic and 'other', and ~ 30% for ores and high REEs. The breakdown is much the same for HH-C except the percentages are somewhat higher, the median RSD being 27% (HH-C, Fig. 5.2.42 for grain size and Fig. 5.2.43 for rock type).

Some examples of data are given in Table 5.2.23. Variability in the surface analysis is quite low compared to that for other elements. Note the similarity between instruments: amazingly low RSDs for surface analysis of the shales 8808 (7-15% RSD) and 8819 (4-7%) and relatively high ones for the high REE GWM-HL (44-81%). There is no consistent difference in RSD or mean values between smooth and round surface analysis.

Table 5.2.23. Results for Rb in various samples by HH-A (Roman) and HH-C (italics), mean in ppm, RSD in %

Sample #	Sample ID	Type	Lab	Powder		Smooth		Round	
				Mean	RSD	Mean	RSD	Mean	RSD
1	558931	Zn-Pb ore	176	174	0.7	113	24	157	25
1	*558931*	*Zn-Pb ore*	*176*	*158*	*1.0*	*122*	*22*	*110*	*22*
9	014 662	Porph. Cu	107	104	2.1	87	24	81	12
9	*014 662*	*Porph. Cu*	*107*	*85*	*2.8*	*83*	*27*	*76*	*27*
10	017 429	Porph. Cu	131	120	1.6	125	32	102	27
10	*017 429*	*Porph. Cu*	*131*	*99*	*0.0*	*103*	*34*	*95*	*33*
36	GWM-HL	High REE	66	78	1.2	71	44	81	47
36	*GWM-HL*	*High REE*	*66*	*64*	*0.4*	*65*	*55*	*59*	*81*
87	AU08803	Shale	77	107	1.9	102	34	90	46
87	*AU08803*	*Shale*	*77*	*101*	*2.2*	*80*	*39*	*75*	*43*
88	AU08808	Shale	80	80	0.7	104	15	108	9
88	*AU08808*	*Shale*	*80*	*75*	*2.1*	*95*	*14*	*97*	*7*
89	AU08818	Shale	77	76	0.5	84	17	97	15
89	*AU08818*	*Shale*	*77*	*66*	*4.7*	*74*	*23*	*85*	*15*
90	AU08819	Shale	81	108	0.8	110	4	127	5
90	*AU08819*	*Shale*	*81*	*103*	*1.7*	*101*	*7*	*113*	*5*
91	AU08825	Shale	120	135	1.2	99	25	116	50
91	*AU08825*	*Shale*	*120*	*126*	*1.2*	*79*	*19*	*79*	*39*

Table 5.2.24 is a summary of Sb results for the Zn-Pb ores. Except for samples 1 and 2, RSDs of direct analysis by the two instruments are similar for the same samples and the median RSD for round surface analysis is equivalent to that for smooth. Again, variability is highly sample-dependent.

Table 5.2.24. Results for Sb in Zn-Pb ores by HH-A and HH-C (italics), mean in ppm, RSD in %

Sample #	Sample ID	Lab	Powder Mean	Powder RSD	Smooth Mean	Smooth RSD	Round Mean	Round RSD
1	558931	126	204	2.4	27	8	34	11
1	*558931*	*126*	*155*	*3.3*	*26*	*53*	*17*	*42*
2	558932	35	44	16.1	46	14	58	69
2	*558932*	*35*	*65*	*4.6*	*38*	*52*	*42*	*57*
3	558933	157	285	3.0	281	69	456	64
3	*558933*	*157*	*333*	*6.8*	*335*	*45*	*242*	*63*
4	558934	>250		2.2	666	20	861	38
4	*558934*	*>250*		*1.9*	*658*	*31*	*522*	*21*
5	558935	>250		7.9	1207	75	3833	99
5	*558935*	*>250*		*1.8*	*1289*	*107*	*1387*	*115*
6	558936	>250			685	45	707	47
6	*558936*	*>250*			*586*	*39*	*562*	*45*
34	SJC 06	>250	1806	6.9	1255	40		
34	*SJC 06*	*>250*	*1026*	*2.2*	*673*	*60*		

Se, selenium (0.1-77.3 ppm)

HH-C reports many more Se values above LOD than does HH-A; most of the samples, for which lab values are available, contain less than 5 ppm. However, the analysis appears to be good, except for some high REE samples which report low concentrations (e.g. samples # 40-42, 598902-a-c, which report 10-19 ppm but contain 61-77 ppm Se).

Table 5.2.25. Results for Se in various samples mostly by HH-C, mean in ppm, RSD in %

Sample #	Sample ID	Type	Lab	Powder Mean	Powder RSD	Smooth Mean	Smooth RSD
2	558932	Zn-Pb ore	18.6	17.8	14.6	11.1	39.7
2	*558932*	*Zn-Pb ore*	*18.6*	*21.8*	*1.6*	*19.9*	*68.5*
5	558935	Zn-Pb ore	13.1	11.8	33.1	16.3	60.7
8	014 696	Por Cu	6.4	2.8	11.6	2.9	46.2
15		Norite	0.3	1.0	39.8	1.5	51.9
16		Norite	35.2	35.8	13.3	31.0	24.8
16		*Norite*	*35.2*	*49.0*	*3.3*	*32.8*	*28.6*
28	SJC 04	Chalc-alt	4.5	5.3	7.6	1.7	55.4
30	SJC 03	Argillite	14.5	13.1	10.5	5.9	39.9
34	SJC 06	Zn-Pb ore	26.6	21.7	10.0	38.1	66.0
35	GWM-PR	High REE	16.8	1.2	118	2.0	68.5

Italics indicates results by HH-A, Roman by HH-C.

Given the very low Se concentrations, the agreement with the lab values and the RSDs for the direct analysis of the smooth surfaces are remarkable (Table 5.2.25).

In the Zn-Pb ore 558936 (lab value of 68.1 ppm Se), HH-A reports 77.9 ppm (RSD 19%) for the smooth surface and 95.7 ppm (RSD 21.6%) for the round; corresponding values by HH-A are 33.2 ppm (RSD 13.0%) and 24.6 ppm (RSD 20.0%). The absolute values differ markedly, which could be caused by different calibrations, but the RSDs are similar for the 10 analyses, indicating the similarity between smooth and rough surface performance. HH-A reports an RSD for Zn-Pb ore 558932 (18.6 ppm Se) of 37% for the smooth surface and 68% for the round but HH-C reports an RSD of 19% for the round (40% for the smooth) so there are inconsistencies when attempting to compare smooth vs round performance.

Low results are evident for the high REE series. For example, in 598902-a whose lab value is 77.3 ppm Se, HH-C reports only 12.1 ppm (RSD of 29.6%) for the powder and 10.7 ppm (RSD of 37.3%) for the rough surface; HH-A reports similarly low or <LOD. These fliers create havoc in the calibration plot of powder vs lab.

The median RSD of 48% (HH-C) in measuring the smooth surface shows a gradual progression from ~ 42% for the very fine to ~ 58% for the coarse and very coarse; no large distinction is seen for rock type.

Sn, tin (0.5-714 ppm)
There are numerous samples reporting erroneously high results by HH-C, for example: several norites (e.g. sample # 16, 46 ppm, cf lab 0.5 ppm), a basalt (sample # 22, 15 ppm, cf lab 0.5 ppm), Cu ore (sample # 32, 30 ppm, cf lab 2 ppm), and the three itabirites (36-49 ppm, cf lab 0.5 ppm). It is interesting that the high REE sample, GWM-PR (sample # 35), which contains 30 ppm Sn, is below detection in the powder by HH-C and is detectable for Sn in only a few analyses of the smooth or rough surfaces; it is reported at 32 ppm in the powder by HH-A. Very few samples are above detection by HH-A (and the mining mode has a high background).

Table 5.2.26 shows the results for the Zn-Pb ores. The results for the means of # 558932 are very consistent across all analyses, and those for # 558933 agree well for surface (smooth and rough) analysis by both instruments, though they are considerably higher than the lab and powder values. The Zn-Pb ore, SJC 06, containing 44 ppm Sn, reports by HH-C at 320 ppm in the powder and 181 ppm in the smooth surface analysis and by HH-A at 173 ppm in the powder and 699 ppm (98% RSD over only 3 analyses, the rest being <LOD): clearly this sample is very inhomogeneous in Sn. Again, there is no consistent difference in RSDs for smooth versus round

surface measurement and RSDs for surface analysis by HH-A and HH-C are similar for the same sample.

Table 5.2.26. Results for Sn in Zn-Pb ores by HH-C and HH-A (in italics), mean in ppm, RSD in %

Sample	Lab	Powder		Smooth		Round	
		Mean	RSD	Mean	RSD	Mean	RSD
558932	46	49.3	12.2	55.6	22.0	68.3	11.7
558932	*46*	*42.5*	*34.9*	*74.8*	*12.3*	*74.6*	*11.8*
558933	131	223	3.9	794	85	770	93
558933	*131*	*190*	*4.5*	*789*	*122*	*741*	*81*
558934	265			258	46.7	193	56.8
558934	*265*			*215*	*44.6*	*351*	*47.4*
558935	714			406	70.3	408	72.5
558935	*714*			*438*	*68.2*	*372*	*39.9*
SJC 06	44	320	2.0	181	68		

Except for the two very coarse REE-enriched samples, the median RSD of 24% associated with the analysis of the smooth surface does not show a dependence on grain size distribution. This RSD breaks down to 12-32% for the felsic, mafic and 'other' categories of rocks and 48-64% for the ores and high REEs.

Sr, strontium (0.5-5590 ppm)
Except for a couple of fliers in the quartz diorite series with high RSDs of 36-38% in the smooth surface analysis, the x-y plots of smooth, rough and round surface analysis versus the powder are very good, with r^2 values better than 0.92, for example, using HH-A (Fig. 5.2.44). Both instruments show that calibration for the REE-enriched samples is different from other rock types (suppressed values, low slope). The HH-C calibration for Sr of powder versus lab result is excellent, with a slope of 0.95 and r^2 value of 0.96 (Fig 5.2.45); one of the few fliers (1074 ppm) is due to an odd lab value of 0.5 ppm provided for the quartz diorite 1689352.

There is no difference essentially between the RSDs in the analysis of the smooth and round surfaces. For example, using HH-C data, the mean RSDs are: 32 and 27% for the Zn-Pb ore 558932; 57 and 53% for another Zn-Pb ore 558933; 22 and 17% for the shale AU 08808; and 29 and 22% for the shale AU 08825.

The median RSD of 20% for the smooth surface determination by HH-C breaks down by grain size distribution to: a progression from ~ 10% (very fine) through 20% (fine, medium) to 40-75% for the coarse and very coarse grained samples. By rock type, the distribution is: ~ 10-20%

RSD for the felsic, mafic and 'other' categories to 40% for the ores and 75% for the REE-enriched rocks.

Te, tellurium (0.005-2 ppm)
Except for several samples containing ~ 1 ppm Te, the overwhelming majority have well under 1 ppm. However, in many of these samples HH-C reports tens or even hundreds of ppm Te. However, an analytical problem is suggested by the standard deviation or `error` of each individual pXRF analysis, typically in this suite at 15-20 ppm (i.e. high) regardless of the Te reading itself.

Th, thorium (<0.05->1000 ppm)
The Pb Lβ line (12.61 keV) is very close to the Th Lα line (12.97 keV) and therefore interference from Pb in the Zn-Pb ores can be expected. Indeed, HH-C reports, for example, 636 ppm Th in the powder and 89 ppm (58% RSD) in the smooth surface of the ore sample # 34 (SJC 06, 9.6% Pb) but the lab value is only 0.11 ppm. Similarly, other Zn-Pb ores 558934 and 558935 (sample #s 4, 5), containing 1-5% Pb and < 1 ppm Th, report by smooth surface analysis 41 and 68 ppm Th, respectively; by HH-A only a few values by smooth surface analysis are reported above LOD for 558934, at ~ 14 ppm, and a value for SJC 06 is not reported at all (i.e. interference detected).

The x-y plots of surface vs powder results by HH-A are very good, with r^2 values better than 0.93 (Fig. 5.2.46, HH-A). The calibration against lab results would be quite good, save for the suppression shown for the three splits of the REE-enriched sample 598901. The itabirites by HH-C read very high, at 51-174 ppm, compared to lab values under 1 ppm (not so by HH-A) but this instrument shows better correlation with the quartz diorite series than does HH-A.

Table 5.2.27 for the shales shows that, in the absence of interfering elements, analysis for Th at low levels can be excellent: means agree well across the nature of the sample surface and the instruments; RSDs by HH-C tend to be higher but other than that there is no consistent difference in RSDs amongst the three categories of surface.

The median RSD for the smooth analysis by HH-A is 21% and 43% by HH-C.

Table 5.2.27. Results for Th in shales by HH-A and HH-C (in italics), mean in ppm, RSD in %

	Lab	Powder		Smooth		Rough		Round	
		Mean	RSD	Mean	RSD	Mean	RSD	Mean	RSD
AU08803	9.1	10.3	6	10.3	41			10.3	23
AU08803	*9.1*	*11.2*	*3*	*6.1*	*73*	*12.7*	*107*	*6.9*	*55*
AU08808	5.2	7.5	7	10.6	56			10.7	54
AU08808	*5.2*	*5.3*	*14*	*10.1*	*83*			*9.8*	*78*
AU08818	12	15.3	11	13.2	20			16.0	15
AU08818	*12*	*13.4*	*13*	*13.9*	*24*	*11.2*	*30*	*14.7*	*21*
AU08819	2.9	6.8	27	5.1	20			5.0	19
AU08819	*2.9*	*2.9*	*29*	*4.3*	*30*			*3.9*	*18*
AU08825	5.7	9.3	7	7.0	29			8.6	43
AU08825	*5.7*	*6.5*	*19*	*5.5*	*49*	*8.8*	*42*	*6.0*	*60*

U, uranium (<0.05-171 ppm)

With a few exceptions, the majority of samples contain less than 10 ppm U. There are very few values provided in the analysis by HH-A, not even for the three splits of REE-rich 598902 which contain 122-144 ppm U or for the Cu-rich schists LM03 and LM04 containing 10 and 97 ppm U. The values for the REE-rich 598901 containing 111-176 ppm are suppressed, at 38-41 ppm U.

The x-y plots of surface analysis versus powder results by HH-C are acceptable, with r^2 values of 0.76 to 0.95 and the calibration, though of good fit (0.99), shows a positive bias at the low end (~ < 40 ppm U) (HH-C, Figs. 5.2.47 and 5.2.48). The high U values (up to ~ 200 ppm) are those for the REE-enriched samples. The median RSD of 28% for the smooth surface analysis comprises: based on grain size, 22-24% for the very fine to medium, and 42-48% for the coarse to very coarse grain size distribution; and, based on rock type, ~ 18% for the felsic rocks and a tight range of 28-35% for all the other samples.

V, vanadium (2.5-730 ppm)

The L lines of the REEs interfere severely with the K lines of V and hence V is reported by both instruments to be very high in the REE-enriched sample suite (e.g. in GWM-HL at 52 ppm V, HH-A reports 2150 ppm V and HH-C reports 456 ppm). Without these samples, the calibration using HH-C would be good (Fig. 5.2.49); the x-y plots of the surface results versus powder are certainly acceptable (Fig. 5.2.50). The 23% median RSD consists of: by grain size, ~ 10% for very fine, through 22-24% for fine and medium, to ~ 45% for coarse; and by rock type, 14% for mafic, 18% for 'other', 23% for felsic, and 30% for ores (ignoring the problematic REE samples).

W, tungsten (0.5-217 ppm)
The W Lα and Lβ lines (8.4 and 9.67 keV) can suffer from overlap with the Zn Kα and Kβ lines (8.64 and 9.57 keV) and therefore severe interference is to be expected in analysis of the Zn-Pb ores. For example, HH-A reports (a) 355 ppm W in Zn-Pb ore 558933 (2.14% Zn) which contains only 1 ppm W and (b) 8728 ppm W in ore SJC 06 (30% Zn) which contains only 0.5 ppm. The software for HH-C has been programmed to recognise such interference and no data are reported for these samples. It is the reverse situation for the high Cu ore: HH-A does not report W in the Cu ore SJC 07 (18.8% Cu) because of the interference from Cu K lines but HH-C does, a value of 508 ppm W compared to a lab value of 6 ppm. The other sporadic results provided by HH-A are very poor. Results by HH-C are certainly better but not good (e.g. results in the tens of ppm for a basalt, rhyolite, and diabase containing < 1 ppm W); the calibration shows a high bias (slope of 1.6, intercept of 47 ppm and r^2 of 0.57).

Y, yttrium (0.25-2330 ppm)
Yttrium by HH-A shows very good results with the glaring exception of two groups of samples: the Zn-Pb ores which show positive interference (e.g. ore SJC 06, 30% Zn and 9.6% Pb, reports 311 ppm Y, cf lab 2.3 ppm); and the splits of the high REE cores which show suppression (e.g. in 598902-c, HH-A reports 694 ppm Y, cf lab 1750 ppm).

Table 5.2.28 shows that for interference-free matrices such as these shales, analysis can be excellent across the different surfaces of the samples. The inferior RSD for the round surface compared to smooth in samples 8803 and 8825 was not apparent in the HH-C mining mode data discussed earlier and therefore this is not a 'real' phenomenon.

Table 5.2.28. Results for Y in shales by HH-A, mean in ppm, RSD in %

		Powder		Smooth		Round	
	Lab	Mean	RSD	Mean	RSD	Mean	RSD
AU08803	94	109	2.7	114	13.0	127	24.8
AU08808	29	28	8.1	22	47.4	26	45.6
AU08818	56	53	1.4	58	16.7	69	19.5
AU08819	29	28	3.2	32	10.0	30	7.8
AU08825	31	32	6.4	21	24.1	29	59.7

Zn, zinc at low concentrations, <1000 ppm (full range is 1 ppm-30.0%)
Without the fliers caused by the three splits of each of the two high REE cores (598901 and 598902; cf 1793-2135 ppm vs 642-761 ppm lab for 598902), the calibration of powder against lab values by HH-C would be excellent; these samples also degrade the calibration by HH-A but not so badly (Fig. 5.2.51, HH-C, Zn values <1000 ppm).

HH-A reports 269 ppm Zn in the powder of the Cu ore SJC 07 (sample # 32, 96 ppm Zn lab value) but <LOD for the surface analysis and HH-C reports <LOD throughout for this ore. Presumably the shoulder of the Cu K lines is an interference for its neighbour Zn and a value of 96 ppm cannot be measured in such a matrix (18.8% Cu). HH-A reports 72 ppm Zn in the smooth surface analysis of the Cu-rich schist LM03 (2.9% Cu); the lab value is only 10 ppm (14 ppm by HH-C).

In the high REE sample, GWM-PR, HH-A reports 440 ppm in the powder (lab is 464 ppm) but only 43 ppm (RSD is 57%) for the 10 smooth surface analyses and 82 ppm (40% RSD) for the 10 rough surface analyses; HH-C performs similarly. This is by far the largest discrepancy between powder and direct surface analysis.

The median RSD (24%) for the smooth surface analysis by HH-A breaks down to: by grain size, ~ 8%, very fine, through ~ 22% for fine to medium and ~ 28% for coarse to 58% for very coarse; by rock type, ~ 10% for mafic, through 20% for felsic, 25% for 'other' and 35% for ores to 52% for the high REEs. For the few samples (e.g. porphyry ores, sample #s 9-12) whose rough or round surfaces were also analysed, there is essentially no difference in RSD compared to smooth.

Zr, zirconium (3->10000 ppm)
The calibration lines for both HH-A and HH-C are very good, with r^2 values of 0.98 and 0.99. The one very high sample is GWM-PR which contains > 10,000 ppm Zr and is reported at 15,761 ppm by HH-A and 16,922 ppm by HH-C.

The 23% median RSD by HH-A by grain size comprises ~ 18%, very fine – 22%, fine - 26%, medium – 36%, coarse - 40%, very coarse; HH-C is similar, with a median RSD of 24% but the RSDs for the two coarse categories are in the range 50-90%. Figure 5.2.52 (HH-A) shows the much higher RSD (~ 60%) of the REE-enriched samples compared to the other rock types (~ 20-25%).

Table 5.2.29 for the shales demonstrates excellent agreement across instruments and surface types except for one sample, AU08825, which is the noisiest in the surface analysis, resulting in a high mean value of 642 ppm for the rough surface. This sample and AU08819, unlike the others, display significantly better RSDs for the smooth rather than round surface analysis.

Table 5.2.29. Results for Zr in shales by HH-A and HH-C (in italics), mean in ppm, RSD in %

	Lab	Powder Mean	Powder RSD	Smooth Mean	Smooth RSD	Rough Mean	Rough RSD	Round Mean	Round RSD
AU08803	304	345	2	263	25			257	30
AU08803	*304*	*356*	*1*	*236*	*21*	*276*	*51*	*242*	*17*
AU08808	154	165	1	188	23			212	21
AU08808	*154*	*168*	*3*	*183*	*20*			*223*	*30*
AU08818	140	152	1	165	18			193	16
AU08818	*140*	*148*	*6*	*159*	*24*	*125*	*50*	*187*	*15*
AU08819	147	153	2	206	9			183	19
AU08819	*147*	*155*	*1*	*200*	*10*			*187*	*21*
AU08825	220	246	3	182	41			238	69
AU08825	*220*	*244*	*1*	*138*	*30*	*642*	*40*	*211*	*73*

Summary of rock surface study

Below are tables (Tables 5.2.30 for HH-A and 5.2.31 for HH-C) summarising the median RSD values for the different surface analyses of the suite of 86 rocks and ores; elements where performance was overwhelmingly very poor (e.g. Au, Cs, Te, W) have been removed. The number of samples whose data are included in the RSD computation is given in the adjacent column; this number is important as it qualifies the validity of the results. Note that the suite of rough surface analyses (14) constitutes mostly the high REE samples and itabirites which are problematic samples, and the suite of round surface analyses (16) includes the Zn-Pb and Cu ores, whose behaviour can be quite distinct from that of many samples in the smooth surface group. It should also be borne in mind that the focus of these data is precision and not accuracy; some of the results included in the RSD calculations are affected by interferences, especially for the ores and high REE samples. Some of the median RSDs for HH-C are significantly higher than those for HH-A but this is due often to the fact that the former instrument reports on many more samples with low concentrations of that particular element.

Both the highly diverse nature of these samples, and the fact that the suites of smooth, rough and round surface analyses are by no means identical, make summarising the results difficult. Major points are:

- There is no consistent trend in the RSD of multiple analyses of a rock or ore with the texture of the surface, i.e. analysis of a rough or round surface does not appear to generate an RSD that is inferior to that of a smooth surface. The difference in RSD across such types of surface is highly sample-dependent. Of course, light elements such as Al and Si show lower absolute concentrations and greater variability for a rough surface

analysis compared to smooth because of the air, between sample and pXRF window, which absorbs low-energy photons.

- As with the granodiorites, the RSDs of powdered samples is on average much lower than surface measurements. For many situations it may be more efficient to grind the samples, and to carry out pXRF measurements on the powder, rather than take multiple shots on the rock surface, particularly for inhomogenous and/or coarse-grained materials.

- For most elements there is a relationship between median RSD and grain size, with significant differences between the very fine and coarse/very coarse, the RSD for the latter group being considerably higher. However, it must be noted that the coarse group comprises two porphyry Cu ores and a peridotite and the very coarse group two Cu ores and two high REE samples, a very different cross-section from the fine and medium groups which are good mixes of rocks and ores. The median RSDs for the fine group are often higher than those for the medium suite, and almost always higher than those for the very fine group. The median RSDs for the very fine, fine and medium samples form a distinct cluster significantly removed from those of the higher coarse/very coarse grouping. In the granodiorite suite, the relationship between RSD and grain size is clearer, because the lithology is much more consistent between samples.

- The median RSDs for the high REE and ore samples are almost always considerably higher than those for the other categories of samples (mafic, felsic and 'other' including shales and Cu-rich schists). These samples, together with the itabirites, are most affected by inter-element interferences (mostly spectral), and certainly require specific calibrations (e.g. suppression of signals in high REE samples is evident for some elements such as Th and Y).

- There is quite a strong tendency in general towards lower mean values for the direct surface results compared to those for the powder (e.g. Cu), especially in situations of high RSDs (but the opposite is true for Ba).

- With respect to trends in RSD across different surface textures for the same sample, generally the two instruments behaved similarly.

- Interference-plagued data are handled differently by the software of the two instruments, HH-A and HH-C. The latter often reports results for samples which are badly affected whereas the former simply does not report any results, presumably programmed to recognise the magnitude of the interference and if, very large, eliminate the result. This

approach needs to be more widespread; interferences were encountered for samples whose matrix was thought to be non-problematic (e.g. a gneiss, norite, basalt).

- Results by pXRF for elements such as Au and Hg, normally present in geological materials at ppb levels, should be viewed with extreme caution as concentrations at the ppb level are often reported erroneously at the ppm level. Other elements also such as Bi, Cs, Te and W could not be determined in this diverse suite. In contrast, pXRF can perform extremely well for trace elements such as Rb, Sr, Nb, Y, and Zr.

Table 5.2.30. Summary of median RSDs in the direct surface and powder analysis by HH-A

	Smooth		Rough		Round		Powder	
	RSD	n	RSD	n	RSD	n	RSD	n
				A. Mining mode				
Si	5.7	78	28.6	9	9.8	16	0.4	64
Al	10.1	77	23.1	9	19.5	16	1.0	61
Mg	17.5	24		0	18.1	1	6.2	9
Ca	17.8	67	29.2	8	40.9	13	0.6	54
Fe	18.1	78	21.9	9	25.6	16	0.5	64
Ti	19.5	72	21.5	7	30.7	13	2.9	60
Mn	20.1	76	26.5	9	22.2	16	3.8	61
Pb	21.7	66	35.1	7	33.9	16	7.1	55
K	23.2	64	50.0	7	29.5	13	0.7	53
Zn	25.8	59	16.6	7	41.6	14	3.1	50
P	32.0	30	17.0	7	70.2	2	3.3	28
Cu	37.2	75	22.6	6	38.8	16	5.2	60
S	38.8	62	64.8	6	34.6	16	1.2	42
				B. Soil mode				
Co	17.5	78	39.9	8	30.1	16	3.9	63
V	17.6	76	44.7	10	20.5	14	2.7	61
Rb	19.2	68	28.0	9	24.8	13	1.4	54
Sr	19.5	75	27.8	9	20.1	14	1.2	63
Mn	20.2	78	34.3	10	26.0	16	1.3	65
Th	20.8	68	24.2	10	23.4	16	11.1	51
Zr	22.6	70	24.9	9	26.2	12	1.5	61
Cr	23.3	73	46.0	9	19.8	15	4.0	58
U	23.4	27	19.1	6	16.7	8	6.2	12
Nb	23.7	74	26.1	10	25.8	16	7.0	62
Mo	24.1	40	20.8	6	40.6	16	7.7	26
Zn	24.2	76	27.2	9	39.2	16	2.8	61
Y	24.6	76	17.2	10	26.1	16	3.7	63
Sb	24.7	17	24.0	5	47.3	7	8.2	12
As	25.5	77	39.4	9	34.1	16	3.8	63
Se	25.7	29	42.0	6	30.6	10	10.4	24
Ni	28.5	39	50.5	7	34.0	6	9.0	17
Pb	28.7	38	41.5	8	37.5	16	2.8	27
Sn	44.6	9	15.5	6	43.7	8	12.7	10
Cu	52.7	75	23.9	9	46.4	16	4.2	60
Cd	54.1	6	34.9	5	38.2	3	10.1	7

Table 5.2.31 Summary of median RSDs in the direct surface and powder analysis by HH-C

	Smooth		Rough		Round		Powder	
	RSD	n	RSD	n	RSD	n	RSD	n
				A.	Mining mode			
Si	3.9	68	17.1	14	8.8	16	0.3	62
Al	8.1	68	22.1	14	24.1	16	1.0	61
K	19.7	74	24.1	12	34.5	14	0.5	60
Fe	19.8	78	29.0	14	30.5	16	0.3	65
Ca	20.3	78	29.5	14	42.3	16	0.5	62
Mn	20.8	72	42.2	14	41.9	15	2.7	57
Mg	23.6	68	25.0	14	34.6	15	9.4	59
P	24.0	66	32.2	14	23.3	16	4.9	60
Y	24.0	67	34.2	14	28.4	16	2.6	59
Zn	24.6	76	30.4	14	42.9	16	2.0	60
Ti	24.9	75	34.6	12	40.1	13	1.6	59
Nb	33.0	54	43.6	13	37.5	14	11.8	51
Pb	36.0	40	35.0	13	37.6	16	2.0	33
Cd	43.1	13	84.9	5	39.0	3	10.1	13
S	49.4	76	41.3	12	27.9	16	1.4	57
Cu	64.6	64	36.7	13	83.9	16	3.7	50
				B.	Soil mode			
Ba	11.0	78	33.0	8	16.4	16	2.0	59
Mn	17.4	78	46.3	14	28.6	16	2.5	64
Ni	17.5	78	36.3	14	27.1	13	8.4	61
Sr	20.3	78	31.5	14	23.5	16	0.8	65
V	23.1	77	32.8	14	25.9	16	3.7	65
Sb	23.3	78	44.7	8	49.6	12	15.1	45
Zr	24.1	72	38.6	12	34.3	15	0.9	61
Sn	24.2	78	41.4	8	32.2	12	11.9	42
Zn	25.9	78	33.0	14	39.0	16	2.7	64
Rb	26.9	77	32.7	14	33.0	16	1.6	66
U	27.5	78	28.3	14	29.2	16	11.3	64
Th	43.4	78	38.8	14	32.4	16	11.0	64
Ag	43.6	77	46.7	8	41.0	11	25.8	47
Se	47.9	78	57.3	13	41.6	11	35.3	54
Pb	52.0	50	60.8	14	48.6	16	3.0	40
Cr	53.2	65	49.4	13	35.6	16	6.0	52
Cu	54.2	78	42.7	14	62.0	16	4.2	66
Co	56.2	74	54.5	8	66.5	8	27.9	43
Mo	60.0	60	57.3	13	69.6	16	10.6	56
As	61.4	76	59.7	13	55.1	16	15.0	59
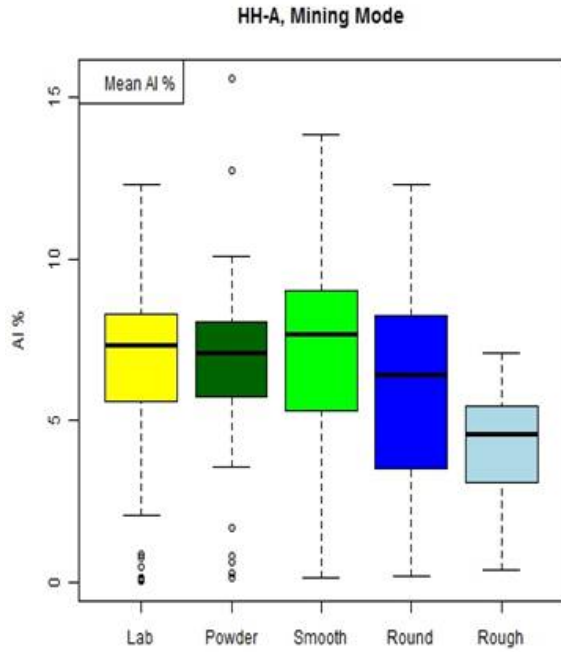
Fig. 5.2.1. Rock_HHA_mining_Al.4.jpg.
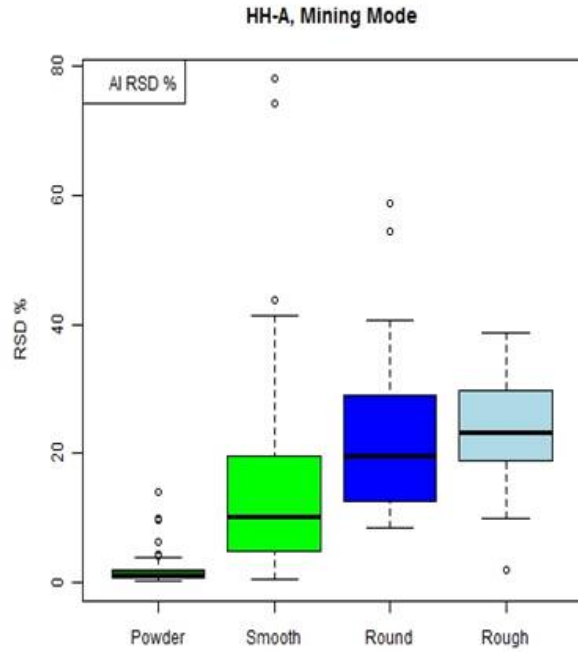
Fig. 5.2.2. Rock_HHA_mining_Al.5.jpg.
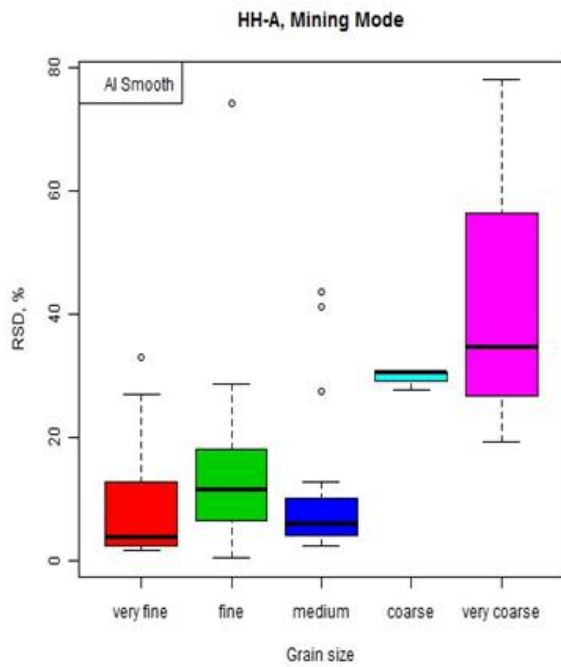
Fig. 5.2.3. Rock_HHA_mining_Al.6.jpg.
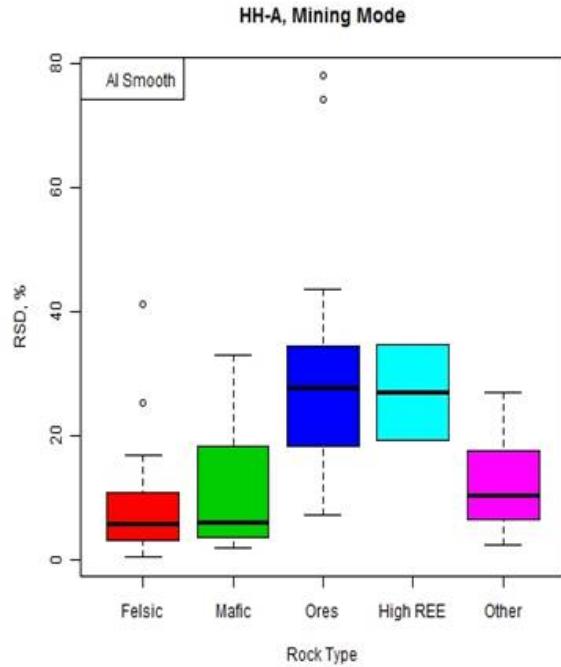
Fig. 5.2.4. Rock_HHA_mining_Al.8.jpg.
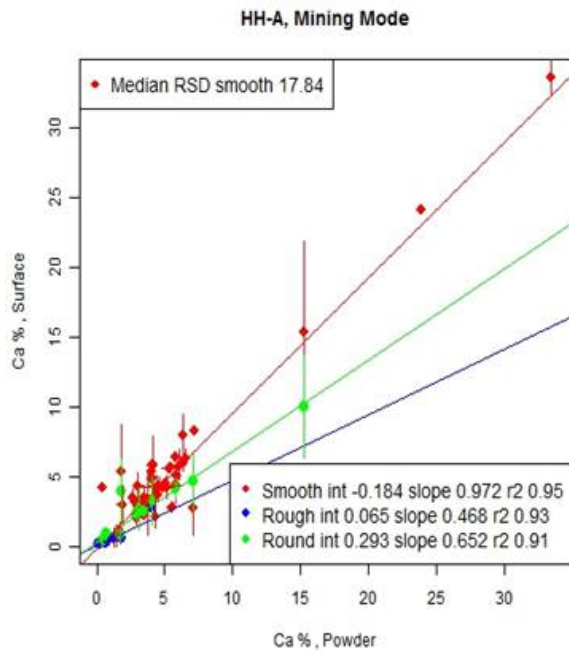
Fig. 5.2.5. Rock_HHA_mining_Ca.2.jpg.
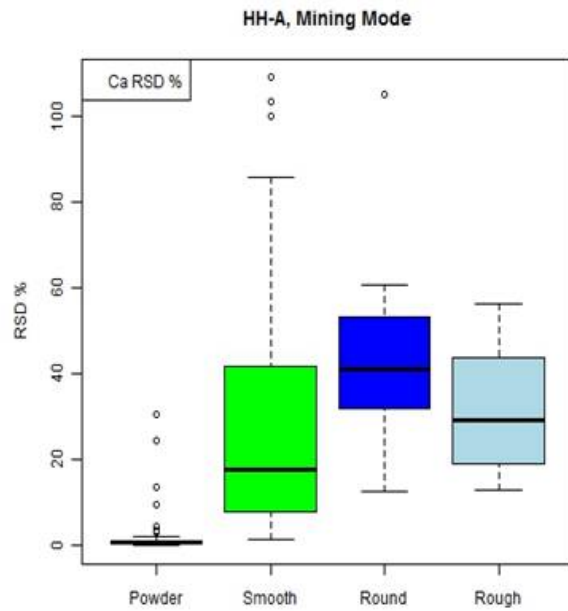
Fig. 5.2.6. Rock_HHA_mining_Ca.5.jpg.
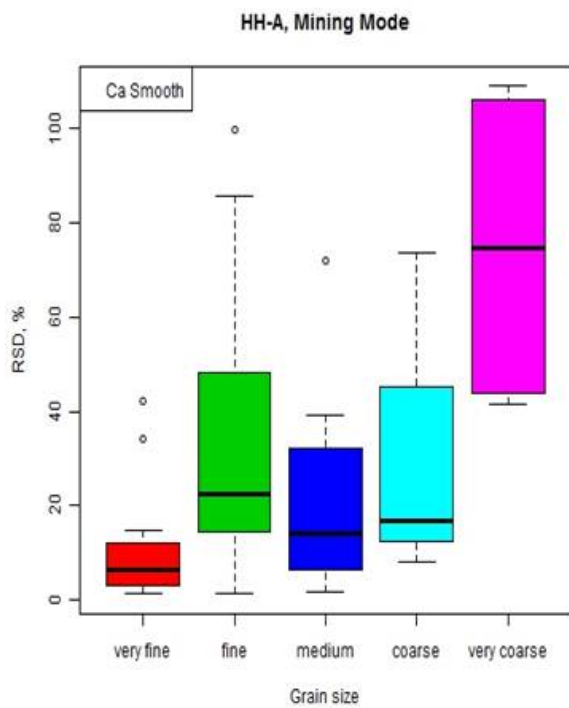
Fig. 5.2.7. Rock_HHA_mining_Ca.6.jpg.
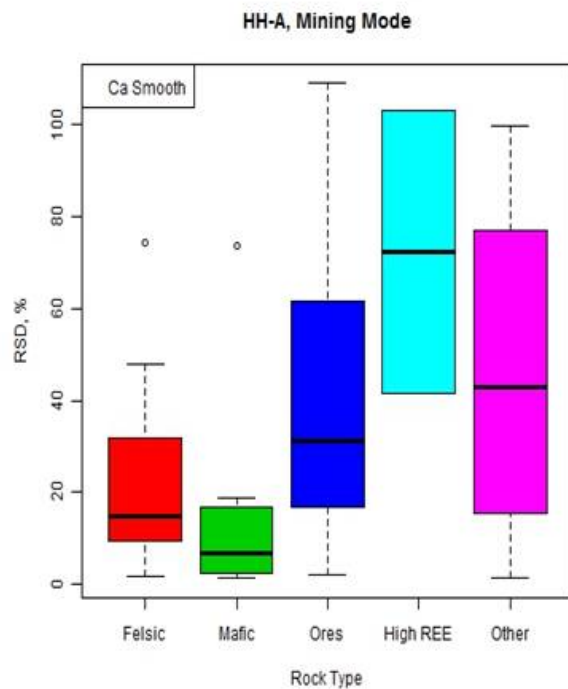
Fig. 5.2.8. Rock_HHA_mining_Ca.8.jpg.
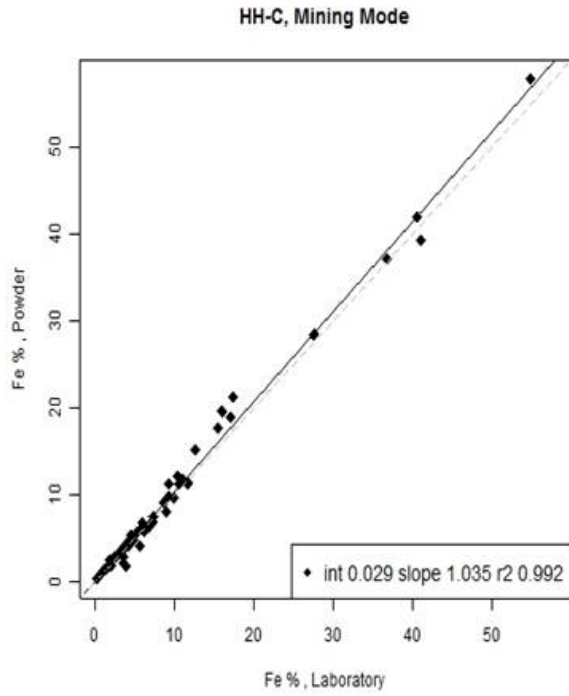
Fig. 5.2.9. Rock_HHC_mining_Fe.3.jpg.
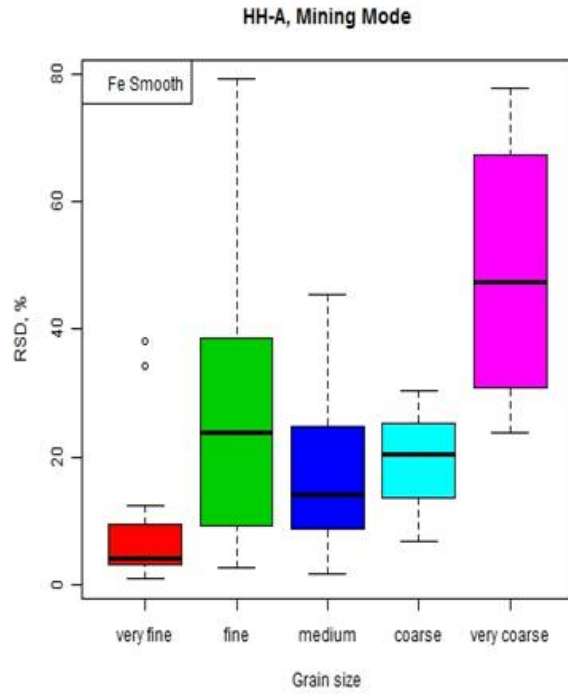
Fig. 5.2.10. Rock_HHA_mining_Fe.6.jpg.
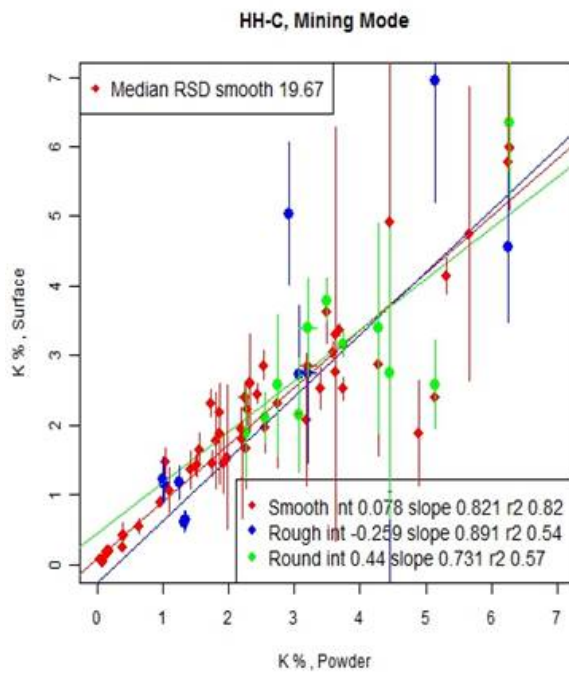
Fig. 5.2.11. Rock_HHC_mining_K.2.jpg.
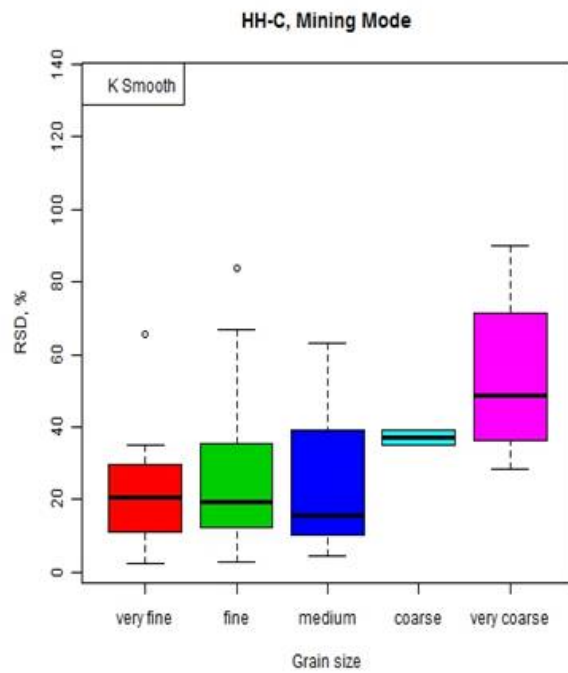
Fig. 5.2.12. Rock_HHC_mining_K.6.jpg.
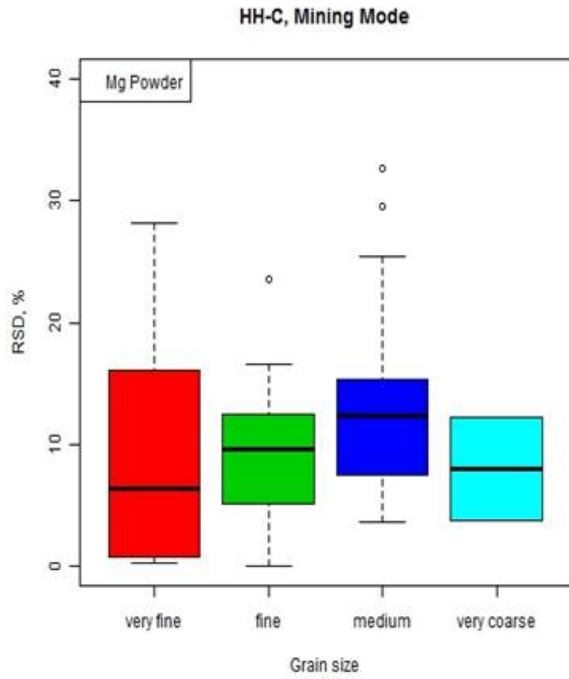
Fig. 5.2.13. Rock_HHC_mining_Mg.7.jpg.
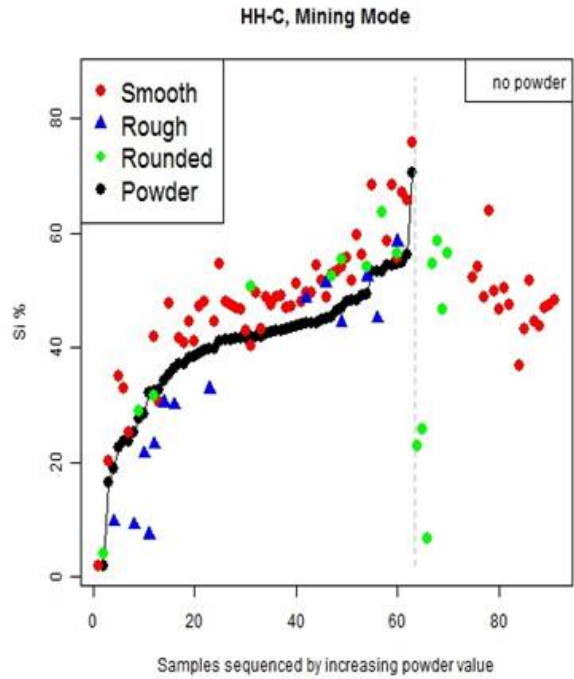
Fig. 5.2.14. Rock_HHC_mining_Si.1.jpg.
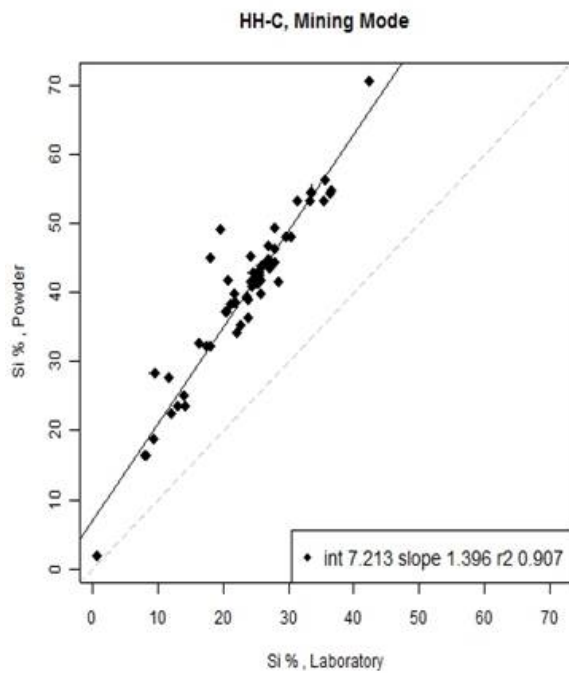
Fig. 5.2.15. Rock_HHC_mining_Si.3.jpg
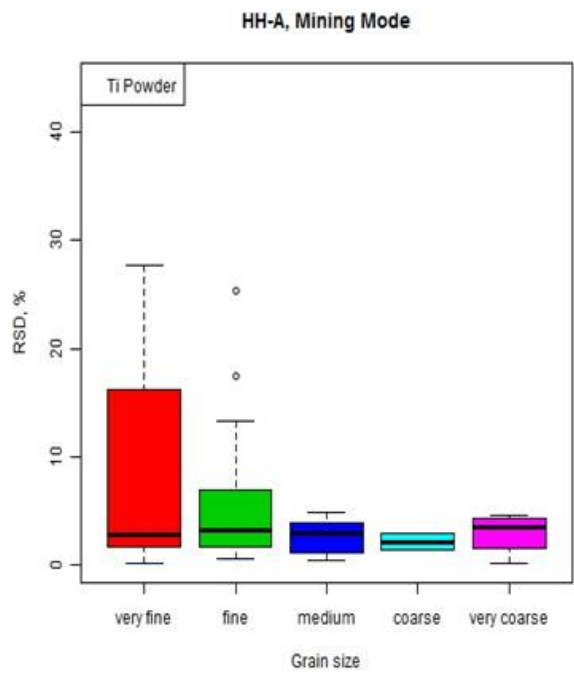
Fig. 5.2.16. Rock_HHA_mining_Ti.7.jpg.
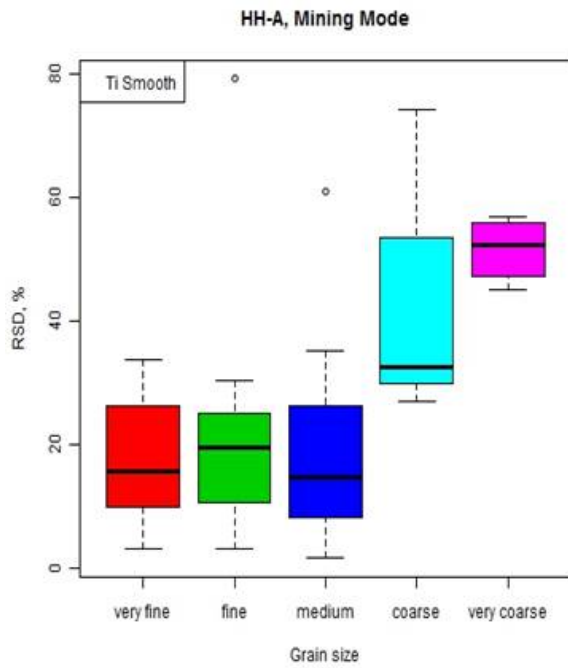
Fig. 5.2.17. Rock_HHA_mining_Ti.6.jpg.
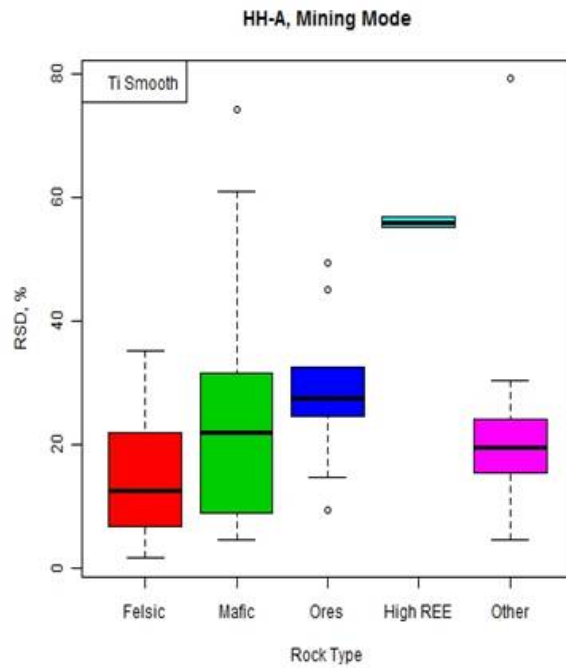
Fig. 5.2.18. Rock_HHA_mining_Ti.8.jpg.
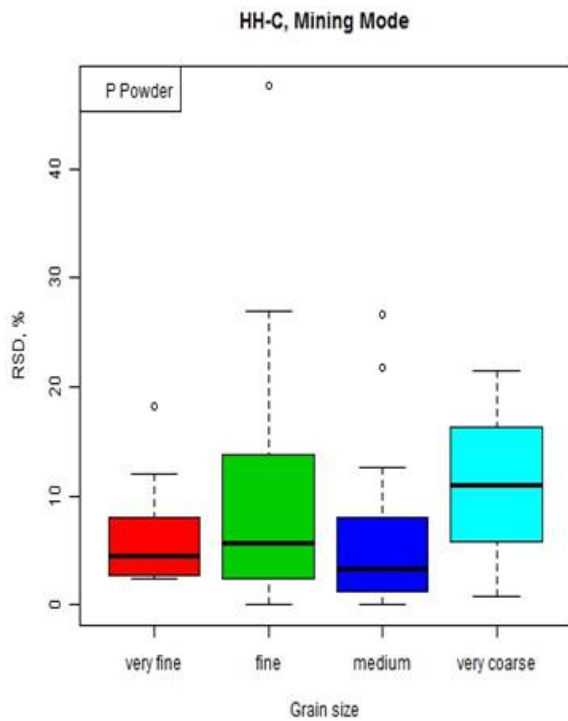
Fig. 5.2.19. Rock_HHC_mining_P.7.jpg.
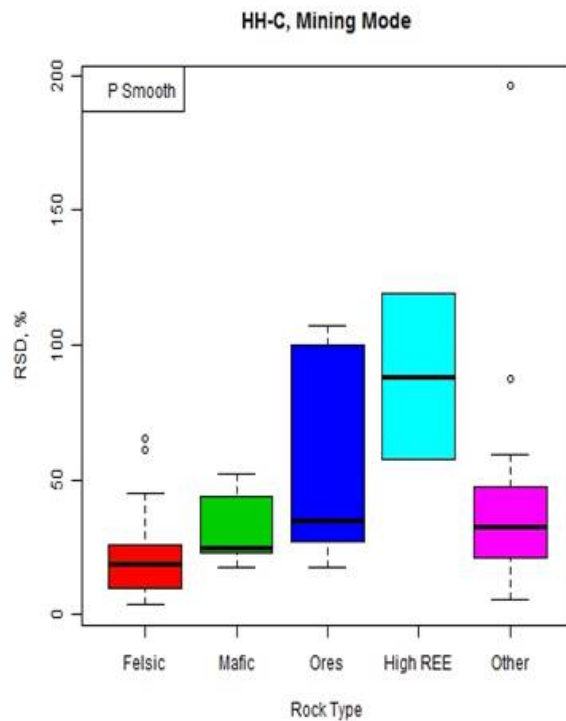
Fig. 5.2.20. Rock_HHC_mining_P.8.jpg.
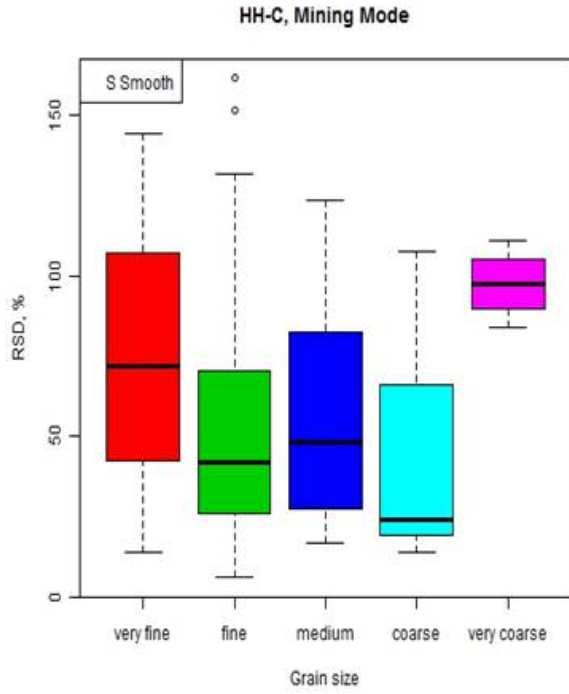
Fig. 5.2.21. Rock_HHC_mining_S.6.jpg.
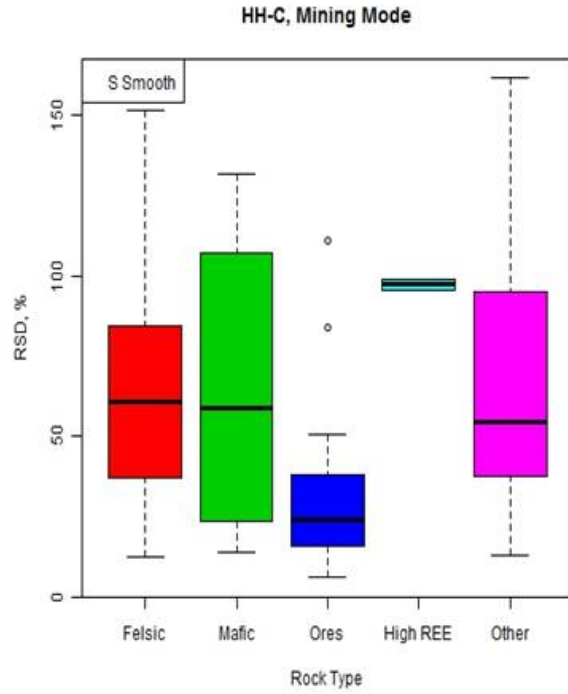
Fig. 5.2.22. Rock_HHC_mining_S.8.jpg.
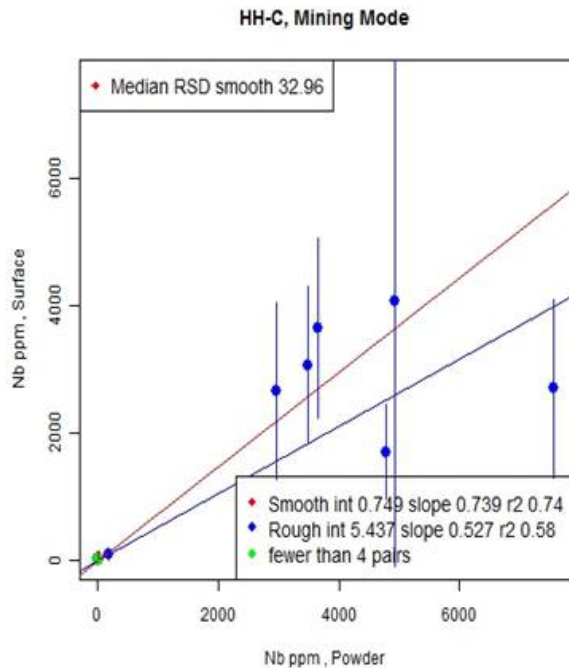
Fig. 5.2.23. Rock_HHC_mining_Nb.2.jpg.
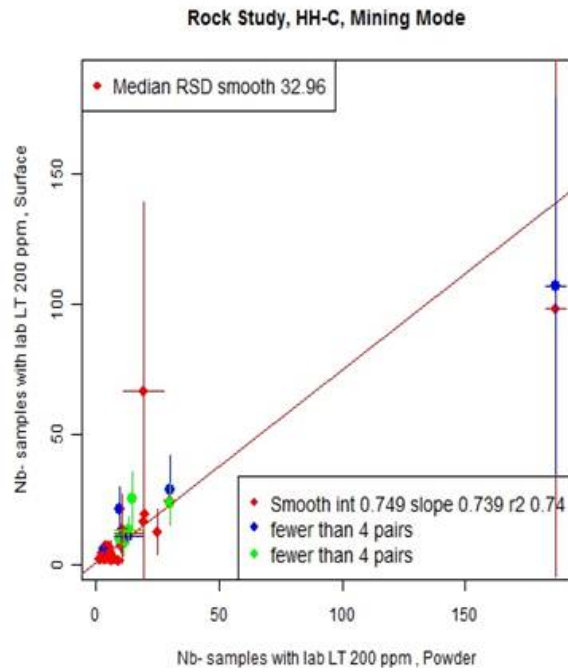
Fig. 5.24. Rock_HHC_mining_Nb.samples with lab LT 200.2.jpg.
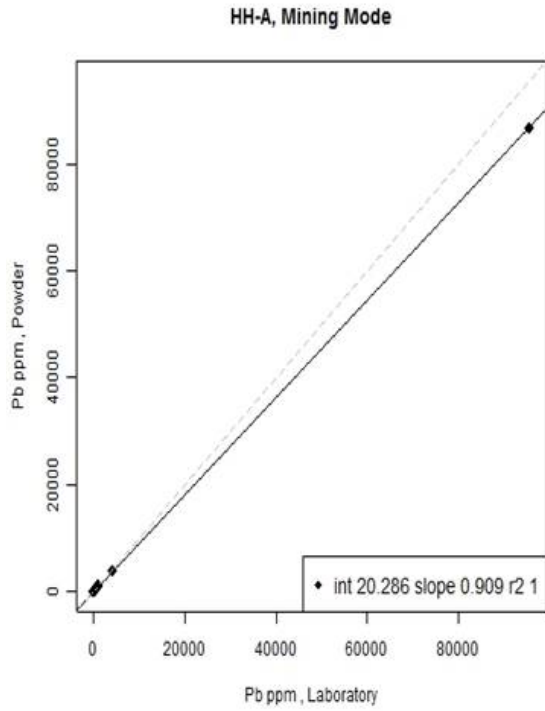
Fig. 5.2.25. Rock_HHA_mining_Pb.3.jpg.
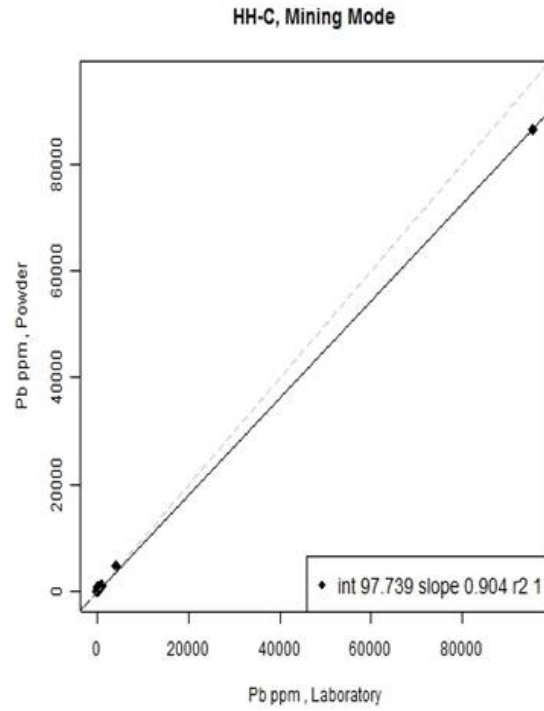
Fig. 5.2.26. Rock_HHC_mining_Pb.3.jpg.
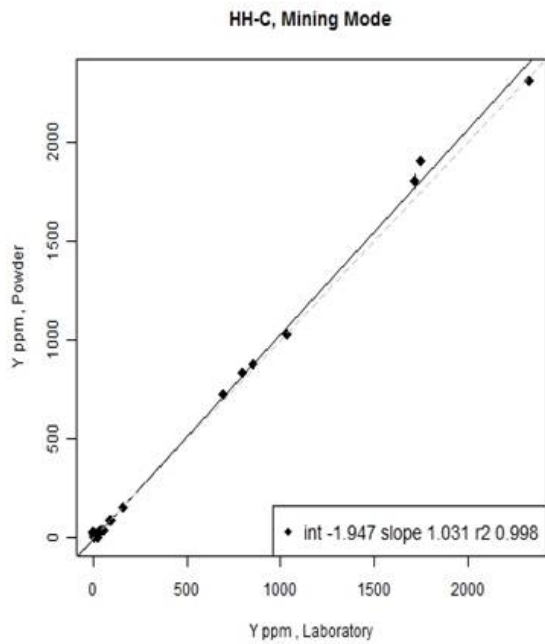
Fig. 5.2.27. Rock_HHC_mining_Y.3.jpg.
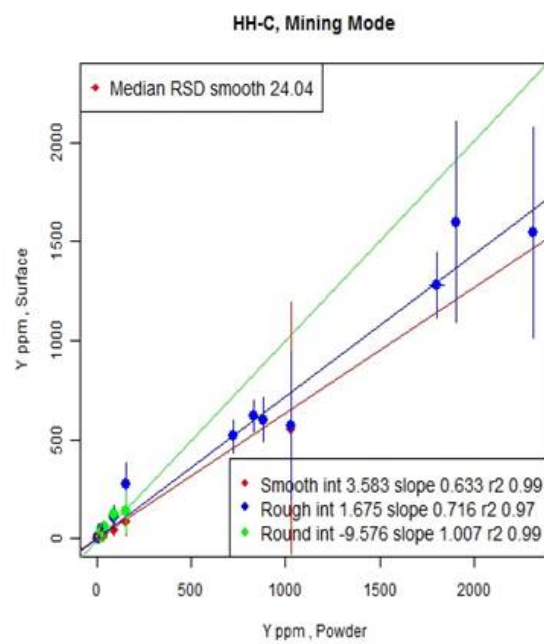
Fig. 5.2.28. Rock_HHC_mining_Y.2.jpg.
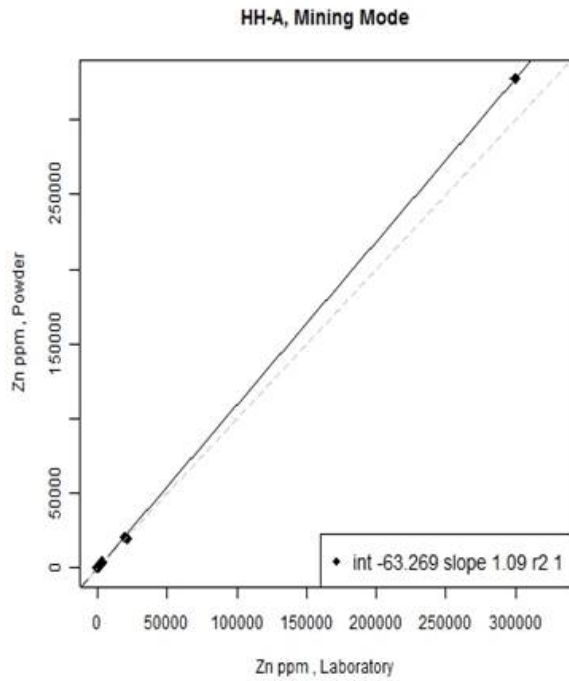
Fig. 5.2.29. Rock_HHA_mining_Zn.3.jpg.
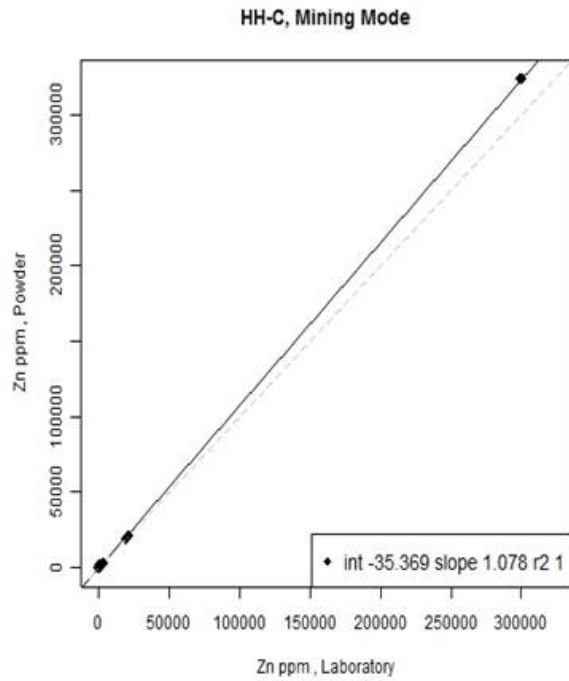
Fig. 5.2.30. Rock_HHC_mining_Zn.3.jpg.
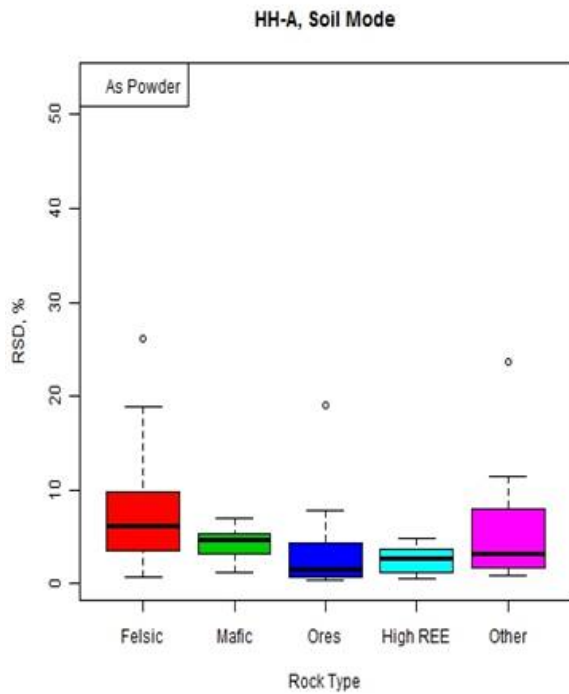
Fig. 5.2.31. Rock_HHA_soil_As.9.jpg.
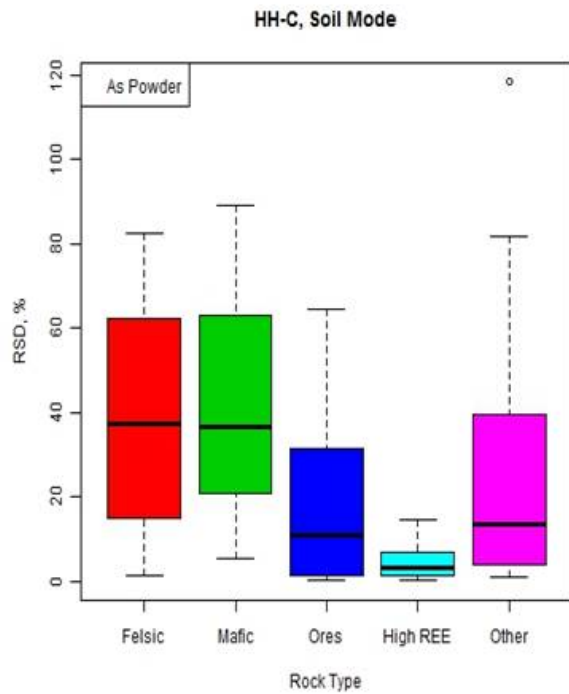
Fig. 5.2.32. Rock_HHC_soil_As.9.jpg.
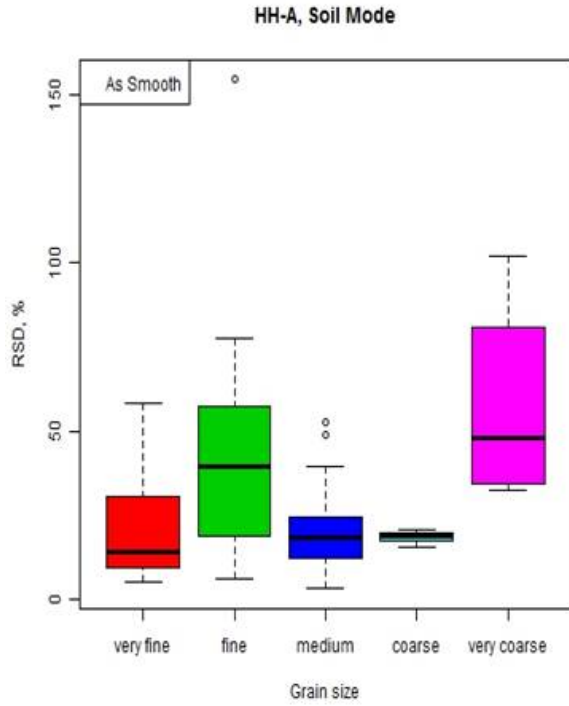
Fig. 5.2.33. Rock_HHA_soil_As.6.jpg.
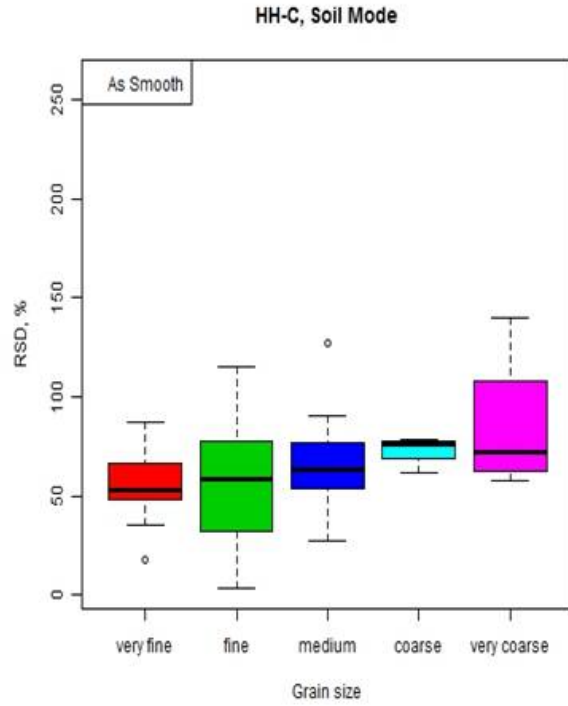
Fig. 5.2.34. Rock_HHC_soil_As.6.jpg.
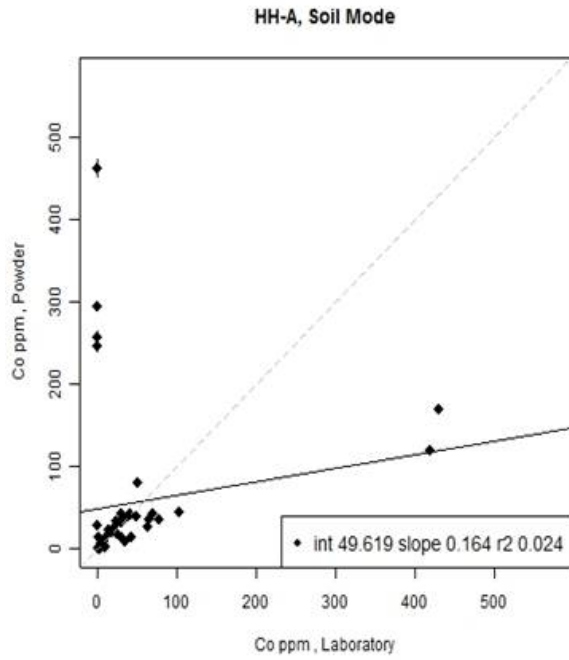
Fig. 5.2.35. Rock_HHA_soil_Co.3.jpg.
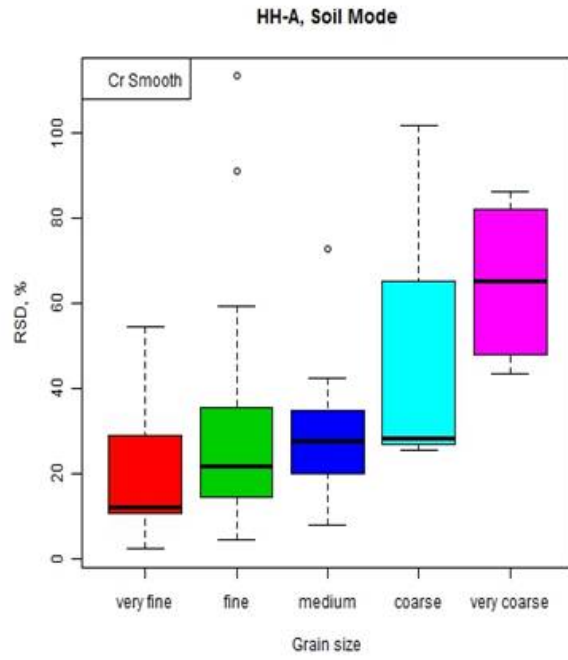
Fig. 5.2.36. Rock_HHA_soil_Cr.6.jpg.

Rock Study, HH-A, Soil Mode
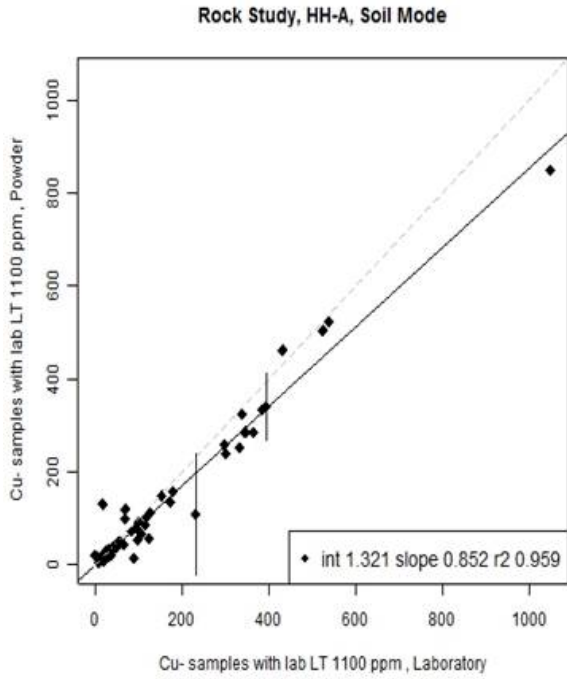
Fig. 5.2.37. Rock_HHA_soil_Cu-samples with lab LT 1100.3.jpg.

Rock Study, HH-C, Soil Mode
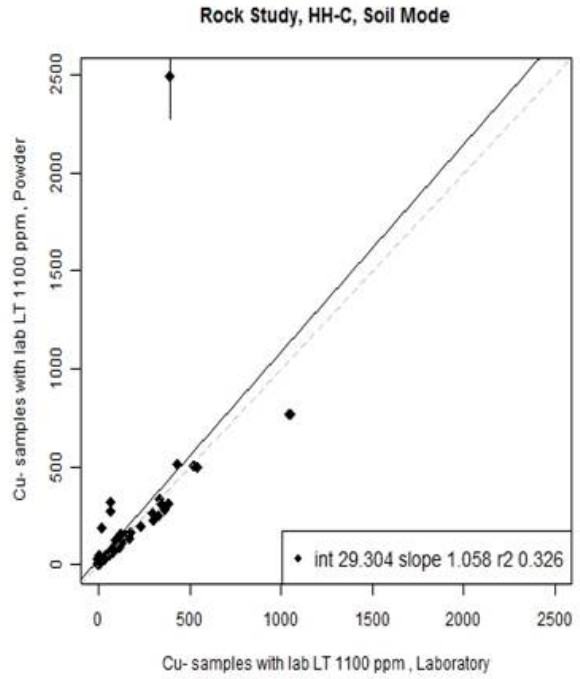
Fig. 5.2.38. Rock_HHC_soil_Cu.samples with lab LT 1100.3.jpg.
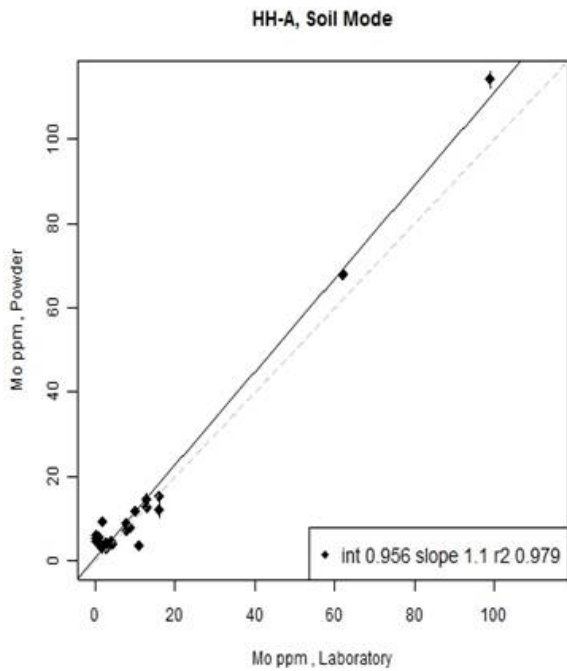
HH-A, Soil Mode

Fig. 5.2.39. Rock_HHA_soil_Mo.3.jpg.

HH-C, Mining Mode
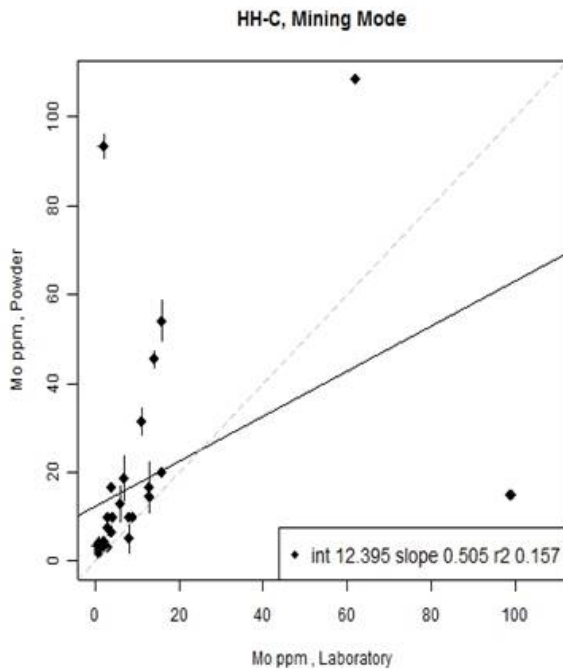
Fig. 5.2.40. Rock_HHC_soil_Mo.3.jpg.
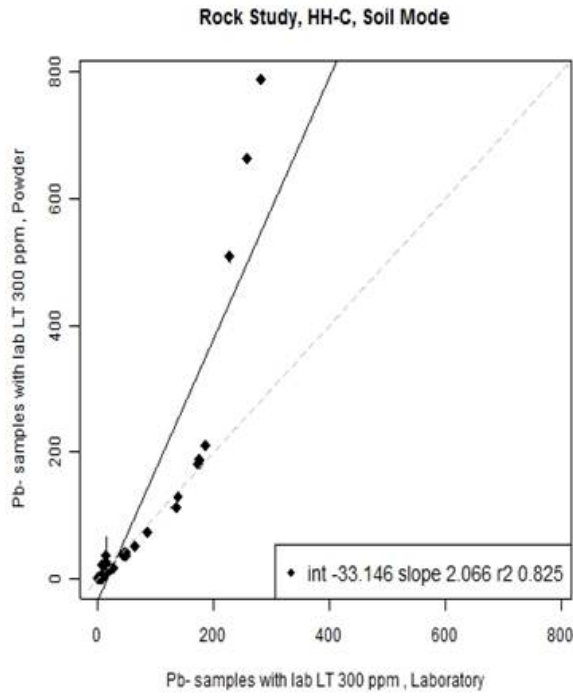
Fig. 5.2.41. Rock_HHC_soil_Pb-samples with lab LT
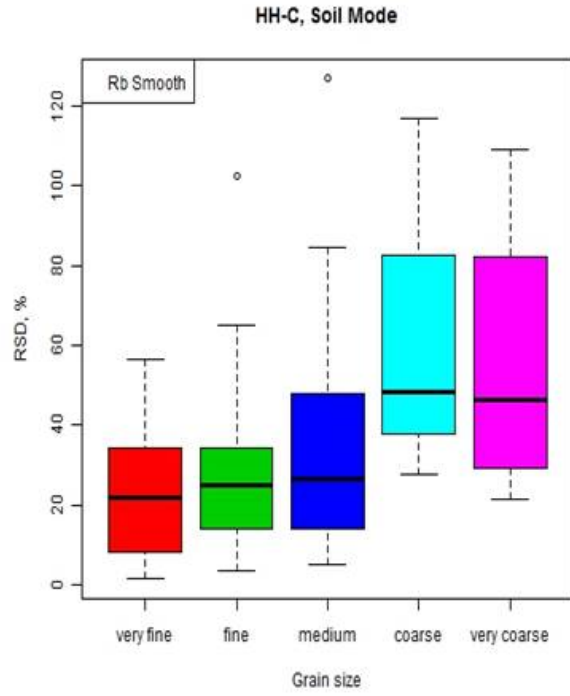
Fig. 5.2.42. Rock_HHC_soil_Rb.6.jpg.
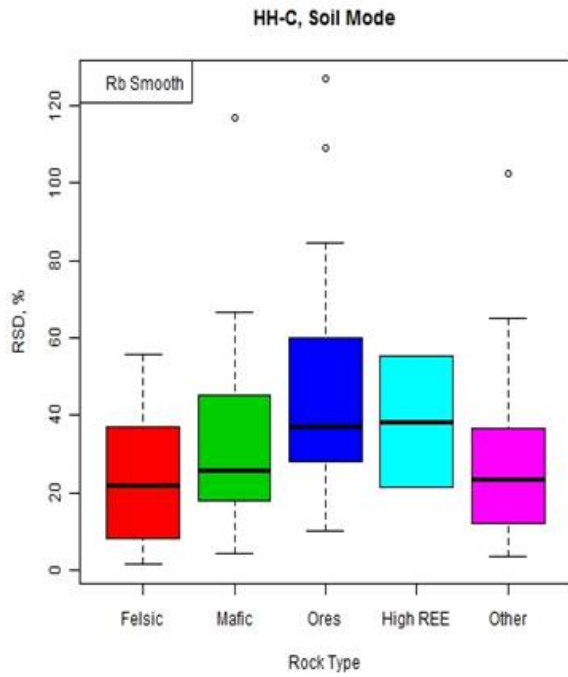
Fig. 5.2.43. Rock_HHC_soil_Rb.8.jpg.
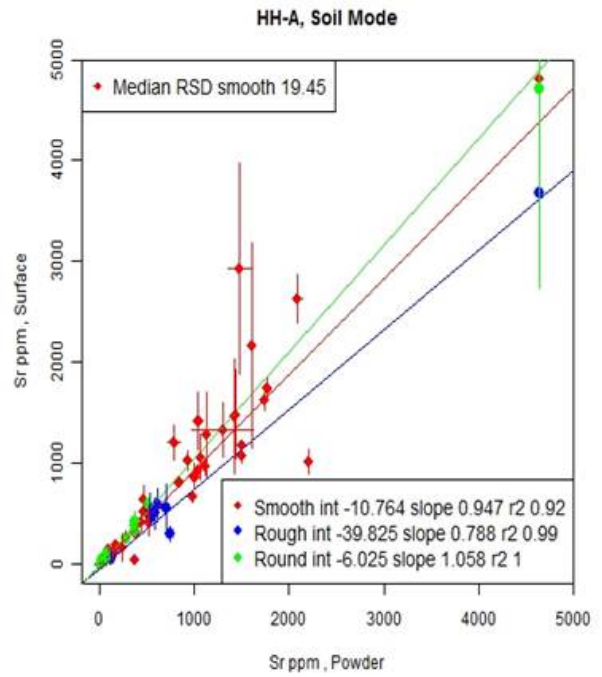
Fig. 5.2.44. Rock_HHA_soil_Sr.2.jpg.
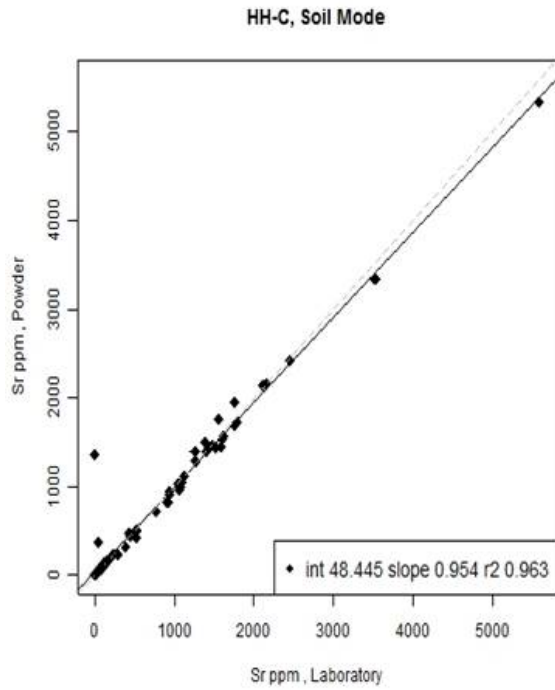
Fig. 5.2.45. Rock_HHC_soil_Sr.3.jpg.
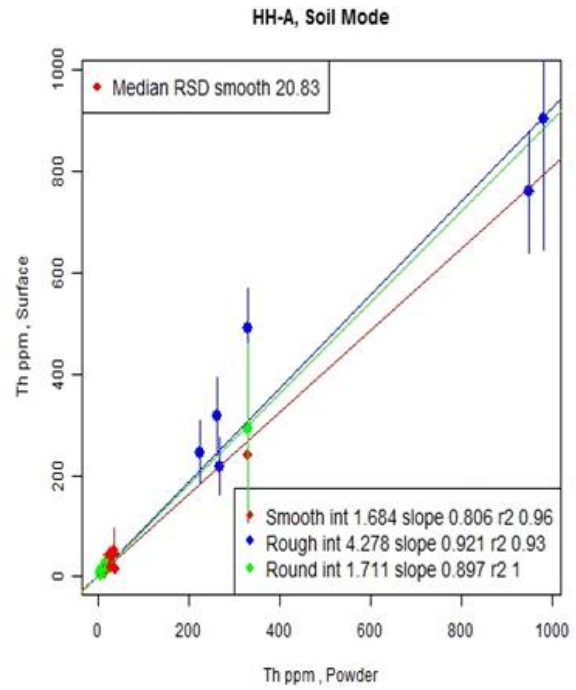
Fig. 5.2.46. Rock_HHA_soil_Th.2.jpg.
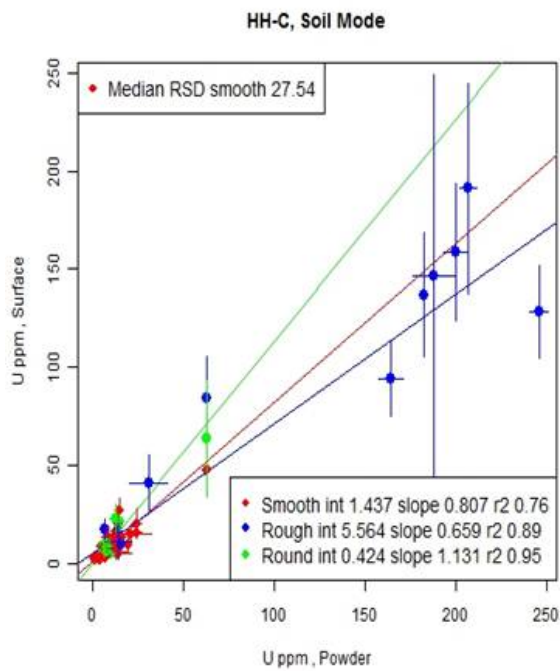
Fig. 5.2.47. Rock_HHC_soil_U.2.jpg.
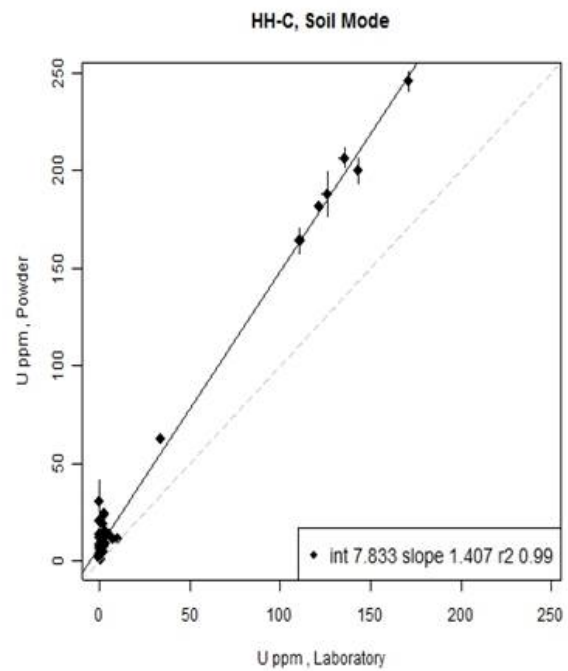
Fig. 5.2.48. Rock_HHC_soil_U.3.jpg.
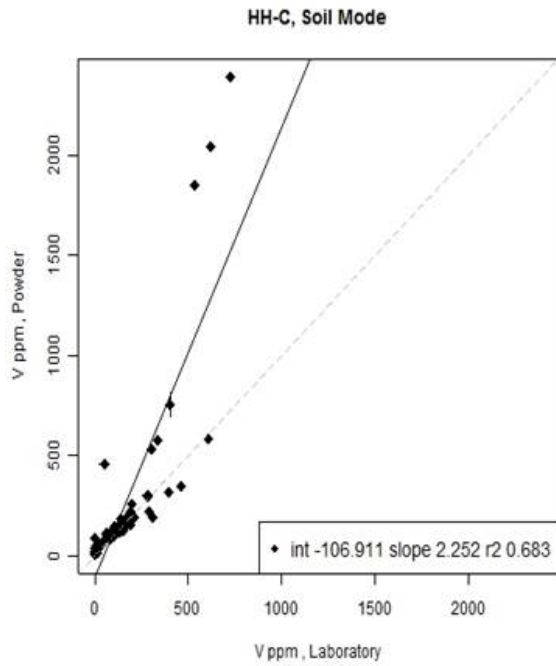
Fig. 5.2.49. Rock_HHC_soil_V.3.jpg.
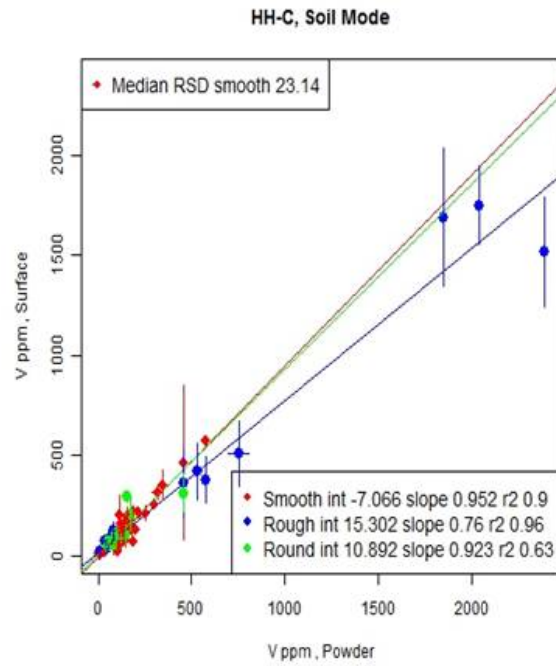
Fig. 5.2.50. Rock_HHC_soil_V.2.jpg.
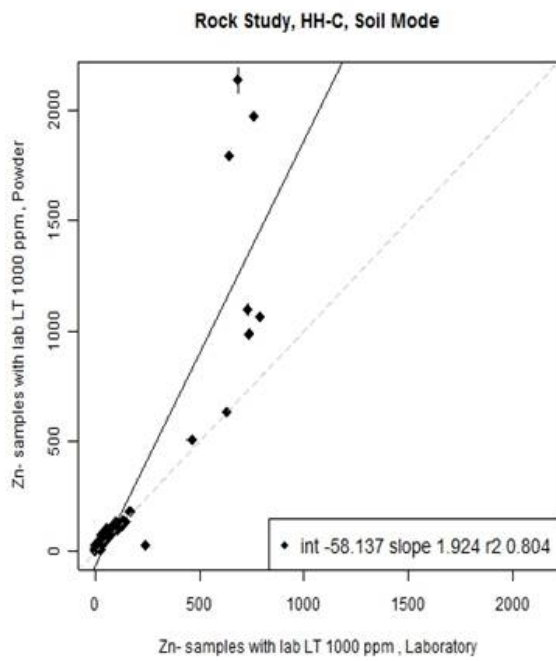
Fig. 5.2.51. Rock_HHC_soil_Zn-samples with
lab LT 1000.3.jpg.
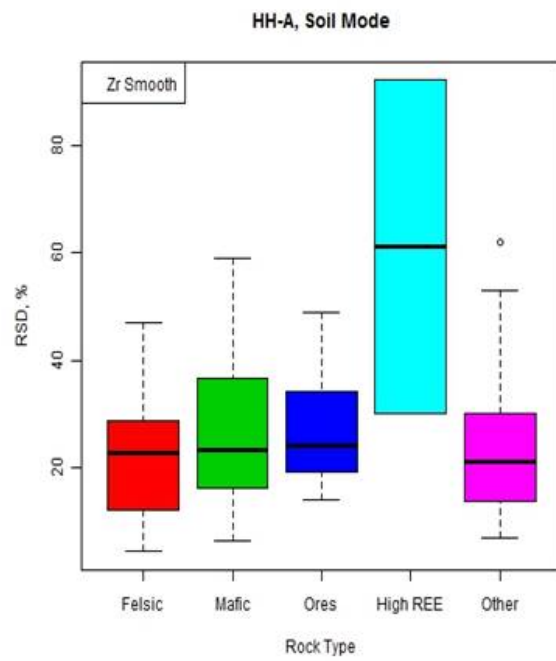
Fig. 5.2.52. Rock_HHA_soil_Zr.8.jpg.

6. SOILS

6.1. GSC soils

A suite of 46 soils collected by the GSC from 2007 to 2009 was chosen to study the variability in precision and accuracy between samples analysed 'as is' (except for coarse sieving at < 2 mm) and analysed following ball-milling, a procedure that would lead not only to diminution in particle size but also to homogenisation. These soils, comprising 36 B-horizon and 10 'humus' samples, come from various eco-regions of Canada and hence comprise different types of soil (e.g. podzol, chernozem, brunisol). The 'humus' samples are actually the so-called 'public health' layer, collected at a depth of 0-5 cm, and so may contain some mineral matter; the range in organic content is 15-43%. One set is simply the '< 2-mm' coarse-sieved fraction whereas the other set has been further prepared and is the '< 2-mm ball-milled'. The sets were not identical in that in a few cases one of the pair was missing. The laboratory data used for comparison with pXRF are based on the '1T' four-acid ($HF-HClO_4-HNO_3-HCl$) 'near-total' package, from Acme Laboratories of Vancouver, and therefore these data may be low for some elements such as Al, Ba, Cr, Hf, Mn, Sn, W and Zr.

Each sample was placed in a cup and analysed three times by each instrument. The cup was moved between analyses for the < 2-mm set but not for the ball-milled samples. The results by pXRF and associated plots are found in the Appendix.

Figures 6.1.1 to 6.1.4 show, for Fe by HH-C, the plots that were made for each element: (a) pXRF ball-milled (BM) vs the lab (four-acid digestion) result; (b) pXRF not ball-milled (NBM) vs the lab; (c) pXRF ball-milled vs not ball-milled; and (d) a box-and-whisker log plot of the mean RSDs for ball-milled and not ball-milled B-horizon and ball-milled and not ball-milled humus samples. Following these four plots is a table of the mean, standard deviation (SD) and RSD value for each element in each sample. This folder is clearly labelled in the Appendix. It is best to open these files using 'Large Icons' under 'View' as they are organised by one element per line this way, with four plots followed by the summary table (open the plots with Picture Manager to sequence through them).

The two types of soil (humus and mineral soil) were separated in order to identify whether samples of high organic content would behave differently from a mineral soil. Results where one or more of the three pXRF readings were below detection limit (labelled in the software as <LOD, a negative number, '1' or '0') were eliminated from computation for that element in that sample. Elements where the overwhelming majority of data (e.g. Cs, W) were below detection are not plotted.

The key questions to be answered in this exercise are:

Ball-milled vs lab: Is the value of r^2 (e.g. > 0.9) good enough such that an accurate calibration would be obtained (regardless of slope and intercept), be it by the factory calibration or one created by soils of similar matrix? Is there a difference in calibration for the humus samples

compared to mineral soils? [It should be borne in mind that the number of humus samples is small compared to the mineral soils]

Not ball-milled vs lab: As above. Is there a significant deterioration in r^2 compared to the ball-milled set?

Ball-milled vs not ball-milled: Allowing for the fact that the ball-milled sample is not the *actual* non ball-milled subsample, is there a difference in the absolute concentrations, that is, is there a significant bias?

Box-and-whisker plot: Is there a significant improvement in precision obtained by ball-milling and is it of such magnitude that it is necessary for a geochemical survey?

From Figure 6.1.1 it is clear that the ball-milled B-horizon set forms an excellent trend-line (r^2 of 0.98) when compared to the lab data (slope of 1.20) and that the humus samples show a slightly different intercept (-0.20 vs 0.38%), though of the same slope and goodness of fit. Almost identical behaviour is seen for the non ball-milled data (Fig. 6.1.2), although error bars on the individual points are certainly greater; the goodness of fit has dropped only to 0.95 from 0.98. Figure 6.1.3 indicates that the two sets of pXRF data agree well (slope of 0.89 and r^2 of 0.98). The box-and-whisker plot (Fig. 6.1.4) shows that a significant drop in RSD occurs by ball-milling for both B-horizon (e.g. ~ 3% to ~0.3%) and humus samples, which is, not surprisingly, typical for many elements. Although these results are summarised here, the reader is encouraged to scan through these plots as there is so much information pertinent to each element.
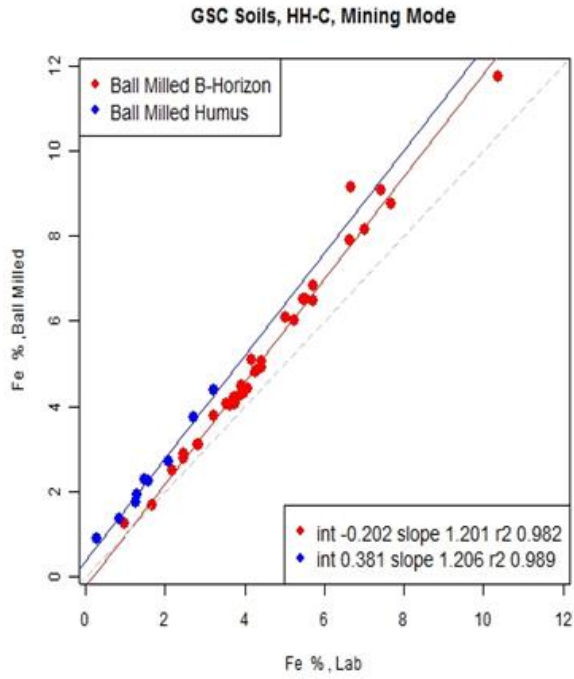
Fig. 6.1.1. GSC_Soils_HHC_mining_Fe.1.jpg
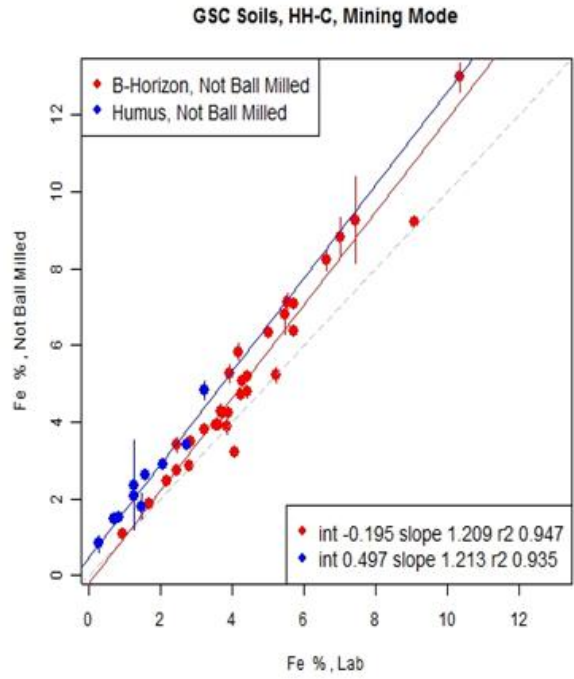
Fig. 6.1.2. GSC_Soils_HHC_mining_Fe.2.jpg
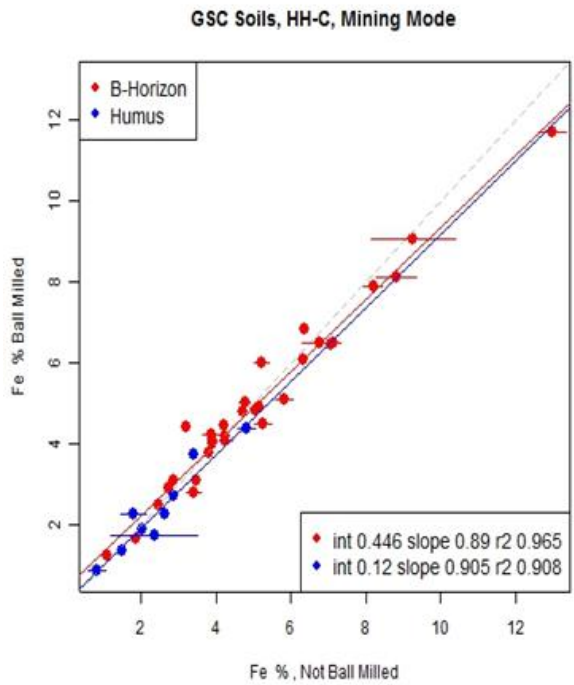
Fig. 6.1.3. GSC_Soils_HHC_mining_Fe.3.jpg
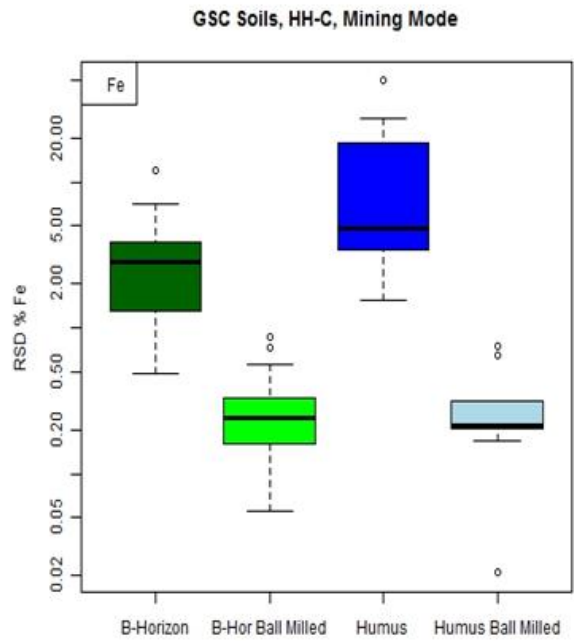
Fig. 6.1.4. GSC_Soils_HHC_mining_Fe.4.jpg

HH-A

The goodness of fit for the mineral soils, represented by r^2 in the three plots, is provided in Table 6.1.1 for various elements in the mining and soil modes.

Table 6.1.1. Values of r^2 for mineral soils by HH-A, for ball-milled versus lab values, not ball-milled versus lab values, and ball-milled versus not ball-milled. [Majors (Al, Ca, Fe, K, Ti) in mining mode, others in soil mode]

	r^2		
Element	**BM vs lab**	**NBM vs lab**	**BM vs NBM**
Al	0.62	0.43	0.77
Ca	0.94	0.97	0.96
Fe	0.99	0.96	0.97
K	0.95	0.87	0.93
Ti	0.55	0.69	0.90
As	0.92	0.87	0.97
Cr	0.99	1.00	1.00
Cu	1.00	0.99	1.00
Mn	0.95	0.87	0.91
Nb	0.91	0.88	0.97
Pb	0.23	0.16	0.83
Rb	0.91	0.87	0.99
Sr	0.99	0.98	1.00
Th	0.46	0.40	0.68
V	0.49	0.63	0.89
Y	0.73	0.77	0.97
Zn	0.99	0.97	0.99

Mining mode
The values of r^2 are not good for Al (0.62 for BM and 0.43 for NBM in mineral soils), a light element, but it is interesting that they are better (0.93, BM; 0.69, NBM) for the humus samples which contain the lowest concentrations of Al. There is no discernible difference between humus and B-horizon calibrations. The BM and NBM sets of data appear to agree well, within the constraints of the goodness of fit. Ball-milling the humus samples improves precision considerably (from ~ 8 to 1.5% median RSD) but only slightly for the B-horizon soils (~ 1.9 to 1.3%).

Figures 6.1.5 to 6.1.7 for Ca show that the humus and mineral soils would require different calibrations. At first glance it would appear that the BM and NBM trend-lines for the mineral soils differ (i.e. a bias present?) because the slopes are so different (1.5 vs 1.1) but this is due to the control of a few samples at high Ca concentrations. The box-and-whisker plot (Fig. 6.1.8) illustrates a common occurrence: drastic improvement in RSDs by ball-milling for the humus

samples (e.g. ~ 15 to 0.5% median RSD) but a more subtle one for the B-horizon (e.g. ~ 3 to 0.8% RSD).

The results for Fe are superb (Fig. 6.1.9-6.1.12), with r^2 values and slopes close to unity for both BM and NBM sets. The worst precision, at just under 5% median RSD for the 'as is' humus, is still excellent.

Although K is a light element, its performance is quite good (Fig. 6.1.13 to 6.1.15). Again, separate calibrations would be required for the organic and inorganic soils and certainly the NBM plots are noisier than the BM set but the non ball-milled median RSDs are only ~ 7% (humus) and 2% (mineral soils), as seen in Fig. 6.1.16.

Nickel is reported as <LOD in the soil mode for all the samples except one: NL091042-B, 341 ppm by the lab and reading 206±16 ppm 'as is' and 241±25 ppm ball-milled. This is very odd as most of the lab values are in the tens of ppm, with several at 100 ppm. Furthermore, the mining mode reports only the one value in the ball-milled set but does report, albeit high, for quite a few samples in the NBM set, as shown in Fig. 6.1.17. Clearly Ni cannot be accurately determined by HH-A in these soils at these concentrations. Phosphorus is another element which cannot be determined in these soils, even though the concentrations are up to 6000 ppm. Only a few samples are reported above detection in the BM set and more in the NBM suite but it is haphazard. [The <LOD pXRF values were eliminated and hence do not appear on the plot with the lab values].

Most of the B-horizon soils contain < 400 ppm S (lab LOD) and therefore essentially the only data reported are those for the humus samples which contain up to 1600 ppm S. However, the pXRF readings are high, with slopes of 3.2 (BM, NBM). There are no lab values for Si; the usual improvement in RSD with ball-milling is evident but the plot of BM vs NBM is rather noisy with an r^2 value of only 0.76 for the mineral soils.

As for Ca, although the trend-lines for Ti appear to be quite different for the BM (Fig. 6.1.19) and NBM (Fig.6.1.20) sets, this is due to control by a sample of high Ti concentration in the NBM set (i.e. there is no bias). Median RSDs are all below 7%.

Soil mode
Arsenic is present in the soils at up to ~ 60 ppm, most concentrations being below 15 ppm. Goodness of fit (r^2 of 0.92, BM; 0.87, NBM) for the As trend-lines are quite good, given this concentration range and the two sets of data agree well. The humus and mineral soils do not show distinct calibrations. Interestingly, As does not show a large improvement in RSD with ball-milling: for the B-horizon soils, the median RSD decreases from ~ 5 to 4% and for the

humus the RSDs are similiar at ~7%, not that much higher than for the B-horizon. This suggests that As is quite homogeneously distributed in the NBM humus.

The results for Cr (Figs. 6.1.21 to 6.1.24) and Cu are excellent, with (a) r^2 and slopes close to unity, (b) the usual improvement in RSDs with ball-milling, and (c) a worst-case median RSD on only ~ 11% (humus, NBM).

Manganese shows distinct calibrations (BM and NBM) for humus and mineral soils, with good values of r^2 (0.87-1.00) for all four plots (not shown here, but all plot files can be seen in the Appendix). Niobium, present at < 20 ppm except for one sample, is remarkable in its behaviour: trend-lines are similar, r^2 values are ~ 0.9, and median RSDs are better than ~ 7% (Figs. 6.1.25 to 6.1.28).

Lead, present at a few tens of ppm up to 34 ppm in the mineral soils, cannot be determined; values reported above LOD are sporadic. In the humus, the Pb concentrations are higher, at 38-85 ppm, and therefore r^2 values improve to 0.63 (BM) and 0.69 (NBM) and trend-lines are similar.

Slopes and r^2 values for Rb are close to unity for all trend-lines and the worst median RSD is still only ~ 7% for the humus (NBM). The same is true for Sr, another superb element by pXRF.

For S in the B-horizon soils only six samples are reported above detection by pXRF in the BM set but 19 are reported in the NBM set, many just below the lab detection of 400 ppm and so do not appear on the plot. The BM humus data suggest that S can be adequately determined in the range 600-1600 ppm (r^2 of 0.97; median RSD of ~ 7%) but not in the NBM suite.

Thorium is not detected in any of the humus samples which contain < 7 ppm Th and its results for the mineral soils, containing up to 19 ppm, are very noisy (median RSDs of ~ 16-18%). Although the concentrations of V are lower in the humus (20-73 ppm) than the mineral soils (38-328 ppm), the results fit the trend-line much better (r^2 of 0.83, BM and 0.89, NBM; cf 0.49, BM and 0.63, NBM in B-horizon). Median RSDs for V are good, at ~ 4% for all but NBM humus at ~ 7%.

Yttrium, present mostly in the range ~ 5-30 ppm, has a poor goodness of fit (e.g. r^2 of 0.73, BM and 0.77, NBM, B-horizon) for both soil horizons, although the precision of measurement is good (~ 4-6% median RSD for all but NBM humus). Essentially all points are above the 45° line which could suggest the lab result (four- acid digestion) is not total; excellent agreement between BM and NBM sets (slope of 1.0, r^2 of 0.97) is evident. Certainly inadequate decomposition is the cause of the lack of agreement between lab and pXRF results for Zr but again BM and NBM data

match extremely well (slope of 1.0, r^2 of 0.96) and median RSDs are below 4% except for NBM humus (~ 15%).

The r^2 values for BM (0.99) and NBM (0.97) mineral soil trend-lines for Zn are excellent, with slopes close to unity. The humus samples appear to form a separate calibration, of considerably higher slope (1.5) in the NBM set and hence the agreement between BM and NBM humus is not as good as that for the mineral soils. The four median RSDs range from ~ 0.8% (humus BM) to ~ 8% (humus NBM).

HH-C

The goodness of fit, represented by r^2 in the three plots, is provided in Table 6.1.2 below for various elements in the mining and soil modes. The mining mode plots are used for the major elements and the soil mode for the minors and traces.

Table 6.1.2. Values of r^2 for mineral soils by HH-C, for ball-milled versus lab values, not ball-milled versus lab values, and ball-milled versus not ball-milled. [Majors (Al, Ca, Fe, K, Ti) in mining mode, others in soil mode]

Element	r^2		
	BM vs lab	**NBM vs lab**	**BM vs NBM**
Al	0.62	0.37	0.78
Ca	0.95	0.98	0.98
Fe	0.98	0.95	0.97
K	0.97	0.90	0.93
Ti	0.52	0.65	0.89
As	0.99	0.95	0.96
Ba	0.57	0.75	0.80
Cr	0.97	0.93	0.96
Cu	0.99	0.99	1.00
Mn	0.93	0.88	0.92
Mo	0.74	0.27	0.02
Ni	0.91	0.90	0.93
Pb	0.86	0.78	0.80
Rb	0.91	0.90	0.98
Sr	0.98	0.97	1.00
Th	0.84	0.83	0.89
U	0.38	0.27	0.79
V	0.86	0.91	0.88
Zn	0.99	0.96	0.98

Mining mode

As seen for Fe shown previously (Figs. 6.1.1 to 6.1.4), other major elements measured – Ca, K and Ti - show a slightly different behaviour for the humus samples as they tend to report higher than the mineral soil trend-line, indicating that indeed a separate calibration is needed for organic-rich media. Calcium and K show excellent values of r^2 (> 0.9) for both BM and NBM sets. Perhaps it is simply happenstance that the r^2 values for Al in the humus samples (0.96 and 0.79 in BM and NBM plots) are much better than those for the mineral soils (0.62 and 0.37); being a light element, it is not surprising that its performance is not that of the other majors (see Figs. 6.1.29 to 6.1.32). It again shows the familiar pattern in mean RSDs: the non ball-milled humus has the highest median RSD (~ 11%) which improves drastically with such preparation (to ~ 1%) and the mineral soil displays a more modest improvement (from ~ 2 to 1% in median RSD). However, the still acceptable levels of RSD and lack of bias suggest that the 'as is' < 2-mm screened soil sample would be suitable for the determination of major elements in a soil survey.

The lab detection limit for S is 400 ppm and most of the data are <LOD. The few data points presented in the plots, most being for the humus samples, show that S reports very high compared to the factory calibration (slopes of ~ 2 and 6 for B-horizon and humus, respectively, in the BM set).

Soil mode

Even though most of the data are below 25 ppm for As, the values for r^2 are excellent (0.95-0.99). A separate calibration for humus is indicated but interestingly there is no improvement in RSD with ball-milling for the mineral soils (~ 10% median RSD) and only a modest one for the humus (~ 18 to 12%) (Figs. 6.1.33 to 6.1.36). These findings are similar to those for HH-A.

Barium is present in the range ~ 50-350 ppm in the humus and ~ 85-1000 ppm in the mineral soils. All results for humus are <LOD in the soil mode, indicating that the Ba signal is severely suppressed. Figures 6.1.37 to 6.1.40 show that Ba in the mineral soils is much better determined in the mining mode (superior r^2 values of 0.84, BM and 0.85, NBM; cf 0.57, BM and 0.75, NBM in soil mode).

For Cr, a few samples at high concentrations show significant improvement in RSD with ball-milling (e.g. 754±332 ppm to 604±15 ppm) but the plots for both BM and NBM are good (the three r^2 values are excellent). There is little difference in the two trend-lines for Cu, both BM and NBM agree well with the lab results (with excellent r^2 values of 0.99) and ball-milling does not improve the RSDs for the mineral soils.

Manganese is well determined in both sample pairs and there does not appear to be a difference in the humus calibration compared to soil. Improvement in RSD with ball-milling is significant for humus (~ 30 to 8% median RSD), and less so for B-horizon (~ 8 to 4%). Although the concentrations of Mo are all below 6 ppm, the plots are still provided to show (a) separate calibration for humus would be required and (b) with ball-milling, measurement even at these very low levels is perhaps possible.

The goodness of fit for the Ni BM and NBM plots (r^2 of 0.91, 0.90) appear much better than they really are because of the dominance of one high Ni concentration at ~ 340 ppm. In fact most of the data are below 50 ppm and are noisy; there is little difference between the BM and NBM plots. Nickel is below detection in all the humus samples (BM or NBM) and yet the lab results are in the range 9-21 ppm. Some mineral soils report above detection at this low range (< 20 ppm) which suggests that the humus samples would require quite a different calibration.

The preferential scavenging by organics for Pb is evident in Figures 6.1.41 to 6.1.44 where all humus data are in the range ~ 40-80 ppm whereas the mineral soils are below ~ 40 ppm in Pb concentration. The huge degradation in precision in the NBM suite, from a median RSD of ~ 3% (BM) to ~ 22% (NBM), and hence poor calibration, suggests that humus samples would need to undergo preparation (sieving or ball-milling). However, the mineral soils behave well (r^2 of 0.86, BM; 0.78, NBM), given their low concentration, and both sets have median RSDs of ~ 18%. Distinct calibrations would be required for humus vs mineral soils (also seen in the mining mode for Pb). These results differ from those found using HH-A where the mineral soils could not be analysed for Pb whereas the humus could, albeit with considerable noise. The degradation in precision for the humus using HH-A is only from ~ 2% to ~ 8%, much less drastic than that seen here for HH-C. Thus, some of the noise encountered in the NBM humus by HH-C must be inherent in the instrumental software/hardware.

Both sets of BM and NBM B-horizon soils show similar calibrations for Rb (slopes of 0.89 and 0.90 with r^2 values of 0.91 and 0.90) and the usual much larger improvement in precision of the humus data with ball-milling. The same holds true for Sr, with r^2 values of 0.98 (BM) and 0.97 (NBM), an excellent element by pXRF. The humus samples do not show distinct behaviour for these elements.

With one exception, all concentrations for Th are below 15 ppm and therefore the data are fairly noisy (r^2 of 0.84, BM; 0.83, NBM) but certainly acceptable (unlike the case for HH-A). No improvement in RSDs (medians of ~ 12, 14%) is evident in the mineral soils with ball-milling; the dominant source of noise in this case is analytical. Uranium, too, is at very low concentrations in these soils, all below 5 ppm by the lab results (four-acid digestion); the reported pXRF data are noisy and high but encouraging for measurement above this 5 ppm level.

The V calibrations versus the lab suffer from a high intercept but the trend-lines for the mineral soils are similar and have r^2 values of 0.86 (BM) and 0.91 (NBM) which is acceptable given the concentrations are almost all < 200 ppm. The BM plot indicates a separate calibration is necessary for the humus.

Figures 6.1.45 to 6.1.48 for Zn shows the excellent calibrations for the BM and NBM sets of mineral soils, with slopes and r^2 values close to unity, and the noise encountered by not ball-milling the humus samples. The degradation in RSDs for humus by not ball-milling is distinctly more severe using HH-C than HH-A.

Zirconium results by pXRF are much higher than the lab results as the latter are four acid- and not fusion-based. Ball-milling improves the median RSDs significantly for Zr, from ~ 30 to 0.7% for the humus and ~ 7 to 0.7% for the mineral soils.

A reason that the NBM mineral soil shows such good results could well be that, in tapping the cup (upside down) to cover the film consistently, the finer material settles to the bottom (i.e. the analysis face), leaving the coarser grains out of the measurement window. The good agreement between BM and NBM data of course suggests that the coarser grains are of the same chemical composition.

Summary for the GSC soils

- Ball-milling leads generally to a significant improvement in precision for the humus samples and to a more subtle one for the mineral soils;
- Given that the < 2-mm *mineral soil* analysed is not the actual subsample that was ball-milled, the agreement between the < 2-mm and < 2-mm ball-milled suites is astoundingly good and indicates that ball-milling is not needed for good pXRF analysis of mineral soils (as represented by this particular suite);
- Different elements show different degrees of improvement in precision in the ball-milled *humus*, presumably due to their distribution and homogeneity in the 'as is' material but for many elements (e.g. As, Rb, Sr) the inferior precision would still be acceptable (i.e. ball-milling not required) but this should be tested for a particular survey;
- Goodness of fit for the plots of pXRF < 2-mm ball-milled and < 2-mm 'as is' versus the lab result for the *mineral soils* is excellent for elements that are well determined by pXRF (e.g. Ca, Fe, K, As, Cr, Cu, Mn, Nb, Rb, Sr, Zn) so accurate calibration would be obtained across such a suite of fairly diverse soils;
- Some elements (e.g. Ca, K, Mn) showed a distinct difference in calibration (trend-lines) between humus and mineral soils and therefore separate calibrations would be required for organic-rich vs inorganic-rich media;
- Though the number (10) of humus samples is small, results indicate that more accurate and precise data would be obtained from mineral soil in the 'as is' material than from the humus.
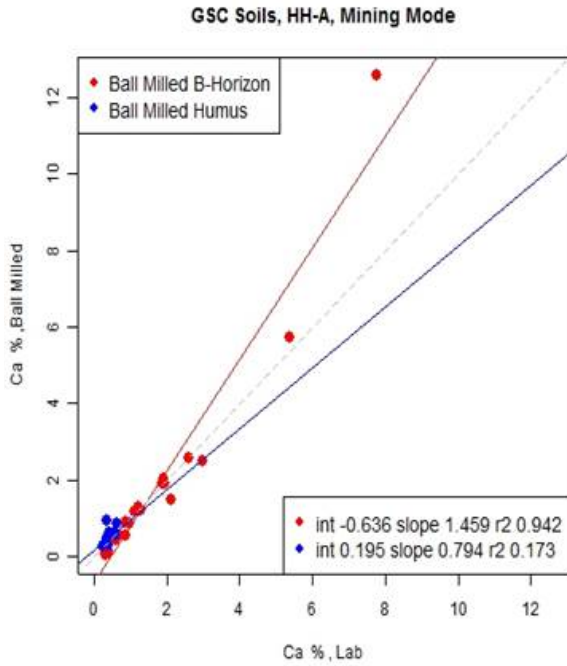
Fig. 6.1.5. GSC_Soils_HHA_mining_Ca.1.jpg
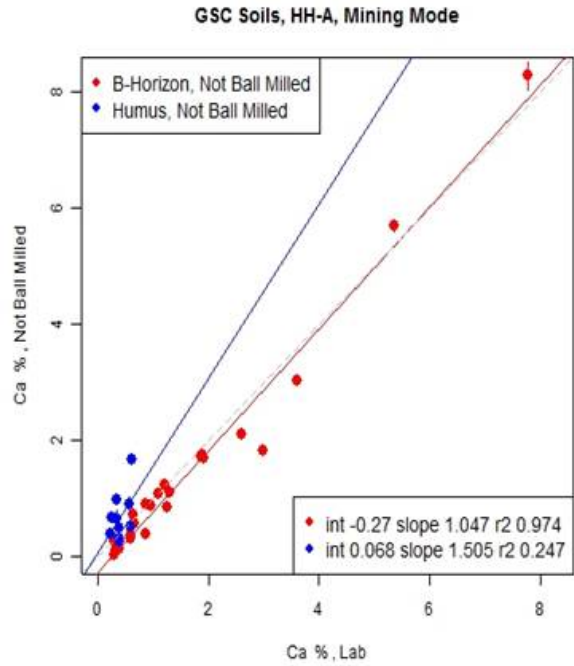
Fig. 6.1.6. GSC_Soils_HHA_mining_Ca.2.jpg
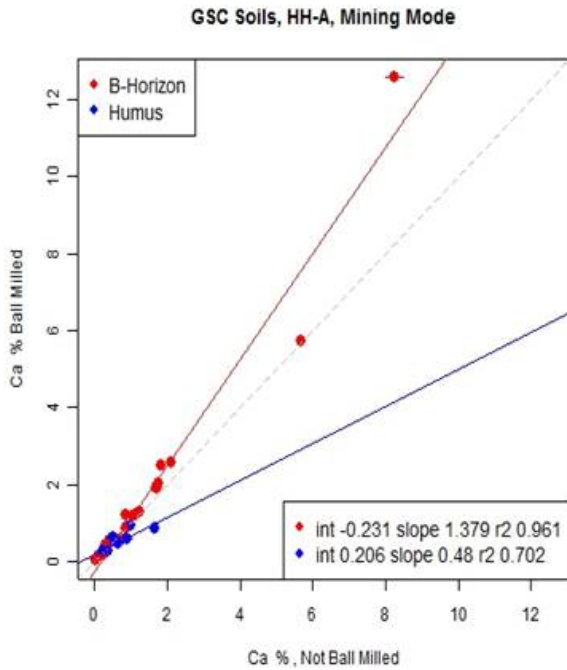
Fig. 6.1.7. GSC_Soils_HHA_mining_Ca.3.jpg
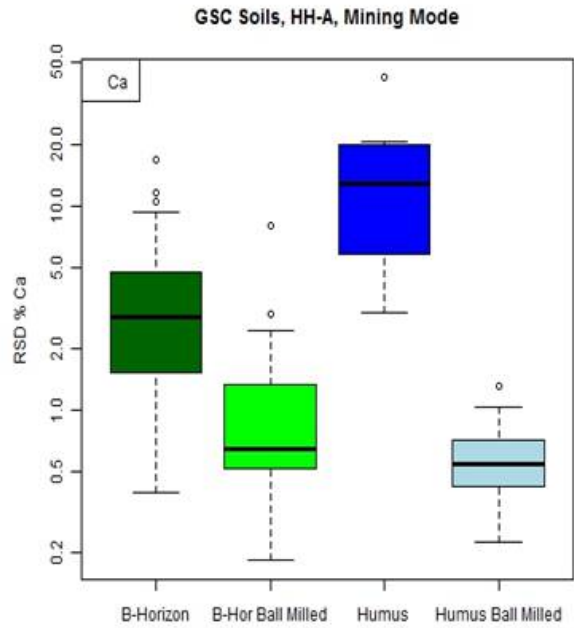
Fig. 6.1.8. GSC_Soils_HHA_mining_Ca.4.jpg
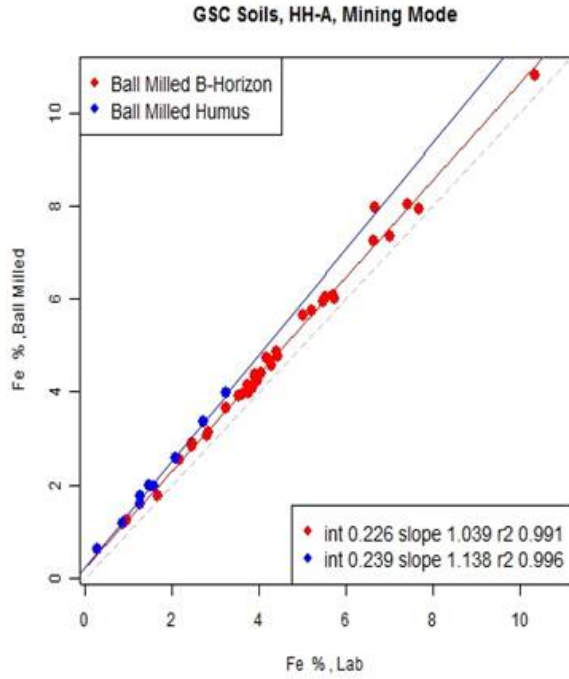
Fig. 6.1.9. GSC_Soils_HHA_mining_Fe.1.jpg
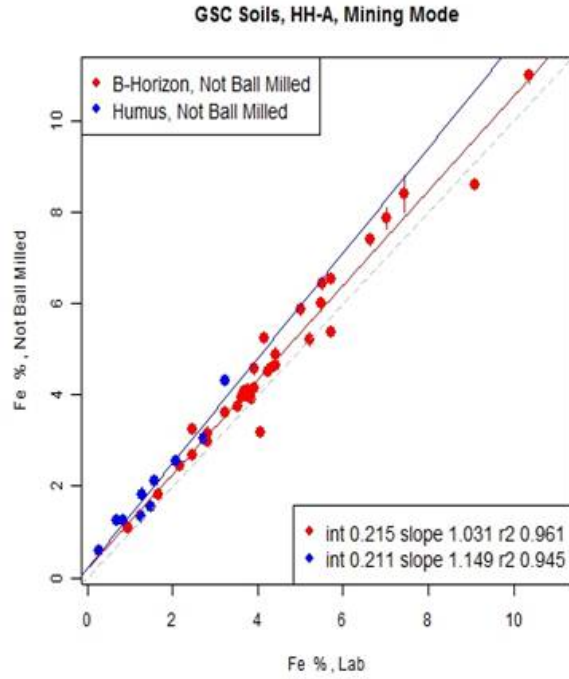
Fig. 6.1.10. GSC_Soils_HHA_mining_Fe.2.jpg
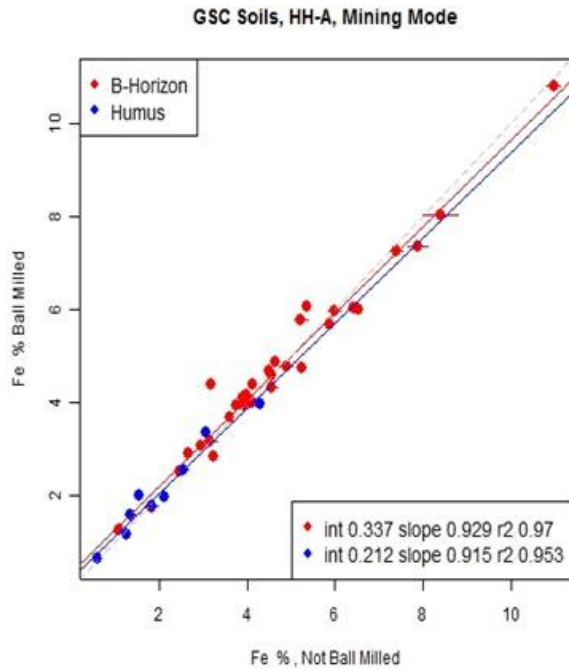
Fig. 6.1.11. GSC_Soils_HHA_mining_Fe.3.jpg
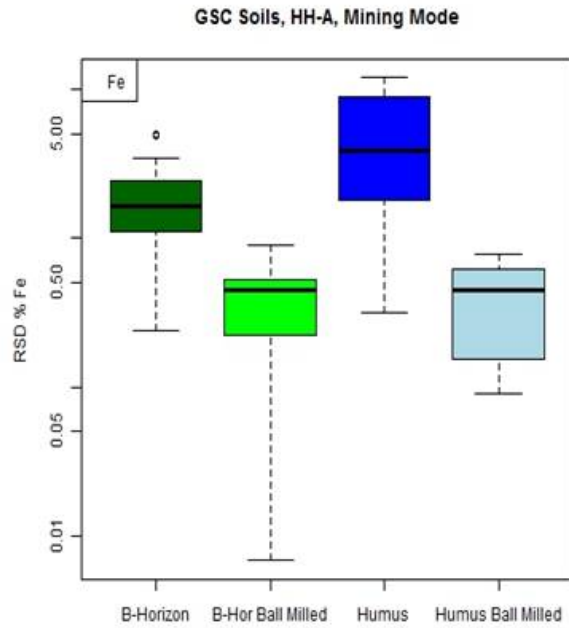
Fig. 6.1.12. GSC_Soils_HHA_mining_Fe.4.jpg
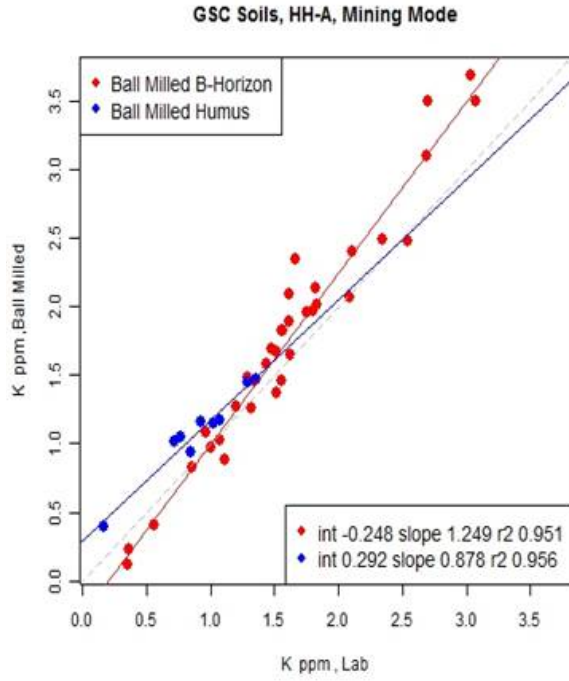
Fig. 6.1.13. GSC_Soils_HHA_mining_K.1.jpg
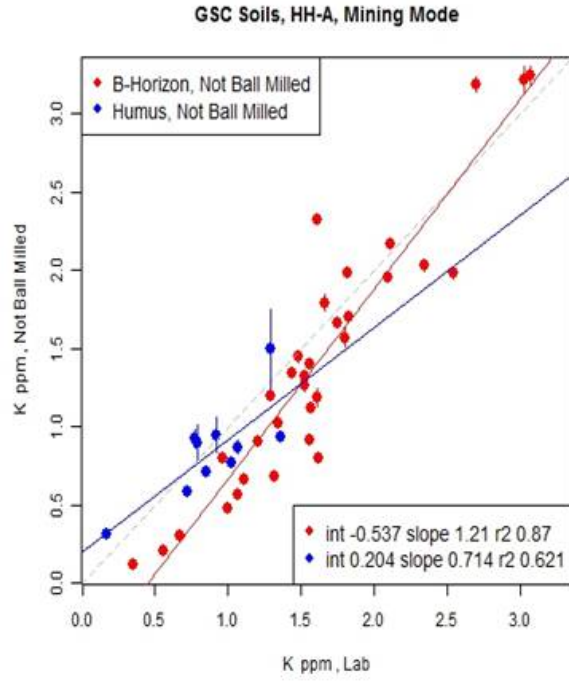
Fig. 6.1.14. GSC_Soils_HHA_mining_K.2.jpg
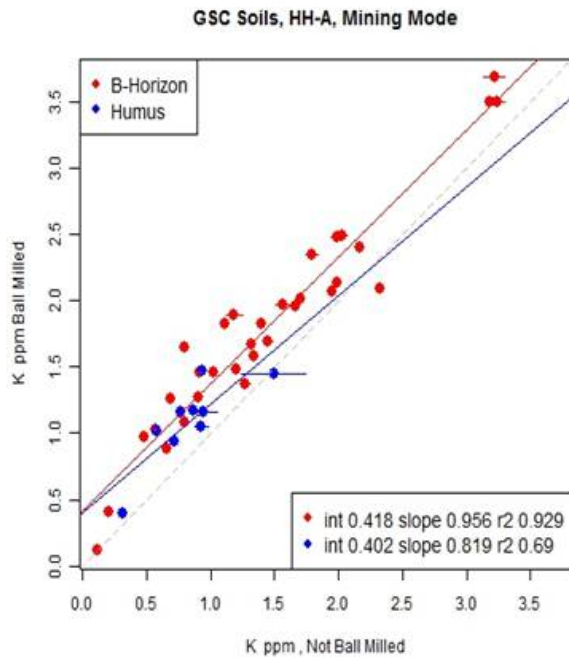
Fig. 6.1.15. GSC_Soils_HHA_mining_K.3.jpg
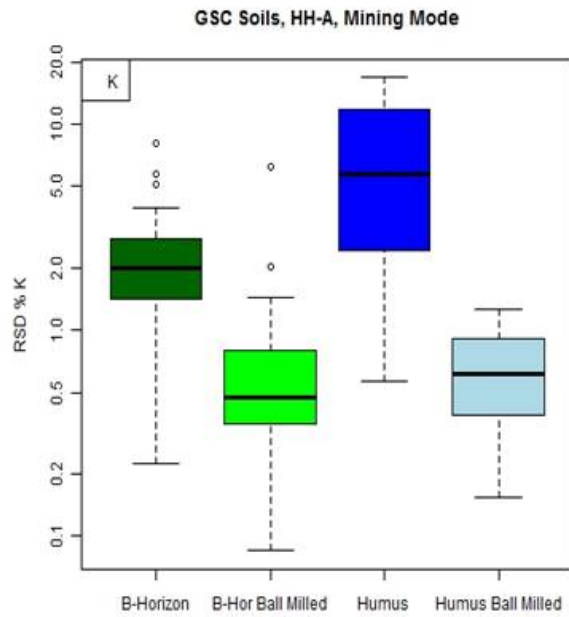
Fig. 6.1.16. GSC_Soils_HHA_mining_K.4.jpg
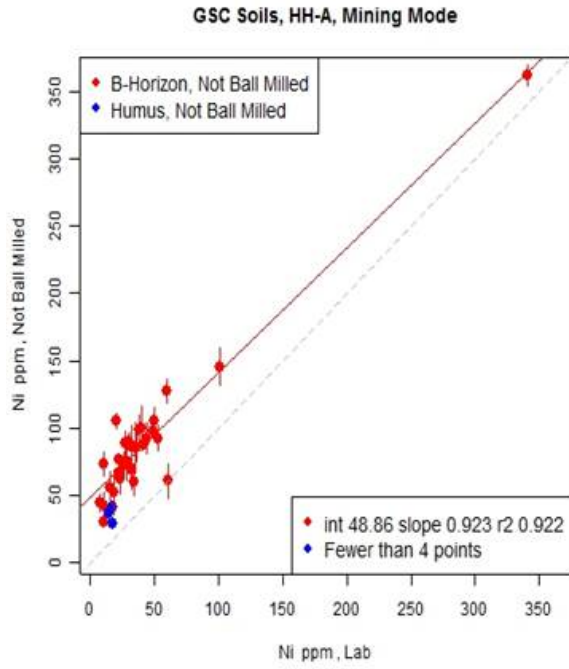
Fig. 6.1.17. GSC_Soils_HHA_mining_Ni.2.jpg
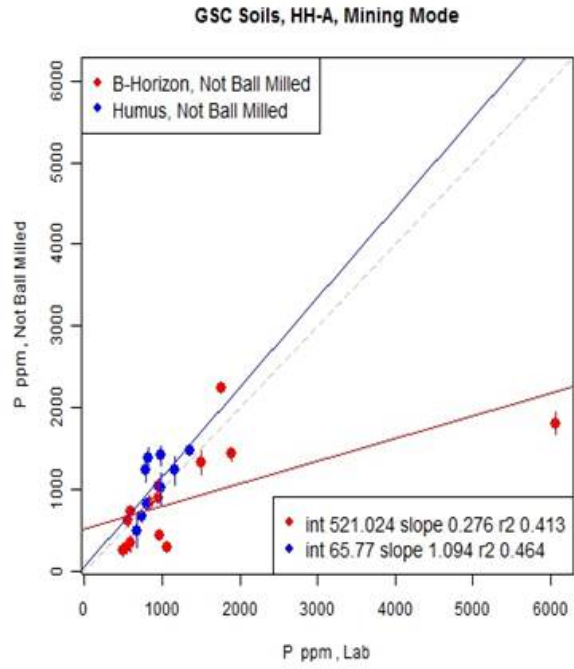
Fig. 6.1.18. GSC_Soils_HHA_mining_P.2.jpg
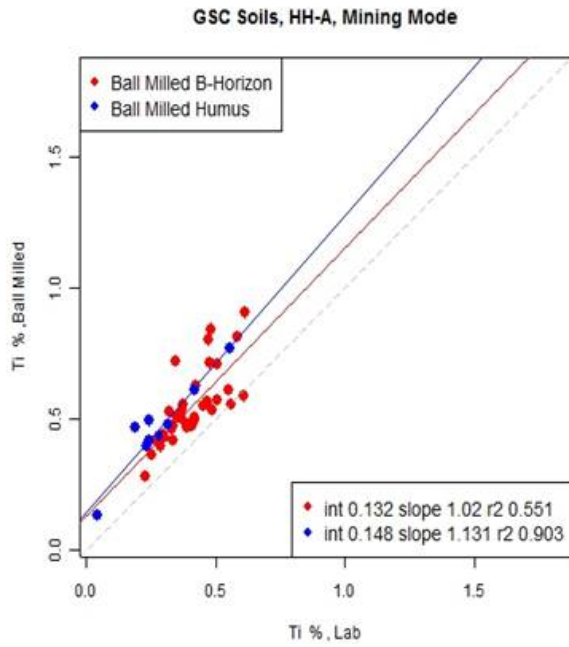
Fig. 6.1.19. GSC_Soils_HHA_mining_Ti.1.jpg
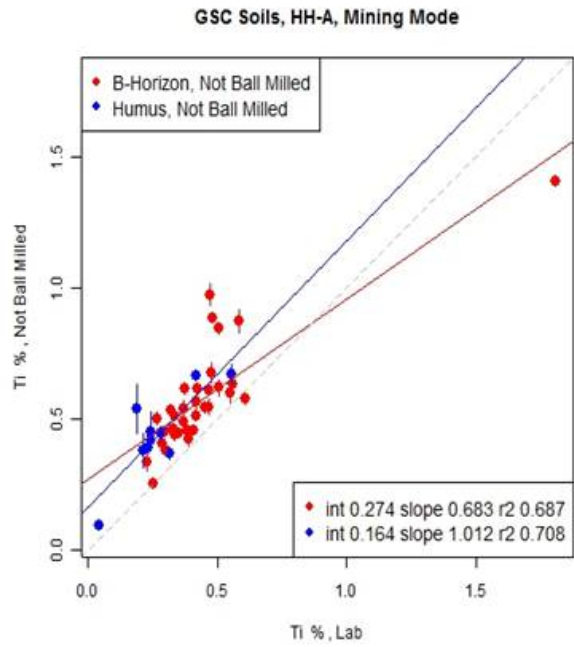
Fig. 6.1.20. GSC_Soils_HHA_mining_Ti.2.jpg
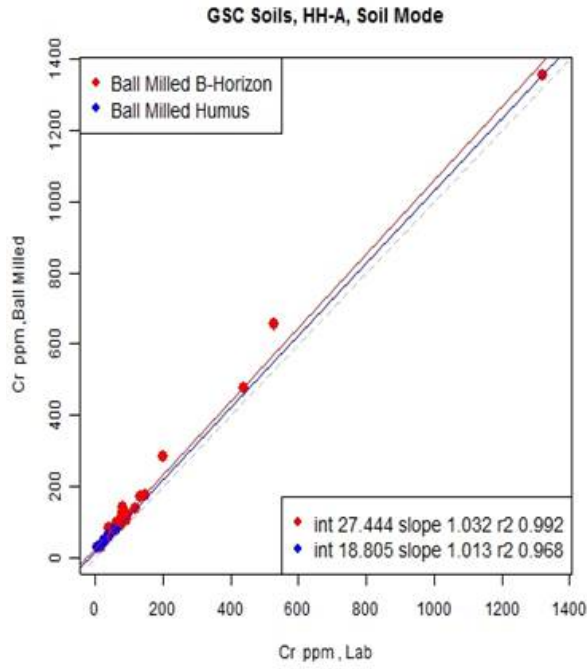
Fig. 6.1.21. GSC_Soils_HHA_soil_Cr.1.jpg
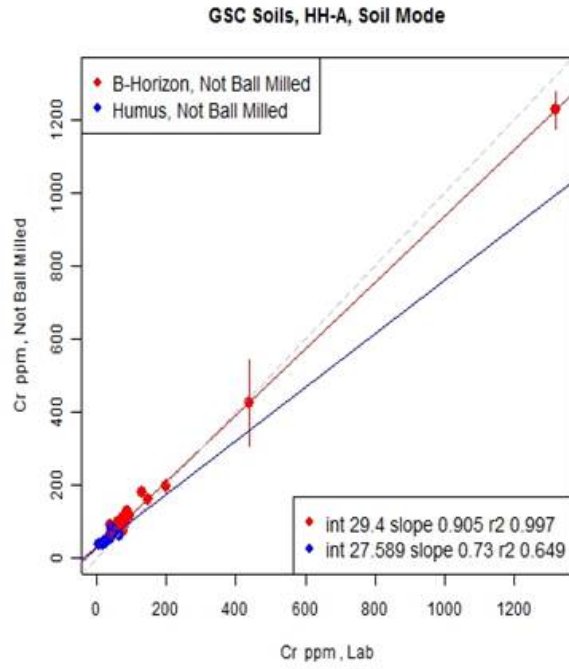
Fig. 6.1.22. GSC_Soils_HHA_soil_Cr.2.jpg
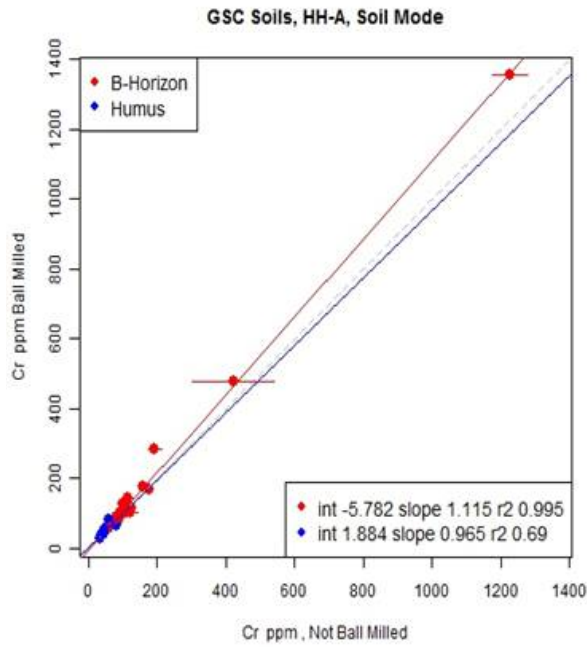
Fig. 6.1.23. GSC_Soils_HHA_soil_Cr.3.jpg
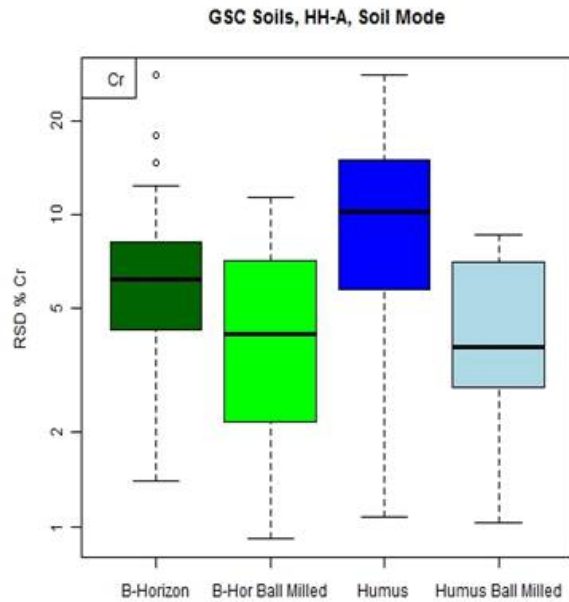
Fig. 6.1.24. GSC_Soils_HHA_soil_Cr.4.jpg

GSC Soils, HH-A, Soil Mode

int 1.644 slope 0.883 r2 0.914
int 1.454 slope 0.822 r2 0.82
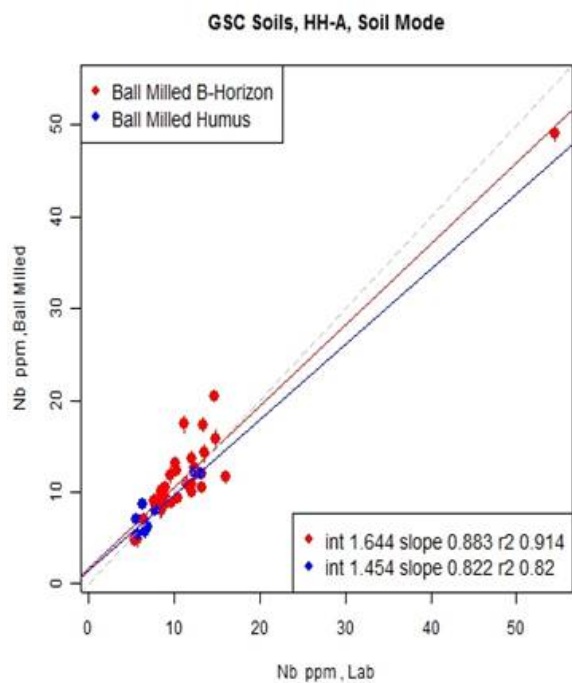
Fig. 6.1.25. GSC_Soils_HHA_soil_Nb.1.jpg

GSC Soils, HH-A, Soil Mode

int 2.822 slope 0.698 r2 0.881
int 0.38 slope 0.864 r2 0.892
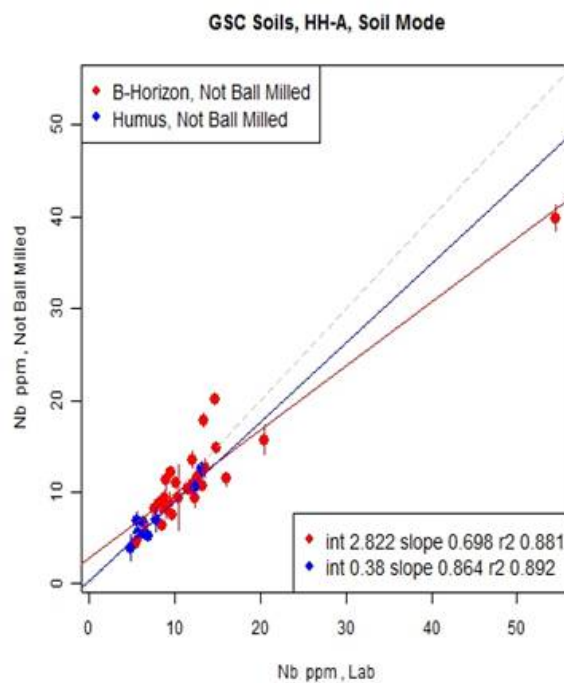
Fig. 6.1.26. GSC_Soils_HHA_soil_Nb.2.jpg

GSC Soils, HH-A, Soil Mode

int -1.442 slope 1.2 r2 0.972
int 0.887 slope 0.968 r2 0.892
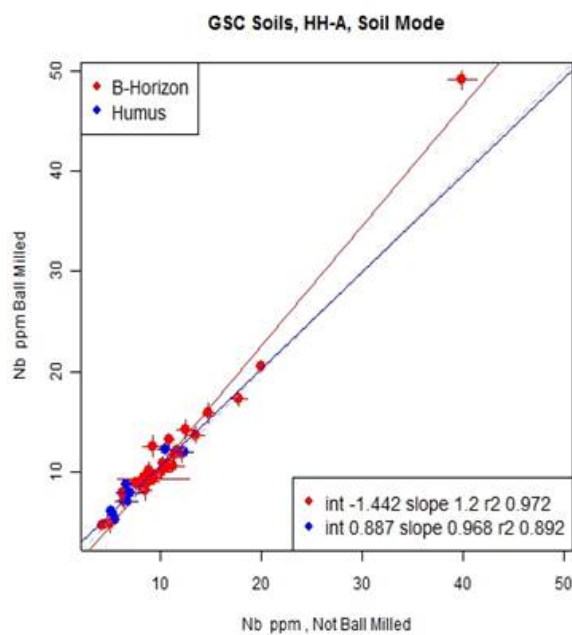
Fig. 6.1.27. GSC_Soils_HHA_soil_Nb.3.jpg

GSC Soils, HH-A, Soil Mode
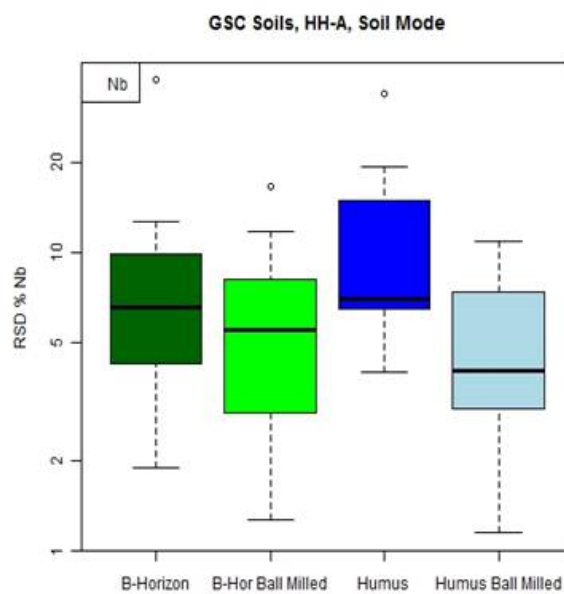
Fig. 6.1.28. GSC_Soils_HHA_soil_Nb.4.jpg

GSC Soils, HH-C, Mining Mode

- Ball Milled B-Horizon
- Ball Milled Humus

int 1.906 slope 0.933 r2 0.618
int 0.151 slope 1.081 r2 0.958

Al % ,Ball Milled

Al % , Lab
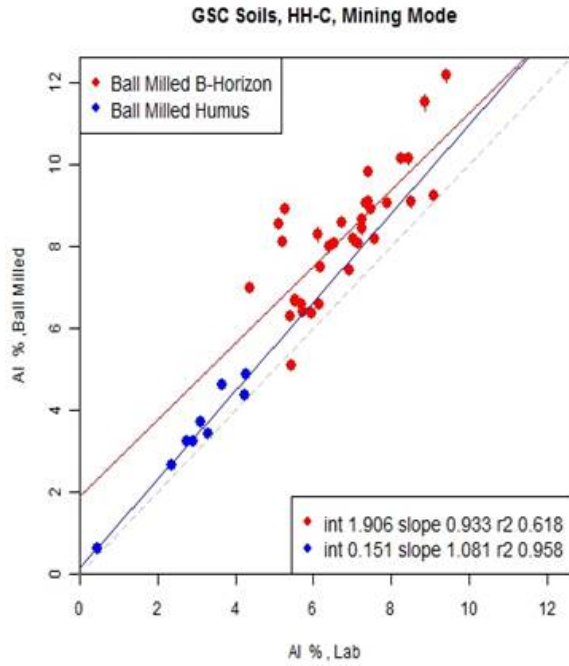
Fig. 6.1.29. GSC_Soils_HHC_mining_Al.1.jpg

GSC Soils, HH-C, Mining Mode

- B-Horizon, Not Ball Milled
- Humus, Not Ball Milled

int 3.195 slope 0.537 r2 0.366
int 0.273 slope 0.841 r2 0.793

Al % , Not Ball Milled

Al % , Lab
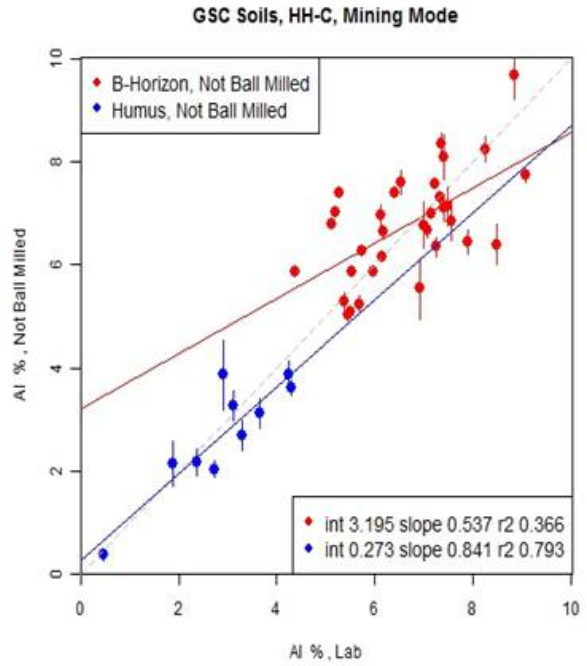
Fig. 6.1.30. GSC_Soils_HHC_mining_Al.2.jpg

GSC Soils, HH-C, Mining Mode

- B-Horizon
- Humus

int 0.217 slope 1.164 r2 0.781
int 0.705 slope 0.974 r2 0.741

Al % Ball Milled

Al % , Not Ball Milled
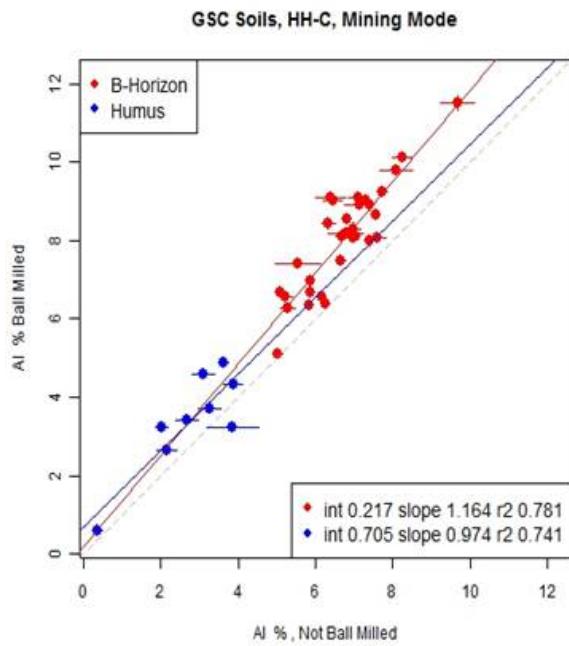
Fig. 6.1.31. GSC_Soils_HHC_mining_Al.3.jpg

GSC Soils, HH-C, Mining Mode

Al

RSD % Al

B-Horizon   B-Hor Ball Milled   Humus   Humus Ball Milled
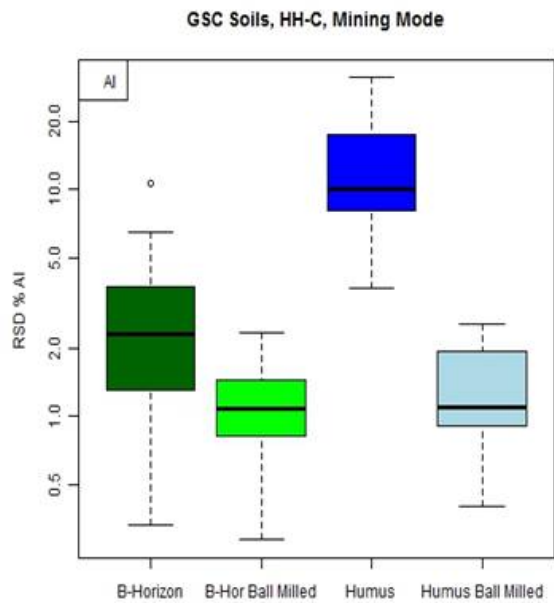
Fig. 6.1.32.GSC_Soils_HHC_mining_Al.4.jpg
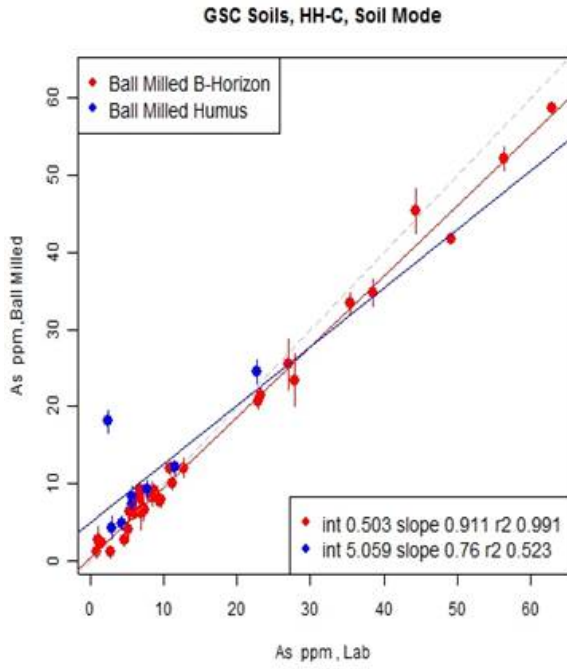
Fig. 6.1.33. GSC_Soils_HHC_soil_As.1.jpg
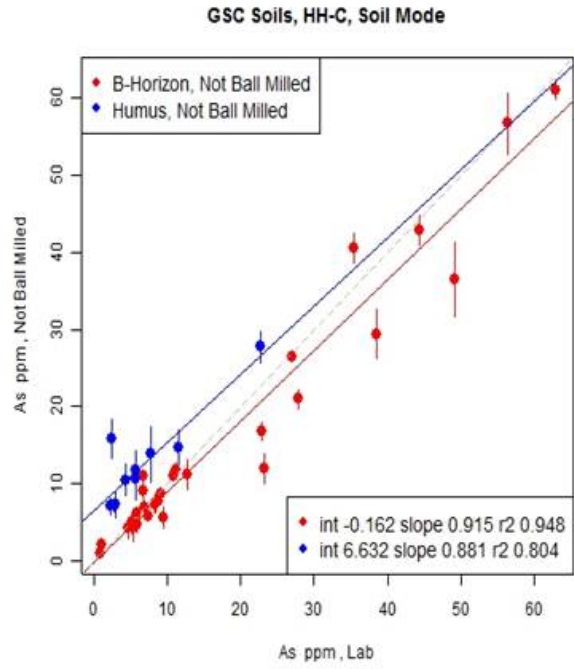
Fig. 6.1.34. GSC_Soils_HHC_soil_As.2.jpg
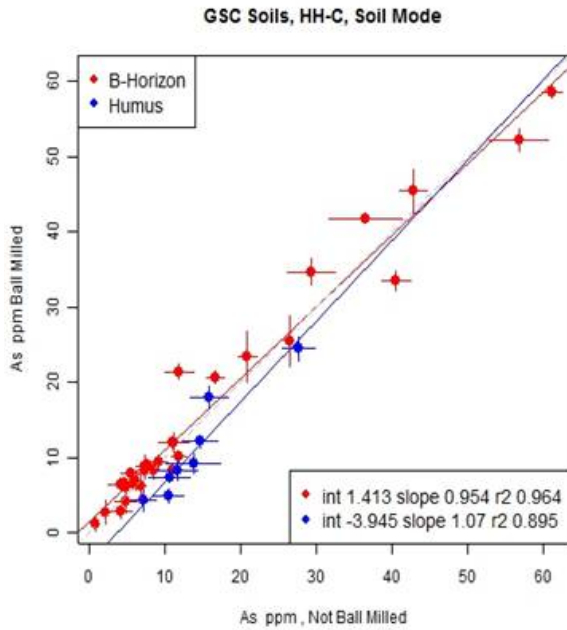
Fig. 6.1.35. GSC_Soils_HHC_soil_As.2.jpg
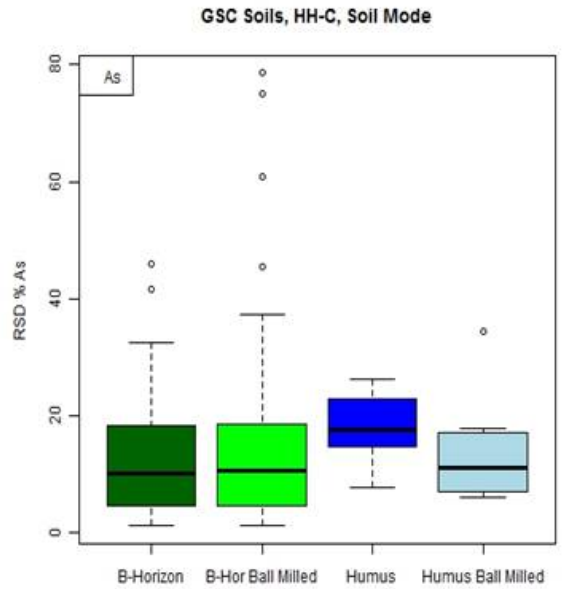
Fig. 6.1.36. GSC_Soils_HHC_soil_As.4.jpg

179
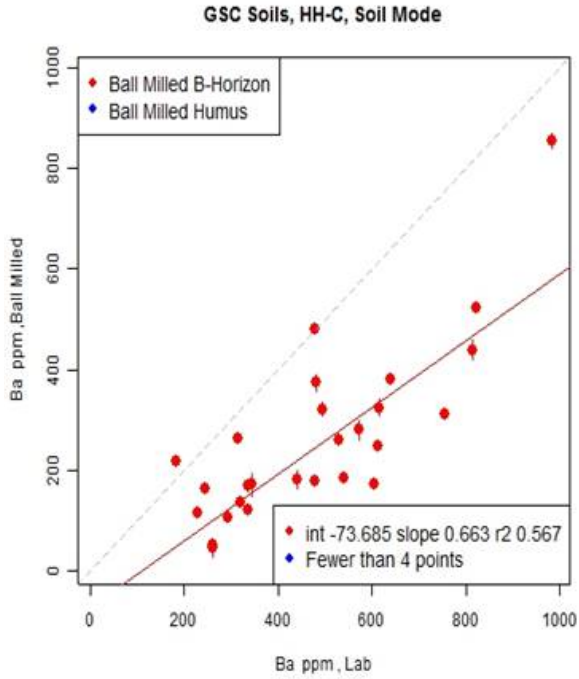
Fig. 6.1.37. GSC_Soils_HHC_soil_Ba.1.jpg
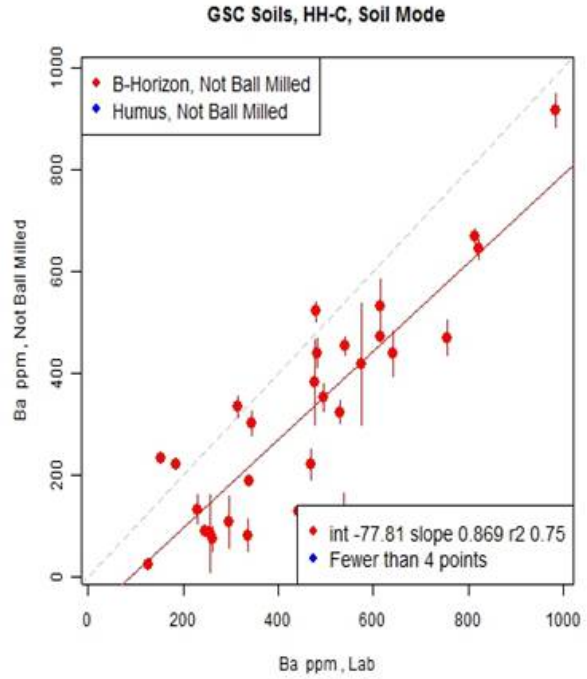
Fig. 6.1.38. GSC_Soils_HHC_soil_Ba.2.jpg
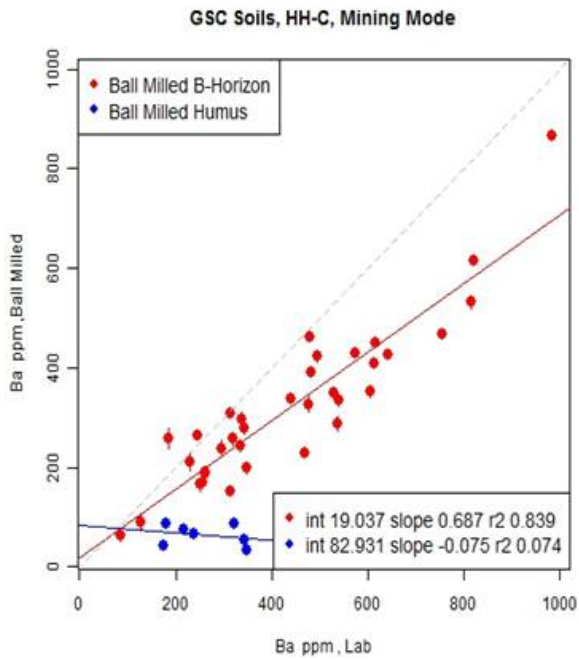
Fig. 6.1.39. GSC_Soils_HHC_mining_Ba.1.jpg
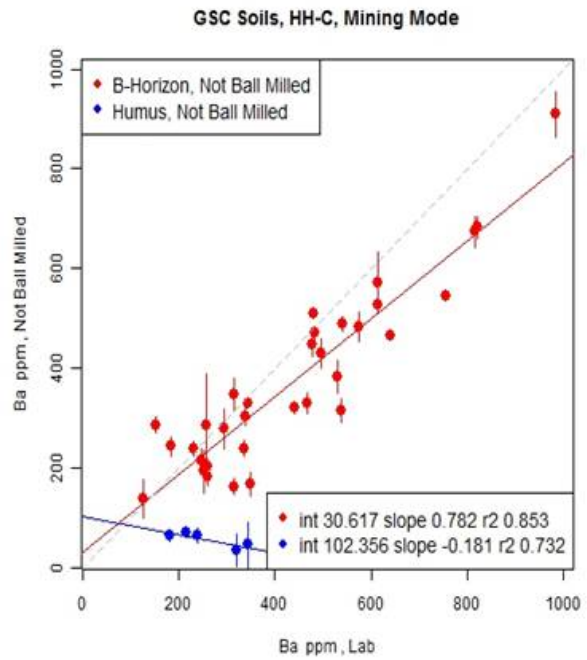
Fig. 6.1.40. GSC_Soils_HHC_mining_Ba.2.jpg
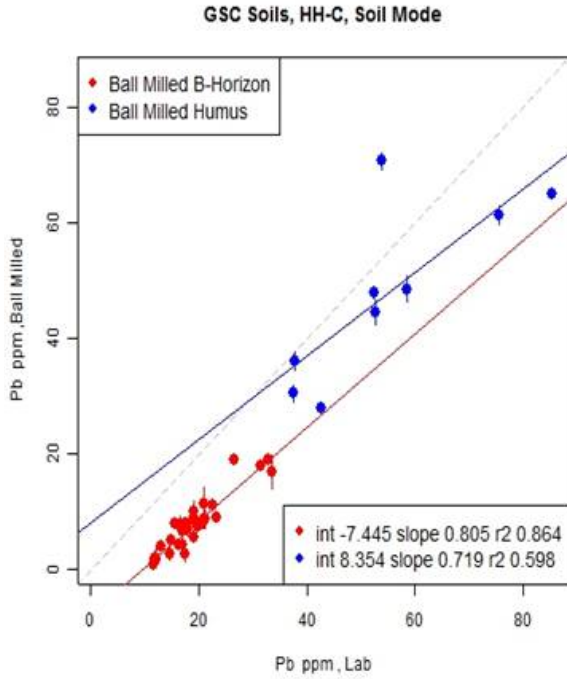
Fig. 6.1.41. GSC_Soils_HHC_soil_Pb.1.jpg
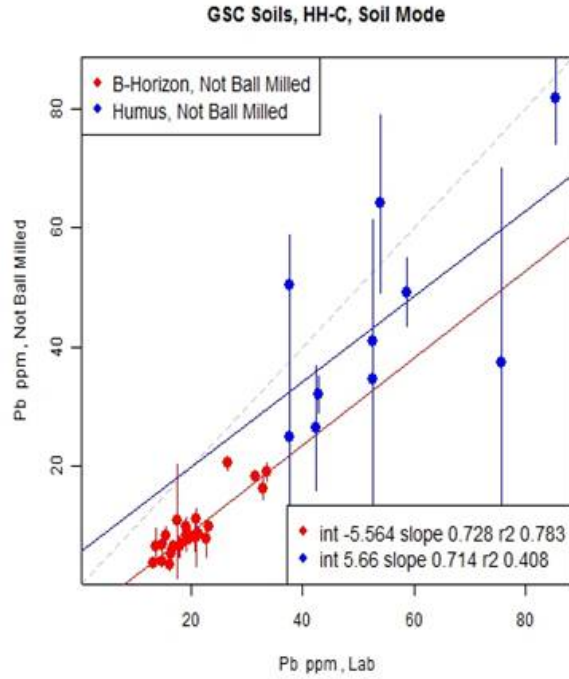
Fig. 6.1.42. GSC_Soils_HHC_soil_Pb.2.jpg
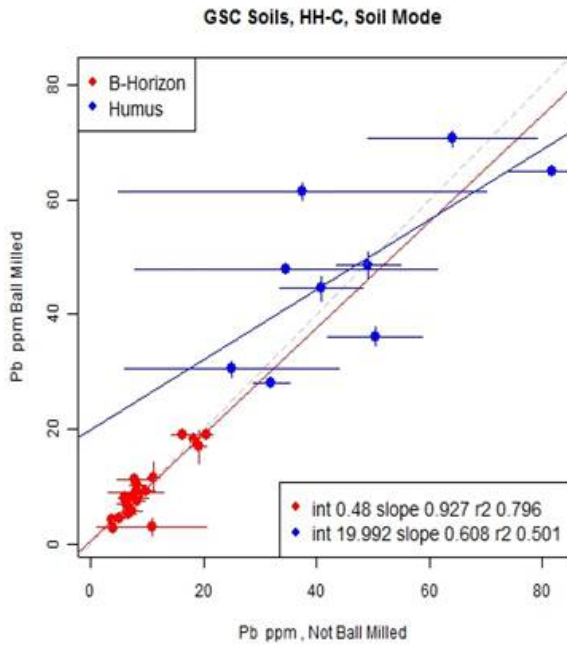
Fig. 6.1.43. GSC_Soils_HHC_soil_Pb.3.jpg
(note much greater error bars on NBM humus)
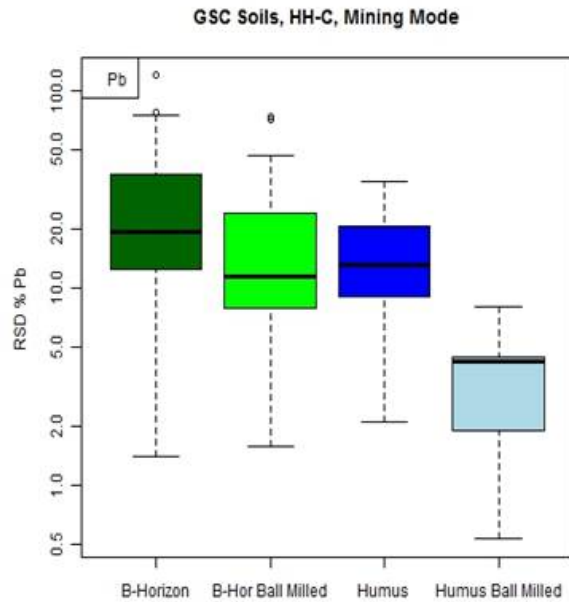
Fig. 6.1.44. GSC_Soils_HHC_soil_Pb.4.jpg
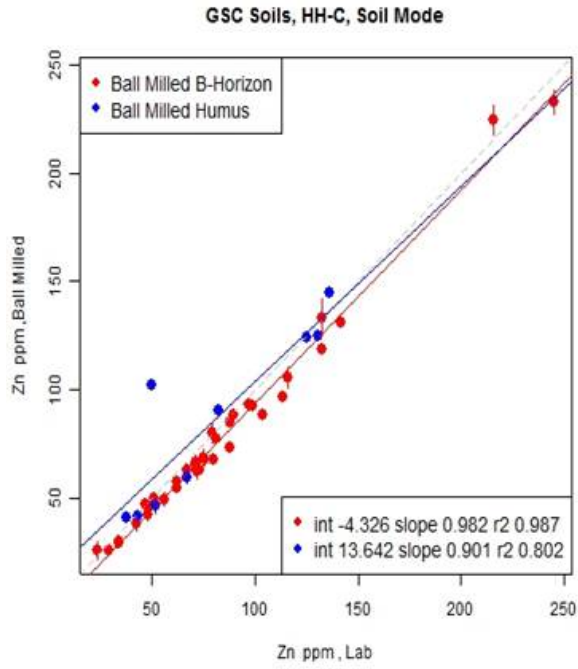
Fig. 6.1.45. GSC_Soils_HHC_soil_Zn.1.jpg
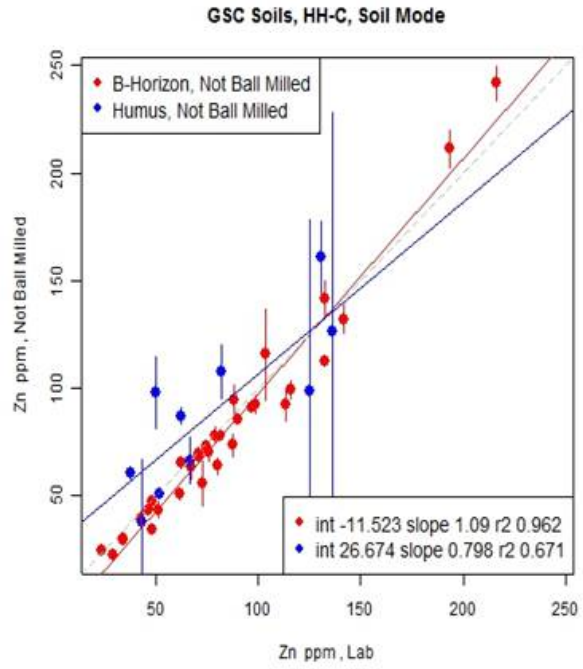
Fig. 6.1.46. GSC_Soils_HHC_soil_Zn.2.jpg
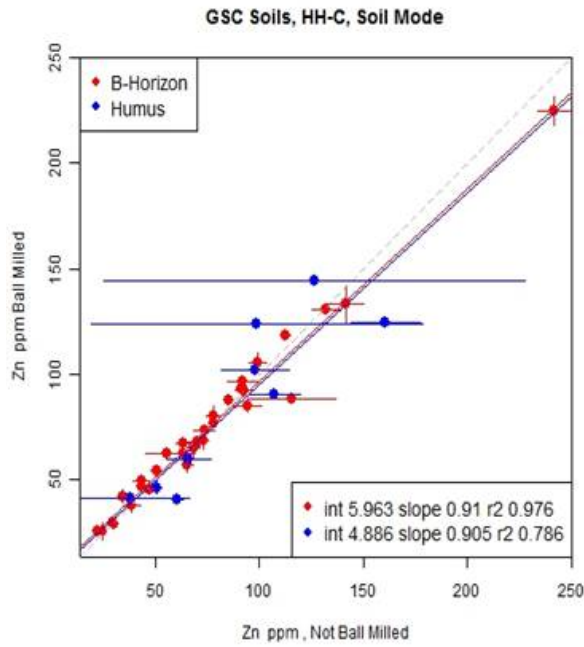
Fig. 6.1.47. GSC_Soils_HHC_soil_Zn.3.jpg
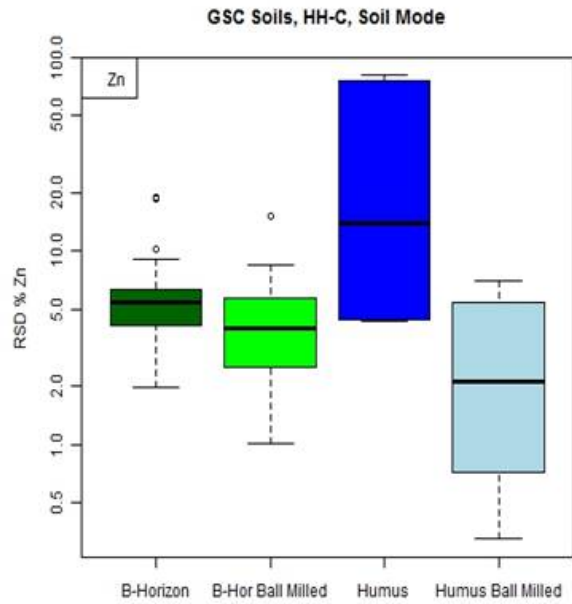
Fig. 6.1.48. GSC_Soils_HHC_soil_Zn.4.jpg

6.2. Vale laterite soils

Peter Winterburn of Vale kindly provided us with a suite of high Fe-Al residual leached tropical soils over Cu mineralisation from Brazil. These soils appeared to be quite homogeneous and fine-grained and have that orange/red colour typical of such enriched-Fe media. Eighteen samples were selected and analysed directly (without any preparation) in cups (n=3, moved between shots) using both handhelds, HH-A and HH-C. A subsample was sent to ALS labs for total analysis where the soils were analysed in triplicate (some actually six times). These samples contain a good range in Al (up to 16%), Fe (up to 42%) and Cu (up to 707 ppm). With these high concentrations of Fe, interferences were to be expected and the factory calibrations, based on a high silica matrix, would certainly not be accurate or suitable. However, a well-fitting line, whatever the slope or intercept, would indicate whether accurate and precise analysis was possible.

The data and results, including plots, are found in the Appendix. The results folders contain, by element and mode: (a) a plot of lab and pXRF values simply organised by increasing lab concentration ('sequence' plot), for a quick view; (b) pXRF vs lab results with trend-line; (c) box-and-whisker plot of both sets of data; and these are followed by a summary of means, SDs and RSDs for each sample. Unlike the case for the GSC soils, where only one (or two) result(s) was (were) above the pXRF LOD, that datum was used to compare to the lab value. If this situation occurred it is obvious in the table for each element (a value less than 3 is shown for 'n'). For the most part, the data used for the plots and discussion are those taken from the mining mode for major elements and from the soil mode for the others, but where data are adequate in number in both modes they are plotted.

HH-A

Mining mode
The sequence and x-y versus lab value plots for Al and Si are shown in Figures 6.2.1, 6.2.2 and 6.2.3, 6.2.4, respectively. Note the poor fit about the trend-line for Al at lower concentrations (< 10% Al), creating an r^2 value of only 0.72, and conversely the good fit for Si at lower concentrations (up to ~ 17% Si) followed by a different trend at higher concentrations with a slope much lower than 1. Thus it appears that simply recalibrating according to this matrix would not be enough to obtain accurate analysis, rather different assumptions would be required in the software.

Analysis for Fe and Ti is excellent, with slopes and r^2 values essentially of unity (Figs. 6.2.5, 6.2.6 and 6.2.7, 6.2.8, respectively).

Calcium and Mg were too low (< 0.1%) to report by pXRF; K was reported in four samples in this mode but in more by the soil mode.

Only five samples are reported for P (lab range of ~ 200-1600 ppm) by pXRF; these data suggest that P cannot be determined by pXRF at these concentrations.

More samples were reported for Pb in the mining mode than in the soil mode. Lead is present at a low range of < 5-33 ppm in the Vale soils but nevertheless the seven samples reported showed a trend-line with an r^2 value of 0.96.

Soil mode
The trace elements As, Co, and W all show the impact of interference (Figs. 6.2.9 to 6.2.12). Arsenic (Fig. 6.2.9) reports up to ~ 200 ppm whereas the lab values are < 20 ppm, the majority being < 5 ppm (lab LOD). These erroneously high As values are associated with high Fe concentrations (> 25%) but interestingly the sample with the highest Fe concentration, SO 00155 with 42% Fe, reports <LOD in As (and W). Cobalt, just next to Fe in the Periodic Table and therefore subject to huge overlap of its Kα (and Kβ) line in this case, reports up to 306 ppm (SO 00155) with lab values rising only to a maximum of 36 ppm (Fig. 6.2.10). The plot of Co by pXRF vs Fe illustrates this spectral overlap nicely (Fig 6.2.11). The lab values for W are < 5 ppm but the pXRF reports 10 samples from ~ 8 to 32 ppm, samples which contain > 25% Fe (Fig. 6.2.12).

Results for Cr, present in the range 50-347 ppm, are extremely noisy, with an r^2 of only 0.21 and most samples report high compared to the lab result (fusion) (Fig. 6.2.13). The reason for the very high result of 369 ppm (cf lab of 77 ppm) in sample 00369 is unclear. This sample is also very high for V, at 541 ppm (cf 77 ppm by lab). Vanadium, present at 44 to 587 ppm, is less noisy than Cr, with an r^2 value of 0.53 and a slope of 0.76 (Fig. 6.2.14). Without sample 00369, results would be far better and acceptable. The lab results for this sample are accurate as it was analysed six times (i.e. six fusions, analysed by both ICP-MS and ICP-ES).

Rubidium and Sr are usually excellent elements by pXRF but they are present at low concentrations in these samples and thus data are noisy. Only seven results are reported for Rb which is present in the range 0.7-36 ppm (Fig. 6.2.15); a concentration of 13 ppm in sample SO 00033 would normally have been detected by pXRF (<LOD in this case). An r^2 value of 0.76 is not bad for Sr given its concentration range of 4-16 ppm (Fig. 6.2.16).

Zinc reads very low in this medium: for example, six samples containing Zn in the range 32-57 ppm are reported as 'VALUE!' or '<LOD' and these are not related to high Fe contents. The r^2 value is 0.79 and the intercept is negative, at -13.2 ppm (Fig. 6.2.17).

The r^2 values of elements which perform well, especially given some of the concentration ranges (in brackets) are: Cu, 0.95 (21-687 ppm); Mn, 0.96 (< 77-4362 ppm); Nb, 0.88 (10-51 ppm); Th, 0.92 (6-58 ppm); U, 0.97 (2-67 ppm); Y, 0.82 (6-50 ppm); and Zr, 0.91 (178-708 ppm). See Figure 6.2.18 (Cu), and Figure 6.2.19 (Zr) for examples. The two samples containing the greatest amount of Mn, SO 00033 and 00034, are reported high for Mn (9342 vs 5344 ppm lab and 7403 vs 4363 ppm lab) but these are not particularly high in Fe (17 and 16%); the plot suggests two trend-lines between low and high concentrations (Fig. 6.2.20).

Molybdenum is too low (2-17 ppm) for the performance to be critiqued but the samples with higher concentrations are reported by pXRF (e.g. 11 ppm by pXRF vs 17 ppm lab; 8 vs 13 ppm; 8 vs 7 ppm). Results for P, present at 232 to 1600 ppm, are random. For the 10 samples that were

reported by pXRF for K (up to 0.7% K), the goodness of fit is excellent at 0.98, with a high slope of 1.6. Nickel is reported as <LOD in all the samples, though it is present at up to 65 ppm; data for the 10 samples reported in the mining mode are scattered and high.

HH-C

Mining mode
As was evident for HH-A, the calibration for Al is poor, with an r^2 value of only 0.70. Calcium is reported by HH-C and considering that the concentrations are so low (~ 0.01-0.07%), an r^2 value of 0.95 is very good. The trend-lines for Fe and Ti are excellent: r^2 values are 0.99 and the slopes are 1.1. Potassium (~ 0.01-0.72%) is reported above LOD (~ 0.1% K) in nine samples: r^2 is 0.98 and the slope is 2.2 for these nine samples (Fig. 6.2.21). Magnesium is reported erroneously above LOD in seven samples, to a maximum of 0.7% (cf 0.06% lab) (Fig. 6.2.22). As noted previously for this instrument, Si reports high and this is the case for Si here up to ~ 20% after which lower relative values are obtained that seem to have their own linearity (Figs. 6.2.23 and 6.2.24). This difference in patterns of response between lower and higher Si, breaking at 20% Si, was observed for HH-A.

Manganese performance is excellent in the mining mode (as opposed to the soil mode): the r^2 value is 0.96, the slope 1.1 and the RSDs excellent.

Phosphorus is reported in almost all samples but it is very noisy, with an r^2 of 0.55 (e.g. in sample SO 00022 P is reported as 940 ppm; cf 233 ppm lab). Niobium and Y are reported only in the mining mode. Data for Nb and Y are excellent at these concentration ranges (10-51 ppm for Nb; 6-50 ppm Y); r^2 values are 0.91.

Soil mode
Unlike HH-A where As results are erroneously high, HH-C reports As, present at < 5-16 ppm, at low (~ < 10 ppm) and random concentrations. This noise is probably due to the large correction being made for Fe and is certainly highly preferable to false highs. Cobalt, the element most severed affected by Fe, is reported as negative numbers in the soil mode and as '1.0' in the mining mode; the actual concentrations are < 1 to 36 ppm. Results for W, present at very low concentrations below 5 ppm but reported by pXRF to 25 ppm (Fig. 6.2.25), are controlled by the Fe concentration as seen in Figure 6.2.26.

The influence of Fe is evident in the high Ni data, reporting up to 141 ppm in SO 00155 (lab value of 59 ppm Ni), as illustrated by the sequence plot (Fig. 6.2.27) and the Ni vs Fe plot (Fig. 6.2.28). Tin is also apparently influenced by Fe, with values reported up to 39.6 ppm for SO 00155 (42% Fe) whereas the lab value is 5 ppm; again, the high Sn values correlate with Fe. Thorium too is reported erroneously high in the six samples containing > 25% Fe; for example, in SO 00155, the pXRF Th value is 97 ppm vs 9.8 ppm by the lab (Fig. 6.2.29). The goodness of fit for U is 0.90 but the impact of the six high Fe samples is still evident in the erroneously high values at the low end of the calibration (e.g. 23 vs 4 ppm for sample 00155).

Calibration for Mn is not good at all by the soil mode (r^2 of 0.71; intercept of ~ -400 ppm, slope of 1.75): this could well be due to an inaccurate correction using Compton normalisation where the Fe peak, between the Mn and Compton peaks, creates a large background.

The plot for Cr would be of much better fit (r^2 of 0.33) if the datum for sample 00369 was removed (373 ppm vs 77 ppm by lab); this sample is also problematic for HH-A (Fig. 6.2.30). Vanadium (44-587 ppm) is well determined in these samples by HH-C, with an r^2 of 0.93; sample 00369 is not so erroneous using HH-C (cf to HH-A).

At concentrations below a few ppm, Rb reports erroneously high, up to 15 ppm, but beyond this level of Rb, results agree well with lab values (Figs. 6.2.31, 6.2.32). The cause of these false highs is not obvious. Strontium is quite well determined at this range of 4-16 ppm; the r^2 value is 0.72.

Lead, present at only up to 33 ppm, is reported in 17 of the 18 samples but many individual RSDs are high and the data are quite scattered, with an r^2 value of 0.73. As for HH-A, Zn shows suppressed values compared to the factory calibration and a rather poor r^2 value of 0.75.

Even though the concentration of Mo in these samples is low (2-17.3 ppm), and some individual RSDs are high, the goodness of fit is excellent at 0.93. Other elements with very good performance comprise Cu (r^2 of 0.96) and Zr (r^2 of 0.91).

<u>Summary for the laterite soils</u>

- The high concentration of Fe has a huge impact on numerous elements, especially Co and As. These results demonstrate the difference between manufacturers in that one reports these impacted elements as <LOD (HH-C) while the other (HH-A) reports false high values into the hundreds of ppm. Conversely, HH-C reports erroneously high results in samples containing > 25% Fe for U and Th whereas HH-A either reports values as <LOD (U) or makes a correction (Th). Other elements influenced by high Fe, particularly at levels > 25%, include W, Ni, and Sn; analysis for these elements is negated.
- Of the major elements, Fe and Ti are well determined but Al and Si are noisy. Calcium can be well determined above 0.015% and K above 0.1%. Magnesium, at 0.006-0.06%, and P, at up to 1600 ppm, cannot be measured in these samples.
- Elements where at least one instrument shows good results comprise Cu, Mn, Nb, Th, U, V, Y and Zr. The performance for Sr, present at low concentrations below 16 ppm, is average to good and that for Cr, Rb and Zn average to poor.
- With the exception of the elements impacted by high Fe concentration, the performance of the remaining elements is good in light of the fact that these samples did not undergo any preparation.
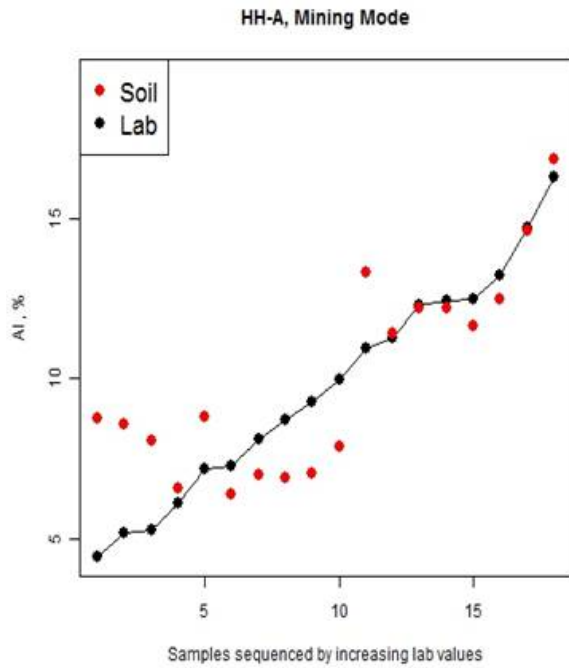
Fig. 6.2.1. Soils_Vale_HHA_mining_Al.1.jpg
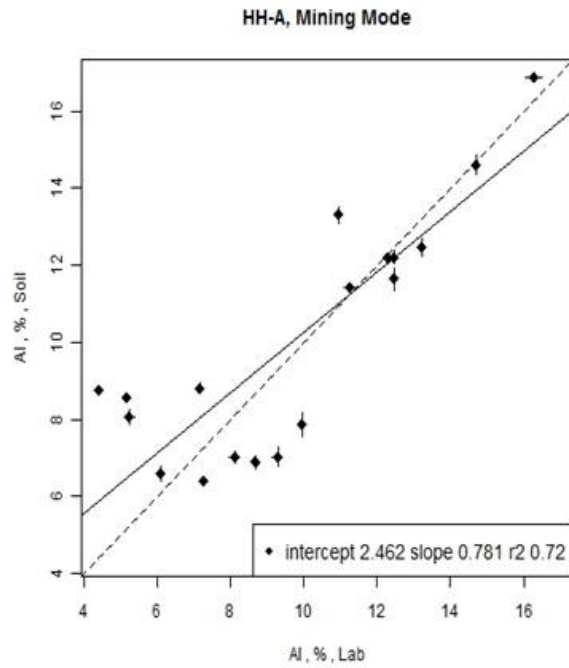
Fig. 6.2.2. Soils_Vale_HHA_mining_Al.2.jpg
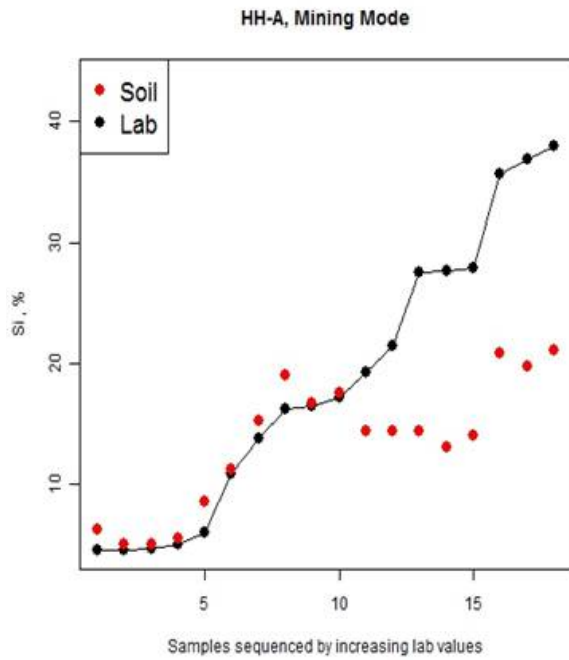
Fig. 6.2.3. Soils_Vale_HHA_mining_Si.1.jpg
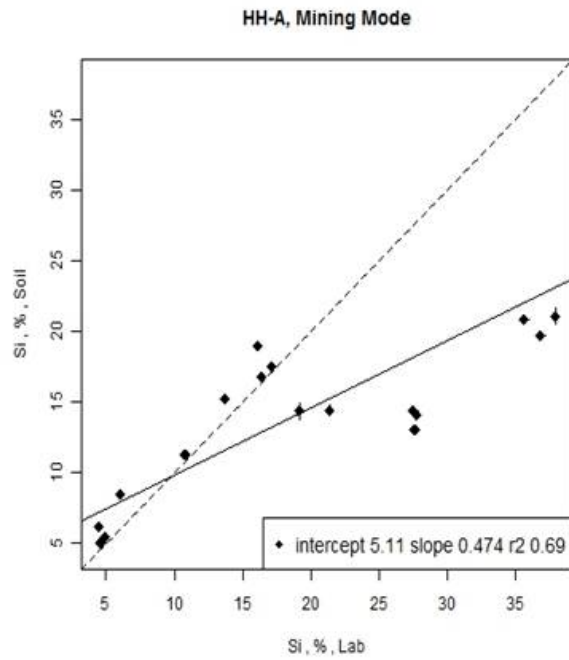
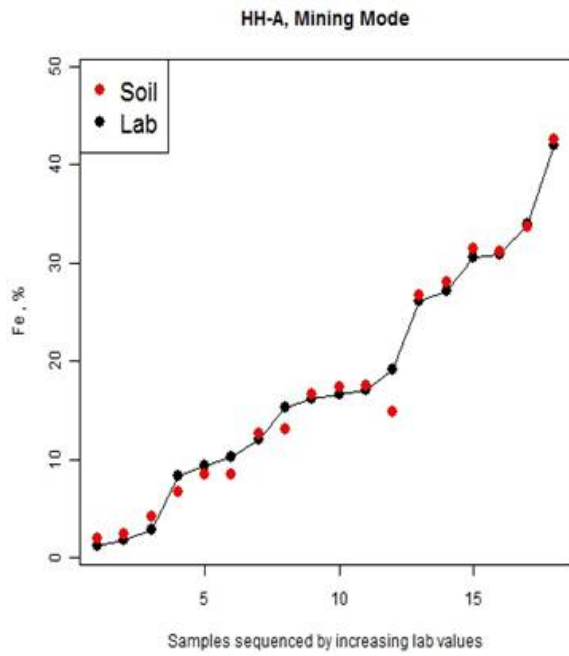**Fig. 6.2.4. Soils_Vale_HHA_mining_Si.2.jpg**
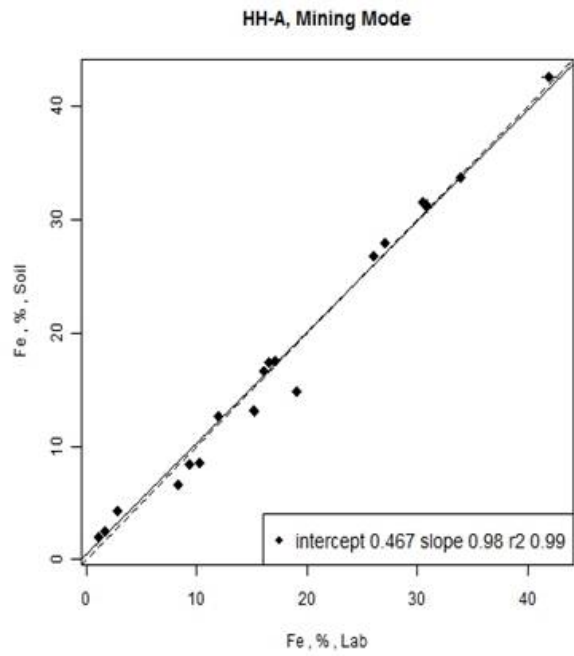
Fig. 6.2.5. Soils_Vale_HHA_mining_Fe.1.jpg

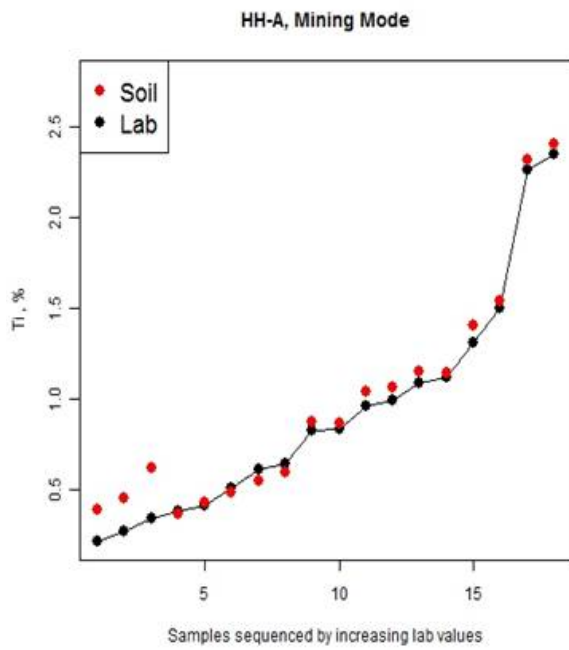**Fig. 6.2.6. Soils_Vale_HHA_mining_Fe.2.jpg**
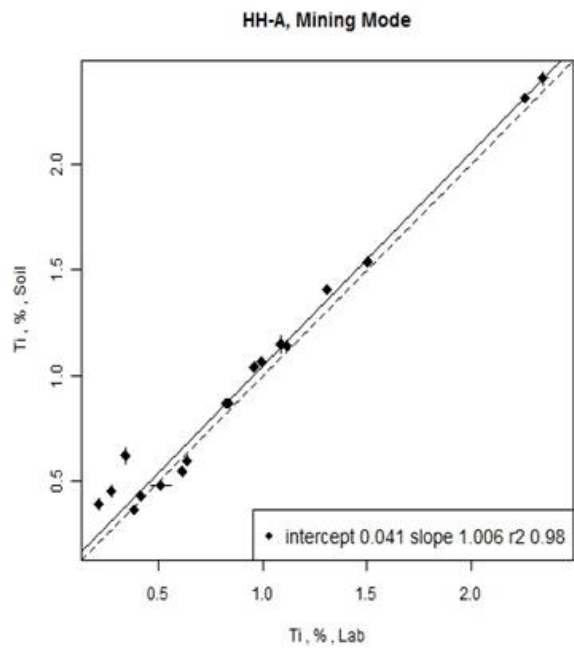

Fig. 6.2.7. Soils_Vale_HHA_mining_Ti.1.jpg
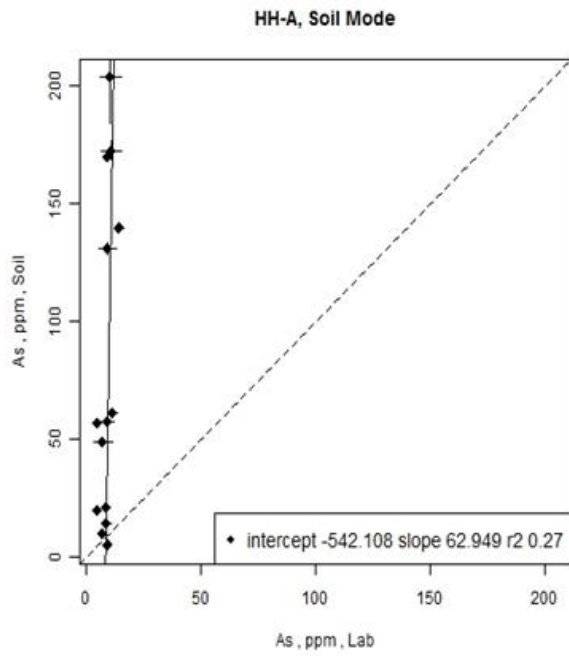

Fig. 6.2.8. Soils_Vale_HHA_mining_Ti.2.jpg
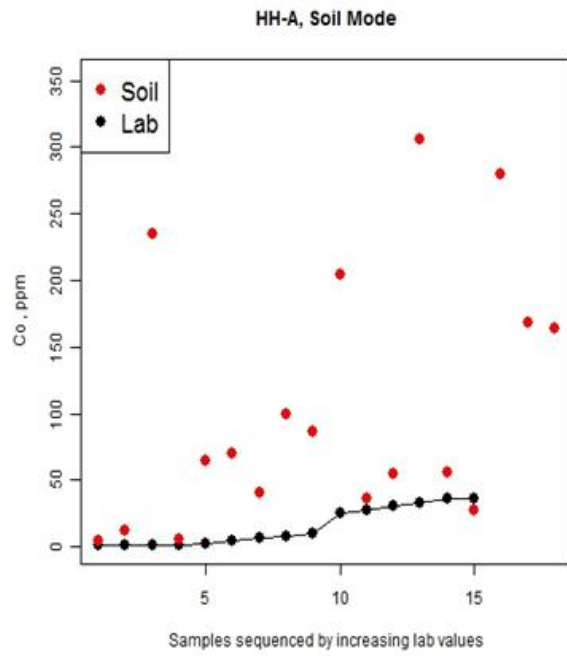
188

Fig. 6.2.9. Soils_Vale_HHA_soil_As.2.jpg

Fig. 6.2.10. Soils_Vale_HHA_soil_Co.1.jpg
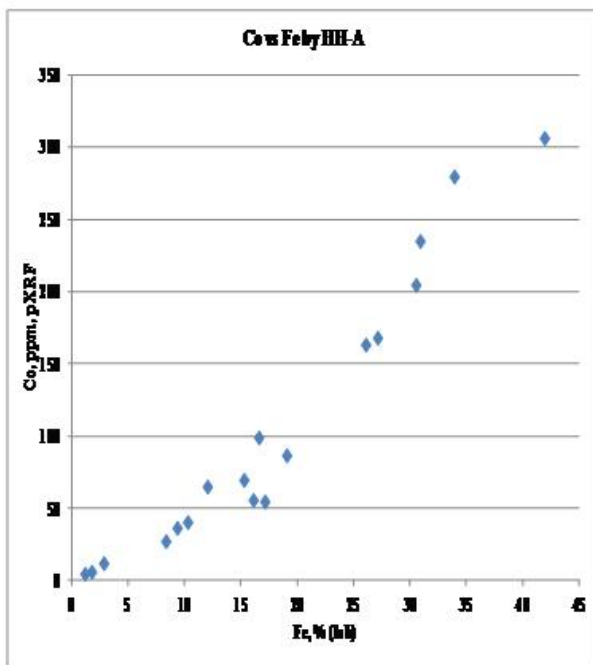
Fig. 6.2.11. Co (pXRF) versus Fe (lab)
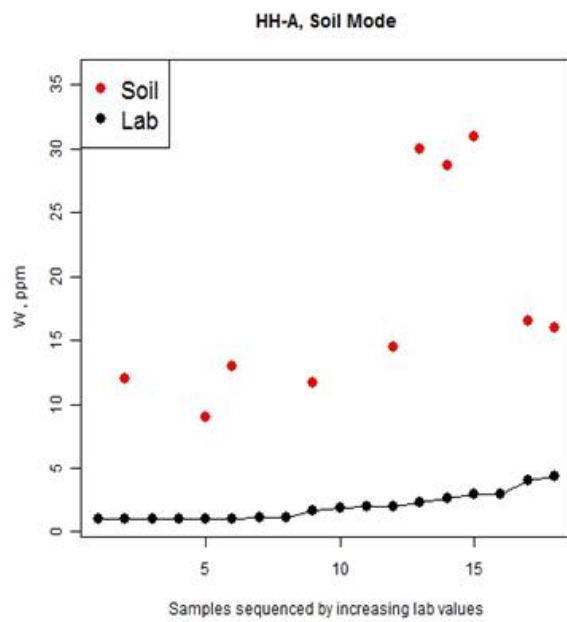
Fig. 6.2.12. Soils_Vale_HHA_soil_W.1.jpg
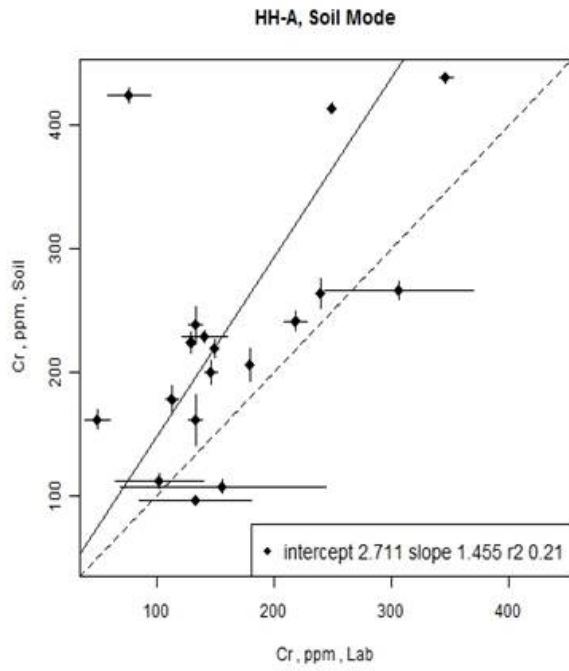
Fig. 6.2.13. Soils_Vale_HHA_soil_Cr.2.jpg
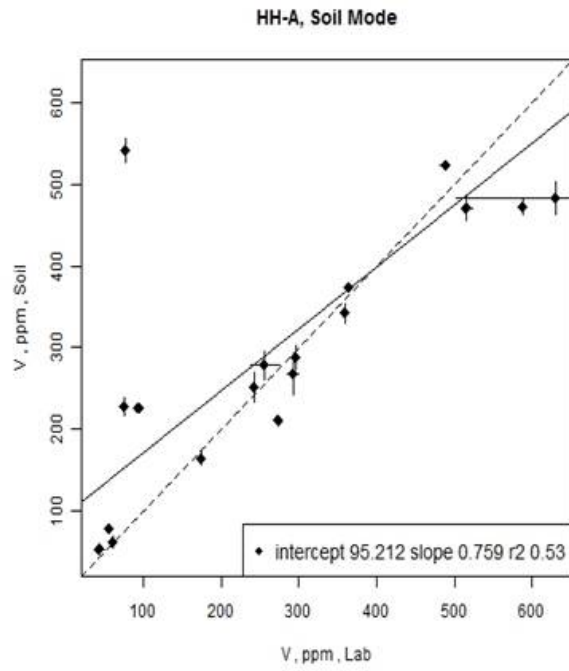
Fig. 6.2.14. Soils_Vale_HHA_soil_V.2.jpg
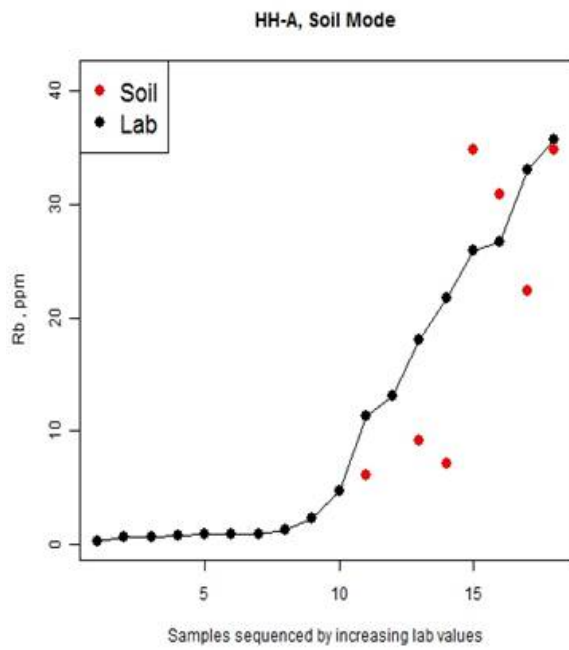
Fig. 6.2.15. Soils_Vale_HHA_soil_Rb.1.jpg
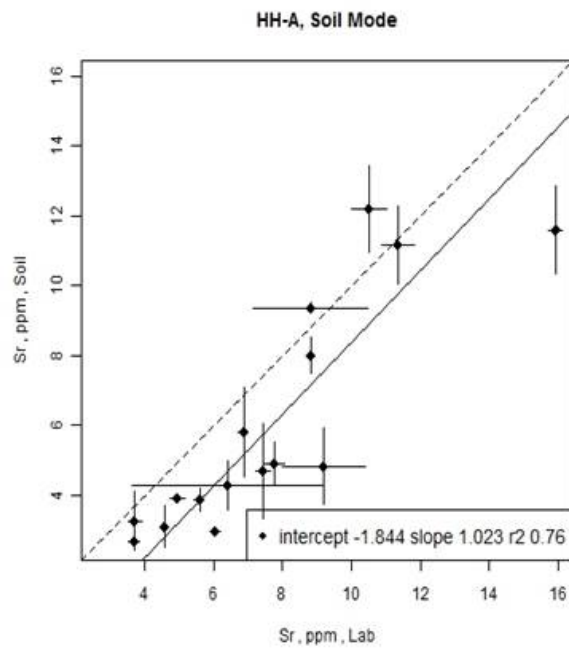
Fig. 6.2.16. Soils_Vale_HHA_soil_Sr.2.jpg
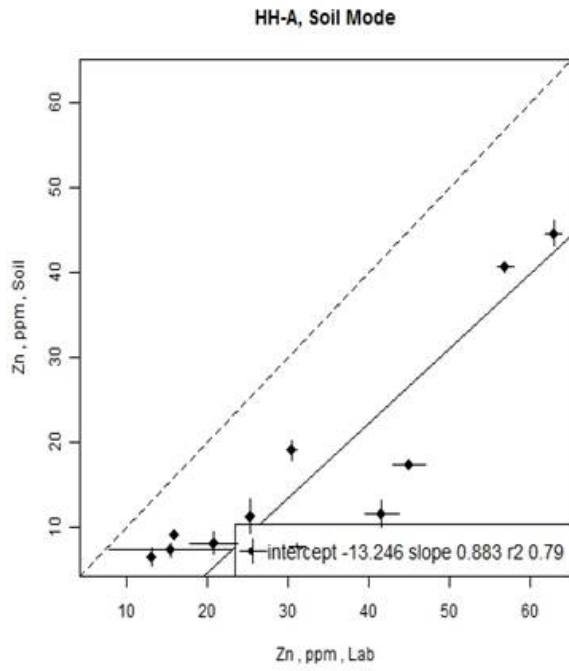
Fig. 6.2.17. Soils_Vale_HHA_soil_Zn.2.jpg
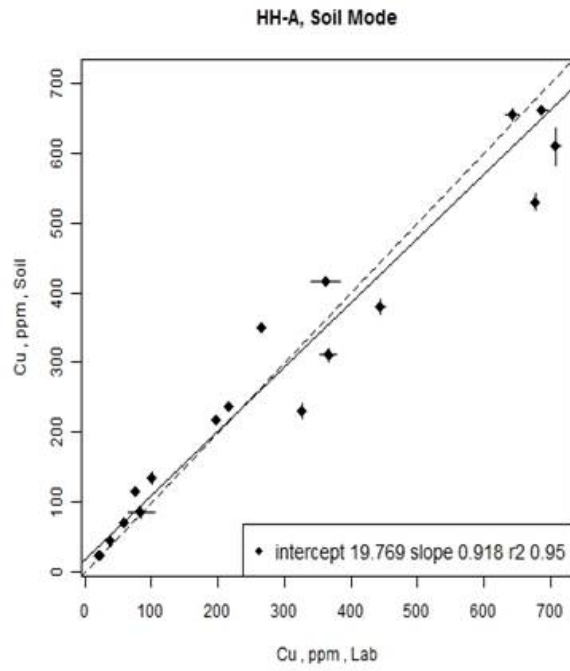
Fig. 6.2.18. Soils_Vale_HHA_soil_Cu.2.jpg
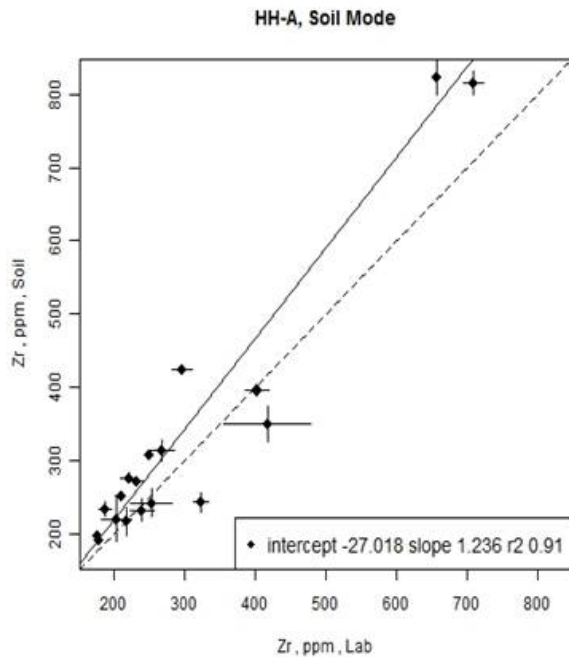
Fig. 6.2.19. Soils_Vale_HHA_soil_Zr.2.jpg
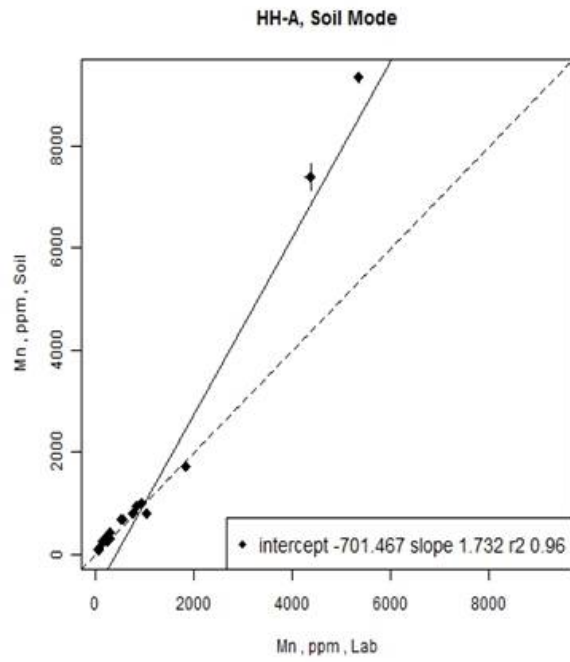
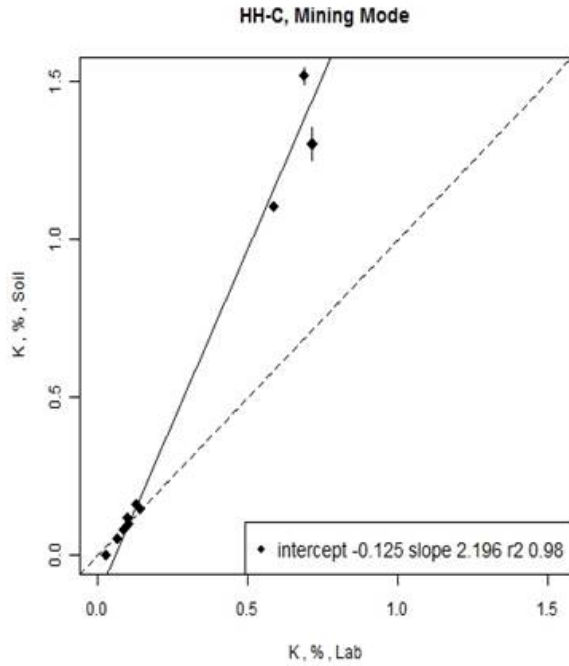**Fig. 6.2.20. Soils_Vale_HHA_soil_Mn.2.jpg**

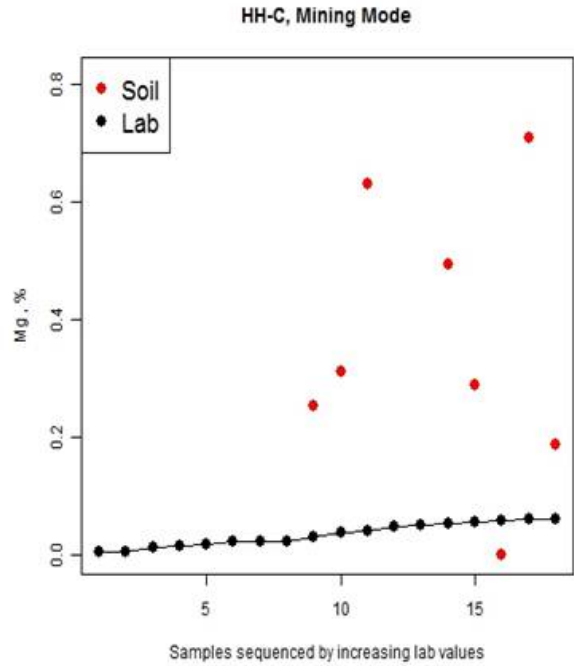**Fig. 6.2.21. Soils_Vale_HHC_mining_K.2.jpg**

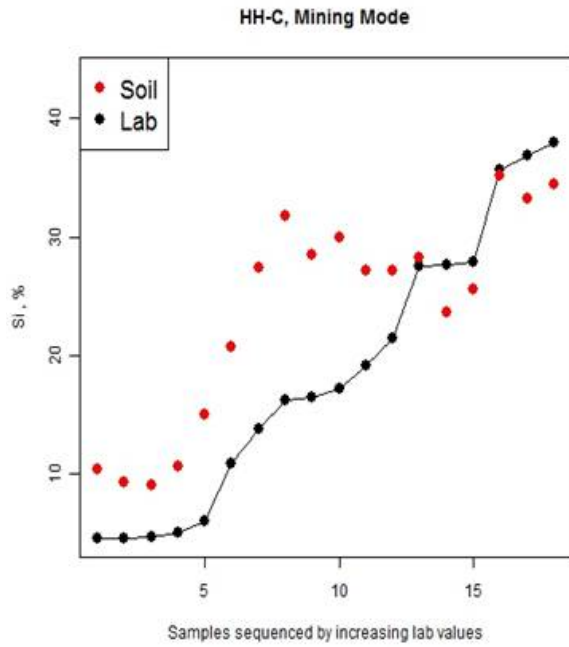**Fig. 6.2.22. Soils_Vale_HHC_mining_Mg.1.jpg**

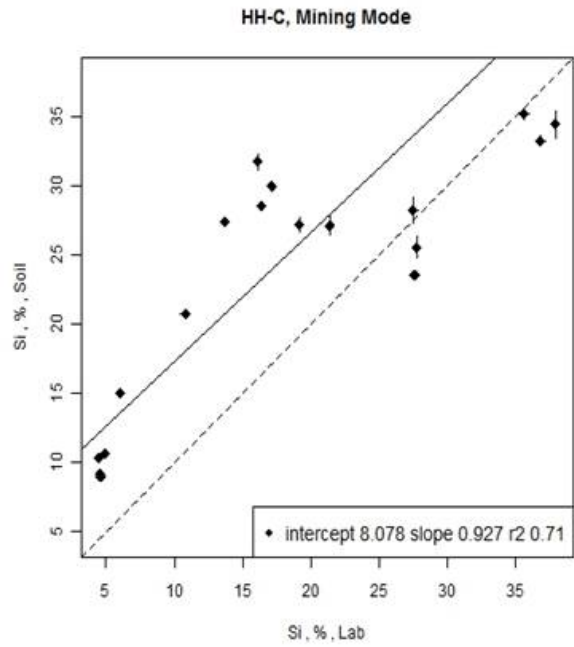**Fig. 6.2.23. Soils_Vale_HHC_mining_Si.1.jpg**

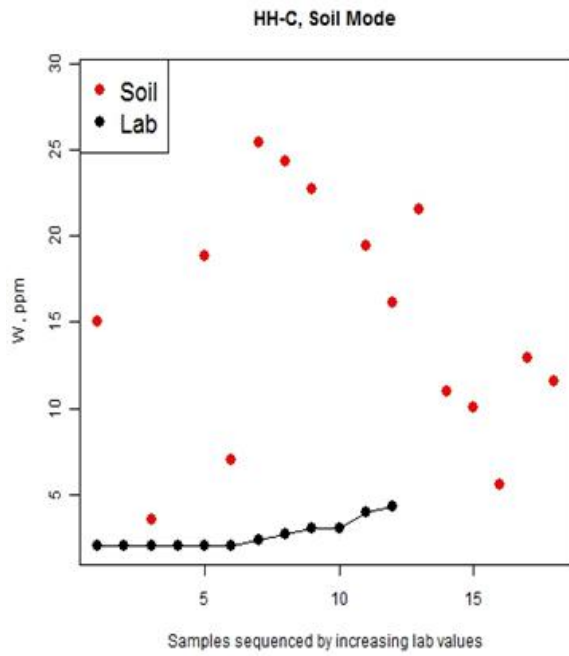**Fig. 6.2.24. Soils_Vale_HHC_mining_Si.2.jpg**

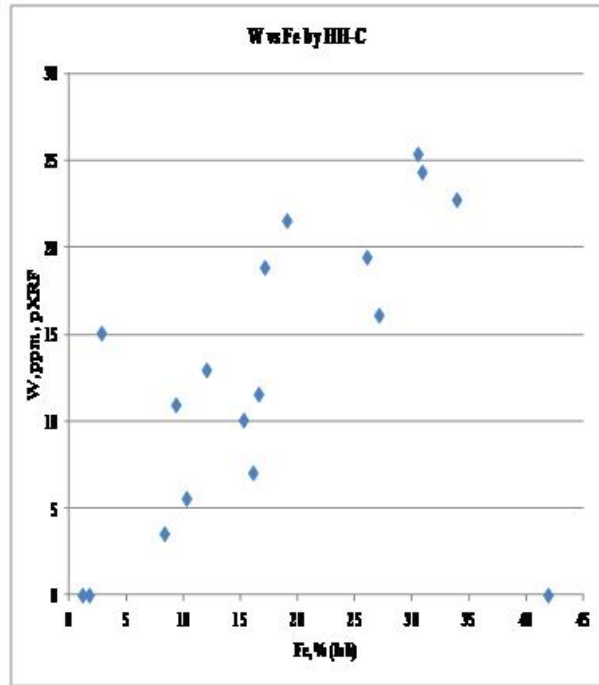**Fig. 6.2.25. Soils_Vale_HHC_soil_W.1.jpg**

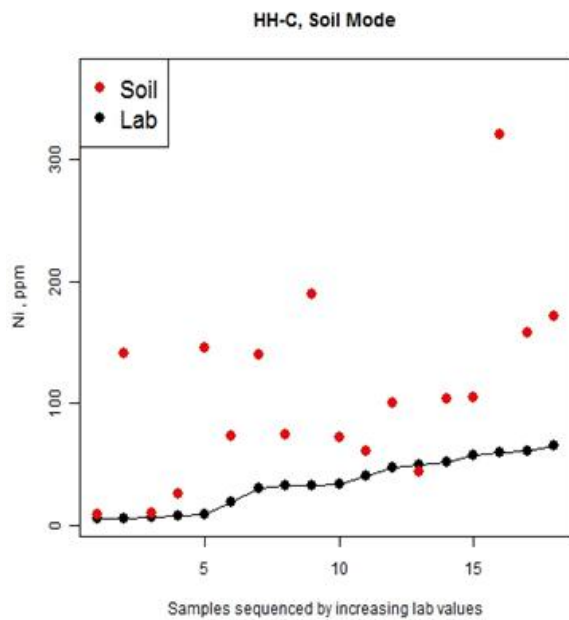**Fig. 6.2.26. W (pXRF) vs Fe (lab)**

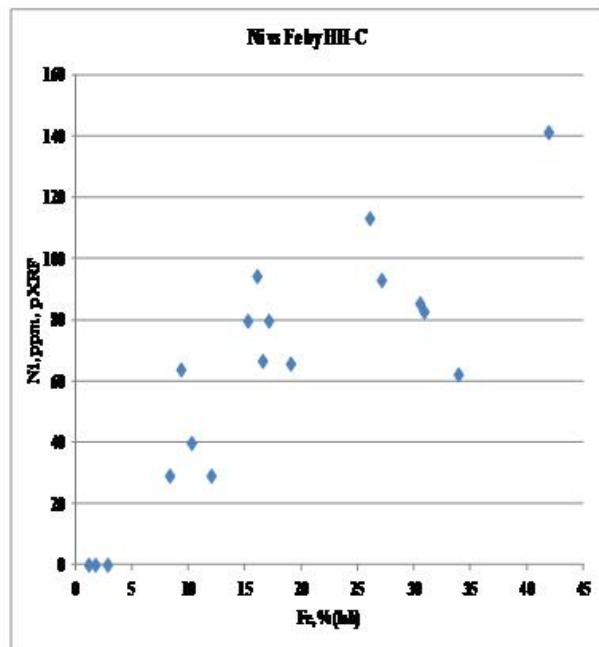**Fig. 6.2.27. Soils_Vale_HHC_soil_Ni.1.jpg**

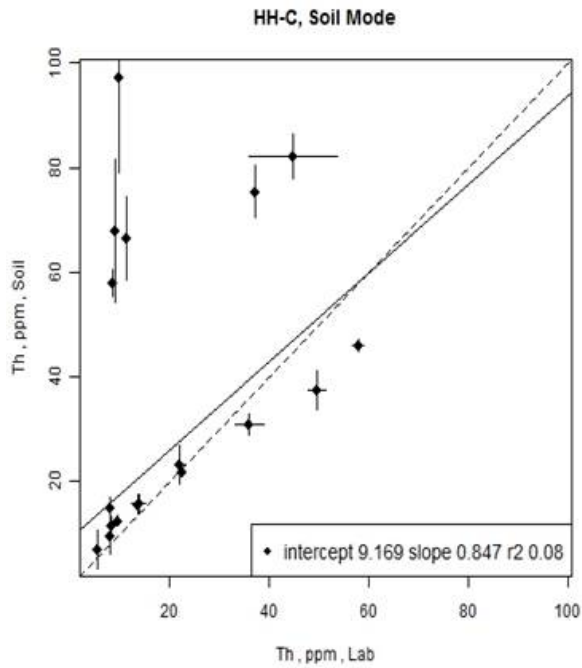**Fig. 6.2.28. Ni (pXRF) versus Fe (lab)**

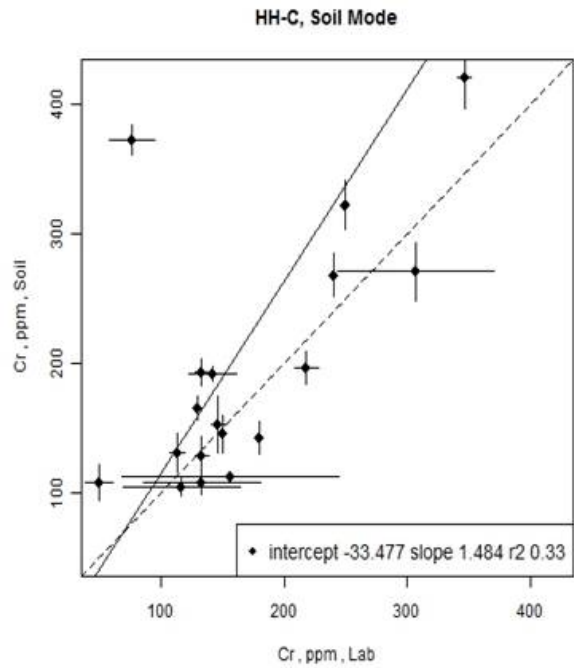Fig. 6.2.29. Soils_Vale_HHC_soil_Th.2.jpg

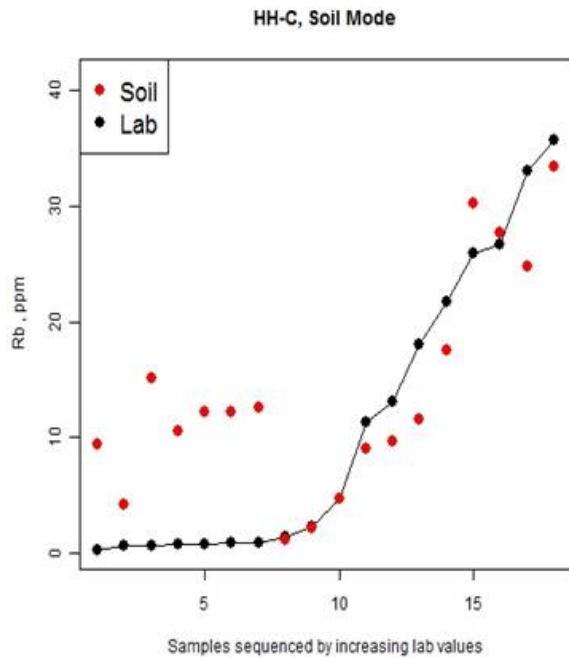Fig. 6.2.30. Soils_Vale_HHC_soil_Cr.2.jpg
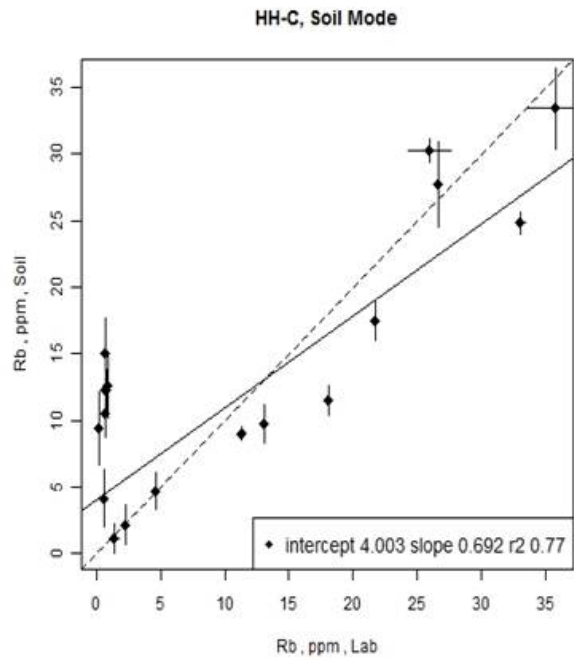

Fig. 6.2.31. Soils_Vale_HHC_soil_Rb.1.jpg

Fig. 6.2.32. Soils_Vale_HHC_soil_Rb.2.jpg

7. MOISTURE STUDY

In order to study the effect of moisture content on pXRF results it is highly desirable to maintain all other parameters except % H_2O constant. Therefore initially we used a very well homogenised, finely powdered, certified reference sample, TILL-2 (Canadian Certified Reference Materials Project, CCRMP), and decided to add water progressively to it. Had we had a saturated homogenous sample at our disposal we might have reversed the experiment and progressively dried it but in that case it may have been difficult to halt the drying at definite stages. Olympus InnovX kindly provided us with 125-ml Nalgene bottles specially fitted with screw caps containing a 4-μm polypropylene window through which we could analyse the wetted sample. However, as water was added to TILL-2 we noticed that some of the sample was sticking to the walls of the bottle and became concerned that the depth of sample being analysed was not always adequate. We then used a Whirl-Pak® bag instead and repeated the experiment; this was an improvement but eliminating air bubbles after each mixing was challenging. Finally we returned to the 125-ml bottles and employed two till samples which were of sufficient quantity that we could use 30 g (rather than 10 g for TILL-2) aliquots.

Till samples 36 and 543

These unsieved till samples were provided by Beth McClenaghan of the GSC. Sample 36 was collected from the vicinity of the Pine Point Pb-Zn deposit (NWT, Canada) whereas sample 543 was obtained from the area of the Sisson Brook W-Mo-Cu deposit (New Brunswick, Canada). The grain size distribution of these samples is: 36.2%/46.3%/17.5% sand/silt/clay for Sample 36 and 62%/32.9%/5.1% for Sample 543.

After drying samples 36 and 543 in an oven overnight at 40ºC, 30 g of each sample were measured into their respective bottles. With the polypropylene-windowed lids in place, the bottles were inverted and tapped on a KimWipe™ tissue on the lab bench to compact the sample against the film. The sample was analysed three times in each mode (soil and mining), alternating between modes. After analysing the sample in each mode once, the sample was shaken within the bottle and then replaced on the analyser in the same position. This was repeated for the final shot. The three shots in each mode were then repeated on the second analyser. Using a 1-ml pipette, 3 ml of deionised (Millipore) water were added to the bottles and mixed with a glass stirring rod until homogenous. The samples were analysed using the same procedure described above. Water was added to the samples by 3-ml increments until 9 ml, at which point the incremental volume was reduced to 1 ml until a total of 18 ml was added. The final two additions were 3 ml, giving a total of 24 ml of water added to each 30-g sample. After each addition the samples were analysed three times following the procedure described above. The experiment was run over three days due to time constraints (0-13 ml on Day 1, 14-21 ml on Day 2 and 24 ml on Day 3).

By the addition of 9 ml, both samples had the consistency of a slurry and hence addition of water was reduced to 1 ml rather than 3 ml. As addition progressed, the excess

solution became more dilute. Under these conditions, there certainly would be settling of heavier particles with time.

Plots of pXRF mean value (n=3) versus # ml of H_2O added were made for those elements that are determined well by pXRF (see the Appendix). There are some 'noisy' responses which is not surprising given that these samples are not sieved and therefore a fair degree of heterogeneity could be present (the triplicate analysis with mixing was designed to minimise noise). Furthermore, it was difficult to mix the added water well in the early stages when a granular texture was noted.

For the graphs presented in this section, data corrected for moisture content are also plotted using the equation

$$C_{dry} = C_{wet} \, (100/(100\text{-}H_2O\%))$$

The corrected data are shown in red on the plots. The uncorrected pXRF results for most elements fall gradually until ~ 15-16 ml of H_2O have been added (33-35% moisture content) at which point the values more or less plateau. These elements include Al, Fe (except sample 543), K, Mn, Si (except sample 543), Sr, Rb, Ti, V, Zr, for both samples by both instruments. This behaviour is illustrated for Fe (sample 36, HH-A), Zr (sample 36, HH-C), Rb (sample 543, HH-A), and K (sample 543, HH-C) in Figures 7.1 to 7.4, respectively. Clearly the correction for moisture content improves the results: for Fe, for example, the corrected data are in the range 1.1-1.3% (cf 1.2% dry) whereas the uncorrected results are in the range 0.7-0.9% Fe; similarly the corrected data for K are in the range 2.2-3.0% (cf 2.8% dry) but the uncorrected data are in the range 1.6-2.1% K. There is a tendency for the corrected results to be rather low at the lower moisture levels (~ 20% moisture; e.g. Fe, K) and high at ~ 35% moisture; nevertheless, for most purposes, the correction would be satisfactory. The reason for this levelling off of signal at ~ 30-35% moisture is that the sample becomes saturated at this point, a slurry forms, and the addition of more water simply rests on the surface of the mixture, no more water infiltrates the grains of the sample and hence the pXRF signal remains more or less the same.

Calcium, Ba and Sr in sample 36 and Ca, Ba and Si in sample 543 show a rise in pXRF results after ~ 15-18 ml of H_2O addition (33-38% moisture). This behaviour is shown in Figures 7.5 to 7.8, respectively, for Ca (sample 36, HH-A), Sr (sample 36, HH-C), Ca (sample 543, HH-A) and Si (sample 543, HH-C). For example, the range in corrected results for Ca in sample 36 is 14.0-15.7% up to 37.5% moisture (cf 17.0% Ca dry and 9.8-12.6% in the uncorrected data) but rises to 20.9% at 44% moisture. The over-correction for sample 543 using HH-A is severe, resulting in a value of 0.89% Ca (cf 0.48% dry), far worse than the actual uncorrected result; similarly the over-correction for Sr in sample 36 at 44% moisture results in a value of 174 ppm, far removed from the dry result of 95 ppm.

Correction for Si up to ~ 35% moisture content is not adequate, generating results in the 22-32% range, substantially lower than the dry value of 40% Si (Fig. 7.8); the same behaviour is evident using HH-A for both samples. In fact, correction for dilution also

fails for another light element, Al, as shown in Figures 7.9 and 7.10 for samples 36 and 543. This suggests the absorption of low energy photons by water.

Responses for Pb and Zn in sample 36 and As, Cu, Fe, Nb, Pb, W and Zn in sample 543 continue to fall after ~ 15-17 ml. This is illustrated in Figures 7.11 to 7.14 for Pb (sample 36, HH-A), Zn (sample 36, HH-C), As (sample 543, HH-A) and Cu (sample 543, HH-A), respectively. After 17 ml (36% moisture) the correction begins to fail for As and Cu and after 18 ml (37.5% moisture) for Pb and Zn; however, the corrected data are still far superior to the uncorrected, as seen in Table 7.1.

Table 7.1. Comparison of corrected and uncorrected data to dry values for 4 elements.

% H_2O	As, ppm			Cu, ppm			Pb, ppm			As, ppm		
	Dry	Corr	UnC	Dry	Corr	UnC	Dry	Corr	UnC	Dry	Corr	UnC
33	32	31	21	92	87	58	150	139	92	466	451	301
44	32	24	14	92	66	37	150	94	52	466	357	198

Corr: Corrected
UnC: Uncorrected

CRM Till-2

Two sets of data were obtained: one using the 'bottle' procedure described above and the other employing a 4-oz Whirl-Pak® bag of 57-µm thickness. The bottle procedure differed in that only 10 g of TILL-2 were used and water was added in 1-ml increments to a total of 10 ml (i.e. 50% moisture content).

In the 'bag' procedure, the top of the bag was carefully rolled down to remove the air and compress the sample. The sample was analysed three times in each mode (soil and mining), alternating between modes. After analysing the sample in each mode once, the sample was shaken within the bag and then replaced on the analyser in the same position. This was repeated for the final analysis. The three analyses in each mode were then repeated on the second analyser. Using a 1-ml pipette, 1 ml of deionised (Millipore) water was added to the bag and mixed with a glass stirring rod until homogenous. The sample was analysed using the same procedure described above. Water was added to the sample by 1-ml increments for a total of 12 ml (i.e. 55% moisture content). After each addition of water the sample was analysed three times following the procedure described above. The sample appeared to be saturated around the 6-ml mark, as indicated by the pooling of water on top of the sample. The experiment was run over two consecutive days due to time constraints (0-6 ml on Day 1 and 7-12 ml on Day 2).

Results using the bottle procedure for TILL-2 agree with those employing the bag and, within experimental error, also match well across the two instruments. The thickness of the bag greatly reduced the signals for Al and Si but the trends remained similar to those seen for the bottle procedure. Figures 7.15 to 7.17 show that correction for dilution works well up to ~ 37.5% moisture (6 ml of water added) for the elements Fe, Zn and Cu. This is the case for most elements determined substantially above pXRF detection levels,

including As, Co, Cu, Fe, K, Mn, Nb, Pb, Rb, Sr and Zn. The pXRF results level off at ~ 37% moisture (to the final moisture content of 50-55%). Thus the saturation point for TILL-2 has been reached at ~ 6 ml of water.

After addition of 5 ml of water (33% moisture content), the elements Al, Ca, Cr, Si, Th, Ti, V, Y and Zr all show increases in signal with water and therefore a serious over-correction results (Figs. 7.18, 7.19 and 7.20 for Ca, Cr, Si). For example, at 8 ml of water or 44% moisture, Ca reads 1.2% corrected (cf 0.6% dry), Cr reads 133 ppm (cf 92 ppm dry) and Si reads 58% (cf 40% dry).

There are several explanations for this increase in intensity of pXRF signal after the saturation point has been reached. Keith McIntosh of Anglo American suggests it is a physical effect of particle separation:

"Fine particles and clay-like minerals may settle, these minerals and their associated analytes will then be preferentially excited and produce an enhancement rather than the dilution you expect. I think this is somewhat confirmed by your data as initially the concentration drops because of dilution and then increases, potentially confirming that when the moisture reaches a specific level it is possible for the minerals to segregate. This cannot be corrected for as it is a physical effect. You may also consider soluble analytes that may concentrate in solution which will separate. To check these theories you may consider measuring the same samples both from below and from above (moving them as little as possible), they should be opposite if there is a segregation. Irrespective of whether this is conclusive I suspect it's a physical effect rather than a measurement problem. We see the same effects in solutions where insoluble salts precipitate."

Stan Piorek of Niton suggests another explanation, that the increase is caused by an enhancement (i.e. spectral) effect:

The fact that we observe an increase of intensity after the initial drop may be explained by enhancement of element X-rays by increased intensity of scattered radiation. Note, that when a layer of free water shows above the soil surface in a sample cup it generates more scattered X-rays which in turn may excite elements in the soil below. Simply put, more water above the soil surface contributes to scatter, which before getting out from the sample to the detector must travel through soil and thus may have a chance to excite its elements, in addition to the primary radiation from the tube. Note also, that this effect will be more pronounced for those elements whose absorption edges are closer to the average energy of scattered radiation; this is why we see zirconium intensity (and results) going up. It is the situation in which the enhancement effect prevails over absorption".

Given the range in X-ray characteristics and chemistry of the elements displaying these increased signals in the three samples tested, a physical effect of particle separation is probably the main cause.

The corrected data for Al and, to a lesser degree, Si are reporting low, as was evident for samples 36 and 543 (Figs.7.21, 7.22). It appears likely that the low-energy photons of these light elements may be absorbed by the water present.

The moisture meter shown below, Model MMD4E from General Tools, can be purchased for under $50 from Amazon.com. It weighs 0.1 kg and operates on a 9-V battery.

Summary of moisture study
- Up to ~ 30-35% moisture content, correction for dilution works well for most elements. Therefore, when working with samples of variable wetness it is recommended that either they be dried or a correction made for dilution after measuring the water content with a moisture meter. The actual point at which the sample becomes saturated (30%, 35% etc) depends on the grain size distribution and mineralogy of the sample.
- However, the light elements (Al, Si) can show a significant degree of under-correction (i.e. the results decrease to a much greater degree than that accounted for by dilution) in the range up to saturation. If these elements are important, drying is the recommended strategy.
- Correction after the saturation point fails to various degrees depending on the element and sample. Any excess water can either be poured off or removed with absorbent tissue and then the sample can be dried or a correction made.

Note: Red dots in Figs 7.1 to 7.22 are for corrected data.
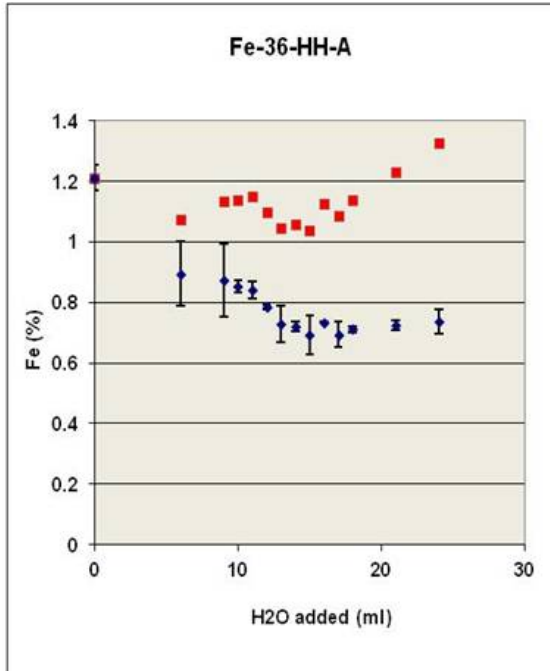
Fig. 7.1. Fe in Sample 36, HH-A.
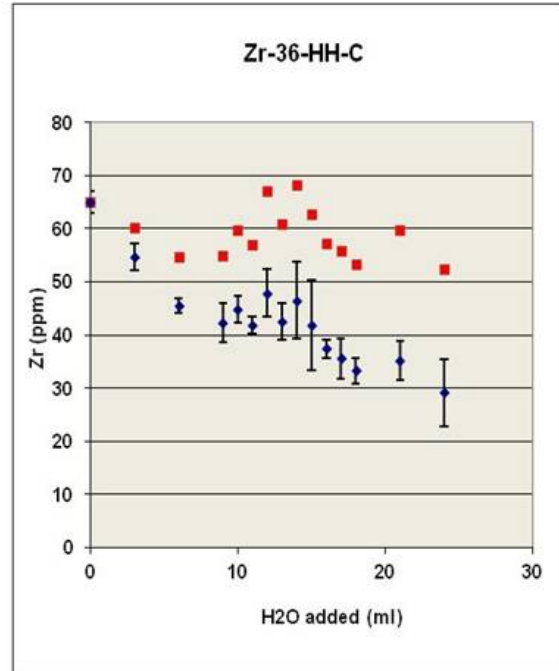
Fig. 7.2. Zr in Sample 36, HH-C.
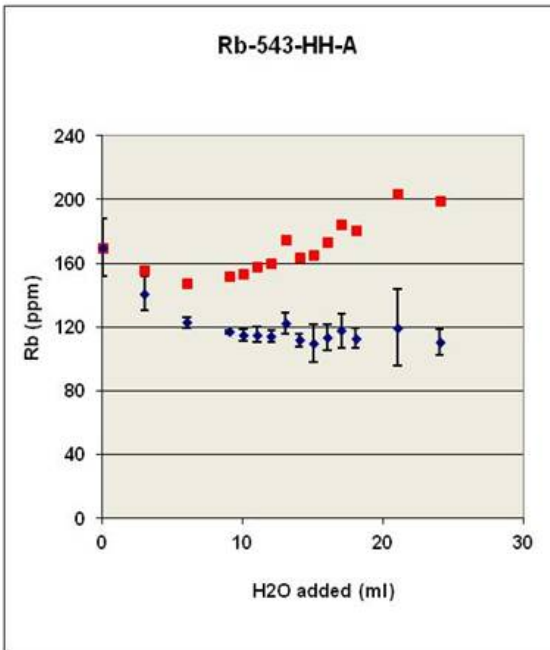
Fig. 7.3. Rb in Sample 543, HH-A.
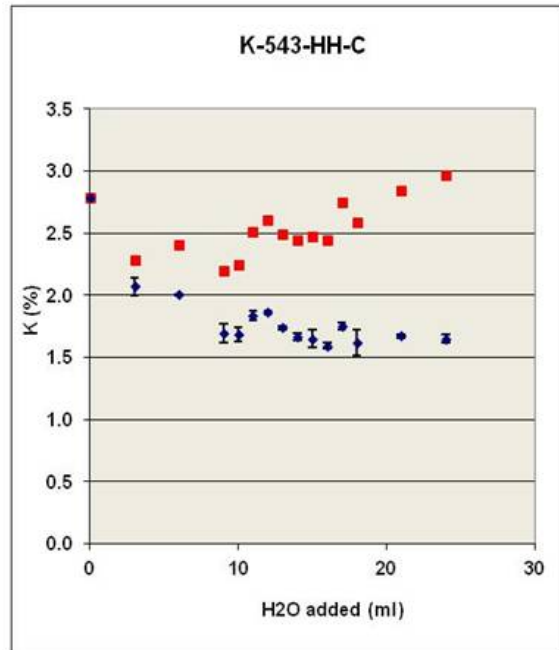
Fig. 7.4. K in Sample 543, HHC.
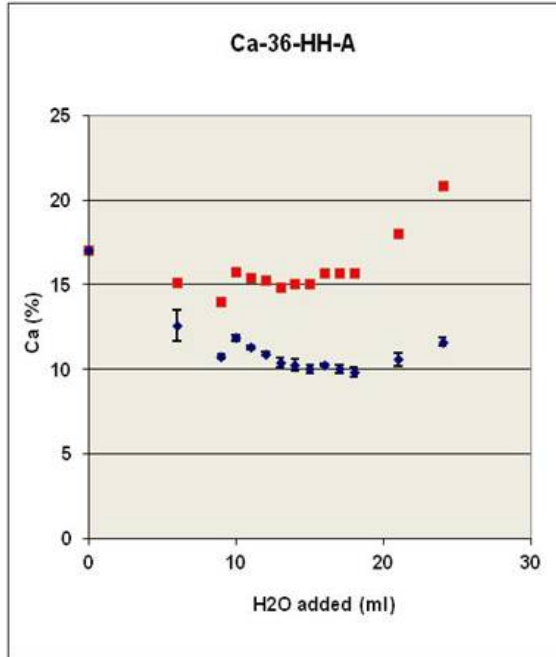
Fig. 7.5. Ca in Sample 36, HH-A.
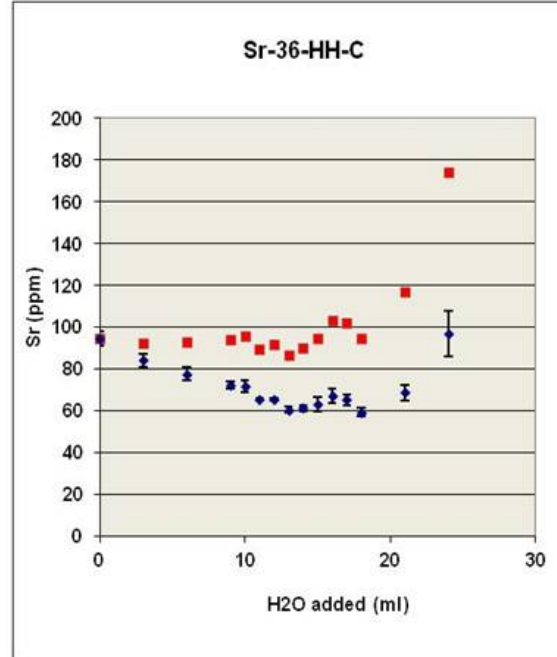
Fig. 7.6. Sr in Sample 36, HH-C.
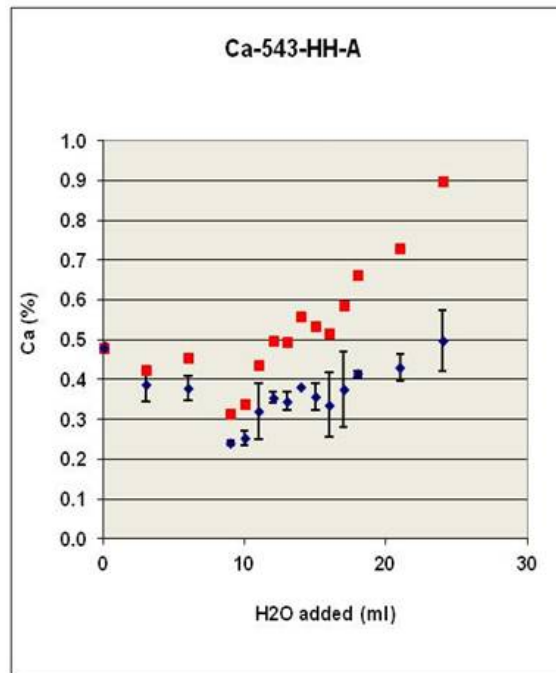
Fig. 7.7. Ca in Sample 543, HH-A.
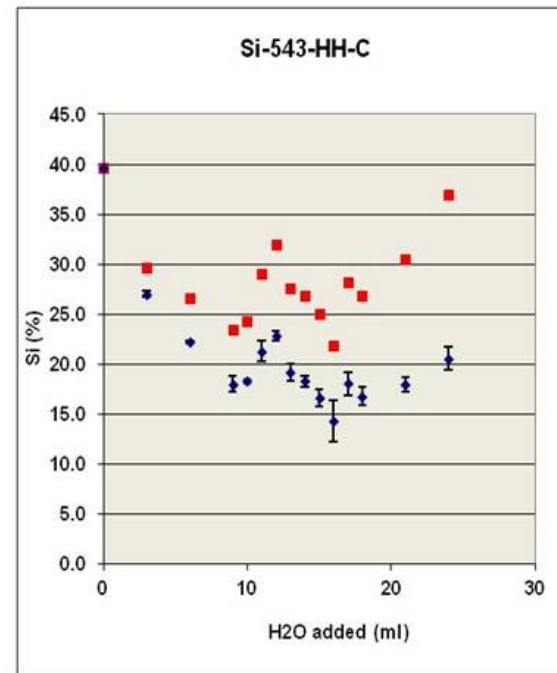
Fig. 7.8. Si in Sample 543, HH-C.
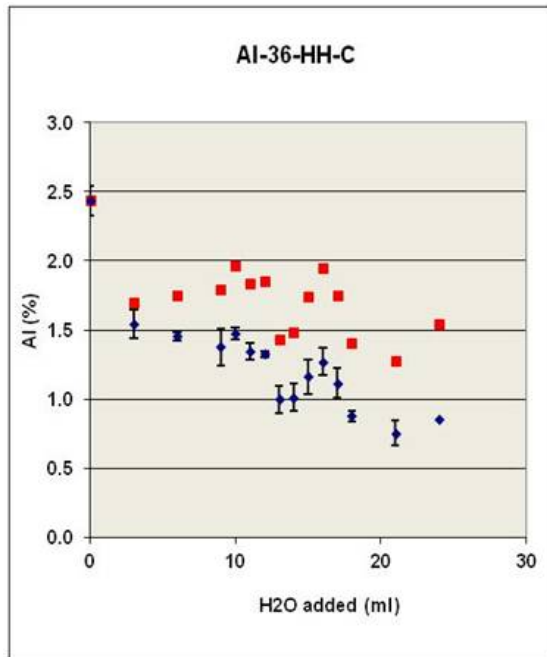
Fig. 7.9. Al in Sample 36, HH-C.
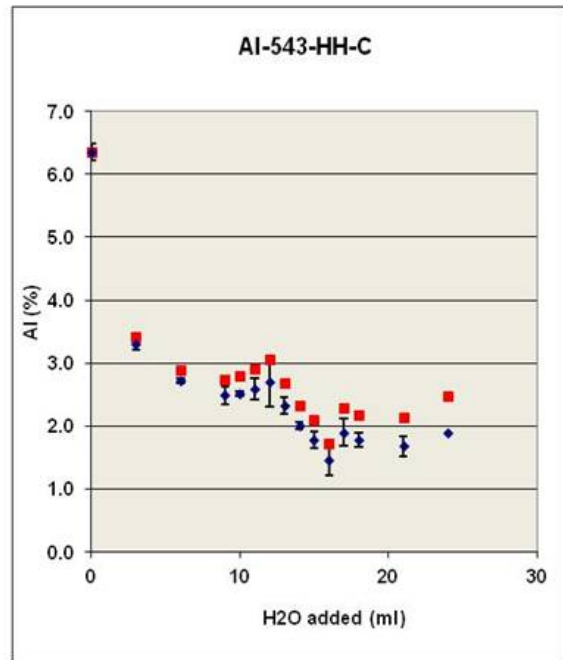
Fig. 7.10. Al in Sample 543, HH-C.
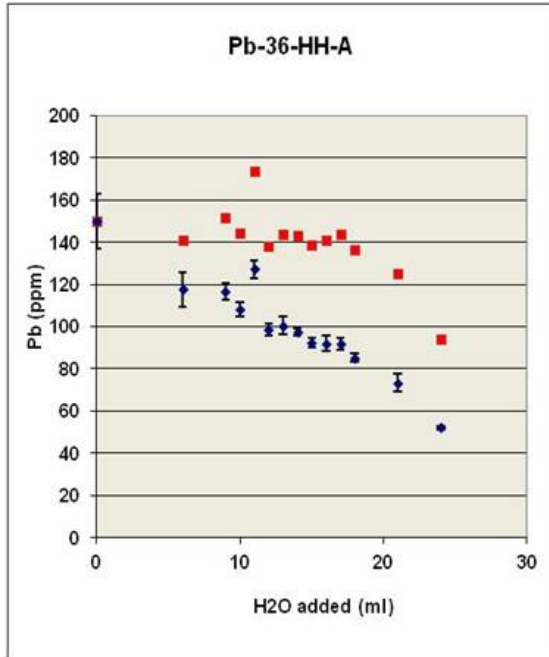
Fig. 7.11. Pb in Sample 36, HH-A.
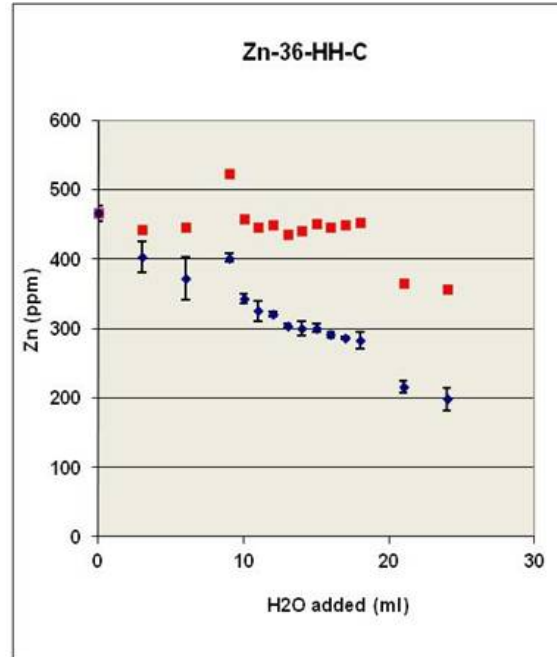
Fig. 7.12. Zn in Sample 36, HH-C.
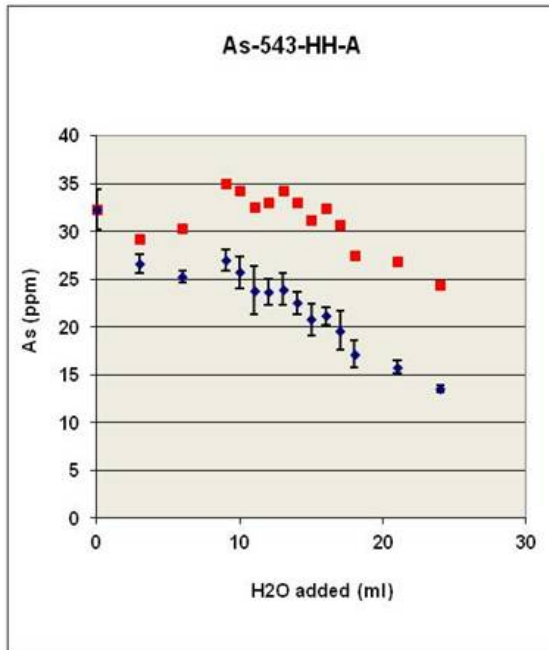
Fig. 7.13. As in Sample 543, HH-A.

Fig. 7.14. Cu in Sample 543, HH-A.

Fig. 7.15. Fe in Sample TILL-2, HH-C.
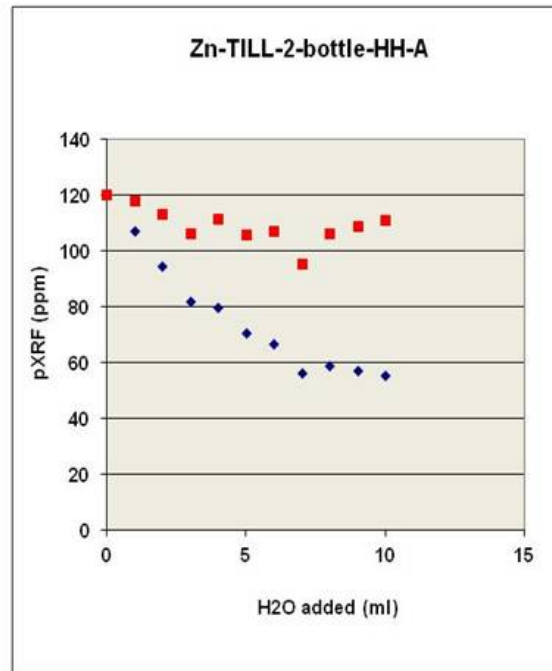
Fig. 7.16. Zn in Sample TILL-2, HH-A.
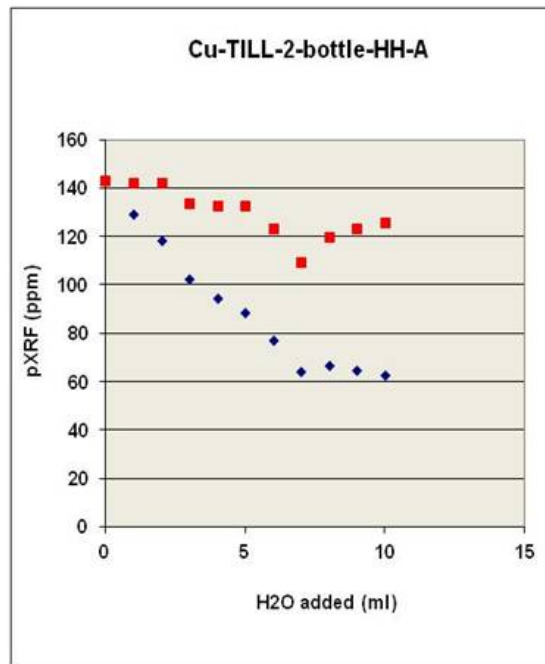
Fig. 7.17. Cu in Sample TILL-2, HH-A.
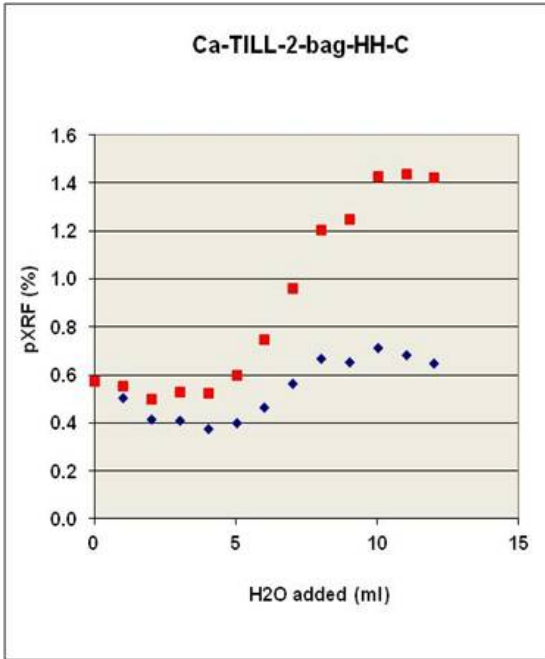
Fig. 7.18. Ca in Sample TILL-2, HH-C.
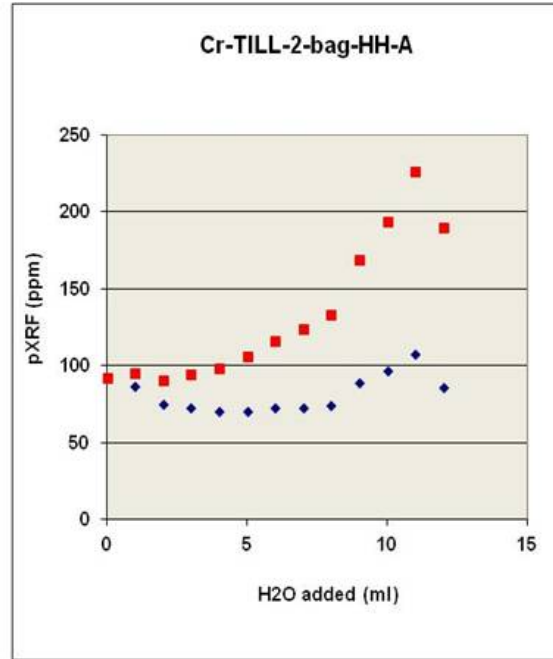
Fig. 7.19. Cr in Sample TILL-2, HH-A.

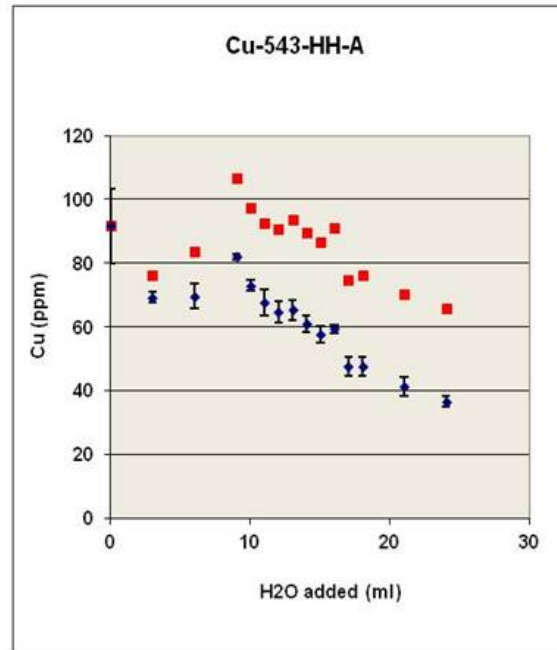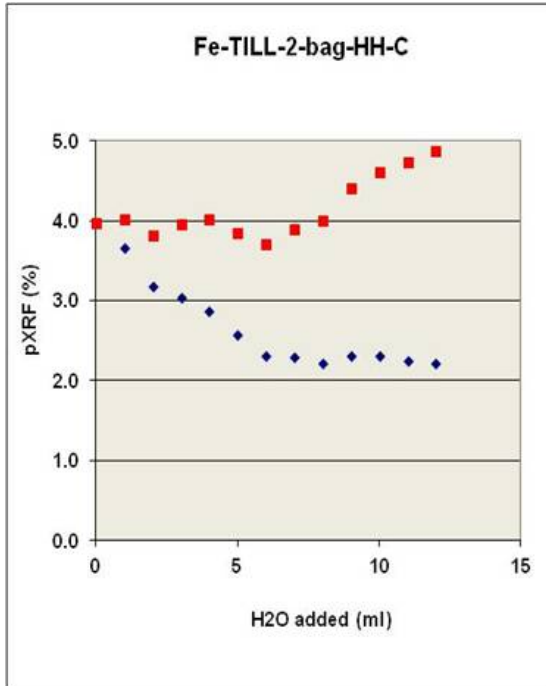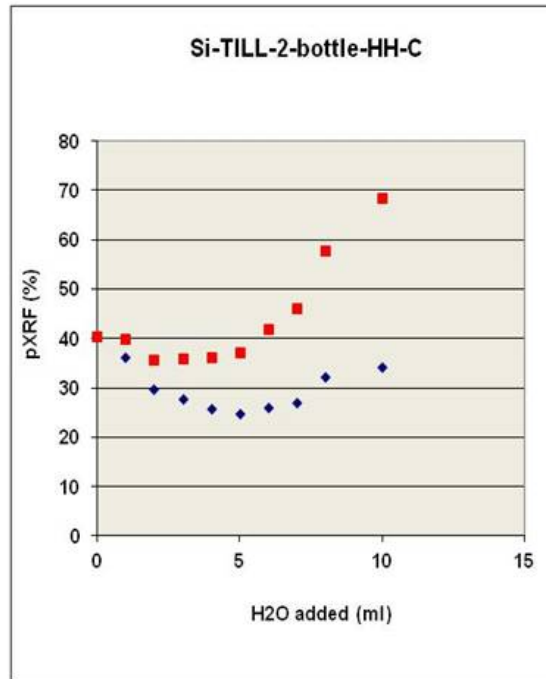**Fig. 7.20. Si in Sample TILL-2, HH-C.**
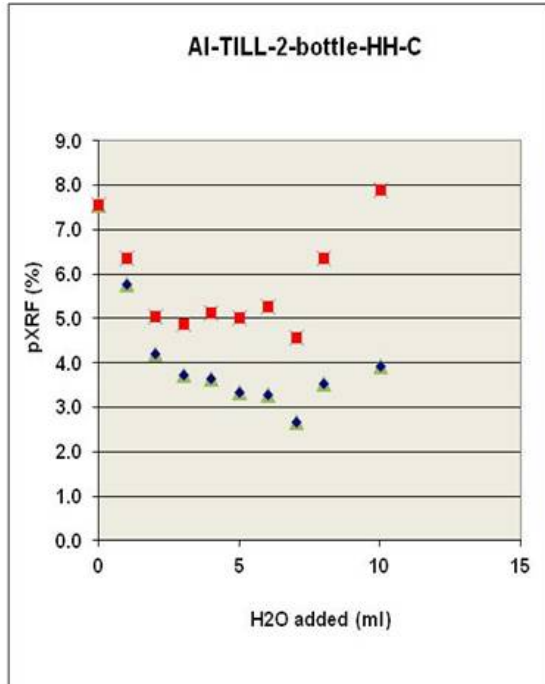
Fig. 7.21. Al in Sample TILL-2, HH-C.
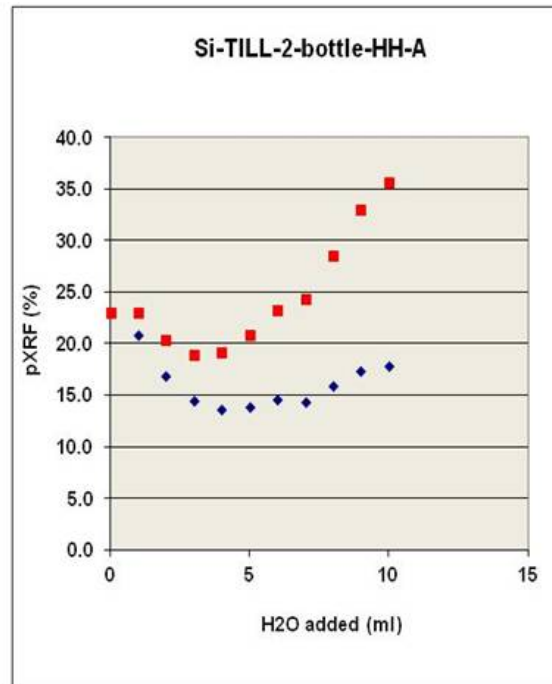
Fig. 7.22. Si in Sample TILL-2, HH-A.

8. MISCELLANEOUS TESTS

All results for these tests are found in the Appendix for both HH-A and HH-C.

8.1. 'Teck Till' sample

Teck Cominco (Steve Cook) submitted, amongst the rock suite, a bulk coarse till sample. This sample was very mixed, comprising small rocks, chunks of aggregated till, roots and fine material. The sample was air-dried and half of it sent off for preparation (sieved to < 2 mm and ball-milled) and analysis at ALS Laboratories of Vancouver. Some of the finer material, avoiding any small stones etc, was separated from the remaining half and quickly ground (~ 2 min) with a mortar and pestle to provide enough sample for two cups for pXRF measurement. This sample was still rather coarse, containing chunks with several mm in cross-section.

The results acquired for this sample comprise those from: (1) total analysis from ALS; (2) pXRF analysis of the coarse till; and (3) pXRF analysis (n=2) of the powder prepared by ALS. As mentioned, the coarse till was split into two cups and each analysed three times but on reviewing the pXRF results it was clear that the data between cups were so similar that means were calculated over all six data per element rather than two sets of three. The results for elements detectable by pXRF are tabulated below; those data where one or more analysis was reported as <LOD or negative were not computed. For the most part, the mining mode data were used for the majors and the soil mode for traces and minors.

Table 8.1.1. Results for Teck Till by ALS (n=1), and pXRF on prepared sample ('powder', n=2) and on coarse sample (n=6). Data in ppm unless otherwise indicated.

| | | HH-A | | | | HH-C | | | |
| | | Powder | | Coarse | | Powder | | Coarse | |
Element	ALS	Mean	SD	Mean	SD	Mean	SD	Mean	SD
Al, %	6.56	6.31	0.04	5.97	0.26	7.82*	0.02	6.82	0.17
As	9.4	17.5	0.3	17.9	1.5	9.1	0.3	11.5	1.6
Ba	1210					730	1	979	57
Ca, %	1.56	1.47	0.01	1.36	0.10	1.41	0.004	1.34	0.04
Co	15	14.7	0.1	13.5	1.0	<LOD			
Cr	160	126	2.8	131	9.2	129	10	127	33
Cu	48	48.5	2.1	53.0	3.3	49.6	0.5	60.0	4.7
Fe, %	3.85	4.15	0.02	4.28	0.23	4.15	0.003	4.51	0.16
K, %	1.55	1.65	0.000	1.52	0.09	1.95	0.02	1.86	0.04
Mg, %	1.16	<LOD				0.71	0.17	0.63	0.14
Mn	775	824	20	929	53	764	5	900	43
Nb	6.8	5.3	0.1	5.9	0.9	6.4	0.2	5.8	1.3
Ni	54.0	<LOD				58.6	0.5	82.4	4.6
P, %	0.096	<LOD				0.26	0.016	0.22	0.013
Rb	49.7	47.4	1.3	46.5	2.6	41.8	1.5	44.7	2.8
Si, %	31.41	31.22	0.09	26.78	1.31	52.69*	0.049	45.78	0.57

Sr	366	365	2	344	20	358	1	350	36
Th	4.6	10.1	3.6	9.8	1.8	2.7	0.5	3.1	0.9
Ti, %	0.366	0.38	0.008	0.43	0.03	0.36	0.000	0.39	0.009
U	1.7	<LOD				9.3	1.2	7.5	1.9
V	170	180	0.7	187	13	166	6	171	6.4
Y	20.3	19.1	1.9	20.0	1.8	18.3	0.4	18.3	1.7
Zn	84	75.4	2.8	79.7	4.8	80.3	1.2	87.3	5.6
Zr	130	121	0.0	120	9.5	122	0.3	125	10.4

Note that HH-C throughout this project reports very high for Si, and, to a lesser extent, for Al

Here we are evaluating degradation in precision rather than accuracy in comparing the fine vs coarse sample results. However, accuracy for most elements appears to be very good, not surprising since this matrix does not contain any unexpectedly high concentrations. The elements for which there are perhaps significant shifts in mean value between fine and coarse are: by both instruments, Mn (824 in fine to 929 ppm in coarse by HH-A, 764 to 900 ppm by HH-C), and Si (31.2 to 26.8% by HH-A, 52.7 to 45.8% by HH-C); and by HH-C only, Al (7.82 to 6.82%), Ba (730 to 979 ppm), and Ni (59 to 82 ppm).

Overall these results are excellent. Examples of degradation in precision in analysing the coarse rather than ball-milled sample include: Fe, 5.3% RSD for coarse from 0.5% RSD for fine (HH-A); Ca, 7.0% from 0.9% (HH-A); Nb, 22% from 3.1% at only ~ 6 ppm Nb (HH-C); Sr, 10.3% from 0.3% (HH-C); and Zr, 8.3% from 0.2% (HH-C). Although these RSDs are inferior to those of the prepared sample, they clearly are reasonable and suggest that a couple of minutes spent sorting and quickly crushing such a sample in the field would be adequate. As very little material is needed to fill a cup or other equivalent vessel for pXRF analysis, using a pestle and mortar to carry out a 1-2 min grind in a field camp would be efficient.

A probable cause of the good agreement between 'powder' and 'coarse' results and the fact that precision for the latter analysis remains acceptable is that each cup is repeatedly tapped, prior to analysis, so that the finer fraction of the coarse material settles evenly to the bottom, leaving the larger grains and 'chunks' on top and for the most part invisible to the X-rays.

[With respect to the individual RSDs associated with each pXRF analysis, the soil mode for Ti appears to be superior to the mining mode for HH-A, unlike the situation for most majors (e.g. Ca, K). Trace elements such as Zn and Zr seem to be equally well determined by both modes but the high background encountered throughout using this instrument for Ag, Cd, Co, Sb, Sn (and at times V) serves as a caution. Using HH-C, the pXRF SDs for Fe, K and Ti are slightly better by the soil mode but results were taken from the mining mode.]

8.2. Great West Minerals (GWM) wet core (# 598903)

One of the three cores submitted by Great West Minerals was quite wet. Prior to drying, three cups were filled with the wet sample and each analysed three times, moving the cup between shots. Most of the sample was then dried in an oven at 40 ^{o}C. The % moisture content was calculated to be 24.9% from the difference in weights before and after drying. A portion of the sample was then ground using a pestle and mortar and split into three cups for pXRF analysis, again moving the cup between each of the three shots per analysis (termed 'dried/crushed' sample). The remaining sample was shipped to ALS for preparation and analysis and the powder was returned to us for pXRF analysis.

The results shown in Table 8.2.1 below are excellent. The mean values for the powder sample agree well with those for the dried/crushed sample and, as expected, are ~ 25% higher than those for the wet clay sample analysed 'as is'. These results are also mostly in good agreement with the lab values, suggesting that the factory calibration for this sample is fitting; recalibration for Ca is probably warranted and for Al, Si and P using HH-C.

Perhaps the most remarkable finding is that there is little to no significant differences in the precision obtained in the pXRF data between all three samples, powder, wet and dried. This reflects the homogeneity and predominantly clay-size characteristic of this core sample. Only the light elements, Al and Si, show substantial degradation in precision in analysis of the wet 'as is' core vs the dried/crushed sample: using HH-A, for example, the RSD increases to 7.5% from 1.3% for Al and to 10.8% from 2.6% for Si. However, even these RSDs are certainly acceptable. As seen for the Teck till, a small time spent in sample preparation in the field camp would yield good results. Alternatively, the sample could be analysed wet and a correction made for the moisture content.

Note: The very low value of Cr found in the wet sample (11 ppm; cf ~ 50 ppm in the powder or dried counterpart) using HH-C is probably a reflection of noisy data and closeness to detection limit; the individual SDs are ~ 12 ppm.

Table 8.2.1. Results for GWM wet core (# 598903) by ALS (n=3), and pXRF on the prepared sample ('powder', n=6), wet core 'as is' (n=9) and on the dried/crushed sample (n=9). Data in ppm unless otherwise indicated.

| | ALS | | HH-A | | | | | | HH-C | | | | | |
| | | | Powder | | Wet clay | | Dried | | Powder | | Wet clay | | Dried | |
Element	Mean	SD	Mean	SD	Mean	SD	Mean	SD	Mean	SD	Mean	SD	Mean	SD
Al, %	4.18	0.05	4.24	0.09	3.62	0.39	4.60	0.12	5.39*	0.06	3.24	0.26	5.53	0.16
As	36.7	0.2	37.4	1.4	26.1	1.2	35.9	1.3	40.7	5.0	28.8	1.7	40.7	3.5
Ca, %	2.68	0.18	1.79	0.04	1.30	0.06	1.87	0.05	1.77	0.02	1.22	0.06	1.86	0.06
Co	7.0	0.0	14.2	0.7	11.2	0.6	12.2	0.7	<LOD					
Cr	50.0	0.0	79.8	5.9	62.3	4.8	81.0	4.8	51.2	11.2	11.3	9.1	49.3	4.6
Cu	26.3	6.7	28.3	3.5	21.8	1.5	27.7	1.9	38.8	2.4	27.6	4.2	38.2	5.7
Fe, %	3.32	0.08	3.48	0.03	2.54	0.11	3.56	0.05	3.93	0.14	2.83	0.07	3.87	0.07
K, %	1.33	0.01	1.22	0.03	1.02	0.04	1.24	0.02	1.67	0.04	1.27	0.04	1.67	0.02
Mn	1420	89	1490	34	1154	43	1491	42	1426	42	1021	107	1428	56
Nb	462	3	387	11	294	11	395	9	476	18	347	10	479	21
Ni	139	3	179	4	133	6	195	7	175	12	132	12	183	8
P, %	1.11	0.08	0.94	0.02	0.75	0.07	1.07	0.03	1.86	0.12	1.07	0.07	1.71	0.05
Pb	76.3	4.2	60	4	43	2	60	2	66	3	43	2	67	5
Rb	36.4	2.4	40	3	25	2	36	2	36	2	26	4	37	1
Si, %	34.42	0.47	29.07	0.17	20.81	1.57	31.00	0.40	52.75*	0.48	37.01	1.27	53.26	0.35
Sr	173	2	150	11	108	6	152	4	179	6	126	9	185	9
Th	205	4	164	11	129	6	170	5	233	4	158	9	233	9
Ti, %	0.29	0.02	0.29	0.003	0.23	0.01	0.30	0.01	0.31	0.01	0.23	0.007	0.31	0.007
U	13.2	0.7	<LOD						23.1	2.3	15.5	1.8	22.2	1.8
V	193	6	122	5	96	6	123	3	197	7	181	9	199	7
W	33.3	1.2	<LOD						64	5	42	7	69	12
Y	304	7	271	18	207	10	278	8	286	4	216	16	291	13
Zn	1077	21	927	16	640	33	939	18	984	24	681	29	1006	31
Zr	910	191	1079	36	823	26	1116	23	1345	36	955	34	1367	56

*Note that HH-C throughout this project reports high for Si and to a lesser degree for Al

8.3. Three pulps (porphyry Cu) from Anglo

These three samples were prepared and analysed at ALS and the pXRF data obtained on return of the powdered sample. The samples were analysed in triplicate by pXRF (moving the sample between shots) and by ALS except for AP-1 which was analysed six times by ALS. The results are tabulated below; the first table presents the data obtained using HH-A and the second using HH-C.

Clearly a calibration should be performed using well analysed samples similar in matrix to these porphyry samples which contain up to 0.56% Cu. Regardless of mode used or instrument, the divergence from the true result at ~ 0.6% Cu (reading 0.9% by pXRF) necessitates recalibration. However, the pXRF data are good for many elements and are indeed excellent for As, Fe, Nb, Rb, Sr, Th, Y and Zr, even at low ppm levels.

Cobalt is not well determined: it is severely suppressed using HH-A, reporting only 9 ppm vs the 109 ppm lab value in AP-3 (0.56% Cu), and is exceedingly noisy by HH-C. There is a high background for Cs by HH-C, negating its determination at the low ppm level. Nickel, next to Cu in the Periodic Table, cannot be determined at these levels ($\leq$ 25 ppm) by HH-A, and reads erroneously high by HH-C. Its Kα line at 7.48 keV is on the shoulder of the Cu Kα line at 8.05 keV and its Kβ line at 8.26 keV would be more severely impacted. HH-A reports <LOD in the mining mode for P in all three samples, containing up to 800 ppm P, and HH-C should probably do the same in light of the erroneously high results reported; the soil mode by HH-A begins to detect P in this matrix at ~ 800 ppm, though it reports low (~ 500 ppm). Response for W is sharply depressed using HH-A, such that AP-3 is reporting only ~ 270 ppm (cf ~ 1500 ppm by lab); HH-C reports ~ 460 ppm for AP-3, also very low (absorption of W fluorescence by Cu?). Zinc, just to the right of Cu in the Periodic Table, is well determined in AP-1 and AP-2 (0.33% Cu) but in AP-3, at 0.56% Cu, it is reported at 85 ppm (cf lab value of 30 ppm) by HH-A and 16 ppm by HH-C. The Kα line of Zn at 8.64 keV is affected by the Cu Kα line at 8.05 keV and Kβ line at 8.26 keV.

Table 8.3.1. Results by pXRF (HH-A) and ALS for Anglo pulps AP-1, AP-2, AP-3; n=3 except for AP-1 where n=6 for the lab data. Data in ppm unless otherwise indicated.

| | AP-1 | | | | AP-2 | | | | AP-3 | | | |
| | ALS | | pXRF | | ALS | | pXRF | | ALS | | pXRF | |
Element	Mean	SD	Mean	SD	Mean	SD	Mean	SD	Mean	SD	Mean	SD
Al, %	8.17	0.06	8.57	0.16	8.09	0.04	7.73	0.22	8.84	0.07	7.83	0.19
As	34.8	3.3	36.9	0.9	201	4	194	6	28.3	0.6	21	2
Ca, %	0.225	0.004	0.229	0.011	2.07	0.019	2.91	0.067	2.24	0.011	2.44	0.024
Co	10.8	0.3	12.6	0.9	63	1.5	21.9	1.2	106	2.3	9.3	0.5
Cr	10	0	25.7	2.3	320	0	280	7	290	10	193	10
Cu	512	17	438	45	3247	136	4395	51	5620	375	9137	86
Fe, %	3.41	0.09	3.27	0.19	5.72	0.04	5.30	0.13	1.90	0.02	1.85	0.03
K, %	3.23	0.02	3.89	0.08	3.06	0.02	3.79	0.07	3.82	0.03	4.51	0.03
Mn	103	40	136	8	1110	45	1082	46	155	0	195	2
Mo	35.5	1.6	37.3	3.1	41.0	1.0	38.9	0.3	184	9	176	1.5
Nb	2.8	0.1	2.0	0.4	4.3	0.3	4.0	1.0	3.9	0.1	3.3	0.8
Ni	2.8	0.8	<LOD		25.3	0.6	<LOD		20.3	0.6	<LOD	
P	393	39	<LOD		669	25	<LOD		800	50	~500	
Rb	170	0.6	163	5	143	2	138	1	98.4	0.5	93	2
Si, %	32.00	0.23	30.25	0.38	25.69	0.16	25.24	0.30	27.76	0.12	26.71	0.25
Sr	105	0	113	1	211	3.2	228	6	360	1.0	384	4
Th	4.8	0.1	8.0	1.7	6.5	0.7	7.9	2.1	4.3	0.1	9.0	2.5
Ti, %	0.161	0.002	0.154	0.004	0.374	0.004	0.407	0.016	0.374	0.004	0.321	0.005
V	45	0.5	69	3	134	3.0	154	7	127	1.0	95	7
W	24	0.4	10.5	0.7	75	0.6	42.0	4.0	1513	38	267	21
Y	3.5	0.1	<LOD		9.6	0.2	9.5	0.3	8.5	0.0	8.5	0.4
Zn	36	0.8	41	2	62	2.1	77	5	30	2.1	85	2
Zr	106	4.5	115	10	132	4	149	4	117	3.8	119	4

Table 8.3.2. Results by pXRF (HH-C) and ALS for Anglo pulps AP-1, AP-2, AP-3; n=3 except for AP-1 where n=6 for the lab data. Data in ppm unless otherwise indicated.

| Element | AP-1 | | | | AP-2 | | | | AP-3 | | | |
| | ALS | | pXRF | | ALS | | pXRF | | ALS | | pXRF | |
	Mean	SD	Mean	SD	Mean	SD	Mean	SD	Mean	SD	Mean	SD
Al, %*	8.17	0.06	8.92	0.11	8.09	0.04	10.2	0.25	8.84	0.07	9.56	0.03
As	34.8	3.3	30.7	1.3	201	4	201	2	28.3	0.6	19.7	0.1
Ba	612	2.4	685	11.2	1043	7.6	1004	6.3	440	4.6	427	17
Ca, %	0.225	0.004	0.236	0.005	2.07	0.019	2.33	0.013	2.24	0.011	2.18	0.013
Co	10.8	0.3	48	36	63	1.5	115	59	106	2.3	72	31
Cr	10	0	<LOD		320	0	315	8	290	10	240	7
Cs	2.4	0.0	52	3	4.7	0.0	46	3	1.9	0.0	25	2
Cu	512	17	385	10	3247	136	4200	16	5620	375	8789	80
Fe, %	3.41	0.09	3.46	0.01	5.72	0.04	5.60	0.003	1.90	0.02	1.90	0.01
K, %	3.23	0.02	3.77	0.01	3.06	0.02	4.05	0.04	3.82	0.03	4.66	0.02
Mn	103	40	186	8	1110	45	1182	25	155	0	195	1
Mo	35.5	1.6	35.8	1.4	41.0	1.0	52	0.8	184	9	190	2
Nb	2.8	0.1	1.7	0.6	4.3	0.3	5.1	0.2	3.9	0.1	4.4	1.2
Ni	2.8	0.8	40	12	25.3	0.6	70	7	20.3	0.6	41	1
P	393	39	1228	12	669	25	1656	158	800	50	1646	59
Rb	170	0.6	148	3	143	2	126	0.5	98.4	0.5	84	0.3
Si, %*	32.00	0.23	47.33	0.09	25.69	0.16	43.04	0.06	27.76	0.12	44.69	0.20
Sr	105	0	115	0.4	211	3.2	222	0.7	360	1.0	380	3.8
Th	4.8	0.1	4.7	0.8	6.5	0.7	8.5	0.9	4.3	0.1	5.6	0.9
Ti, %	0.161	0.002	0.135	0.004	0.374	0.004	0.371	0.005	0.374	0.004	0.342	0.009
V	45	0.5	58	1.4	134	3.0	135	8	127	1.0	115	7
W	24	0.4	33	3.9	75	0.6	98	12	1513	38	455	11
Y	3.5	0.1	<LOD		9.6	0.2	7.7	1.6	8.5	0.0	7.2	1.0
Zn	36	0.8	39	1.4	62	2.1	62	1.8	30	2.1	16	5.4
Zr	106	4.5	100	0.3	132	4	145	1.4	117	3.8	129	3.4

Note that HH-C throughout this project reports high for Si and to a lesser degree for Al

8.4. Test of a portable mill for rock preparation in the field

A field portable rock mill, operated by a 12V DC battery, was tested using several of the project`s samples. The mill is shown in Figures 8.4.1 and 8.4.2. Several versions of such a mill are commercially available.

Selection of the samples chosen for preparation was based on the availability of spare small 'chunks', which eliminated most of the larger-sized cores, and unfortunately these three samples turned out to be have a high degree of heterogeneity. These samples comprise: the shale sample AU08818, the granodiorite CDB-10-102 and the friable itabirite (highly heterogeneous and interference-prone due to high Fe content). However, the purpose of the investigation was to test test the ease and speed of preparation and secondly to compare the precision of the pXRF measurement of the milled sample versus (a) that of the unprepared sample ('smooth' surface for the first two samples and 'rough' surface for the itabirite) and (b) that of the powder (obtained from ALS labs using a different and much larger subsample than that used to obtain the surface or milled data). Under ideal circumstances, cleaning the mill between samples with a shot of air under pressure would have been carried out to avoid carry-over. Contamination from the previous sample was evident as indicated by colour; effort was made to separate this early-milled part of the sample from that analysed but the results suggest carry-over. Hence the accuracy of measurement is not under scrutiny here, rather it is the *precision*.

The preparation itself took only about 3-5 minutes for each sample, the longest time being that required to crush the sample, with a hammer and chisel, ready for the mill. The milled sample appeared to be very fine (<100 µm?). The samples were placed in the usual cups and analysed twice by both HH-A and HH-C.

Data for a selection of elements are shown in the table below; much the same results in terms of both accuracy and precision were obtained using HH-A. It is clear that the precision (standard deviation) obtained by using this mill for preparation is certainly equivalent to that found by analysing the lab-prepared powder and far superior to that obtained by directly analysing the surface. In light of the fact that the inferior surface results on the unprepared samples were based on ~ 10 separate measurements, the time taken to produce a ground sample with such a mill is justifiable. Furthermore, the representativity inherent in the milled sample is much better than that of the very small surface analysed directly. Users must first check for any contamination from metal parts by running pure silica through the mill several times and definitely incorporate a routine cleaning procedure to minimise carry-over between samples.

214

Table 8.4.1. Mean and standard deviation results by HH-C for the prepared (by ALS) powder (n=3), original surface material (n=10, along the surface) and milled material (n=2) for: shale sample AU08818, granodiorite CDB-10-102 and friable itabirite. Values for Al, Ca, Fe, S, and Ti are in % and the rest are in ppm.

	AU08818		CDB-10-102		Itabirite (friable)	
Element	Mean	SD	Mean	SD	Mean	SD
Ag, powder					37.6	1.4
Ag, milled					43.0	5.0
Ag, surface					47.2	11.2
Al, powder	6.88	0.11	8.05	0.30	2.87	0.05
Al, milled	7.89	0.09	7.69	0.21	17.36	0.24
Al, surface	6.34	0.11	9.60	1.56	9.67	1.97
Ba, powder	246	41	854	11	546	20
Ba, milled	285	21	1156	17	649	63
Ba, surface	707	136	1613	943	622	132
Ca, powder	2.59	0.76	0.31	0.01	0.028	0.006
Ca, milled	0.53	1.15	0.43	0.001	0.052	0.005
Ca, surface	2.59	0.76	0.43	0.12	0.021	0.004
Cu, powder	85.8	7.0				
Cu, milled	49.1	1.7				
Cu, surface	44.2	19.9				
Fe, powder	1.96	0.004	0.84	0.02	57.7	0.3
Fe, milled	2.07	0.014	0.96	0.001	62.2	0.1
Fe, surface	1.35	0.34	0.55	0.47	64.7	5.0
K, powder	3.29	0.08	4.06	0.05		
K, milled	3.79	0.03	3.51	0.04		
K, surface	2.86	0.57	3.57	1.45		
Mn, powder	441	64	181	11		
Mn, milled	198	3	208	16		
Mn, surface	366	79	289	203		
Ni, powder	77	2.1	13.7	2.4		
Ni, milled	89	0.7	50.3	1.8		
Ni, surface	91	12	54.7	13.4		
Pb, powder	38	4	3.6	0.3	36	29
Pb, milled	65	0.7	84	4	80	10
Pb, surface	29	8	3.9	3.1	53	19
Rb, powder	66	3.1	89	1.1	12.5	2.2

Rb, milled	85	0.9	91	0.02	22.6	0.4
Rb, surface	74	17	89	34	22.2	4.6
S, powder	0.98	0.01				
S, milled	0.91	0.01				
S, surface	0.68	0.24				
Si, powder	55.3	0.08	54.4	0.93	28.4	0.09
Si, milled	57.4	0.23	51.0	0.08	19.8	0.13
Si, surface	55.4	3.45	59.7	3.3	21.4	6.2
Sr, powder	57.9	4.0	472	4.3		
Sr, milled	65.9	2.0	477	1.5		
Sr, surface	37.8	10.3	497	86		
Ti, powder	0.10	0.002	0.069	0.004		
Ti, milled	0.12	0.001	0.072	0.001		
Ti, surface	0.12	0.05	0.046	0.048		
U, powder	9.6	1.3	10.4	1.0		
U, milled	6.5	1.2	10.4	1.1		
U, surface	8.8	1.9	12.4	2.8		
V, powder	50	1.7	33.0	2.3		
V, milled	60	4.4	33.8	7.9		
V, surface	44	5.3	30.0	22		
Zn, powder	2139	130				
Zn, milled	2353	35				
Zn, surface	2285	880				
Zr, powder	148	9.2	73	1.8		
Zr, milled	152	0.3	91	1.8		
Zr, surface	159	38	56	34.2		

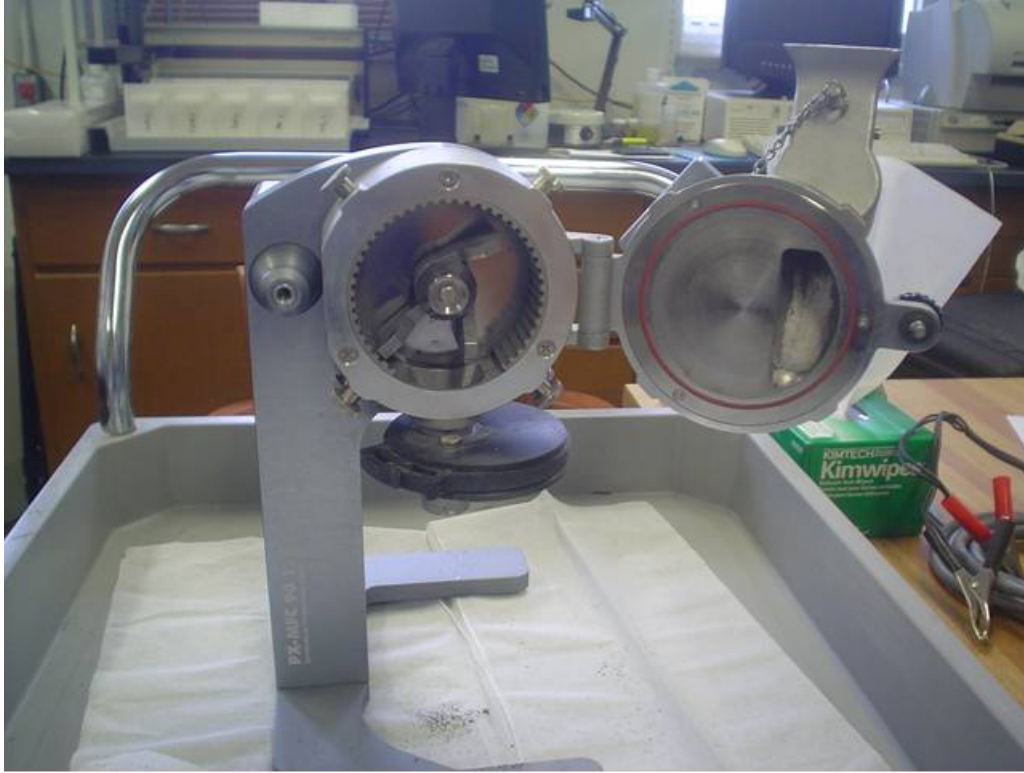*Blue highlights simply for ease of reading separate elemental data sets*

Fig. 8.4.1. Inside of the mill

Fig. 8.4.2. Loading the mill; note the collection bag below
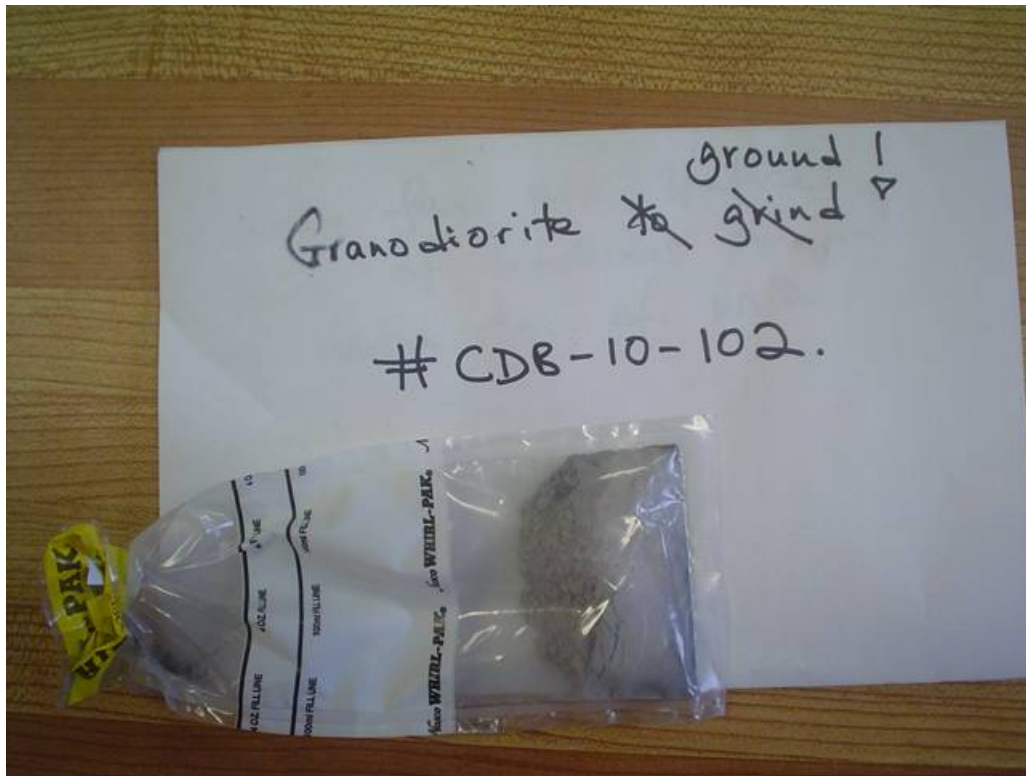
Fig. 8.4.3. Finished product

9. APPENDIX

The appendix is all in digital form (nearly 180 Mb) and contains data and results for Calibration (section 3), Rock study (sections 5.1 and 5.2), Soils (sections 6.1 and 6.2), Moisture study (section 7) and Miscellaneous (section 8).

Data files are in Excel format, whereas plot files are jpegs. The data organization is self explanatory, using a hierarchy of folders.

Note that some sections have summary tables separated out from graphs. These are particularly useful for granodiorites and rocks.

In the Introduction folder in each section there are text files with explanatory notes that explain what is in the various plots and tables.

This is obviously not something to be read (there are an awful lot of graphs and tables), but is a resource to search out results and interpretive graphs for particular elements, suites of rocks, instrument and mode that may be of interest to particular companies or researchers.